2006

Detection, Identification and Classification of Suck, Swallow and Breathing Activity In Premature Infants During Bottle-Feeding

Fedra Adnani
Virginia Commonwealth University

Detection, Identification and Classification of Suck, Swallow and Breathing Activity in Premature Infants During Bottle-Feeding

A dissertation submitted in partial fulfillment of the requirements for the degree of Doctor of Philosophy at Virginia Commonwealth University.

by

Fedra Adnani
Bachelor of Science in Computer Engineering, Sharif Technical University, 1996
Master of Science in Biomedical Engineering, Virginia Commonwealth University, 2003

Director: Paul A. Wetzel, Ph.D.
Associate Professor,
Department of Biomedical Engineering

Virginia Commonwealth University
Richmond, Virginia
December, 2006

To Prophet Mohammad (Peace Be Upon Him),
a meteor whose light is shining
a flint whose spark is bright
a candle whose flame is burning
and
a light for those who seek guidance…

ACKNOWLEDGMENTS

Thanks are due first to my best friend and husband, Mojtaba, for his everlasting love, support and patience during the past four years it has taken me to graduate. I would like to thank my son, Seyed Hussein, and my daughter, Seyedeh Zeinab, for their love, cooperation and support. I could not have made it without your support.

I express my gratitude for my beloved mother who is not alive to celebrate this moment with me. I would also like to thank my father for his unending love, support and encouragement and my sisters who believed in me and supported me along the way.

I would like to thank my advisor, Dr. Wetzel, for his great insights, prospective and guidance in making this educational process a success. My sincere thanks go to Dr. Pickler for her unending directions and providing me the research grant (R01 NR005182, Pickler (PI), NIH). I wish to thank my committee members: Dr. Primeaux, Dr. Lenhardt and Dr. Fei who have shown interest in my project and provided valuable suggestions. And finally, but not least, I am thankful to Ms. Patricia Russo for her enormous help in editing my dissertation.

TABLE OF CONTENTS

LIST OF TABLES

Table 4.87: The second minute of sucking of baby #81, 10th feeding.........................214

Table 4.88: The evaluation of the second minute of sucking of baby #81, 10th feeding..214

Table 4.95: The sixth minute of sucking of baby #81, 10th feeding.......218
Table 4.96: The evaluation of the sixth minute of sucking of baby #81, 10th feeding.......218
Table 4.97: The seventh minute of sucking of baby #81, 10th feeding.......219
Table 4.98: The evaluation of the seventh minute of sucking of baby #81, 10th feeding.......219

LIST OF FIGURES

LIST OF ABBREVIATIONS

A/D	Analog to Digital
AR	Autoregressive
AOP	Apnea of Prematurity
CWT	Continuous Wavelet Transform
DWT	Discrete Wavelet Transform
FFT	Fast Fourier Transform
Hz	Hertz
MTM	Multitaper Method
NICU	Neonatal Intensive Care Unite
NN	Neural Network
PDAS	Ponemah Data Acquisition System
PSD	Power Spectrum Density
STFT	Short Time Fourier Transform
WPT	Wavelet Packet Transform
WT	Wavelet Transform

ABSTRACT

DETECTION, IDENTIFICATION AND CLASSIFICATION OF SUCK, SWALLOW AND BREATING ACTIVITY IN PREMATURE INFANTS DURING BOTTLE-FEEDING

By **Fedra Adnani, Ph.D.**

A dissertation submitted in partial fulfillment of the requirements for the degree of Doctor of Philosophy at Virginia Commonwealth University.

Virginia Commonwealth University, 2006.

Director: Paul A. Wetzel, Ph.D.
Associate Professor, Department of Biomedical Engineering

Prematurity, especially if extreme, is one of the leading causes of problems and/or death after delivery. Among all the problems encountered by premature infants, feeding difficulties are very common. Many premature infants are fed intravenously at first, and they progress to milk feedings provided by a tube passed into the stomach. At around 34 weeks of gestation, premature infants should be able to breastfeed or take a bottle. At the same time such premature infants are usually faced with difficulty making the transition from tube-feeding to full oral feeding. In this study three physiological measurements of premature infants including sucking, swallowing and breathing were measured. The objective of this work was to detect, identify and classify these three signals independently and in relation to each other. The goal was to look at the specification of sucking, swallowing and breathing signals to extract the ratio of suck-

swallow-breath coordination. The results of this study were used to predict the readiness of a premature infant for introduction to oral feeding.

To accomplish this, three different methods were examined. In the first method, the integration of the wavelet packet transform and a neural network was investigated. According to results of the first approach, integration of the wavelet packet transform and the neural network failed due to the inefficiency of the feature extraction method. Thus, the wavelet packet energy nodes did not provide a good feature extraction tool in this specific application.

In the second approach, the frequency content of each signal was investigated to study the relationship between the shape of each waveform and the frequency content of that specific signal. Spectral analysis for suck, swallow and breathing signals showed that the shape of the signal was not tightly related to the frequency content of that specific waveform. Therefore, the frequency content could not be used as a method of feature extraction in this specific application.

In the third method, the integration of correlation and matched filtering techniques was investigated and demonstrated promising result for the detection of suck and breathing signal but not for the swallowing waveform. Based on the results for sucking and breathing signals, this method should also work for good quality swallowing signal. To understand the relationship between the suck, swallow and breathing signals a matrix containing information on the time of occurrence of each event was developed.

Introduction

1.1. Introduction

History has seen many distinguished premature infants. Isaac Newton, Albert Einstein, Daniel Webster, Napoleon Bonaparte, Mark Twain, Winston Churchill and Charles Darwin all were born premature (Linden *et al.*, 2000). Because birth occurs before the internal organs have completed forming, premature infants will encounter problems related to their immature vital organ systems, specifically the respiratory and nervous systems. As a result premature infants will often require specialized care (in a hospital or nursery) until their vital organ systems have developed enough to sustain life without specialized support. Depending upon the extent of the infant's prematurity, this may take weeks to months.

Gestational age is the number of weeks a fetus has been in the uterus determined by counting the date of the mother's last menstrual period. Gestational age provides essential information about the growth and development of a fetus during pregnancy and may help determine whether an infant can live outside the uterus.

Every newborn infant is classified at birth as one of the following: premature (less than 37 weeks gestation), full-term (37 to 42 weeks gestation), or post-term (more than 42 weeks gestation). Although many medical and anatomic disorders are involved in premature labor, in most cases, the cause of premature labor is not well-known.

Risk factors that lead to premature labor include (Weismiller, 1999):

- Illness of the mother, such as high blood pressure or diabetes
- Vaginal infection that has spread to the uterus
- A large fetus or more than one fetus

- Abnormalities of the placenta
- The early rupture of the membranes
- A previous preterm labor
- Smoking while pregnant
- Excessive alcohol consumption throughout the pregnancy
- A hormone imbalance

Immature vital organ systems such as respiratory or nervous systems may cause problems for premature infants. For example, an infant may not be able to breathe immediately following the birth or the respiratory efforts are so poor the premature infant cannot expand its chest to deliver oxygen to its body. In such cases, artificial breathing is delivered using a breathing tube which is inserted into the infant's trachea (Conners *et al*, 1989). As a result, the premature infant will need specialized care in NICU (Neonatal Intensive Care Unit) until the organ systems have developed sufficiently to sustain life without medical support.

Prematurity, especially when extreme is one of the leading causes of problems and/or death after delivery (Linden *et al.*, 2000). Since a majority of organs on premature infants' body are not fully developed, expert intervention and constant monitoring is required, for example:

- Premature infants often encounter difficulty breathing. This is mainly because of underdeveloped lungs. Such infants may need extra oxygen and/or assistance with their breathing from a ventilator (Conners *et al*, 1989 and Berne and Levy, 2004).

- The surface area of a premature infant's body is large when compared to its volume. Also, since premature infants have very little body fat, their body temperature drops. Therefore, they must be kept in an incubator to monitor the body temperature (Linden *et al.* ,2000).
- Premature infants' immune system is not fully developed, therefore, they are highly susceptible to life-threatening infections (Linden *et al.*, 2000).
- Because their stomach and intestines are not fully developed in many premature infants, their digestive systems cannot handle breast milk or formula adequately, and must get part or all of their nutrition through an IV (Redshaw *et al,* 1985).
- The brain is not fully developed. As a result, many premature infants don't breathe regularly and reliably on their own without assistance, or cannot suck, swallow, and breathe in a coordinated fashion during feeding (Mathew, 1988).

Among these problems, feeding difficulties are very common in premature infants. Premature infants have very little muscle mass and almost no fat. During the premature infant's first few days of life, total intravenous feeding is widely used because the various mechanisms for ingestion and digestion of food are not fully developed. The exact amounts of nutrients, electrolytes, minerals, vitamins and water to be given are calculated on the basis of the infant's weight and as a result of blood and urine tests (Redshaw *et al,* 1985).

The more premature the infant, the more difficult the feeding problem. Immature development of the brain may initially prevent the premature infant from sucking and swallowing normally. Many premature infants are fed intravenously at first,

and progress to milk feedings provided by a tube passed into their stomach. Around 34 weeks gestation, premature infants should be able to breastfeed or take a bottle. At the same time, such premature infants are usually faced with difficulty in making the transition from tube-feeding to full oral feeding (Lau *et al,* 2000). This is because the coordination of sucking, swallowing and breathing is often not achieved much before 34 weeks gestation (Lau *et al,* 2000).

1.2. Sucking in Premature Infants

A fetus has the ability to suck as early as 13 weeks gestation (Conway, 1994). Physiologically, sucking is a complicated process involving a complex integration of the muscular activities of the lips, jaws, tongue, cheeks and palate (Lau and Schanler, 1996). Two modes are used to describe the sucking process: nutritive and non-nutritive. Nutritive sucking, which occurs after the consumption of a liquid, the infant sucks with lower speed in comparison with non-nutritive sucking (Medoff-Cooper *et al,* 2001). The sucking pattern of a mature infant consists of the alternation of two components: suction and expression. Suction is the negative intraoral pressure produced to draw milk into the mouth. Expression is believed to correspond with the compression and/or stripping of the nipple between the tongue and hard palate to express milk into the mouth (Lau *et al,* 2000; Medoff-Cooper and Ray, 1995).

Although full term pattern of sucking would appear to be the most efficient method of transferring milk from the breast/bottle to the infant, it is not necessary for successful oral feeding. Premature infants who can use only the expression component as

a result of their immaturity can also be successful in oral feeding (Lau and Schanler, 1996). For premature infants, in comparison with full term infants, the feeding bouts are shorter in duration with significantly lower sucking pressure, lower sucking rates and shorter bursts of sucking (Medoff-Cooper *et al*, 2001). By increasing the gestational age and providing more opportunities for infants to suck, the pattern of sucking starts to change. As the number of suck/burst and the sucking rates increase, the pauses between sucking become shorter and the infant sucks with higher pressure (Nyqvist, 1999).

1.3. Swallowing in Premature Infants

Studies indicate that a fetus has the ability to swallow as early as 18 weeks gestation (Conway, 1994). Actually, at a gestational age of between 11-13 weeks, the fetus engages with jaw opening and rhythmical bursts of jaw movements at a rate of one per second (Nyqvist *et al,* 1999). At 15 weeks gestation, swallowing starts to appear and by 20 weeks gestation, the rate of swallowing is 1-2 swallows per second (Nyqvist *et al,* 1999).

The swallowing process consists of three stages. Nerves connecting the digestive tract to the brain are responsible for controlling these phases (Reddy and Ryan, 2001).

- ***Oral preparation stage***: In the first stage, food is chewed and moistened by saliva; then is pushed back by the tongue towards the throat.
- ***Pharyngeal stage:*** In the second stage, as food enters the pharynx, the epiglottis, a cartilage-like structure positioned on the tongue blocks the passage of air to

prevent the leakage of food or liquid into the lungs. When the muscles in the throat relax, food and liquid are quickly passed down the pharynx into the esophagus. At the end of this stage, the epiglottis opens up again allowing the air to enter into the lungs.

- ***Esophageal stage:*** In this final stage, food is pushed down towards the stomach by muscles in the esophagus. There is a muscular area between the end of the esophagus and the upper portion of the stomach (esophageal sphincter) where the esophagus meets the stomach. As this muscle relaxes in response to swallowing, food and liquids enter the stomach.

Despite the current studies about the process of swallowing in adults, there has been very little research on infant swallowing function and pathophysiology. On the other hand, the relationship between anatomic structures involved with swallowing is different in infants while the neurological relationship between these structures is still immature. For example, the larynx and epiglottis are located at a higher level in infants (Newman 1996) as a result, the infant often accumulates food and liquids in the valleculae (the wedge-shaped space formed between the base of the tongue and epiglottis) during multiple sucks with the pharyngeal stage triggering from the valleculae (Newman *et al* 2001).Therefore, the parameters engaged with swallowing in an adult cannot always be used to investigate this process in infants.

1.4. Breathing in Premature Infants

As early as 10 weeks gestation, the human fetus has the ability to perform episodic, spontaneous breathing movements (Conners *et al.* 1989). By 11 to 12 weeks gestation, the fetus is breathing fluid steadily and continuously while the placenta provides exchange of O_2 and CO_2 for the fetus. It appears that, this form of breathing develops the organs of respiration and is essential for neuromuscular control of breathing. Fetal breathing movements occur in an irregular fashion, usually during rapid eye movement sleep (Koos *et al.* 2001). Even though, in the 11th week of gestation fetal breathing is intermittent, the breathing movements tend to be more vital and rapid as gestation continues. Development of fetal lungs continues as the fetus grows, and fairly well developed alveoli (the small air sacs) are usually present by 25 weeks gestation (Koos *et al.* 2001).

The lungs are totally collapsed before birth, as the infant takes his or her first breath, the lungs must expnad to inflate the alveoli. To lower the tension surface of alvioli, the fetus starts secreting a fluid called surfactant into the alveoli during the last trimester of pregnancy. One reason that premature infants often have difficulty breathing is surfactant deficiency. Actually, their lungs are not mature enough to produce adequate surfactant therefore, surfactant therapy might be applied to help them until their own lungs are able to produce sufficient surfactant (Wu and Carlo 2001).

Another problem premature infants face is an immature nervous system. Premature infants are not usually engaged with a nonstop breathing pattern because the part of the central nervous system that controls breathing is not yet mature. As a result

premature infants usually have large bursts of breathing followed by periods of shallow breathing or stopped breathing. This condition is usually referred as "Apnea of Prematurity", or AOP (Wu and Carlo, 2001).

1.5. Suck-Swallow-Breath Coordination

Sucking, swallowing and breathing utilize common anatomical structures. The anatomical pathways for inspired air and ingested food cross in the pharynx of mammals, implying that breathing and swallowing must be separated in time. Sucking results in filling the mouth with liquid which in turn triggers swallowing. Although swallowing can be triggered voluntarily, it is mainly considered a reflexive process (Berne and Levy, 2004). The frequency and timing of the swallow is determined by the rate and intensity of sucking as well as the amount of liquid obtained during sucking (Mellins, 1985). As the liquid reaches the pharynx, chemoreceptors in pharynx and larynx are stimulated to initiate the swallowing reflex. An area in the medulla called the swallowing center will receive a sensory impulse from these receptors. Motor impulses are then transmitted from the swallowing center to the pharynx and the upper esophagus to initiate the apnea and as a result the epiglottis closes the air passage temporarily (Berne and Levy, 2004).

The ability to orally feed successfully is highly dependent on the proper coordination of sucking, swallowing and breathing activities. Beginning in utero, the fetus is able to suck and swallow amniotic fluid, but the coordination between the two processes is usually achieved between 32 to 34 weeks (Nyqvist *et al,* 1999). With increasing the gestational age, the suck-swallow pattern becomes more mature and

rhythmic with up to 30 consecutive sucks and frequent swallows during sucking (Nyqvist, 1999). Suck, swallow and breathing processes are usually coordinated by 34 weeks gestation although it may occur even later, at 36 to 37 weeks gestation (Lau *et al,* 2000)

The timing of a swallow relative to the inspiration/expiration cycle is critical to protect the airways. This coordination is especially important for premature infants due to their immature nervous system. Studies suggest that swallowing occurs during all parts of the breathing cycle (Mizuno *et al*, 2003). In other words, swallowing may happen during expiration, during inspiration, at the transition (cusp) between inspiration and expiration or between expiration and inspiration.

In healthy adults, breathing and swallowing are well coordinated during eating and drinking, with 75-95% of swallows beginning in the expiratory phase (Hiss *et al*, 2001). In healthy full term infants, nutritive swallowing mostly occurs at the transition between inspiration to expiration, otherwise in mid-expiration and infrequently at the transition between expiration to inspiration (Selley *et al.*, 1990; Bamford *et al.* , 1992). In premature infants (32 and 33 weeks gestation), swallowing predominantly occurs during pauses in respiration, but by 35 weeks of gestation, swallowing usually occurs at the end of inspiration (Mizuno *et al*, 2003).

Investigations suggest that the coordination between swallowing and breathing happens in the form of brief periods of breathing cessation during swallow with an overall decrease in ventilation (Mathew, 1988). Reduction in inspired oxygen concentration in premature infants leads to a transient increase in ventilation for

approximately one minute, followed by a sustained depression. Therefore, the respiration pattern will be slower, more irregular and shallow form as the infant's level of oxygen decreases (Pickler, 1999).

The respiratory rate of a premature infant is between 40 and 60 breaths per minute. The epiglottis closes the airway passage for about one second therefore; swallowing can easily interfere with respiration in a premature infant. For well coordinated sucking, swallowing and breathing, the ratio is theoretically 1:1:1 or 2:2:1. However, if the coordination between sucking and breathing is not well established the ratio is more sucking to breathing around 2:1 to 4:1 (Pickler, 1999)

As feeding performance improves, sucking and swallowing frequency, bolus size, and suction amplitude increases. It is speculated that feeding difficulties in preterm infants are more likely to result from inappropriate swallow-respiration interfacing than suck-swallow interaction (Lau *et al*, 2003).

1.6. Significance

Effective hospital discharge planning can be difficult and is often influenced by uncontrollable factors such as the infant's medical status. Physiological criteria are generally used to determine readiness for discharge and include: growth, feeding tolerance and the ability to maintain and regulate temperature outside of an incubator (Linden *et al.,* 2000). An infant's ability to tolerate feeding is a major concern since all infants need to have proper nutrition in order to grow and develop. Due to physiological immaturity and lack of a suck-swallow-breathe coordination in premature infants, tube-

feeding is widely used to feed them at the beginning. Introduction to bottle-feeding seems logical when the infant is more mature and the suck-swallow-breathe coordination has developed demonstrating that the infant is ready to progress from tube to oral feeds(Lau *et al.* 1997) .

The decision to initiate oral feeding in a premature infant is an important clinical decision. While there are no universally accepted criteria used to determine when to initiate oral feeding for premature infants, there are several factors involved in the process of determining bottle-feeding readiness. Specifically, readiness is defined as "the maturational readiness to begin the oral, bottle feeding process rather than readiness to feed at a bottle when it is offered" (Pickler, 1999). The infant's gestational age, respiratory status, heart rate, muscle tone, behavioral organization and sucking ability are some of the factors that are used to assess an infant's readiness for bottle-feeding (Conway, 1994). Usually somewhere between 33 to 34 weeks gestation, oral feeding is initiated. However, there is no empirical evidence showing that this process cannot be started earlier (Lau *et al,* 2000). The following rationale for initiating oral feeding as soon as the infant is ready may include:

- Extending nursery length of stay increases health care costs.
- The inability of the infant to feed and gain weight is frustrating for nurses and parents and may affect the parental attachment process (Redshaw *et al*, 1985) .
- Although success in oral feeding is highly dependent on infant maturity, there are some mechanical factors involved in delivering milk from a bottle that may affect the premature infant's performance. The hydrostatic pressure generated by the

volume of milk in an inverted bottle, results in a net positive of milk flow. Therefore, such continuous milk flow may affect the premature infant's ability to coordinate sucking, swallowing and breathing, regardless of whether the infant is sucking actively (Lau, 1997).

- Premature infants experience breathing irregularities that lead to significant and frequent episodes of hypoxemia especially during bottle-feeding (Berne and Levy, 2004). Recurrent, transient hypoxemia may cause the development of dysfunctional oral-motor feeding patterns, increased expenditure of energy and poor growth, and neurological injury (Lau *et al*, 2000).
- When premature infants are born, non-oral feeding methods (e.g. tube-feedings) are used to feed them due to their inability to coordinate the suck, swallow and breathe processes. As a result of using these methods, sensory input to the mouth will be less in comparison to bottle-feeding and this may delay the development of oral feeding ability (Pickler, 1999).

All these facts emphasize the importance of initiating bottle-feeding at the earliest time when the infant is able to coordinate the suck-swallow-breath process.

1.7. Objectives

In order to predict the appropriate time to introduce bottle-feeding to premature infants, the heart rate, oxygen saturation, respiratory rate, sucking and swallowing activities are measured. These physiological measures are recorded directly into a Ponemah Data Acquisition System (PDAS). The objective of this work is to detect and

identify breathing, sucking and swallowing waveforms independently and in relation to each other. The goal is to look at the specification of these three waveforms to extract the ratio of suck-swallow-breath coordination and predict if the premature infant has reached the point of coordinating of these three processes.

1.8. Physiological Measurement and Methods

Heart rate, oxygen saturation, sucking, respiratory and swallowing activities are the primary physiological measures that are used in this study. These physiological measures are recorded directly into the PDAS.

1.8.1. Ponemah Data Acquisition System (PDAS)

The Ponemah Data Acquisition System is multi-application platform that uses digital technology to record physiological data. This complete and accurate data acquisition system is responsible for accurate, continuous and non-interrupted multi-channel data acquisition in a validated, standardized environment. The PDAS consists of hardware and software that can be installed in a personal computer (Gould Instrument System, 2001).

The PDAS has modular software that allows the user flexibility along with accurate, multi-channel, non-interrupted data acquisition. This feature provides the opportunity for the user to custom design the configuration in order to meet the research objectives without the need for extra programming (Gould Instrument System, 2001).

. The PDAS can communicate with variety of different types of hardware. In this application, five channels were used to record oxygen saturation, heart rate, respiratory, sucking and swallowing activities. Before the analog signal can be used by the PDAS it must be digitized. The analog input was transferred to an analog to digital (A/D) converter device with 12-bit resolution and a sampling rate ranging from 5 Hz to 50 KHz. In the current application, the sampling rate was 1 KHz per channel. Sampled data from all channels were directly stored to the resident hard disk drive into a single file with a .RAW extension but due to the difficulty extracting the data from .RAW files, a Matlab based data acquisition system was working in parallel to acquire data and save it in a single file with a .DAQ extension. In latter case, data from different channels can be easily extracted using Matlab commands.

The PDAS has the ability to provide the user with a variety of different graphs and data windows not only on-line but also during subsequent replay. The software is able to illustrate the derived data and raw signals on the monitor at the same time. The user can define the X and Y scales. Figure (1.1) illustrates the suck, swallow, breath, oxygen saturation and heart rate signals, which were acquired by the Ponemah system.

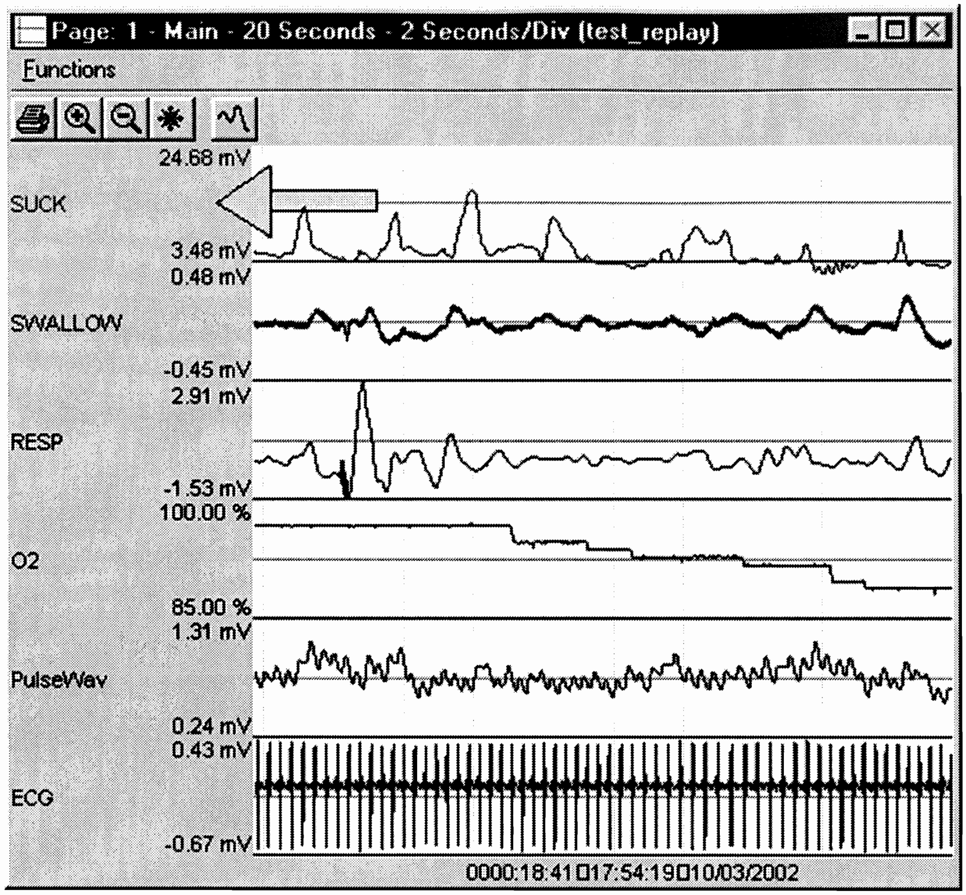

Figure 1.1: Sucking, swallowing, breathing, oxygen saturation and heart rate signals acquired by Ponemah system.

In order to measure the heart rate continuously during the whole process, standard cardiorespiratory leads were interfaced with a Gould ECG/Biotah Signal Conditioner, Model 13-6615-65. This signal conditioner was responsible to send the analog data to the A/D device and then the Ponemah Data Acquisitions System (Pickler, 1999).

To record the respiratory data two different methods have been used. In the first method, a Dymedix PVDF piezoelectric sensor was placed under the premature infant's

nose. Piezoelectric sensors, which are used to measure physiological displacements, generate an electric potential when mechanically strained and due to their high sensitivity to mechanical movement, artifacts are not avoidable (Webster, 1998). In the second method, a nasal thermistor (US Sensors, Model # H1744) was placed beneath the infant's nostrils to detect temperature changes that occur during inhalation and exhalation (Pickler, 1999). Thermistors are semiconductors made of ceramic materials that are small in size, have relatively large sensitivity to temperature changes and have excellent long-term stability characteristics (Webster, 1998). Very small differences in temperature can be measured by the thermistor and the small size of this type of sensors makes possible their placement beneath the infant's nostrils. This sensor was connected to Ponemah system via a signal conditioner. Figure (1.2) illustrates a breathing waveform recorded using a nasal therimistor.

Oxygen saturation is a measure of how much oxygen the blood is carrying as a percentage of the maximum it could carry (Berne and Levy, 2004). Oxygen saturation provides more effective evaluation of ventilation. Investigations suggest that pulse oximetry is a reliable indicator of arterial oxygenation in neonates (Deckardt and Steward, 1984). In this study, the pulse oximeter was connected to the A/D device via a signal conditioner (Criticare Model #540). The range was of value between zero and one volt when one volt corresponds to 100% saturation. The PDAS then received sampled data from the A/D device. In order to connect the pulse oximeter probe to the infant, "premie" sized sensors were used to attach to the infant's hand or foot (Pickler, 1999).

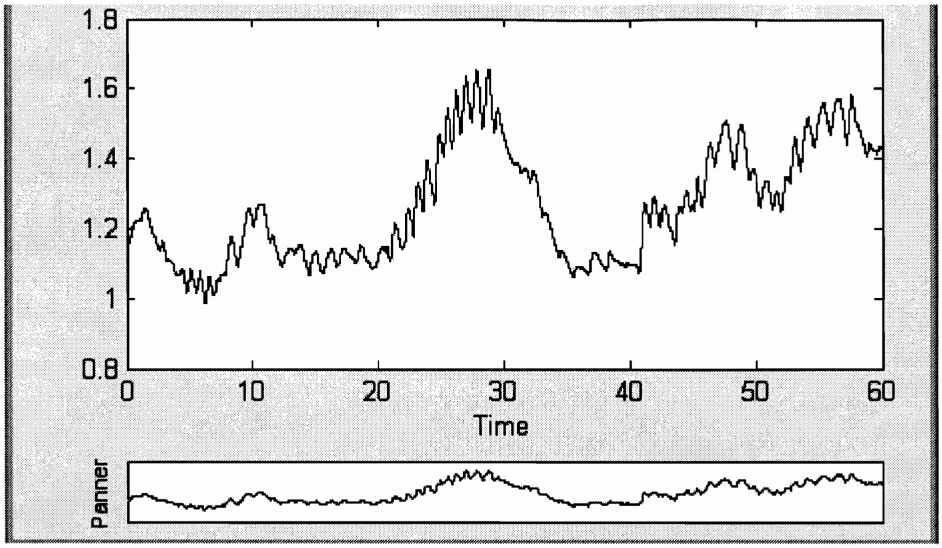

Figure 1.2: Breathing Waveform

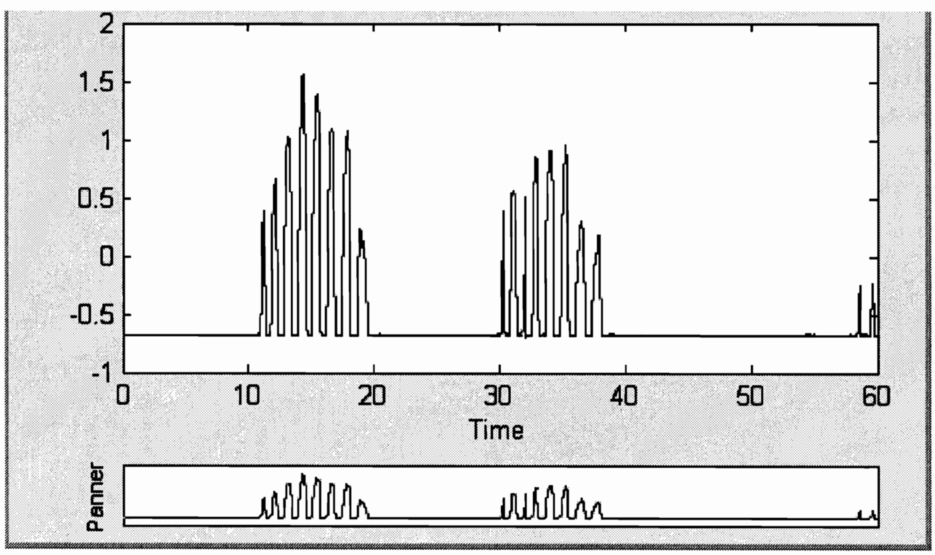

Figure 1.3: Sucking Waveform

A chin strain gauge was used to measure sucking events. Mercury filled strain gauges, which are sensitive to stretch, were placed under the infant's chin. When sucking occurred the strain gauge was stretched and the plethysmograph, which was connected to

strain gauge, detected the changes in electrical resistance. As a result of the change in electrical resistance a waveform was recorded (Figure 1.3). The A/D device received the analog signal from Mercury Strain Gage Plethysmograph Model #272 and digitized it. Digitized data was then transferred to the PDAS. Therefore sucking activity was recorded as it occurs (Pickler, 1999).

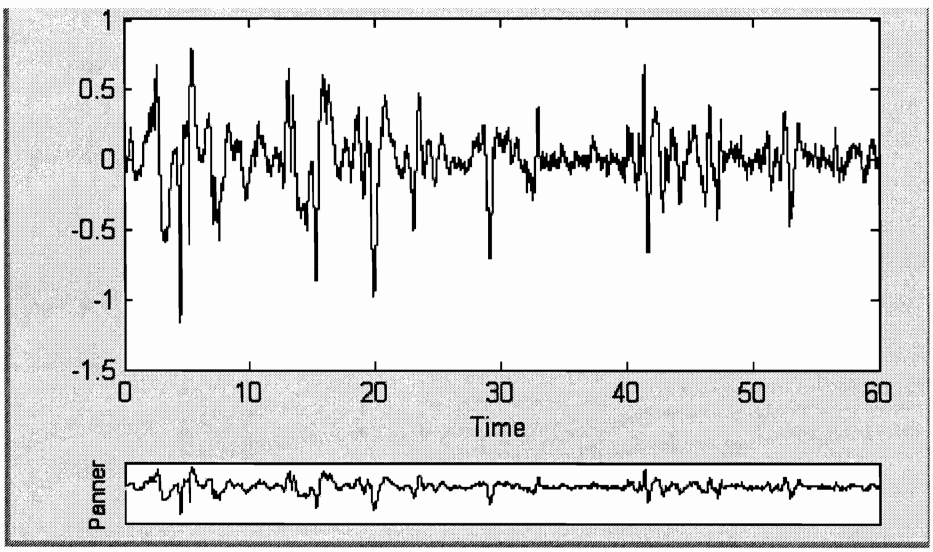

Figure 1.4: Swallowing Waveform

Figure (1.4) illustrates a swallowing waveform acquired by Ponemah system. In order to measure a swallowing event during feeding, surface electromyography (EMG) was used. Electrodes were placed on the skin overlying the muscle and the electrical potential that results from the generation and propagation of an action potential along muscle fiber was amplified. The contraction of the muscles for swallowing was detected by using two EMG electrodes. These two bar electrodes were attached externally to either side of the left digastric muscle. EMG electrodes are very sensitive to movement and are able to detect even slight movement of the muscle (Pickler, 1999). The PDAS received

the signal via EMG probes, which were connected to the Bioelecteric Signal Conditioner, Model 13-6615-58. The input range could vary between 50 μV to 5 V AC full scales. In Figure (1.5) the block diagram of PDAS is shown.

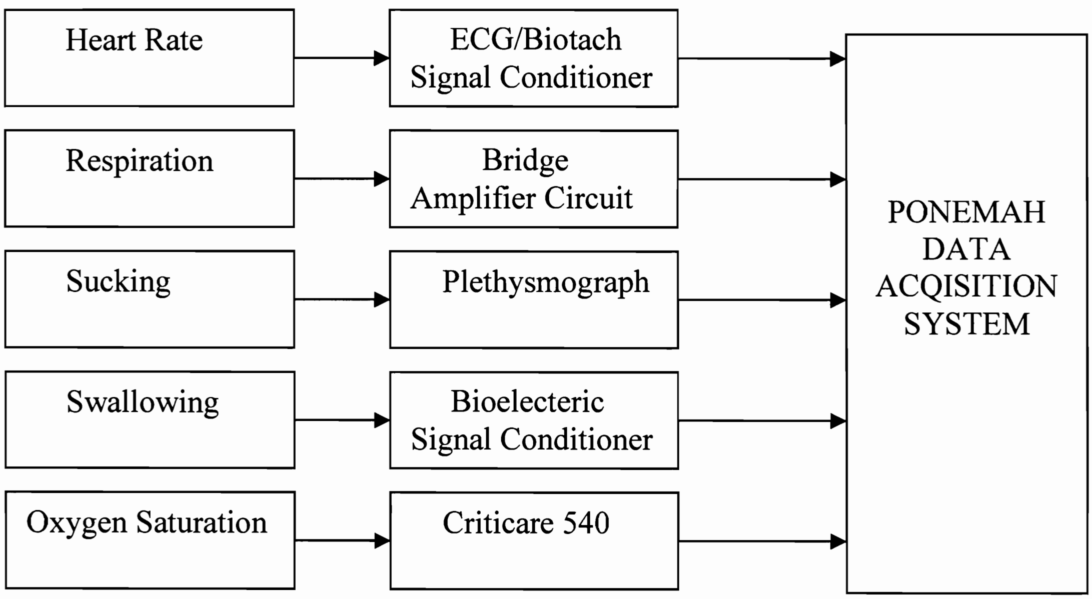

Figure 1.5: The block diagram of PDAS

In this study, in order to detect suck, swallow and breathing activities three different methods have been investigated. In chapter two, the integration of wavelet packet transform and neural network methods will be examined to detect the suck, swallow and breathing events in corresponding signals. In chapter three the spectral analysis of these three signals will be investigated to see whether the frequency content of the signals can provide a practical tool to extract the features of each signal. In chapter four, integration of correlation and matched filtering method will be investigated to detect the activities in each specific waveform.

Wavelet Packet Transform and Neural Networks

2.1. Introduction

The goal of this study is to develop a set of algorithms to detect, identify and classify three physiological measures: respiratory rate, sucking and swallowing activities. The results of this study will be used to predict the readiness of a premature infant for introduction to oral feeding.

Signals can be classified as being deterministic or random (Proakis and Manolakis, 1996; Castanie, 2006). Deterministic signal behavior is predicted by mathematical functions and rules. For example, the future value of a deterministic signal can be predicted if information about its past is available. Periodic signals, like sine waves, are a good example of deterministic signals (Proakis and Manolakis, 1996). Some biosignals like an ECG will be treated as deterministic, even though they are not true deterministic signals. Random or stochastic signals cannot be precisely described by mathematical functions. With most biosignals falling into this category, due to their unpredictability, they can only be expressed in term of statistical properties. Therefore statistical techniques are often used to analyze random signals (Bruce, 2001).

There are several methods to analyze and process different types of signals. These methods include: wavelet analysis, neural network, Fourier Transform, fuzzy logic techniques and expert systems. Choice of a method to process data depends upon the application, each having its own advantages and disadvantages. It is beneficial to use several of them such that quality of one method compensates for the disadvantages of another.

2.2. Background

In this section wavelet transform, wavelet packet transform, neural network and expert systems will be reviewed.

2.2.1 Wavelet Transform

A wavelet is a waveform of limited duration with an average value of zero. Wavelets as the name suggests are waves; wavelets oscillate and their curves yield zero net area. This feature makes a wavelet an appropriate candidate for scaling (dilation) and shifting (translation) to make the time-frequency window flexible (Sarkar *et al*, 2002). A wavelet expressed as the function $\psi_{a,b}(t)$ is acquired by scaling (dilation) and shifting (translation) of the original or mother wavelet, $\psi(t)$.

$$\psi_{a,b}(t) = \frac{1}{\sqrt{a}}\psi\left(\frac{t-b}{a}\right) \qquad a,b \in \Re \ \text{ and } \ a>0 \qquad \text{Eq. (2.1)}$$

a is scale factor and b is position factor. Therefore, $\psi(t)$ should satisfy Equation (4):

$$\int_{-\infty}^{+\infty} \psi(t) = 0 \qquad \text{Eq. (2.2)}$$

In wavelet analysis, a given signal is broken down into shifted and scaled versions of the original or mother wavelet, $\psi(t)$. The approximation of function $f(t)$ by wavelet $\psi_{a,b}(t)$ can be expressed using the coefficients C given by:

$$C(a,b) =< f;\psi_{a,b} > \qquad \text{Eq. (2.3)}$$

where notation <• ; •> defines inner products. Wavelet transform of the function $f(t)$ is defined as:

$$Wf(a,b) = \int_{-\infty}^{+\infty} f(t) \frac{1}{\sqrt{a}} \psi\left(\frac{t-b}{a}\right) dt = f * \xi_a \qquad \text{Eq. (2.4)}$$

where $*$ is the convolution operation and ξ_a is given by:

$$\xi_a(u) = \frac{1}{\sqrt{a}} \psi(\frac{-u}{a}) \qquad \text{Eq. (2.5)}$$

where $u = b - t$.

Due to the complexity and long-time computation, discrete wavelet transform (DWT) and wavelet packet transform (WPT) is used instead of continuous wavelet transform (CWT). Computing the DWT of a signal can be obtained using digital filter banks that are a function of the mother wavelet (Qian, 2002 and Mallat, 1998). This concept is reviewed in more detail in next section. Assuming $a = 2^k$ and $b = 2^k nT$, DWT of signal $p(t)$ using a mother wavelet given by $w(t)$ can be obtained by:

$$WT[p] = \int_{-\infty}^{+\infty} p(t) 2^{-k/2} w(2^{-k} t - nT) dt \qquad \text{Eq. (2.6)}$$

The difference between wavelet analysis and both Fourier transform and Short Time Fourier Transform (STFT) is that the constituent signals are not required to be sinusoidal and the windows are no longer of fixed length. With the Fourier transform the signal values are weighted with an exponential of imaginary and harmonic frequency dependent argument, while in wavelet transform, the signal values are weighted by wavelet functions. When comparing wavelets with sine waves (the basis of Fourier analysis), sinusoids do not have limited duration and extend from minus to plus infinity. In addition, sinusoids are smooth and predictable while wavelets tend to be irregular and

asymmetric. As a result, signals with sharp changes might be better analyzed using an irregular wavelet than a smooth sinusoid.

There are quite a few mother wavelets available in the literature (Mallat, 1998). Most of these mother wavelets were developed to satisfy important properties such as the invetibility and the orthogonal propery. Figure (2.1) illustrates two examples of wavelets: Haar and Daubechi (db2). The optimal choice of the wavelet basis will depend on the application.

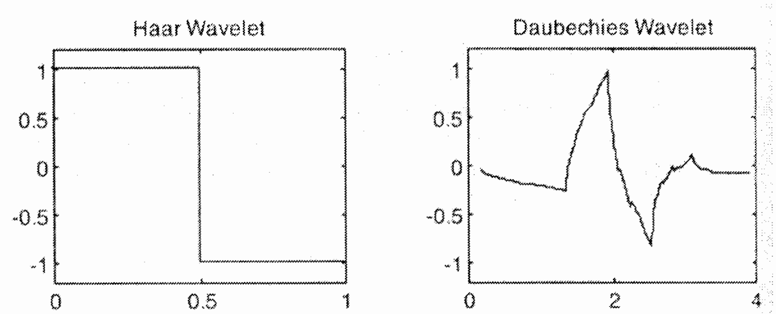

Figure 2.1 : The general shape of two wavelets which are commonly used in wavelet analysis (Enderli *et al*, 2000).

According to Figure (2.1), these wavelets have sharp corners that enable them to match up with local details. One major advantage afforded by wavelets is the ability to perform local analysis; that is, to analyze a localized area of a larger signal.

A disadvantage of STFT is that the width of the window stays fixed during the analysis but in wavelet analysis the signal is decamped by a set of wavelets which are shifted (translated) and scaled (dilated) versions of mother wavelet.

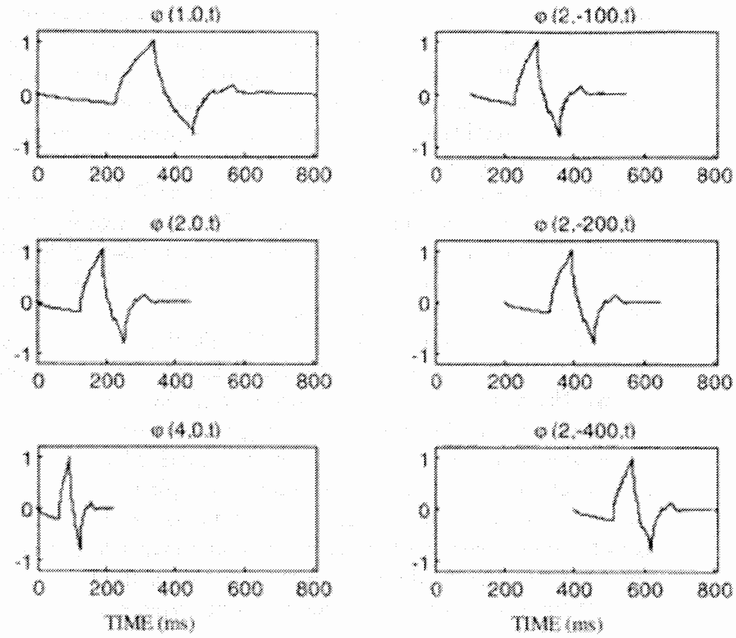

Figure 2.2: Illustrations of the db2 at several scales and positions (Enderli *et al*, 2000).

Figure (2.2) illustrates the db2 wavelet at several scales (dilations) and positions (translations). The upper left-hand corner shows the mother wavelet φ(t). The illustration is denoted using the form φ(scale, delay, t). Thus, φ(t)= φ(1,0,t) and φ(2t-100)= φ(2,-100, t), etc.

2.2.2. Wavelet Packet Transformation (WPT)

Wavelet transform (WT) is a mathematical tool that can decompose a temporal signal into a summation of time-domain basis functions of various frequency resolutions. This simultaneous time-frequency decomposition gives the WT a special advantage over the traditional Fourier transform in analyzing nonstationary signals. Wavelet transform decomposes a signal into successive bands of low to high frequencies using filters that

are a function of the mother wavelet (Mallat, 1998; Kaiser, 1994 and Qian, 2002). The decomposed signal from the low-pass filter is called the approximation or high-scale signal while the decomposed signal from the high-pass filter is called the detail or low-scale signal. This decomposition is obtained by consecutive two channel filtering and downsampling operations applied only on the low frequency band at each stage of the decomposition (Figure (2.3)). The amount of data is doubled after each filtering. The redundancy in the data can be removed by deleting every other data point of output sequence. This operation is called downsampling or decimation by two (Sarkar,2002).

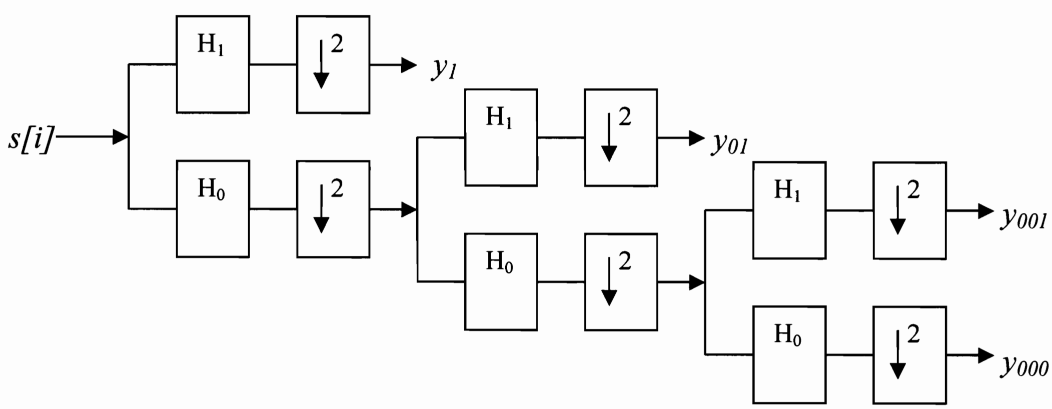

Figure 2.3: Implementation of WT. H_0 and H_1 are low-pass and high-pass filters respectively (Sarkar, 2002)

In Figure (2.3), the subscript "0" and "1" corresponds to low-pass and high-pass filters respectively. Therefore, the symbol y_{00} indicates the sequence after two stages of low-pass filtering and the symbol y_{011} denotes the sequence after one stage of low-pass filtering followed by two consecutive high-pass filters. In order to compute DWT of

discrete signal *s[i]*, the signal will be passed through the filter bank and repeatedly split, filtered and down-sampled. The output of a high-pass filter at each level of decomposition, such as y_1, y_{01} and y_{001}, is the DWT of the signal at that level.

Due to consecutive filtering the output of low-pass filter at each stage, the frequency resolution is rather poor in the high-frequency region (Sarkar, 2002; Walnut, 2002). Wavelet packets can solve this problem by consecutive two channel filtering and downsampling operations applied to both the low frequency and the high frequency band at each stage of the decomposition (Mallat, 1988). Figure (2.4) illustrates this concept.

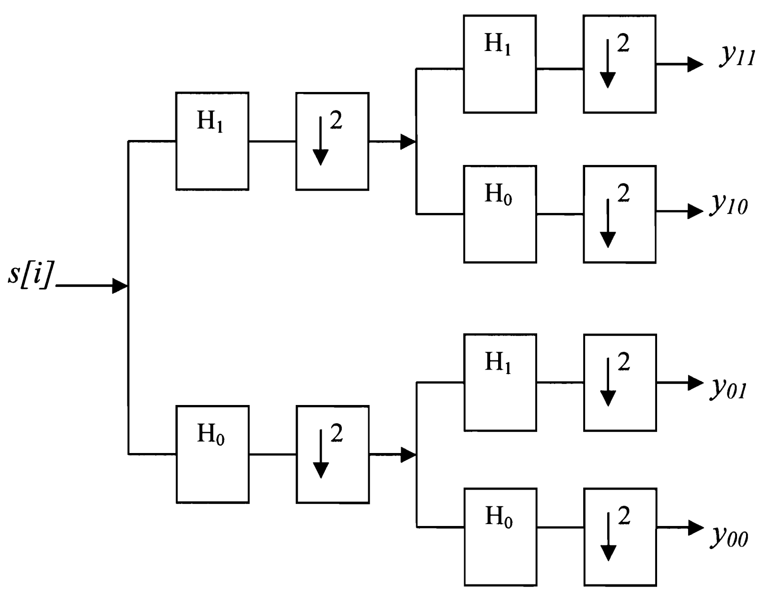

Figure 2.4: Implementation of WPT. H_0 and H_1 are low-pass and high-pass filters respectively (Sarkar, 2002).

The wavelet packet transform (WPT) is an alternative to traditional wavelet analysis and offers a more detailed description of scaling behavior into position, frequency, and scale terms. Therefore, the wavelet packet transform provides a flexible

analyzing function, which is well suited to characterizing signals and includes stationary and nonstationary features. Wavelet packet functions are also localized in time, but offer more flexibility than wavelets in representing different types of signals (Mallat, 1998; Sarakr, 2002).

Yen and Lin (2000) investigated the application of WPT for classification of vibration signals. In their study, the wavelet packet node energy was defined and it was concluded that the node energy representation could provide a more robust signal feature for classification than using the wavelet packet coefficient directly. The wavelet packet energy component can be considered as energy stored in each component of decomposed signal. Therefore, the level of decomposition and number of energy components are case dependent. In this approach, the use of wavelet packet component energies, as a parameter that characterizes the signal is proposed.

2.2.3. Neural Network

Neural network (NN) is an advanced artificial intelligence technology that mimics the brain's learning and decision making process (Rumelhart and McClelland, 1986). Biological neural networks, which are composed of biological neurons, are highly complex and may consist of billions of neurons, each connected to thousands of others. NNs are simpler than biological neural networks. A neural network consists of a number of nodes with "neuron" connections between the nodes. Different types of neurons can be represented in a NN. Neurons are arranged in a layer, and the different layers of neurons, which are connected to other neurons, form the neural network. The manner in which the

neurons are interconnected determines the architecture of the NN. (Guez *et al.*, 1988; Eberhart and Dobbins, 1990). When a training process is being conducted, the neural network learns from the input data and gradually adjusts its neurons to reflect the desired outputs (Haykin, 1999; Looney, 1997).

NNs are simply mapping functions that map values of one or more inputs to single or multiple outputs (Hornik *et al.*, 1990). In this sense, they are similar to ordinary transfer functions that map inputs to outputs. However, their structures provide a great degree of flexibility in mapping that makes them distinguishable from ordinary transfer functions. Specifically, it is not necessary to know the form of the function governing the inputs to a NN to map them to desired outputs. In addition, NNs can adapt to changes in input and output. That is, if the inputs change, the elements of the ANN can be adjusted to continue to map the new inputs to the same output and vise versa. This feature can be highly advantageous in signal processing and pattern recognition(Hornik *et al.*, 1990).

NNs are well suited for variety of biosignals processing applications and may be used as a tool for nonlinear statistical analysis (Eugene, 2001). They are often used for pattern recognition and classification (Looney, 1997). In addition, NNs have been shown to perform faster and more accurately than conventional methods of signals, which are highly complex or contain noise especially in robotic and control area (Guez *et al.*, 1988). NNs also have the ability to solve problems that have no algorithm solution. In other words, they are particularly useful in cases where the problem to be solved is intractable and development of an algorithmic solution is difficult (Hornik *et al.*, 1990). In signal processing area, the efficacy of NNs is mostly evident when they are used in conjunction

with other signal processing techniques such as fuzzy logic or wavelet transform (Akay, 2000).

2.2.4. Expert System

An expert system is a computer program designed to simulate the problem-solving behavior of a human who is an expert in a narrow domain or discipline (Gallant, 1993 ; Klein and Methlie, 1995). Firebaugh defines an expert system as:

"Expert systems are a class of computer programs that can advise, analyze, categorize, communicate, consult, design, diagnose, explain, explore, forecast, form concepts, identify, interpret, justify, learn, manage, monitor, plan, present, retrieve, schedule, test and tutor. They address problems normally thought to require human specialists for their solution." (Firebaugh, 1988)

According to Figure (2.5), an expert system is normally composed of (Klein and Methlie, 1995) :

- Knowledge base (information, heuristics, etc.)
- Inference engine (analyzes the knowledge base)
- User interface (accepting inputs, generating outputs) .

The path that leads to the development of expert systems is different from that of conventional programming techniques. The concepts for expert system development come from the subject domain of artificial intelligence (AI), and require a departure from conventional computing practices and programming techniques. A conventional program consists of an algorithmic process to reach a specific result while an AI program is made

up of a knowledge base and a procedure to infer an answer. Expert systems are capable of delivering quantitative information as well as heuristics to interpret qualitatively derived values, or for use in lieu of quantitative information (Gallant, 1993; Klein and Methlie, 1995).

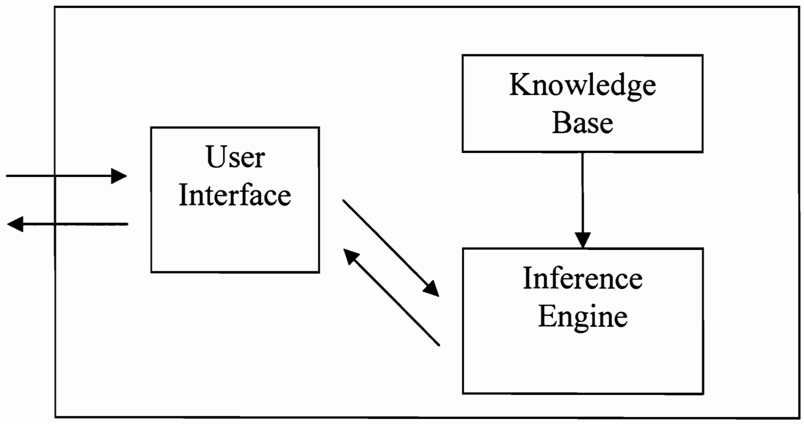

Figure 2.5: Expert System Architecture

One of the most powerful attributes of an expert system is the ability to explain reasoning. Since the system remembers its logical chain of reasoning, a user may ask for an explanation of a recommendation and the system will display the factors it considered in providing a particular recommendation. This attribute enhances user confidence in the recommendation and acceptance of the expert system (Medsker, 1994).

One of the fundamental limitations of expert systems is that the experts do not usually think in term of rules. Therefore, in these cases the expert system does not really mimic the way that a human expert thinks and reasons. Another limitation is knowledge acquisition. Although expert system development tools are widely available and becoming more effective, extensive effort is still required to acquire data from human

experts and written materials. In addition, for real-world applications, management of the development process is difficult and time-consuming (Medsker, 1994).

2.3. Method

To predict the appropriate time to introduce bottle-feeding to premature infants, the heart rate, oxygen saturation, respiratory rate, sucking and swallowing activities are measured. The purpose of this research is to detect, identify and classify respiration, sucking and swallowing waveforms independently and in relation to each other to extract the ratio of suck-swallow-breathe patterns. This can determine if the premature infant has reached the point at which coordinating of these processes has occurred.

In this study, 97 babies were enrolled. For each baby, several feedings were observed and physiological measurements were recorded using PDAS and Matlab-based data acquisition system. However, due to the poor quality of the swallowing signal most of the babies recorded, there are just two babies that have all three signals in an acceptable quality (baby #81, 10th feeding and baby #87, seventh feeding). At the beginning of this study, it was not known which babies would have acceptable data. Therefore, the respiration signal of baby #97's, seventh feeding was selected to perform preliminary studies. But later on, (in next chapters) baby #81, 10th feeding and baby #87, seventh feeding was selected for investigation due to the satisfactory quality of all three signals.

The general system architecture of this approach is discussed in the following sections. The leading steps involved in this process are as follows:

- Data extraction
- Segmentation , feature extraction and classification of each signal
- Analyzing the relationship between signals

2.3.1. Data Extraction

The digitized data from all channels are directly stored as one file to the resident hard disk drive. Therefore, the first step was to extract the data from each channel. The ultimate output of this task includes three arrays: respiratory data, swallowing data and sucking data (Figure (2.6)). These arrays can be saved separately as data files.

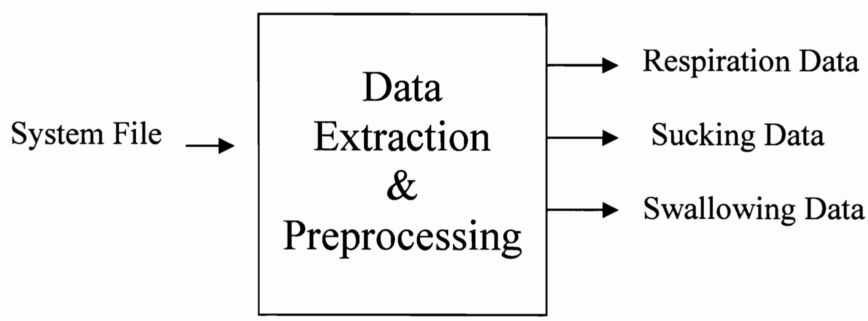

Figure 2.6: Data extraction and preprocessing task.

2.3.2. Segmentation, Feature Extraction and Classification

In order to detect an activity in a specific waveform, it was necessary to divide that waveform into smaller frames (windows), process each frame separately and move to the adjoining frame which had an overlap with the previous frame. This procedure is referred to as segmentation.

To classify each frame, first, it was necessary to characterize it. The feature extraction task was to convert each frame to some type of parametric representation which describes that frame uniquely. In this application using wavelet packet energy nodes (see section 2.2) as parameters was proposed. In next step (classification of each frame), the time of occurrence and length of a specific activity were determined. For example, for the swallowing waveform it needed to be determined whether the swallowing had occurred in the current frame or not. To accomplish this task, the extracted features (parameters) for the current frame were fed as input vector to a neural network with a feed forward architecture that used backpropagation algorithm (for training/adjustment of weights).

The neural network was trained to classify the input vector. The output of this neural network was either one (the activity has happened) or zero (the activity has not happened). If the activity had occurred in the current frame, the time of occurrence and length of the activity were stored in a matrix called the occurrence matrix. The first row was the time of occurrence and the second row was length of the activity. For instance, for a frame of sucking waveform starting at 100^{th} sample with a length of 1003 samples, if the output was close to one (sucking has occurred), it can be assumed that the baby had sucked at t=100/1000=0.1 s of data recording and it had lasted for 1.003 seconds (recall that sampling rate in this application is 1 KHz)

When classification was accomplished for the current frame the adjoining frame was classified and this procedure continued along the waveform. Therefore, at the end of classification of whole waveform, the occurrence matrix was filled out. An example of

the occurrence matrix for the sucking waveform is presented in Equation (2.7). For example the first column indicates that the infant has sucked at the 5^{th} second of the feeding and it had lasted for 0.835 seconds.

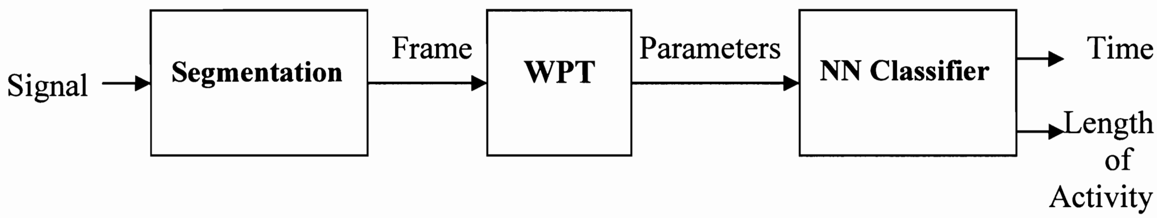

Figure 2.7: Segmentation, Feature Extraction and Classification Task.

$$\begin{bmatrix} 5 & 10 & 35 & 50 & \ldots & 120 \\ 835 & 1002 & 800 & 531 & & 1200 \end{bmatrix} \quad \text{Eq. (2.7)}$$

After classification of the current frame, the adjoining frame (with an overlap with the previous one) was processed and this procedure continued for the whole waveform. Each signal had its own neural network classifier. Therefore, at the end of the classification process of all three signals, three occurrence matrices were filled out. These matrices were utilized in the next step to analyze t

he relationship between the signals. Figure (2.7) shows the block diagram of this step.

2.3.3. Analyzing the Relationship between Signals

In this step, the occurrence matrices created in previous step were loaded into an analyzer to determine the SSB ratio (suck-swallow-breathe ratio) based on the physiological measurements for the current observation (Figure (2.8)). After determining

the SSB ratio, the baby was assessed and categorized according to group. These categories were predefined by the subject expert and were loaded as an input into the analyzer. For example, if the SSB ratio is 1:1:1 the baby falls to Class 1, which means the infant has established a well coordinated suck-swallow-breathe pattern. In general, if the infant's SSB ratio falls between $x_1:y_1:z_1$ and $x_2:y_2:z_2$ then the baby is in class C (x_1 and x_2 are the number of sucks, y_1 and y_2 are the number of swallows and z_1 and z_2 are the number of breaths).

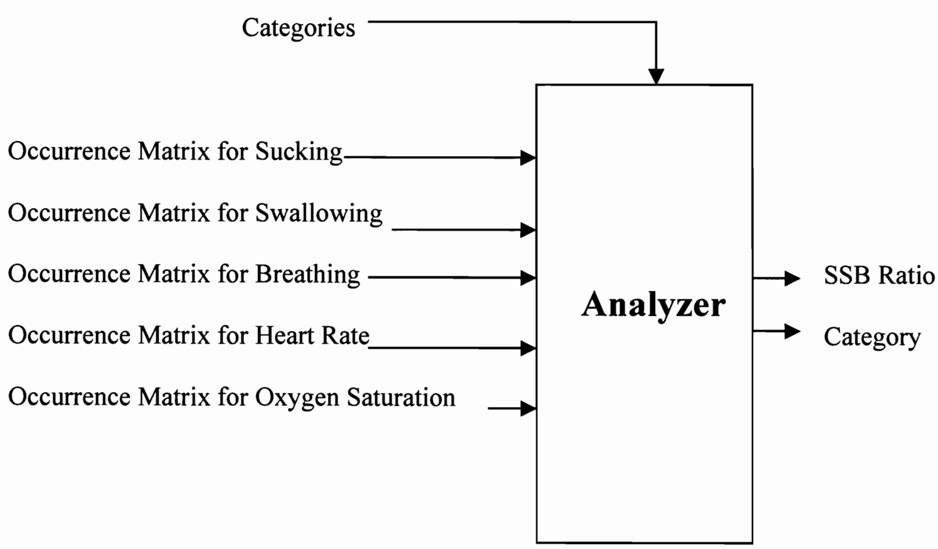

Figure 2.8: Analyzing task.

The analyzer will be implemented using neural network and expert systems. These two methods have their own advantages and disadvantages. It was therefore beneficial to use both of them as complementary elements of a general data processing system, taking advantage of the synergy between them such that quality of one method

can compensate for the disadvantages of another one. Figure (2.9) illustrates the overall system architecture.

2.4. Implementation

To implement the software of this system, Matlab (version 7) was used. Matlab (abbreviation for MATrix LABoratory) is a high-level programming language and interactive environment created by The MathWorks, Inc. MATLAB is an interactive, matrix-based system for specific scientific and engineering computations. It provides a high performance, numerical computing environment that enables the user to preform numeric computation and visualization. The programming language is very straightforward due to the wide range of commands and functions that permit users to solve and analyze difficult computational problems from science and engineering without programming in a general purpose language (Matlab User's Guide, 2000). In in this study Matlab sofware is used because:

- Matlab allows easy matrix manipulation, plotting of functions and data and the implementation of algorithms (Matlab User's Guide, 2000).
- Matlab includes a number of subject specific toolboxes such as Neural Network Toolbox, Signal Processing Toolbox and Wavelet Toolbox. These provide the user with very useful built-in functions and supplied m-files to perform numeric computation in a short period of time (Matlab User's Guide, 2000).
- Matlab also has functions that allows the user to intregate with external apllications and languages such as C, C++ and Java (Matlab User's Guide, 2000).

- Matlab includes mathematical functions for linear algebra, statistics, Fourier analysis and filtering (Matlab User's Guide, 2000).

Next, the implementation of Data Extraction, Segmentation, Feature Extraction and Classification of each signal will be explained. This approach failed in feature extraction and classification of the respiration signal. Therefore, analysis of the relationships between the signals (the third step of the overall system architecture) was not implemented.

2.4.1. Implementation of Data Extraction

As mentioned previously, for each feeding, data was stored in a file with the extension .DAQ and can be extracted using the *daqread* command in Matlab. The following set of commands will result in extraction of suck, swallow and respiration data of seventh feeding for baby # 97.

```
>> swallow_data = daqread('B09701-07.daq',...
        'Channels', [3]);

>> suck_data = daqread('B09701-07.daq',...
        'Channels', [4]);

>> respiration_data = daqread('B09701-07.daq',...
        'Channels', [1]);
```

where 'B09701-07.daq' is the data file name. In this application, Channel1, Channel3, and Channel4 are assigned for respiration, swallowing and sucking data respectively.

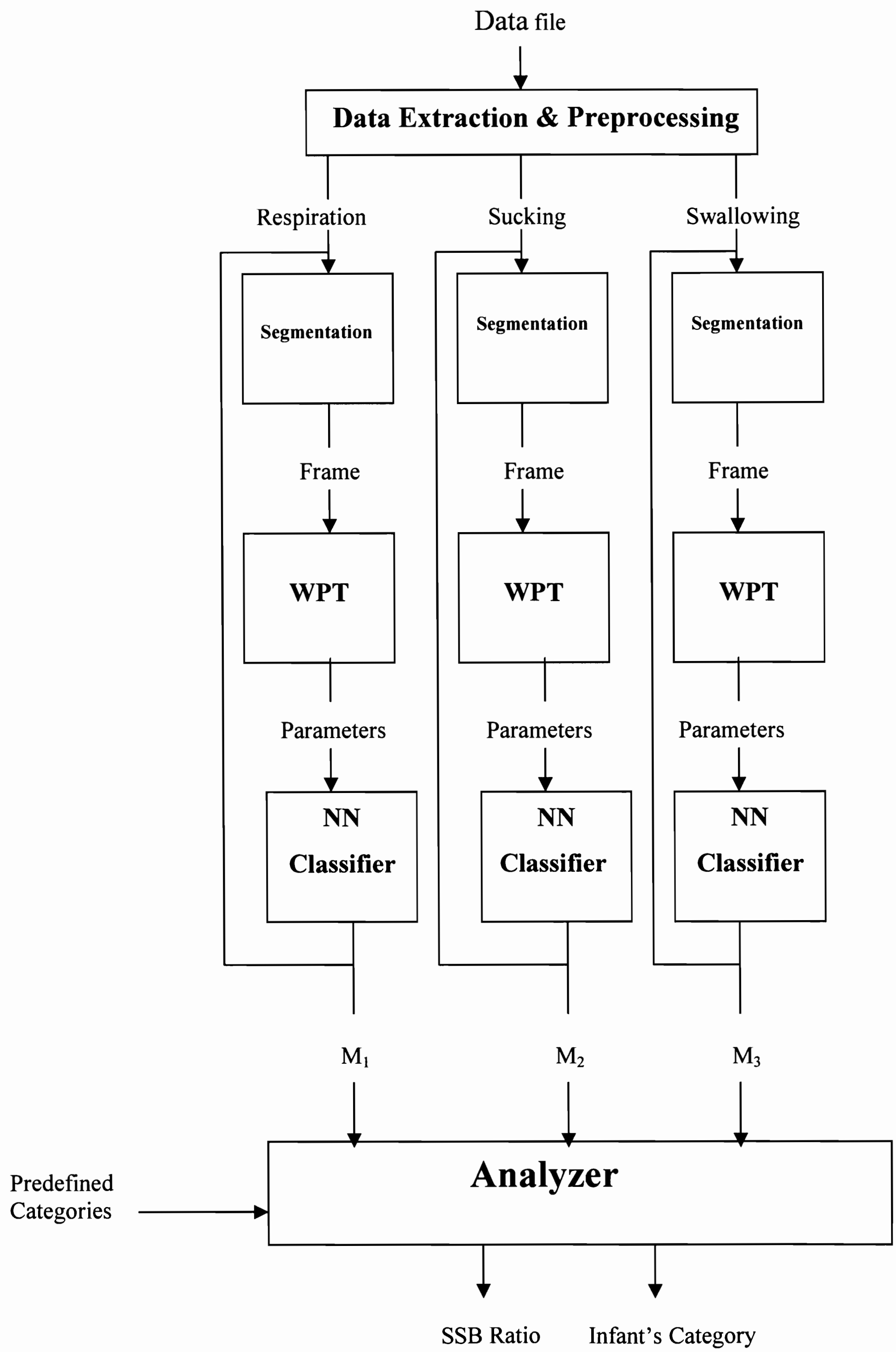

Figure2.9: The overall system architecture of the first approach (integration of WPT and NNs) where M_i is the corresponding occurrence matrix.

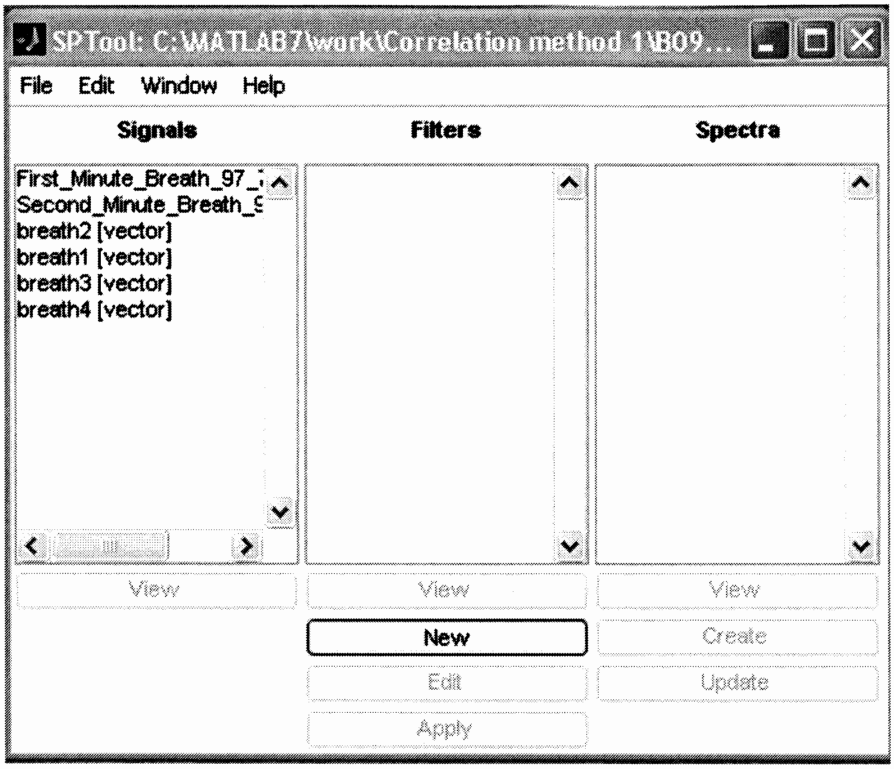

Figure 2.10: Signal Processing Toolbox in Matlab

After data extraction, each signal was divided into one minute segments loaded in *SPTool* (signal processing tool) environment using the following command.

>> SPTool

This command will open a graphical user interface which enables the user to import, analyze, export and manipulate signals, filters, and spectra (Figure (2.10)).

2.4.2. Implementation of Feature Extraction

In this study, the parameters used to characterize each frame of a waveform were wavelet packet energy nodes. Matlab provided a very user-friendly environment for the manipulation of wavelet packets using Wavelet Tool Box.

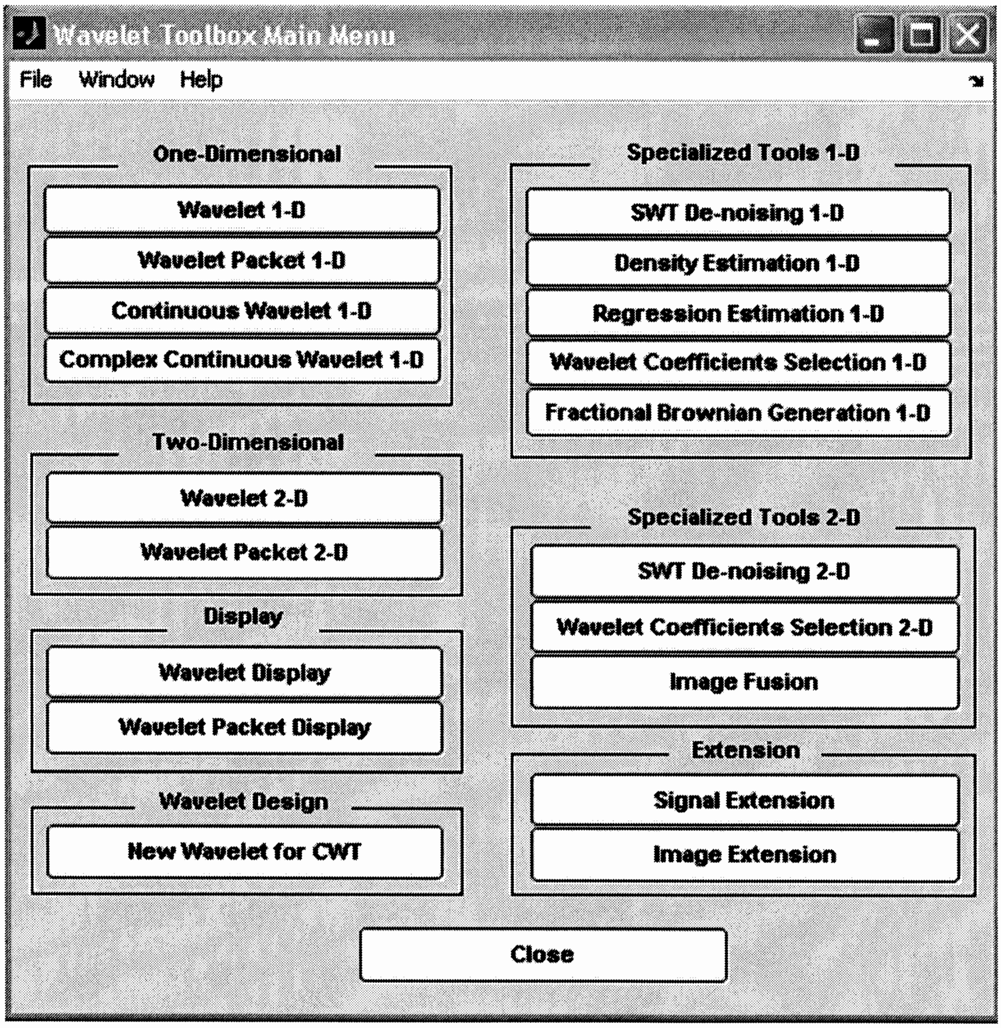

Figure 2.11: Wavelet Toolbox in Matlab

The following command the user will start the Wavelet Toolbox graphical user interface tools (Figure (2.11)).

```
>> wavemenu
```

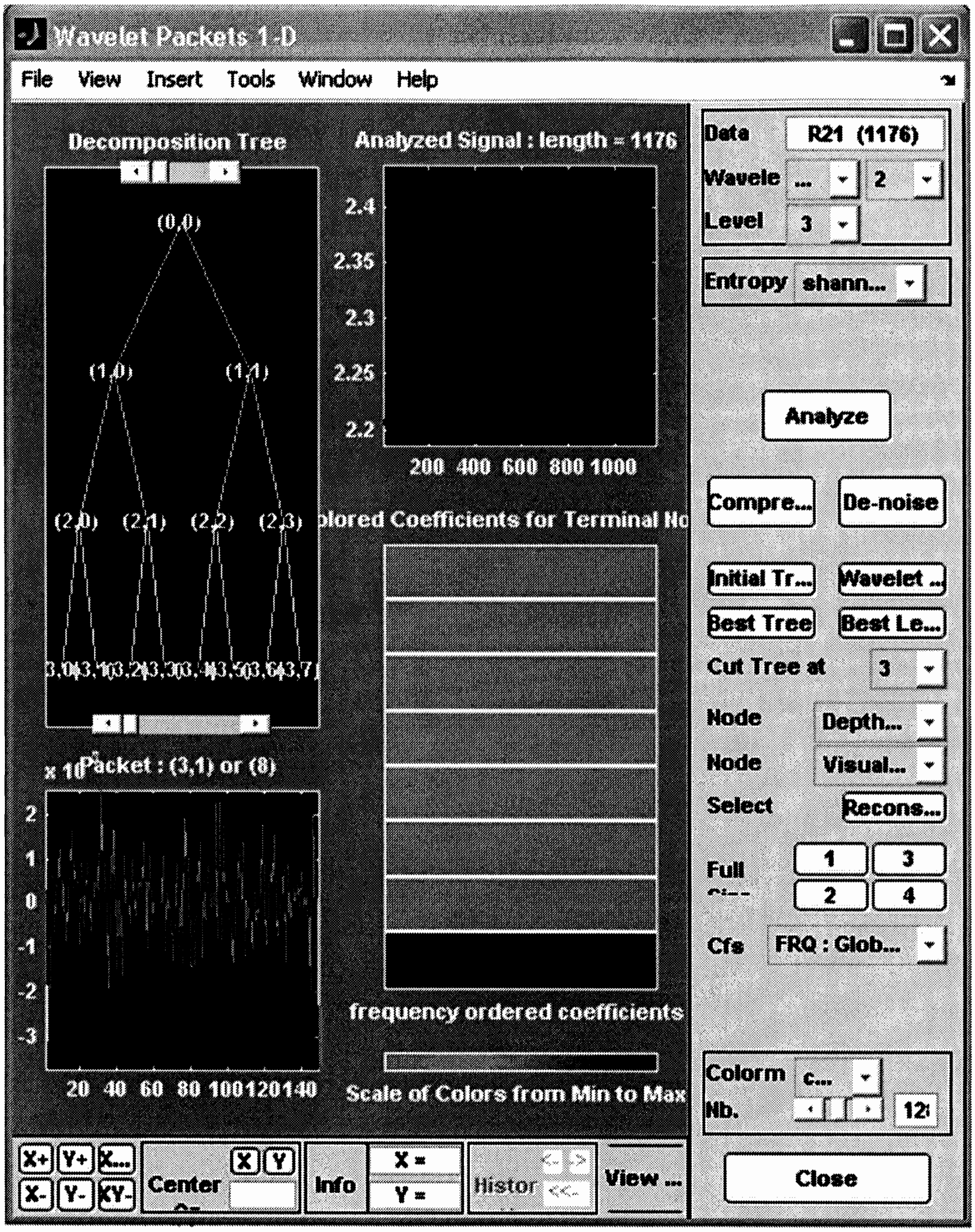

Figure 2.12: Wavelet Packet Transform

Clicking on *wavelet packet 1-D* opens a window allowing the user to perform wavelet packet transform using different methods and up to desired level (Figure (2.12)). In this application db2 family of wavelets are used to perform the wavelet packet transform up to third level (8 parameters).

To calculate the parameters corresponding to each frame (wavelet packet energy nodes), a user-defined function named *parameters* is used. This m-file is included in Appendix 1. Therefore the following command will compute the parameters corresponding to one frame.

>> P=parameters (frame)

where *P* is an vector with eight elements. This vector will be loaded as input to NN classifier.

2.4.3. Implementation of Classification

As the first attempt, a small neural network with three layer (17,10,1 neurons in each layer respectively) and feed forward architecture was established. The network has eight inputs (parameters) and one output (activity or non-activity). This neural network (named *net_8_1*) was trained using *trainrp* (resilient backpropagation) algorithm (see Appendix 1). To train, seven breath patterns and ten non-breaths patterns were selected from the first minute feeding of baby #97. The parameters of each pattern were extracted using user-defined function *parameters*. These parameters were combined together in a 8X 17 matrix named *train_set_8*. The target set using to train the neural network was *target_set_8* (see Table (2.1) and Equation(2.7)).

Generally, it is beneficial to scale the inputs and targets of a NN before training (Neural Network Toolbox User's Guide, 2000). As a result of scaling, inputs and targets always fall within a specified range. One approach for scaling network inputs and targets is to normalize the mean and standard deviation of the training set. This procedure is

implemented in Matlab by a built-in function named *prestd*. This function normalizes the inputs and targets in a way that the mean will have zero and standard deviation will have a value of one.

.

2.4.5. Implementation of Segmentation

In this application segmentation (windowing) is the combination of stretching and moving the frame. To explain the algorithm, the respiratory signal is considered. The minimum and maximum length of a breath is 300 samples and 2000 samples respectively. The algorithm to detect a breath in whole respiration signal is as the following:

1. Set the smallest_window as the minimum size of a breath (300 samples).

2. Set the widest_window as the maximum size of a breath (2000 samples)

For the whole respiration signal

3. Set the window_size as the smallest _window

4. Read the current frame (the size of the frame is window_size)

5. Extract the feature using WPT

6. Feed the parameters to the NN

7. If a breathe occurs in this frame

7.1 Save the time and the length in occurrence matrix

corresponding to the respiration

7.2 Move to the end of the current frame

7.3 Go to 3

8. Stretch the window for 20 samples (window_size would be increased by 20 samples) and Go to 4

9. If the window_size is equal to the widest_window

9.1 Move the window for 20 samples

9.2 Go to 3

The implemented algorithm can be found in Appendix 1 as a user-defined function named *scan.*

2.5. Results

Using subject expert opinion, ten non-breath patterns and seven breath patterns of seventh feeding for baby #97 were selected from the first minute of feeding to train the network (Table (2.1)). The shapes of these patterns are available in Appendix 1. The parameters of each pattern were extracted using user-defined function *parameters.* These parameters were combined together in a 8X 17 matrix named *train_set_8* and the expected outputs (targets) for training data was associated with a 1X 17 matrix named *target_set_8* (Equation (2.8)).

Table 2.1: Training data

Non-breath patterns	R60	R70	R30	R50	R100	R130	R140	R220	R230	R240
Breath patterns	R11	R41	R111	R91	R21	R121	R161			

Table (2.2) shows the parameters for each pattern where E_{ij} corresponds to the parameters of R_{ij}. The network was trained with normalized *train_set_8* and *target_set_8*.

train_set_8= [E11 E41 E111 E91 E21 E121 E161 E60 E70 E30 E50 E100 E130 E140 E220 E230 E240]

target_set_8=[1 1 1 1 1 0 0 0 0 0 0 0 0 0 0] Eq. (2.8)

Table 2.2: Parameters corresponding to training data

E11	**E41**	**E111**	**E91**	**E21**	**E121**	**E161**
4.3824e+003	3.1535e+003	4.3996e+003	5.4773e+003	6.5612e+003	4.2727e+003	6.4447e+003
8.7488e-005	5.1258e-005	1.0056e-004	1.2272e-004	1.3923e-004	1.2507e-004	1.4723e-004
5.3518e-005	4.1853e-005	7.3602e-005	7.9107e-005	8.0230e-005	8.1954e-005	8.6843e-005
7.3210e-005	4.4466e-005	6.3358e-005	8.1571e-005	9.2704e-005	7.3941e-005	7.7157e-005
6.1194e-005	2.7550e-005	5.3318e-005	7.5250e-005	7.1799e-005	5.3238e-005	6.4720e-005
6.0620e-005	3.0857e-005	6.2961e-005	7.7040e-005	6.6026e-005	5.8256e-005	7.4975e-005
5.4138e-005	3.6879e-005	5.6132e-005	6.1004e-005	7.7582e-005	8.0701e-005	7.5661e-005
4.4692e-005	4.1896e-005	7.2512e-005	6.6153e-005	7.2643e-005	5.4870e-005	6.9731e-005
E60	**E70**	**E30**	**E50**	**E100**	**E130**	**E140**
6.7140e+003	6.9128e+003	3.4628e+003	5.5914e+003	4.5906e+003	5.3063e+003	4.7916e+003
1.3894e-004	1.2697e-004	8.0797e-005	3.2235e-004	9.9532e-005	2.2046e-004	1.8594e-004
7.9430e-005	9.1301e-005	6.0008e-005	1.0251e-004	6.1597e-005	9.6397e-005	7.2748e-005
8.2729e-005	9.1252e-005	5.8050e-005	8.5435e-005	6.6885e-005	9.5623e-005	7.6050e-005
8.5498e-005	6.2944e-005	4.4027e-005	6.1166e-005	8.8619e-005	8.2336e-005	6.4966e-005
7.1741e-005	5.2695e-005	5.4104e-005	8.6752e-005	7.9931e-005	8.1078e-005	8.1308e-005
9.1352e-005	6.7350e-005	5.6280e-005	9.3752e-005	7.3985e-005	6.9435e-005	9.1990e-005
7.0986e-005	7.7244e-005	4.2225e-005	7.1518e-005	7.4531e-005	6.0782e-005	7.0026e-005
E220	**E230**	**E240**				
6.0824e+003	2.7762e+003	5.9387e+003				
1.2893e-004	4.4830e-005	1.0482e-004				
7.6520e-005	3.9414e-005	6.3440e-005				
6.7472e-005	3.9156e-005	8.9791e-005				
5.8973e-005	2.7871e-005	5.9643e-005				
7.1815e-005	3.0253e-005	7.6157e-005				
7.5974e-005	2.8929e-005	8.5527e-005				
6.3928e-005	2.5384e-005	6.5322e-005				

A set of five breaths and three non-breaths was selected using subject expert opinion to test the neural network. Shapes of these signals are available in Appendix 1. Table (2.3) and Table (2.4) represent the testing data and their corresponding parameters respectively.

Table 2.3: Testing data

Testing Data	R171	R181	RR11	R80	R190	R200	R210	R151

Table 2.4: Parameters corresponding to testing data

E171	E181	ER11	E80	E190	E200	E210
4.9686e+003	4.4551e+003	5.2968e+003	9.5971e+003	6.2922e+003	1.2239e+004	1.1908e+004
8.2912e-005	5.0626e-005	6.8586e-002	1.6212e-004	1.7770e-004	1.8441e-004	2.3218e-004
6.3535e-005	5.7989e-005	5.4862e-003	1.1386e-004	9.7232e-005	1.3537e-004	1.5774e-004
7.2309e-005	5.1891e-005	2.9827e-002	1.0419e-004	8.6094e-005	1.6982e-004	1.9279e-004
4.3565e-005	4.8391e-005	1.9202e-001	1.0143e-004	7.9997e-005	1.1372e-004	1.3460e-004
3.5675e-005	5.2147e-005	4.5748e-001	8.3954e-005	9.4192e-005	1.5633e-004	1.4996e-004
6.3771e-005	5.2050e-005	1.2739e-001	1.0468e-004	1.0598e-004	1.3110e-004	1.6407e-004
4.8233e-005	4.4236e-005	2.5844e-001	1.0423e-004	1.0811e-004	1.3691e-004	1.8828e-004

E151
4270.6
8.339e-005
6.0125e-005
5.9429e-005
4.8109e-005
6.3845e-005
4.5561e-005
4.9585e-005

For evaluation of the NN, first the network was tested with the training data to see whether the network is trained successfully or not. Next the network was simulated with testing data. The results are shown in Table (2.5) and Table (2.6) respectively. O_{ij} corresponds to output of NN when it is simulated by E_{ij}.

Table 2.5: The Output of NN when simulated by training data

O11	O41	O111	O91	O21	O121	O161	O60
1.0671	1.0672	1.0672	1.0672	1.0670	1.0674	1.0676	0.0532
O70	**O30**	**O240**	**O100**	**O130**	**O140**	**O220**	**O230**
0.0526	0.0526	0.0530	0.0524	0.0527	0.0530	0.0532	0.0537
O50							
0.0526							

Table 2.6: The Output of NN when simulated by testing data

O80	O190	O200	O211	O171	O181	OR11	O151
0.3242	0.2042	0.2542	0.7897	0.1857	1.0672	-0.0629	0.59245

In other to test the segmentation procedure, part of signal was selected (Figure (2.13)) and function *scan* was run for this portion of waveform. The result is the following occurrence matrix.

$$occurrence = \begin{bmatrix} 1 & 821 & 1651 & 2526 & 3541 \\ 820 & 830 & 875 & 1015 & 1035 \end{bmatrix} \qquad \text{Eq(2.9)}$$

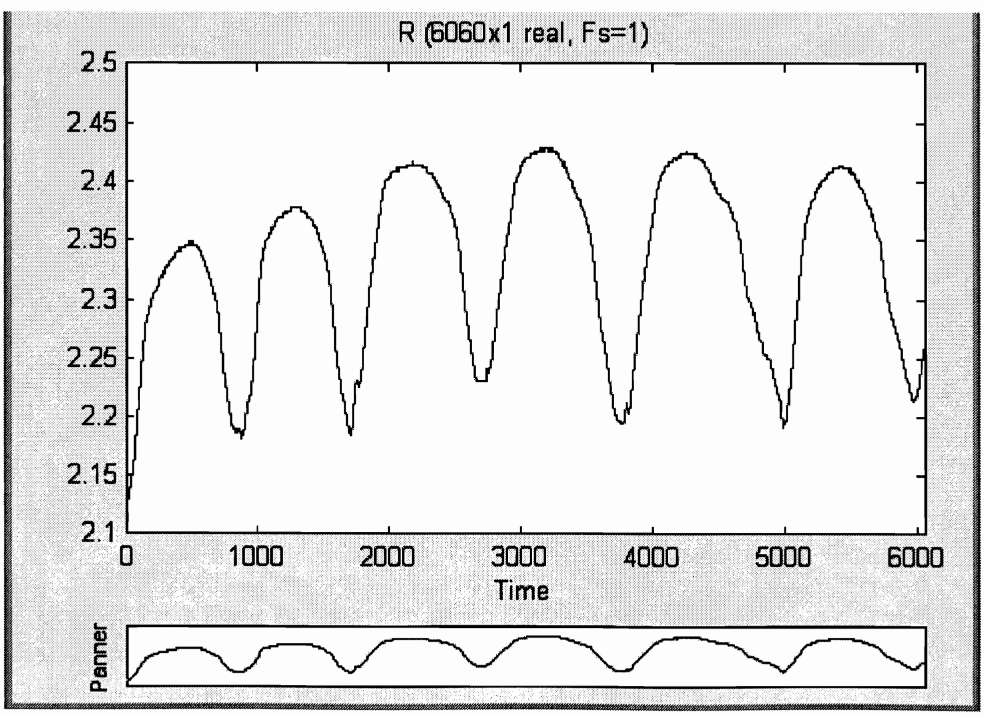

Figure 2.13: Part of respiratory signal selected to test.

2.6. Discussion

As the Table (2.5) shows, the output of the NN for training data is acceptable (it is close to one for breath patterns and close to zero for non-breath patterns). However, according to Table (2.6) the output of NN is not acceptable for testing data. It seems that the parameters were not efficient for classification. For example, according to Figure (2.14), RR11 and R11 are very similar but with different size. In fact, RR11 is build by resampling of R11 with different sampling rate. Knowing that the NN was trained for the parameters of R11, output of NN was expected to be close to one. However, according to Table (2.6) the output was -0.0629.

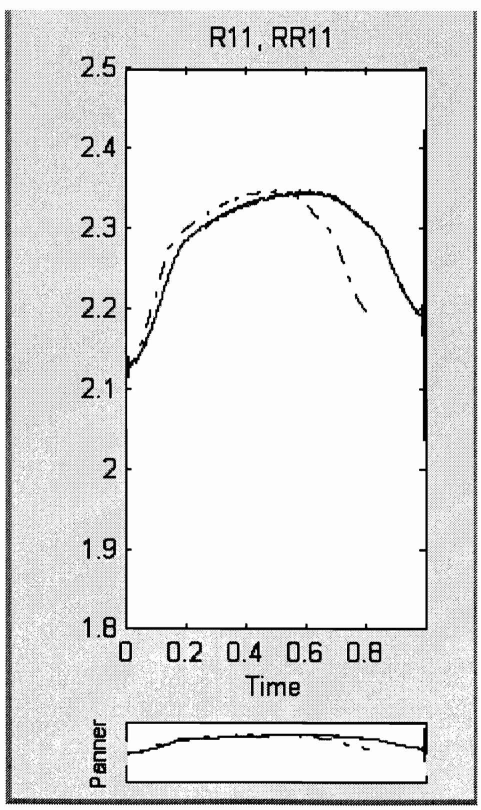

Figure 2.14: R11 and RR11

R151 and R11 are another example for this issue. As Figure (2.15) illustrates, R151 is actually R11 with a larger size. In fact, R151 is the same pattern as R11 with different size. Recalling that The NN was trained for R11, the output for R151 was expected to be close to one but according to Table (2.5) it was not as expected. Therefore, it can be concluded the feature extraction method was very sensitive to the length of the patterns.

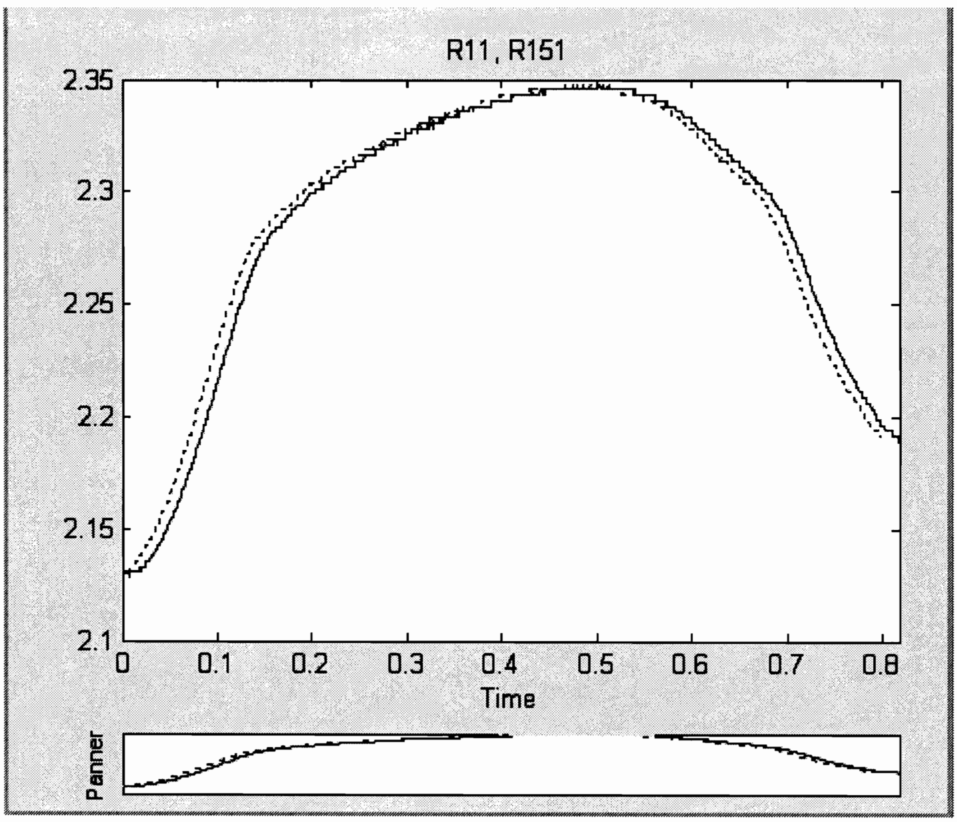

Figure 2.15: R11 and R151

As Figure (2.16) shows R171 is very similar to R41 but with different size. R41 was part of the training data set. Therefore, simulating the NN with the parameters of R171 must result in an output which is close to one. But the result does not confirm this (Table (2.5)).

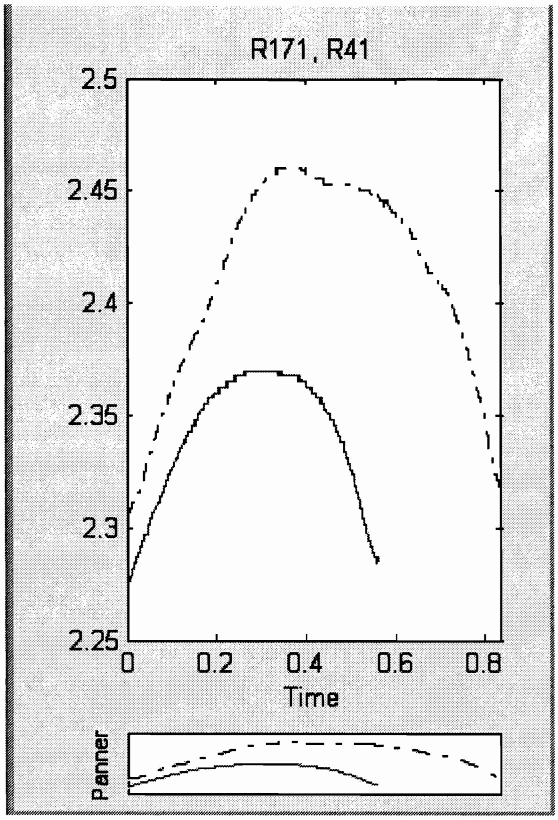

Figure 2.16: R171 and R41

To evaluate the detection procedure, according to Equation (2.9), a breath has been detected at t=2.526s that has lasted for 1.015 s. This is shown approximately in Figure (2.17). Based on the subject expert, this pattern can not be considered as a breath and therefore it questions the validity of detection. According to Equation (2.9), a breath is detected at t=3.541s with a length of 1.035s and is shown in Figure (2.18). However, the subject expert does not agree with this detection.

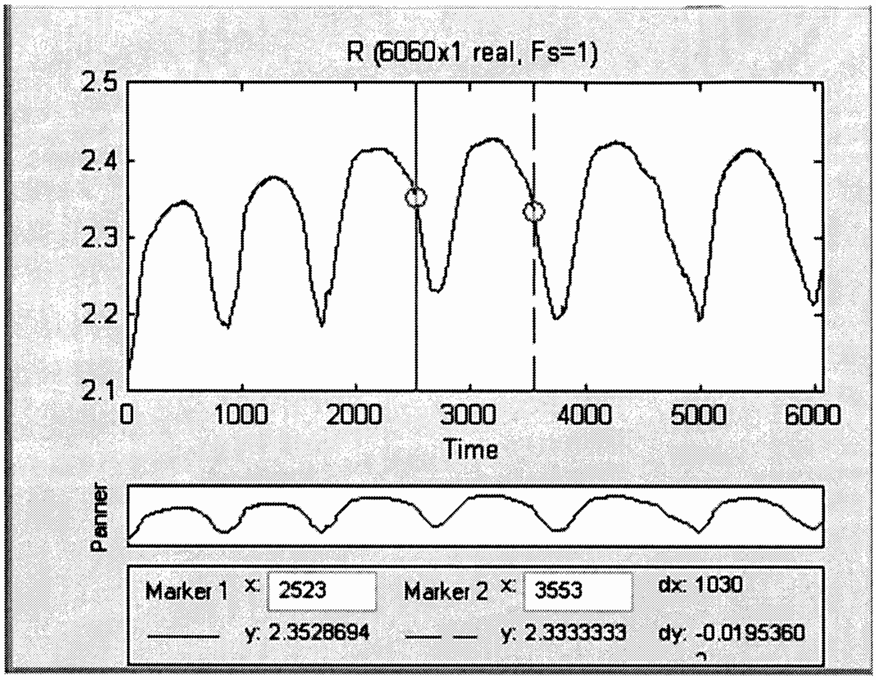

Figure 2.17: A non-breath is detected as a breath

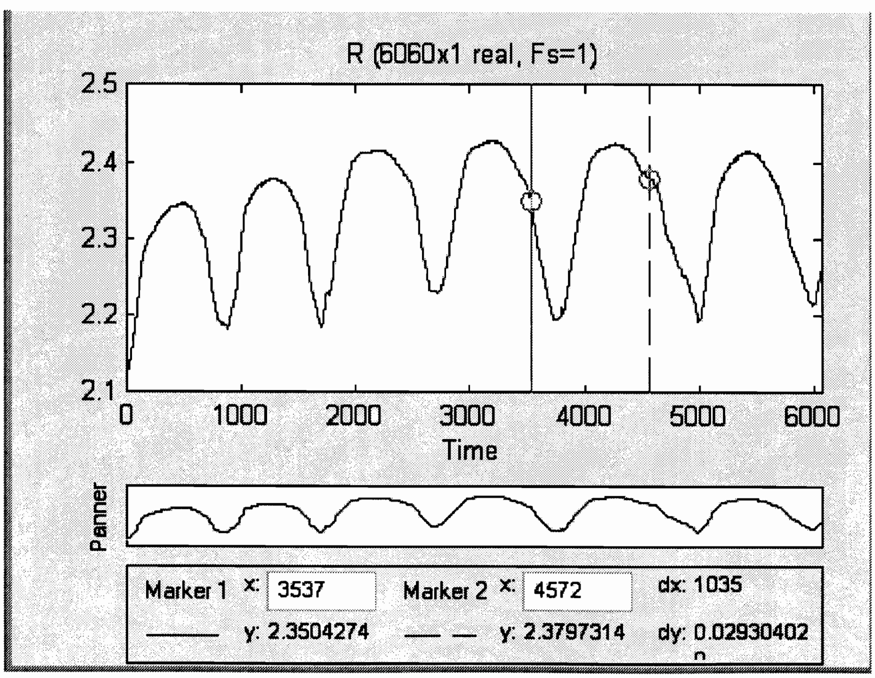

Figure 2.18: A non-breath pattern is detected as a breath

2.7. Conclusion

Feature extraction is generally considered a data mapping procedure. Regardless of how data transformation is implemented the feature extraction algorithm must be designed to preserve the information of interest for a special problem.
In this study, integration of WPT and NN failed due to the inefficiency of the feature extraction method. In other words, wavelet packet energy nodes do not provide a good feature extraction tool in this specific application resulting in failure of classification by NN.

Wavelet packet energy nodes are formed based on the existing decomposition coefficients. Although this method is compact and avoids the use of a large number of coefficients, it fails to emphasize localized time property. In order to reveal the localized time property and shape differences of the waveforms, another category of feature extraction method that directly uses the decomposition coefficients may be investigated.

Wavelet packet energy nodes are formed based on the existing wavelet packet decomposition coefficients. Although this method is compact and avoids the use of a large number of coefficients, it fails to emphasize the localized time property. In order to reveal the localized time property and shape differences of the waveforms, another category of feature extraction method that directly uses the decomposition coefficients may be investigated.

Spectral Analysis

3.1. Introduction

In chapter 2, the combination of WPT and NN was examined to see whether it could be applied as an integrated system to detect suck, swallow and breathing activities in corresponding signals. The results show that WPT is not appropriate to characterize the signals uniquely in this specific study. In this chapter the spectral analysis of these three signals are performed to study whether the investigation of the signals in the frequency domain will provide sufficient information to characterize the signals in a unique manner.

Spectral analysis describes the process of calculation and interpretation of a spectrum. A spectrum may be considered the scale breakdown of phenomenon in space or time and presents a different and often extremely revealing way of looking at a sample sequence. Spectral analysis provides a deeper understanding of data and the system which produces those data (Preistley, 1981).

The essence of the spectral estimation problem is to estimate how the total power is distributed over frequency (Stoica and Moses, 1997). Analysis of the Power Spectral Density (PSD) allows us to investigate the dominant frequencies in a signal, as the dominant frequencies are likely to be important to the physical process

There are two broad approaches to spectral analysis: nonparametric (classic) and parametric. In nonparametric methods, power spectrum density is estimated directly from the signal (Stoica and Moses, 1997; Proakis and Manolakis, 1996). To do this, the studied signal is applied to a bandpass filter with a narrow bandwidth (frequency band of interest) and the filter output power divided by the filter bandwidth is used as a measure of the spectral content of the input to the filter (Stoica

and Moses, 1997). Periodogram, Welch's method and multitaper method (MTM) are examples of nonparametric methods.

In parametric approach, the second approach to spectral estimation, the studied signal is assumed to be the output of a linear system. In this approach, the spectral estimation problem is reduced to estimating the parameters in the assumed model. Examples are Yule-Walker autoregressive (AR) method and the Burg method (Stoica and Moses, 1997; Priestly, 1981).

3.2. Nonparametric methods

Nonparametric methods rely on the definition of the PSD to constitute the "classical means" for PSD estimation. In the following sections, the periodogram, Welch and multitaper methods of nonparametric estimation are discussed.

3.2.1. The Periodogram

In the periodogram method that is based on the definition of the PSD, the discrete-time Fourier transform of the samples of the process is calculated and the magnitude squared of the result is assumed as the spectral estimation. The periodogram estimate of the PSD of a length-L signal $x_L[n]$ is (Signal Processing Toolbox User's Guide, 2000; Castanie, 2006):

$$\hat{P}_{xx}(f) = \frac{|X_L(f)|^2}{f_s L} \qquad \text{Eq. (3.1)}$$

where f_s is the sampling frequency and $X_L(f)$ is given by:

$$X_L(f) = \sum_{n=0}^{L-1} x_L[n] e^{-2\pi j f n / f_s} \qquad \text{Eq. (3.2)}$$

$X_L(f)$ can be computed performing only at a finite number of frequency points, N, and usually applies the FFT. However, in implementations of the periodogram method, the N-point PSD estimate is calculated.

$$\hat{P}_{xx}[f_k] = \frac{|X_L[f_k]|^2}{f_s L}, \qquad f_k = \frac{kf_s}{N}, \qquad k = 0,1,\ldots,N-1 \qquad \text{Eq. (3.3)}$$

.

where

$$X_L[f_k] = \sum_{n=0}^{N-1} x_L[n] e^{-2\pi jkn/N} \qquad \text{Eq. (3.4)}$$

It helps to choose $N>L$ so that N is the next power of two larger than L.

The periodogram provides reasonably high resolution for relatively long data. However, from the statistical point of view, this method has a serious variability problem: the variance does not converge to zero as the sample size increases (Stoica and Moses 1997). Several modified methods have been developed to solve the high variance of the periodogram at the cost of reduced resolution. The most popular methods are Welch and multitaper methods (Priestly ,1981 ; Signal Processing Toolbox User's Guide, 2000).

3.2.2. Welch Method

An improved method to estimate the PSD is Welch method. This method splits a set of data into (possibly overlapping) smaller sets of data and calculates the periodogram of each set. Then the frequency domain coefficients arising from

calculating the periodograms are then averaged over the frequency components of each data set (Signal Processing Toolbox User's Guide, 2000).

. To explain Welch method mathematically, one must assume that there are N samples avaiable. The idea behind Welch method is to split up the available N samples to $S = N/M$ subsamples of M observations each, and then average the periodograms obtained from the subsamples for each value of frequency . Let

$$y_j(t) = y((j-1)K + t) \qquad t = 1,\ldots,M \qquad j = 1,\ldots,S \quad \text{Eq. (3.5)}$$

describes the jth data segment and $(j\text{-}1)K$ denotes the starting point for the jth sequence of observations. The value for K is $M/2$ (50% overlap between succesive segments).

The windowed periodogram corresponding to $y_j(t)$ is obtained as (Proakis and Manolakis, 1996)

$$\hat{\phi}_j(\omega) = \frac{1}{MP}\left|\sum_{t=1}^{M} v(t) y_j(t) \exp(-i\omega t)\right|^2 \qquad \text{Eq. (3.6)}$$

where P is the "power" of the segment $\{v(t)\}$:

$$P = \frac{1}{M}\sum_{t=1}^{M} \left|v(t)\right|^2 \qquad \text{Eq. (3.7)}$$

Therefore, the PSD estimation using Welch method can be computed by averaging the windowed periodograms as:

$$\hat{\phi}_W(\omega) = \frac{1}{S}\sum_{j=1}^{S} \hat{\phi}_j(\omega) \qquad \text{Eq. (3.5)}$$

Overlapping between data segments and getting more periodograms to be averaged over frequency components lead to a decrease of the variance of the estimate relative to a single periodogram for the whole data record. Overlap between

segments may introduce redundancy of information. Howevere, using a nonrectangular window, which gives less weight to the end sample of each segment, can significantly diminish this effect (Priestley, 1981; Bendat and Piersol, 1993) .

3.2.3. Multitaper Method

The basic idea behind the multitaper method is to window the data with different orthogonal tapers, and then average over the spectra for each taper (Signal Processing Toolbox User's Guide, 2000). In multitaper method, to estimate the PSD, time series data are multiplied by a single time series with the same size as a taper or window function. These windows are usually Slepian functions, which form a set of orthogonal functions. Hamming, Hanning and Cosine tapers are examples of these types of tapers (Mitra and Pesaran, 1999).

The first step in the multitaper method is to calculate the Slepian functions (Mitra and Pesaran, 1999). There two parameters that describe a Slepian function are: length, N, and bandwidth parameter, W. The parameters N and W determine the maximum number of functions that can be used, $K = \lfloor 2NW \rfloor$. The maximum number of functions is dependent upon the processes under investigation. Given frequency half-bandwidth W and length N, approximately $2NW$ Slepian functions ($wt\,(k)$, $k = 1,\ldots,\lfloor 2NW \rfloor$ and $t = 1,\ldots, N$) exist with their power concentrated in frequency range $[-W,W]$.

The next step is to calculate the tapered Fourier transforms of the data x_t ($t = 1,\ldots, N$), for each taper $w_t\,(k)$ ($k = 1,\ldots,K$).

$$\tilde{x}_k(f) = \sum_{t=1}^{N} w_t(k) x_t \exp(-2\pi i f t) \qquad \text{Eq. (3.6)}$$

Before performing this task, the data is usually padded with zeros to the nearest power of 2 (Mitra and Pesaran, 1999). The zeros are added to one end of the time series after they are multiplied by the tapers. The simplest example of the multitaper method is the direct multitaper spectral estimate, $S_{MT}(f)$ which is simply the average over individual tapered spectral estimates (Mitra and Pesaran, 1999),

$$S_{MT}(f) = \frac{1}{K} \sum_{k=1}^{K} \left| \tilde{x}_k(f) \right|^2 \qquad \text{Eq. (3.7)}$$

Although the multitaper method tends to reduce spectral leakage and include the beginning and end of the time series data, it involves more computation in comparison to Welch method (Signal Processing Toolbox, 2000).

3.3. Parametric Methods

If the signal length is short, parametric methods tend to provide higher resolutions than nonparametric methods (Bendat and Piersol 1993; Castanie, 2006). In parametric or model-based methods, instead of estimating the PSD directly from the data, the data are assumed to satisfy a model with a known functional form. This model is usually assumed to be a linear system driven by white noise. The next step will be to estimate the parameters in the assumed model and then the signal's spectral characteristic are derived from the estimated model (Castanie, 2006; Proakis and Manolakis, 1996).

One of the most common models in parametric methods is the all-pole filter or autoregressive models. The all-pole filter is a filter that all of its zeros are located at

the origin in z-plane. Considering white noise as an input for such a filter, calculating the output is actually an autoregressive process (Signal Processing Toolbox User's Guid, 2000; Castanie, 2006).

3.3.1. Yule-Walker Method

The Yule-Walker method fits an autoregressive model to the windowed input data by minimizing the forward prediction error in the least square sense (Signal Processing Toolbox User's Guide, 2000). This formulation results in Yule-Walker equations that can be solved using Levinson-Durbin algorithm. Levinson-Durbin algorithm is an algorithm that is used to solve normal equations efficiently. Normal equations can be described by (Proakis and Manolokis, 1996)

$$\sum_{k=0}^{p} a_p(k)\gamma_{xx}(l-k) = 0 \qquad l = 1,2,\ldots,p \qquad a_p(0) = 1 \qquad \text{Eq(3.8)}$$

where $\gamma_{xx}(m)$ is autocorrelation sequence.

In this method the PSD ids given by (Proakis and Manolakis, 1996):

$$P_{xx}^{YW}(f) = \frac{1}{\left|1 + \sum_{k=1}^{P} a_p(k)\exp(-j2\pi fk)\right|^2} \qquad \text{Eq. (3.9)}$$

where $a_p(k)$ is the estimated AR parameters.

The advantage of this method is the AR parameters computed always result in a stable all-pole model. However, this method performs poorly for short data records (Stoica and Moses 1997).

3.3.2. Burge Method

Burge method minimizes the forward and backward linear prediction errors while satisfying the Levinson-Durbin recursion. In this method, instead of attempting to calculate the autocorrelation function, the reflection coefficients are estimated directly. The PSD is given as (Proakis and Manolakis, 1996):

$$P_{xx}^{BU}(f) = \frac{E_P}{\left|1 + \sum_{k=1}^{P} a_p(k)\exp(-j2\pi fk)\right|^2} \qquad \text{Eq. (3.10)}$$

where $a_p(k)$ is the estimated AR parameters and E_p is least-square error.

The Burge method obtains a higher resolution, produces stable AR parameters and is computationally efficient. However, peak locations are highly dependent on initial phase (Priestley 1981, Bendat and Piersol 1993; Proakis and Manolokis, 1996)

3.4. Method

Where the data satisfy the assumed model, parametric methods may offer a more accurate spectral estimate than the nonparametric ones (Stoica and Mosese 1997). In most cases, however, the assumed model is not a close approximation of the reality. Due to the sensitivity of the parametric methods to model specification, the nonparametric approaches may be preferred to the parametric ones. Among the nonparametric methods, Welch method tends to be more accurate than the periodogram and requires relatively less computation in comparison to the multitaper method. As a result, Welch method has been used to estimate the PSD in this study. The window size is arbitrary selected as one minute.

3.5. Results

Suck, swallow and breathing waveforms of baby #87, seventh feeding and baby #81, 10^{th} feeding are analyzed using Welch method in Matlab environment. The results are as following.

The Spectral Analysis of the Breathing Waveform of Baby # 87, Seventh feeding

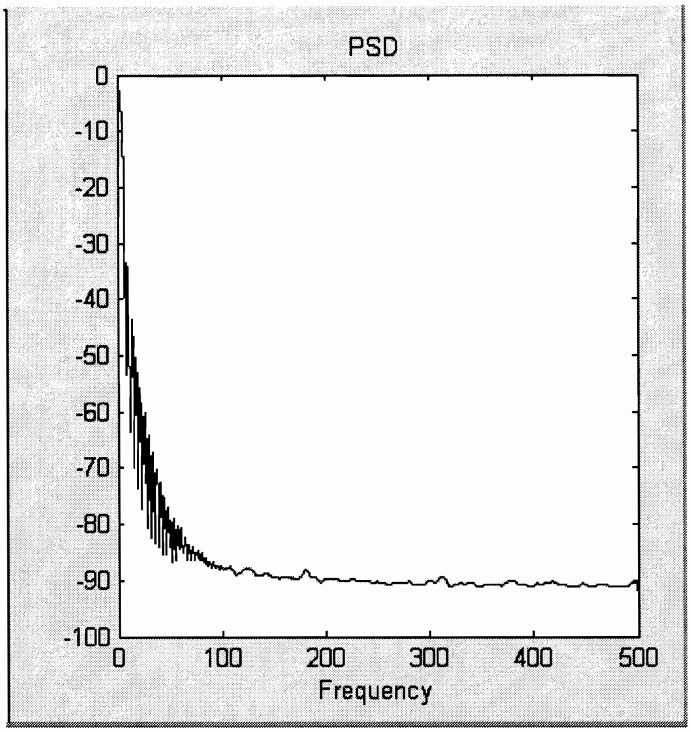

Figure 3.1: The spectral analysis of the first minute breathing of baby #87, seventh feeding

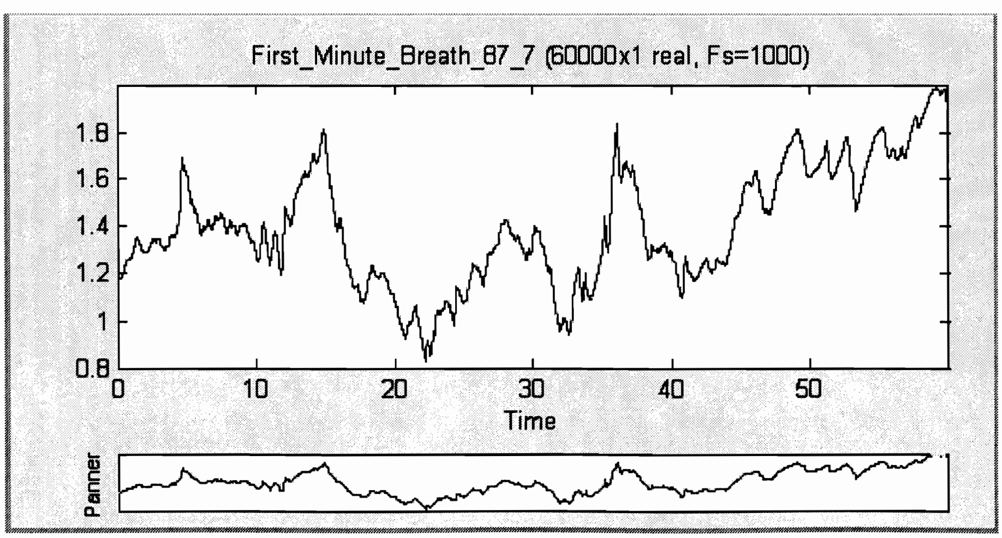

Figure 3.2: The first minute breathing of baby #87, seventh feeding

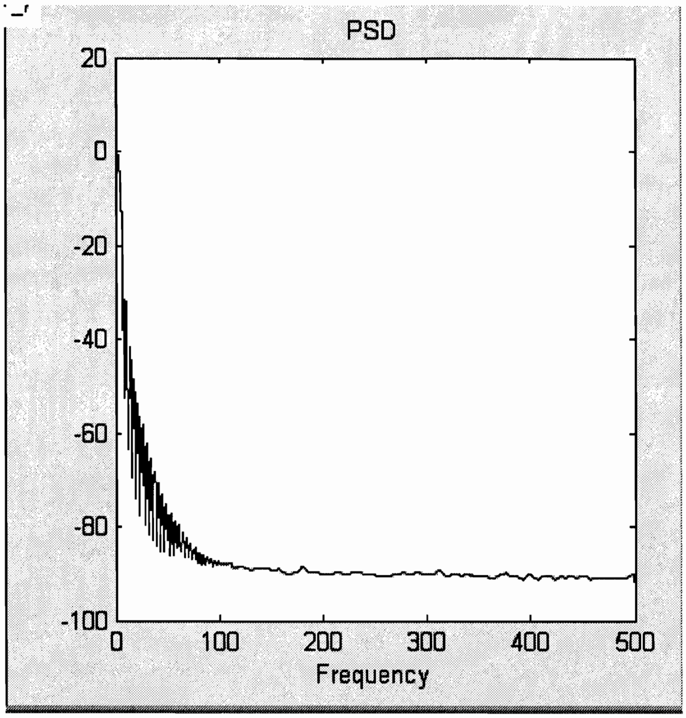

Figure 3.3: The spectral analysis of the second minute breathing of baby #87, seventh feeding

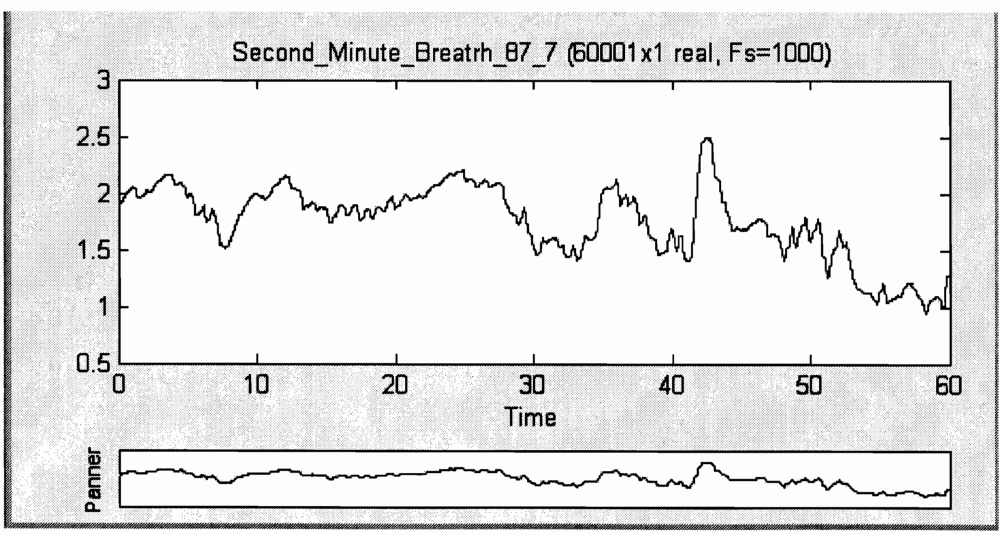

Figure 3.4: The second minute breathing of baby #87, seventh feeding

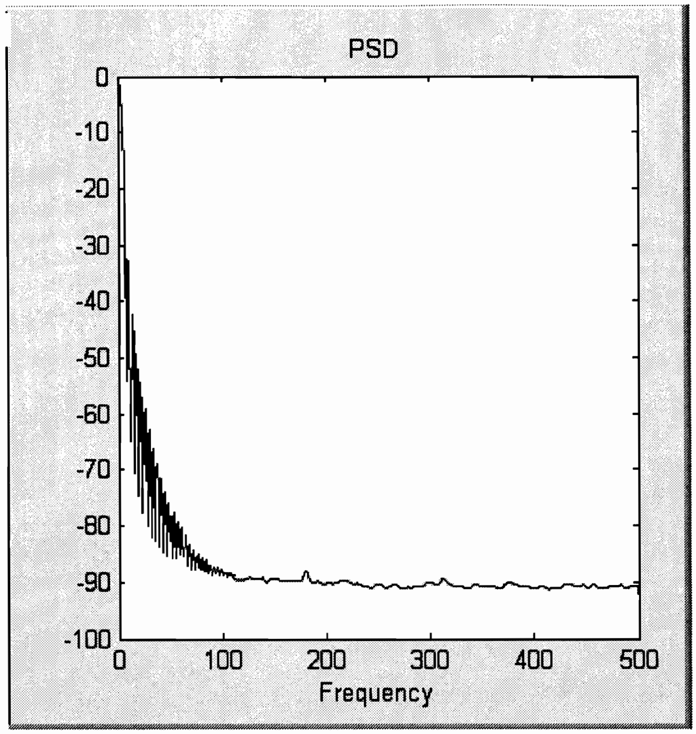

Figure 3.5: The spectral analysis of the third minute breathing of baby #87, seventh feeding

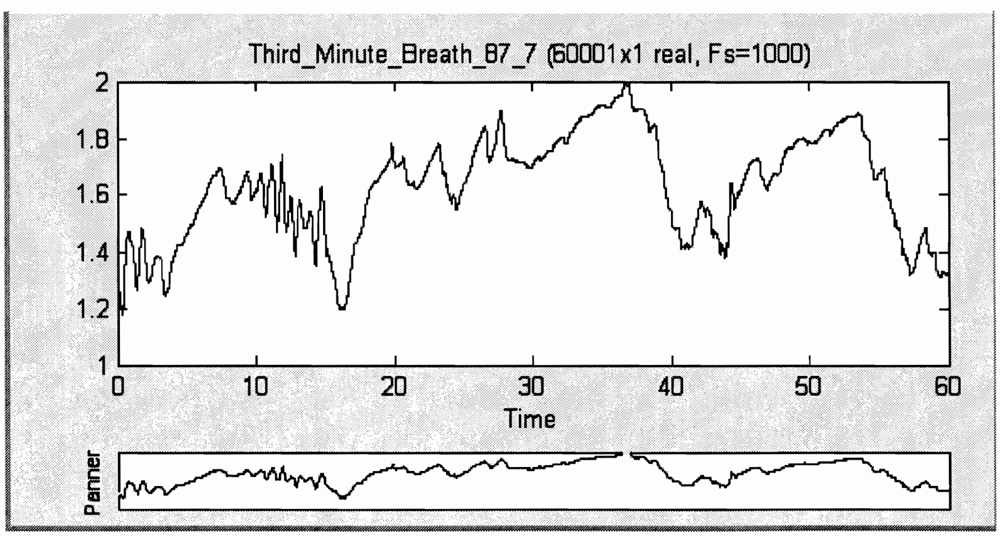

Figure 3.6: The third minute breathing of baby #87, seventh feeding

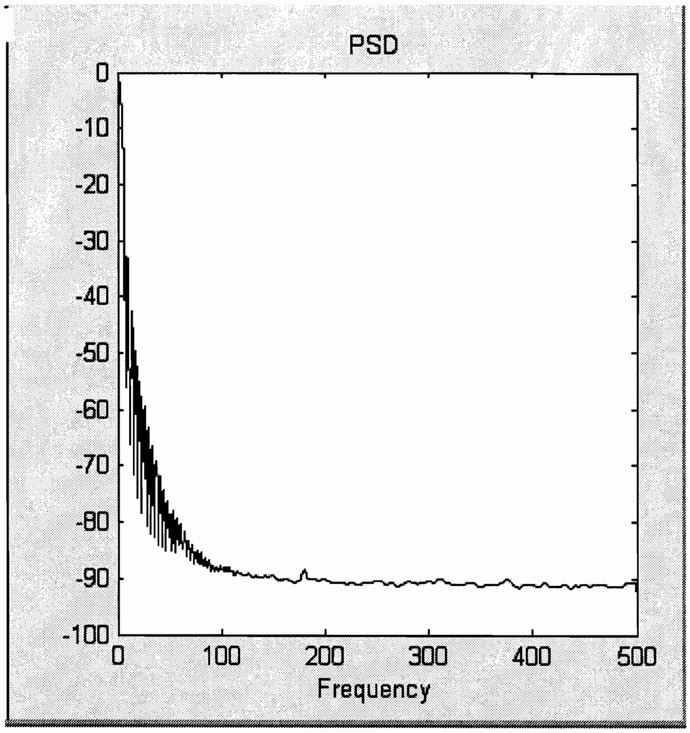

Figure 3.7: The spectral analysis of the forth minute breathing of baby # 87, seventh feeding

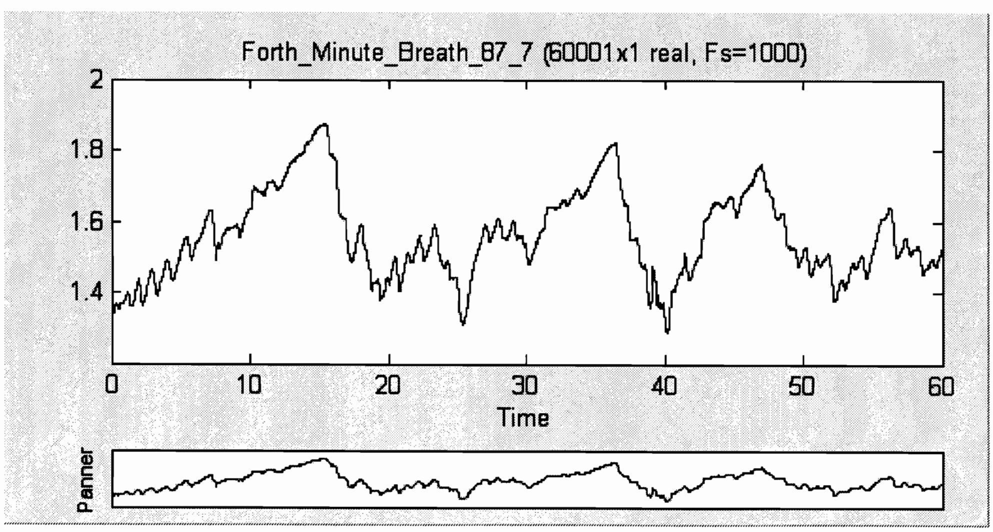

Figure 3.8: The forth minute breathing of baby #87, seventh feeding

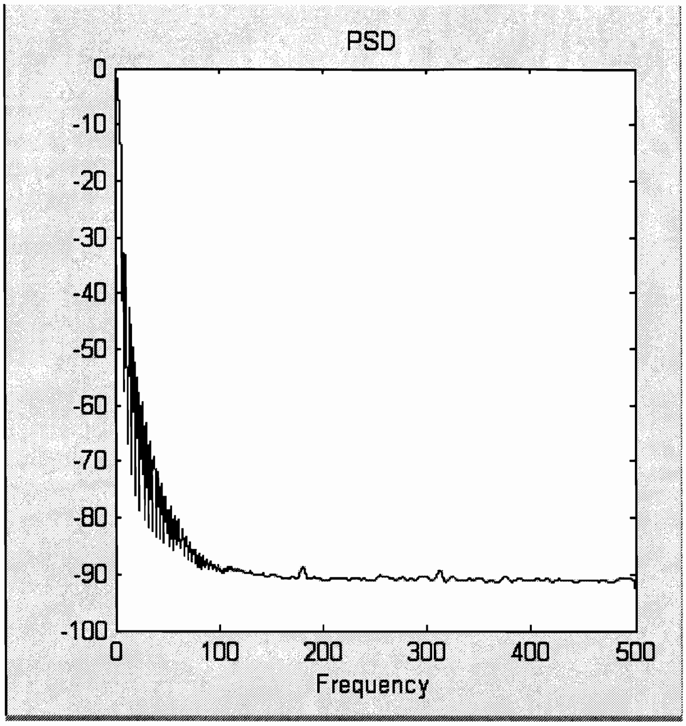

Figure 3.9: The spectral analysis of the fifth minute breathing of baby #87, seventh feeding

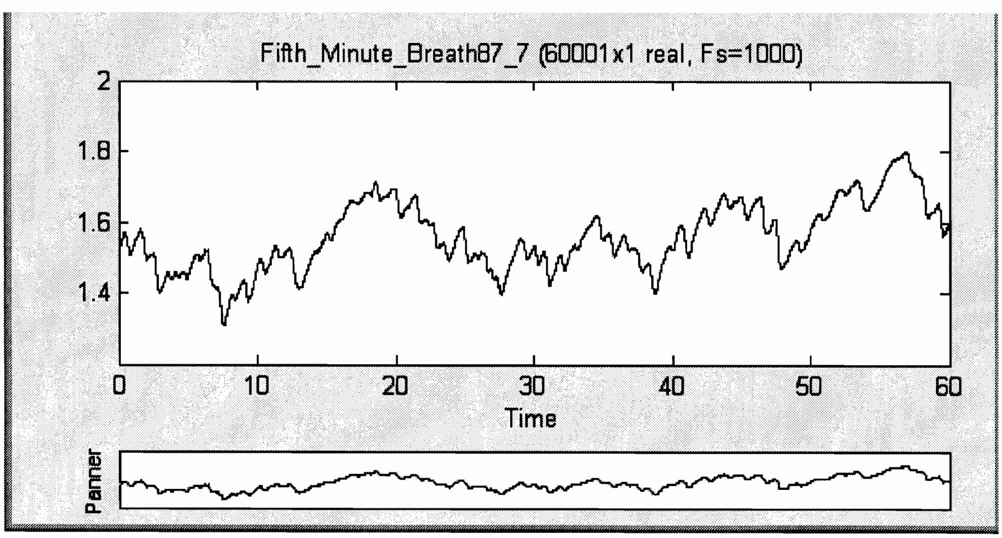

Figure 3.10: The fifth minute breathing of baby #87, seventh feeding

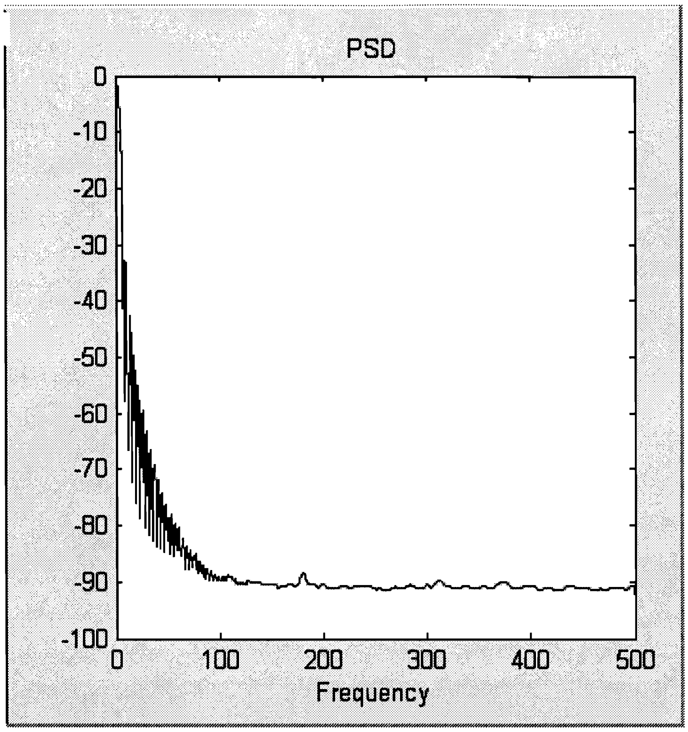

Figure 3.11: The spectral analysis of the sixth minute breathing of baby #87, seventh feeding

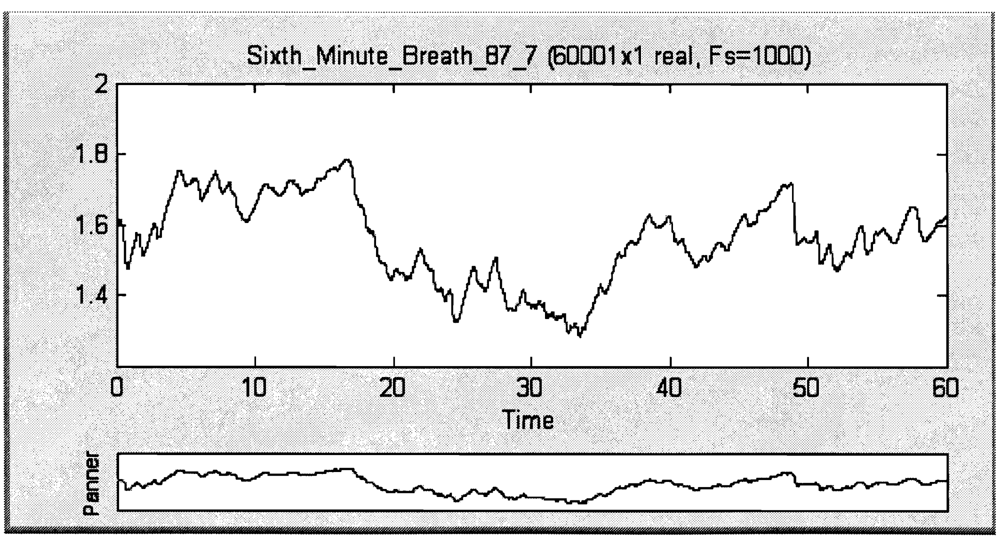

Figure 3.12: The sixth minute breathing of baby #87, seventh feeding

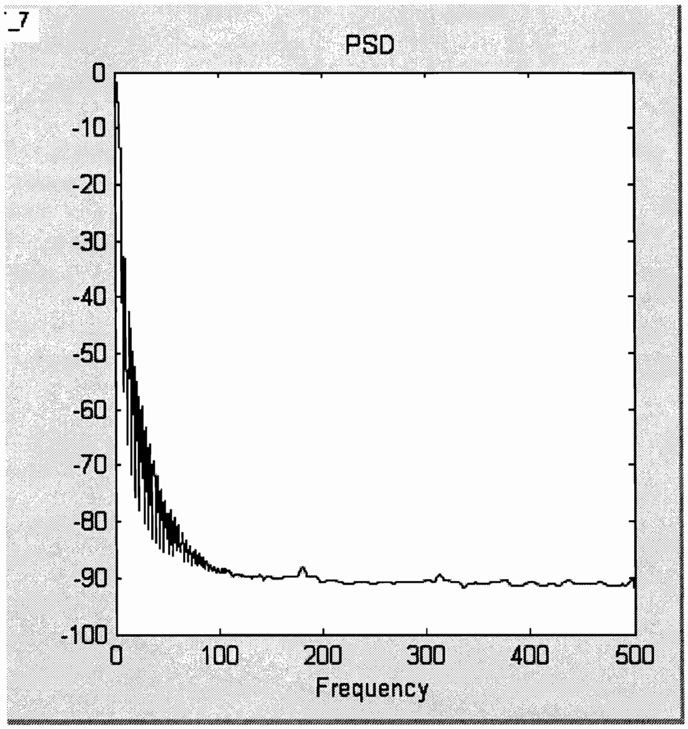

Figure 3.13: The spectral analysis of the seventh minute breathing of baby #87, seventh feeding

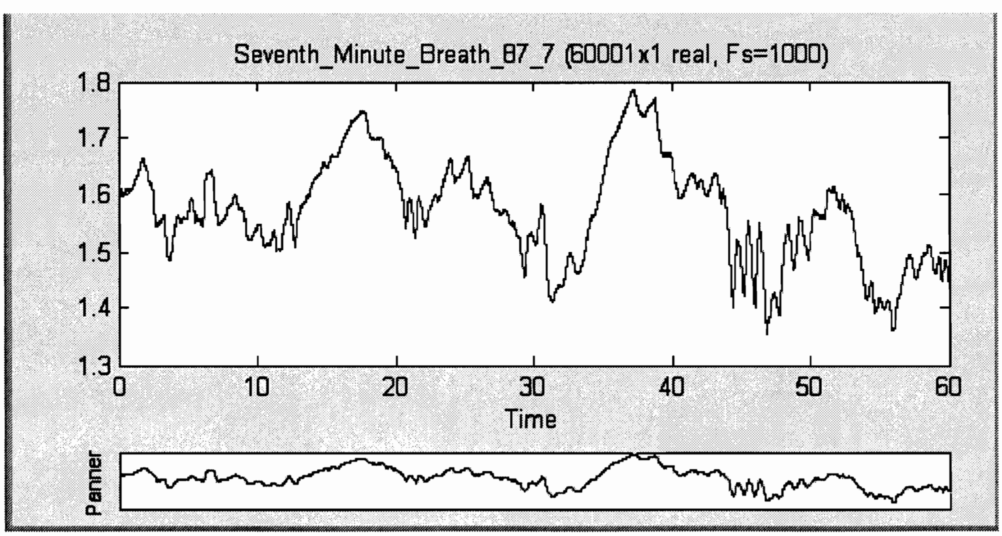

Figure 3.14: The seventh minute breathing of baby #87, seventh feeding

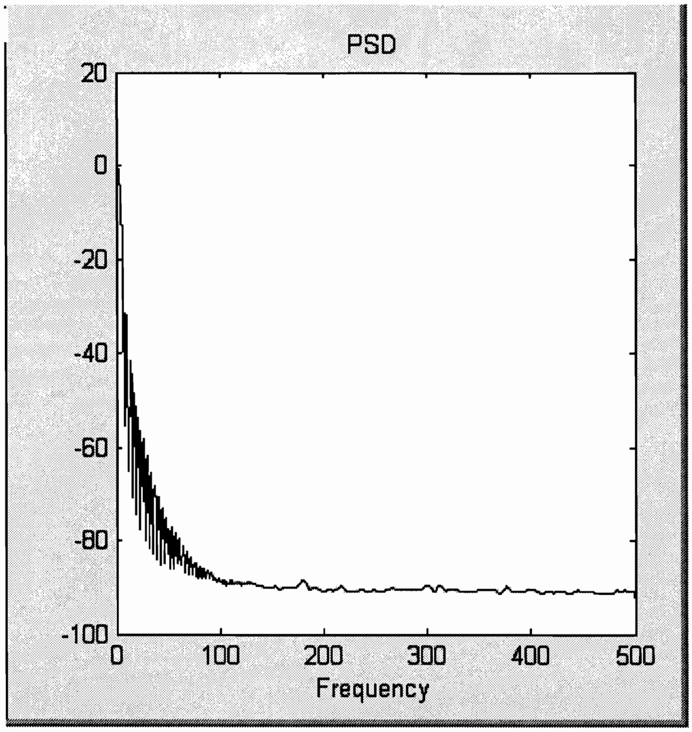

Figure 3.15: The spectral analysis of the eighth minute breathing of baby #87, seventh feeding

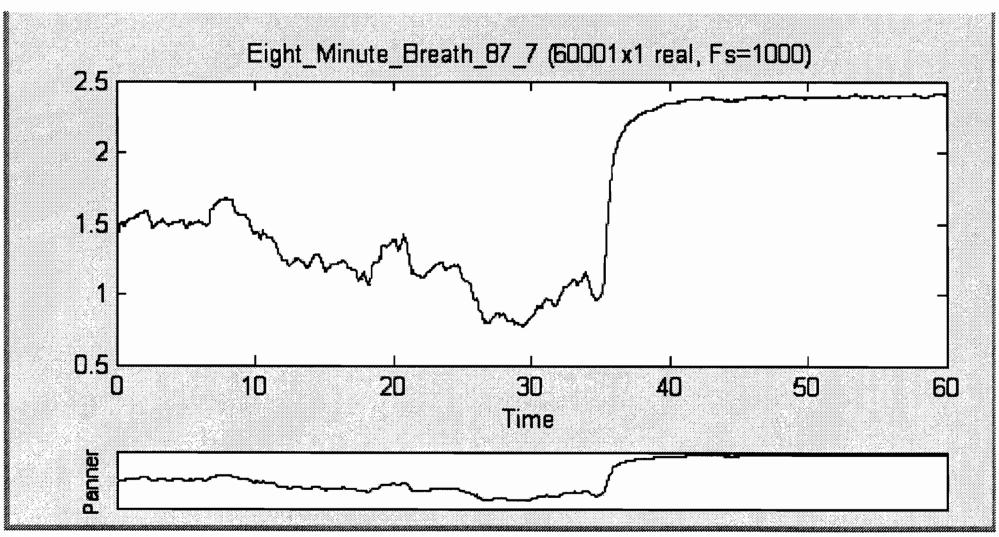

Figure 3.16: The eight minute breathing of baby #87, seventh feeding

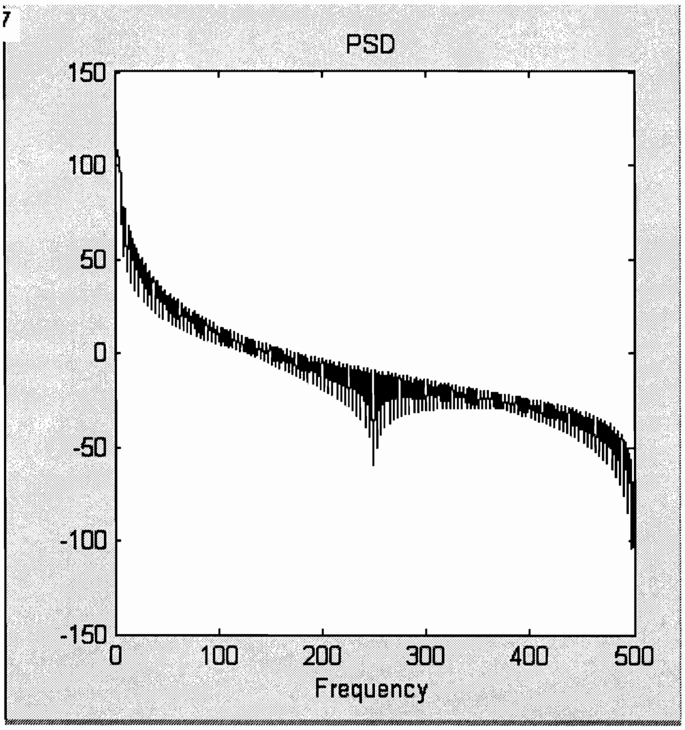

Figure 3.17: The spectral analysis of the ninth minute breathing of baby #87, seventh feeding

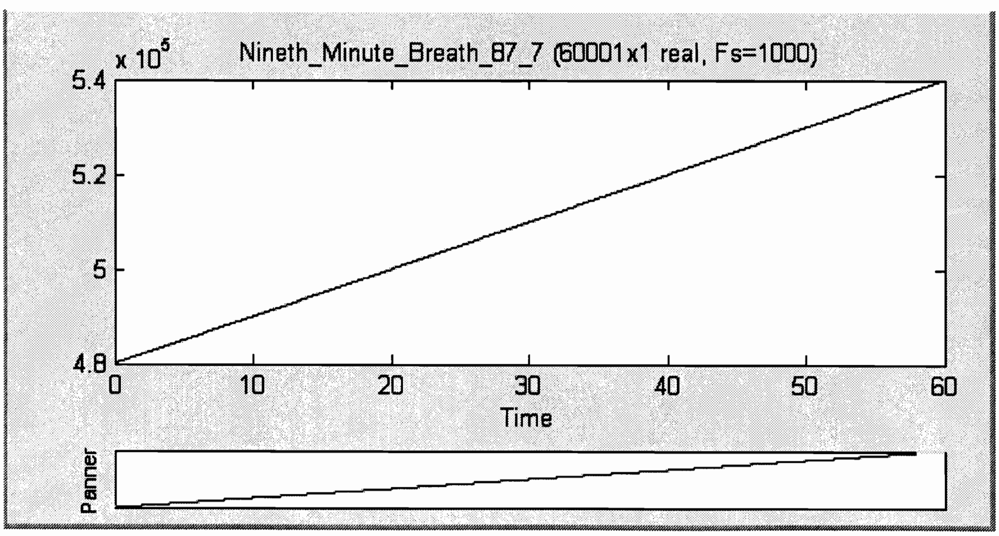

Figure 3.18: The ninth minute breathing of baby #87, seventh feeding

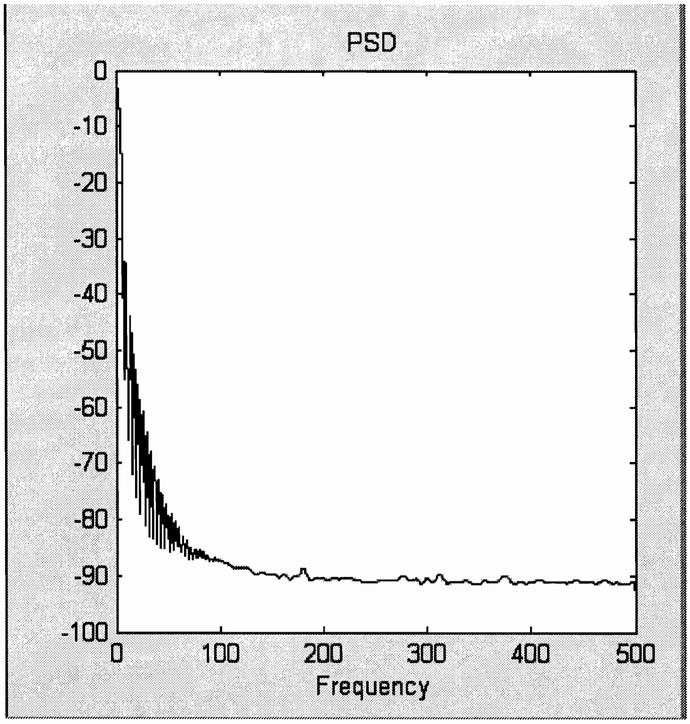

Figure 3.19: The spectral analysis of the10th minute breathing for baby #87, seventh feeding

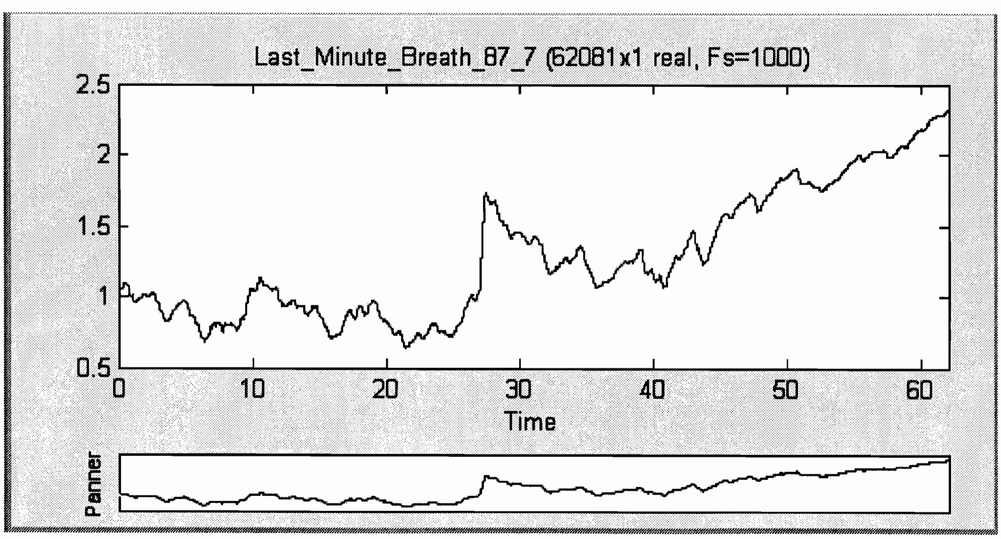

Figure 3.20: The 0th minute breathing of baby #87, seventh feeding

The Spectral Analysis of the Sucking Waveform of Baby # 87, seventh feeding

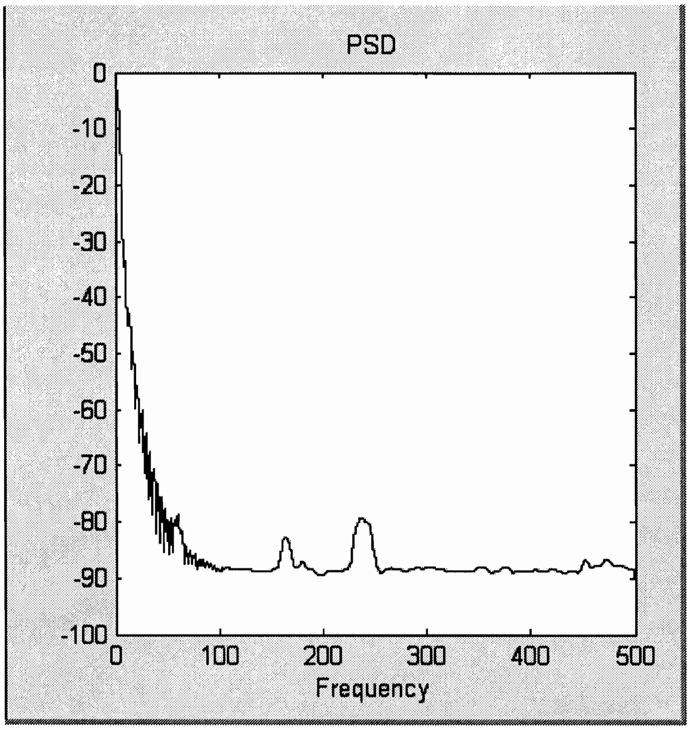

Figure 3.21: The spectral analysis of the first minute sucking of baby #87, seventh feeding

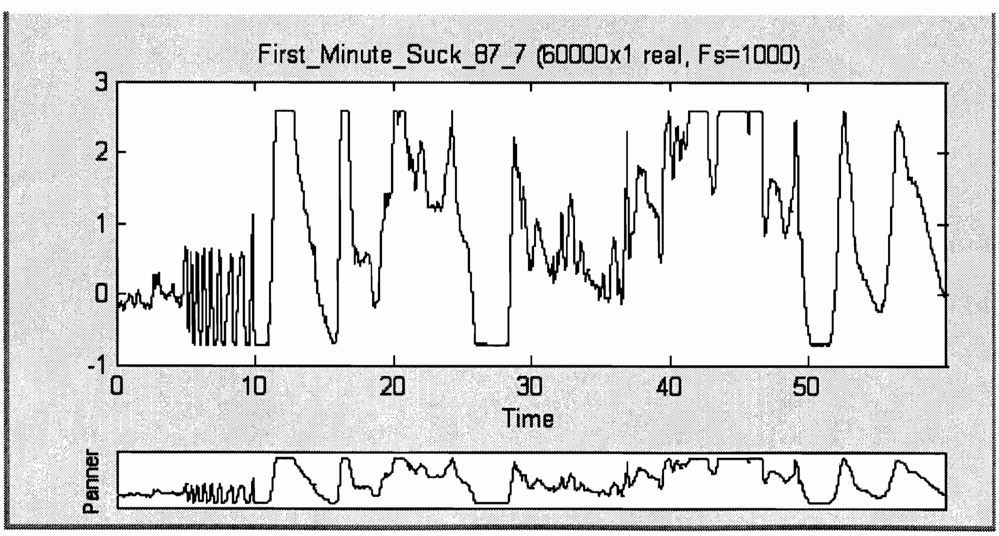

Figure 3.22: The first minute sucking of baby #87, seventh feeding

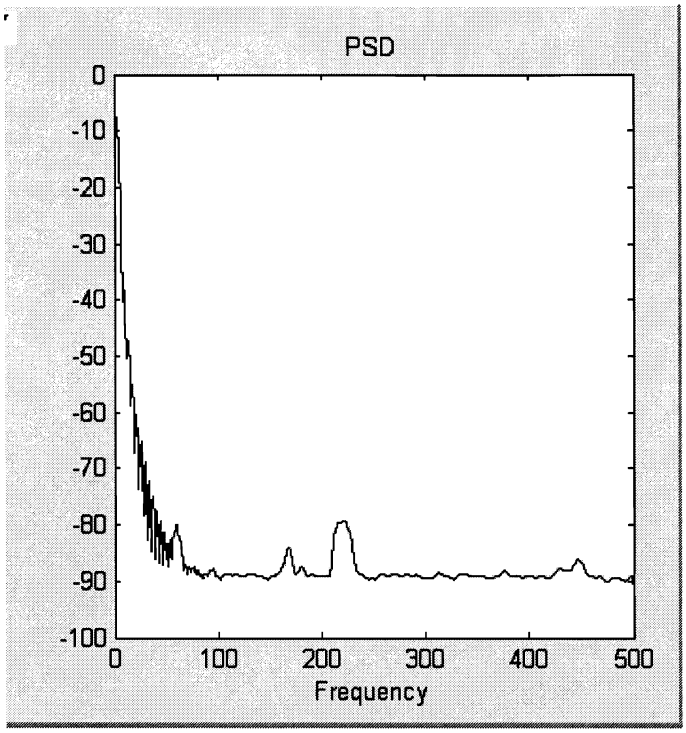

Figure 3.23: The spectral analysis of the second minute sucking of baby #87, seventh feeding

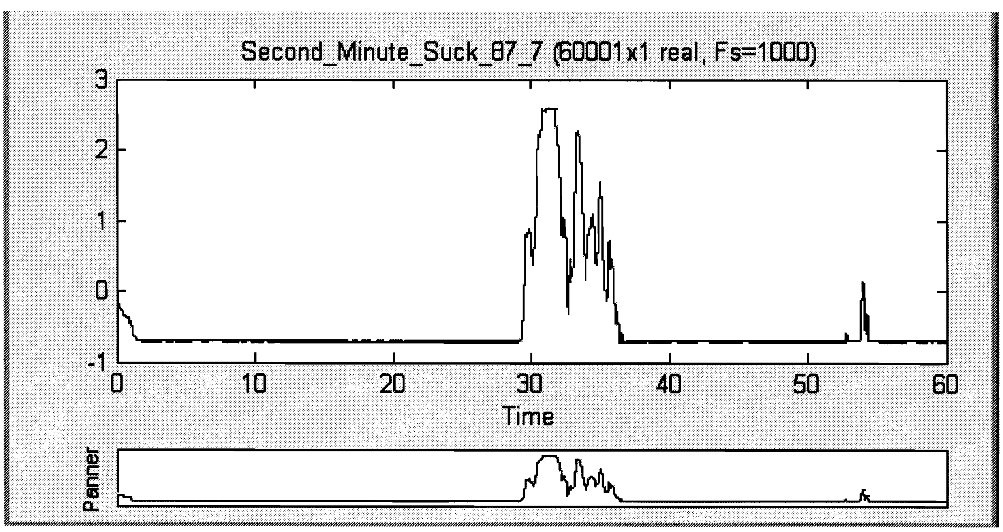

Figure 3.24: The second minute sucking of baby #87, seventh feeding

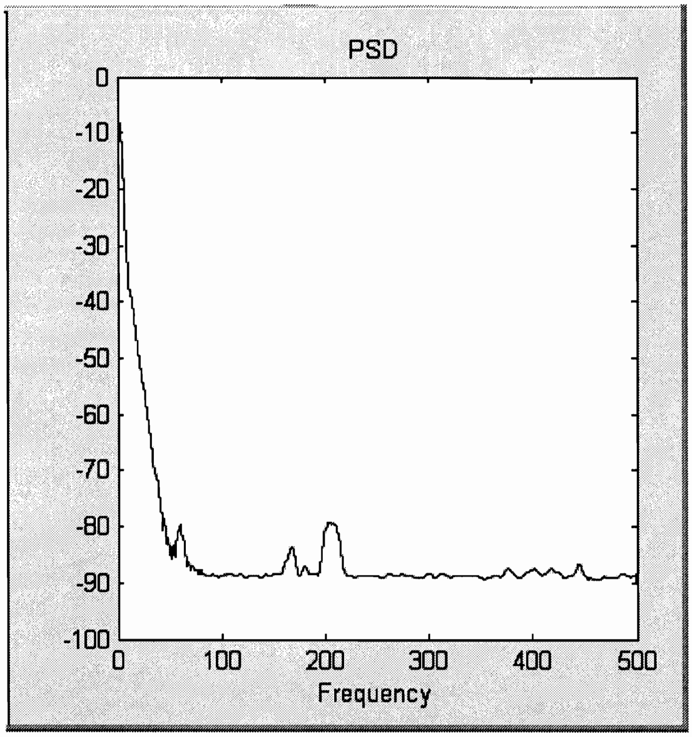

Figure 3.25: The spectral analysis of the third minute sucking of baby #87, seventh feeding

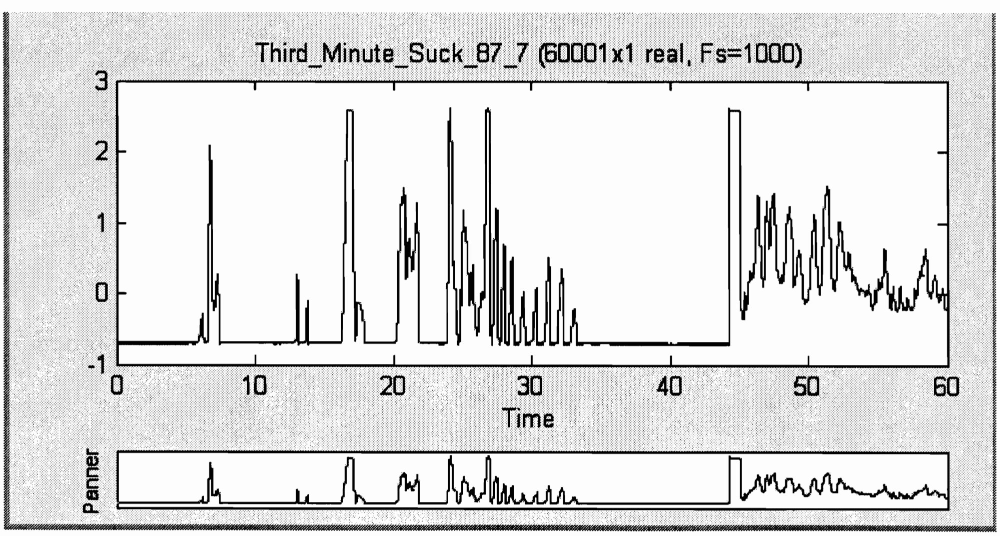

Figure 3.26: The third minute sucking of baby #87, seventh feeding

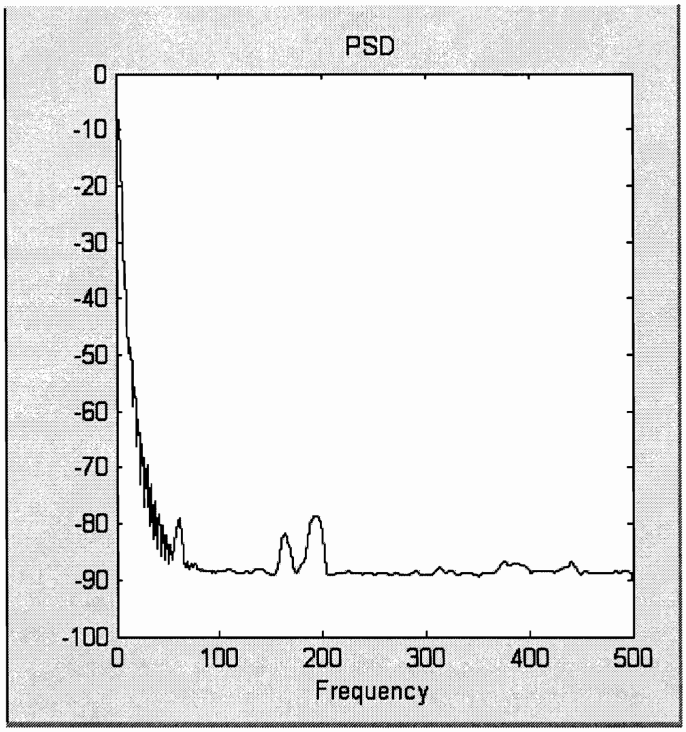

Figure 3.27: The spectral analysis of the forth minute sucking of baby #87, seventh feeding

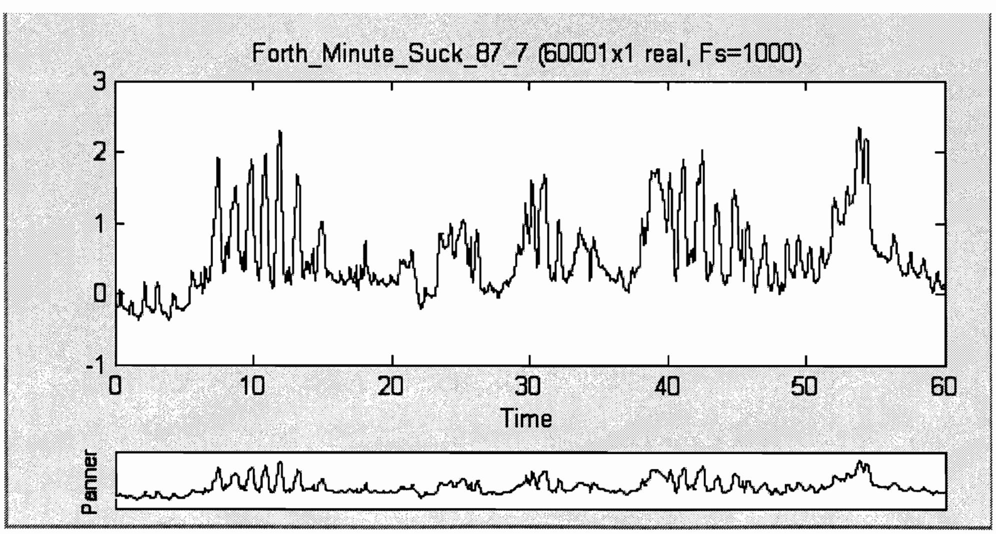

Figure 3.28: The forth minute sucking of baby #87, seventh feeding

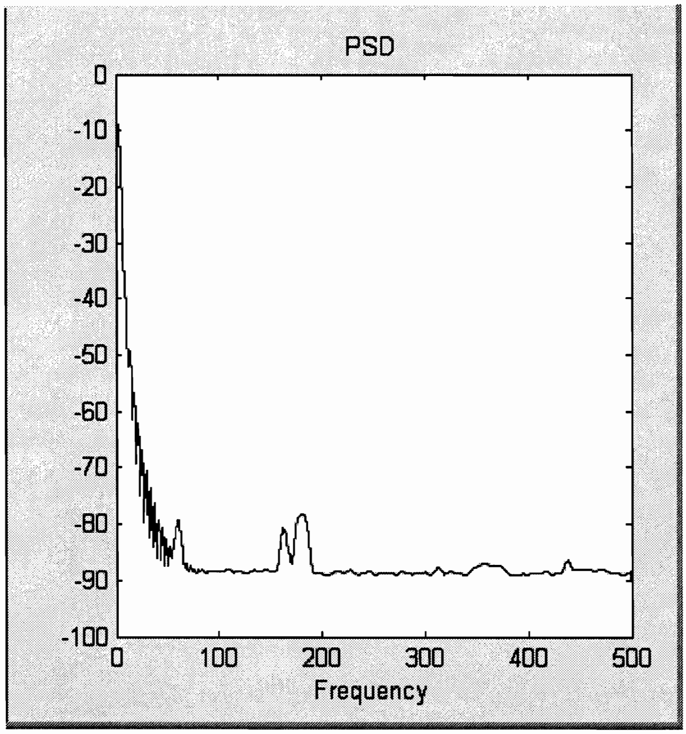

Figure 3.29: The spectral analysis of the fifth minute sucking of baby #87, seventh feeding

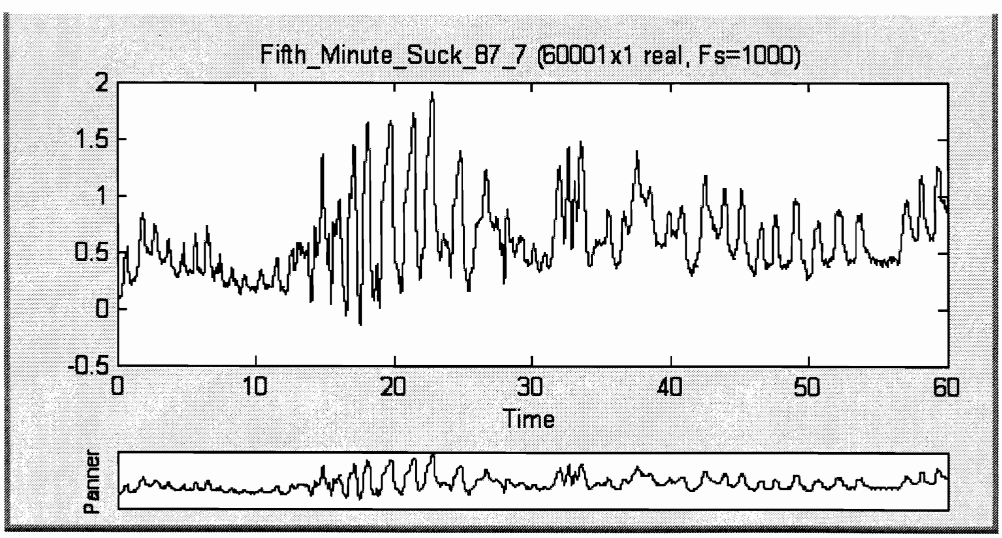

Figure 3.30: The fifth minute sucking of baby #87, seventh feeding

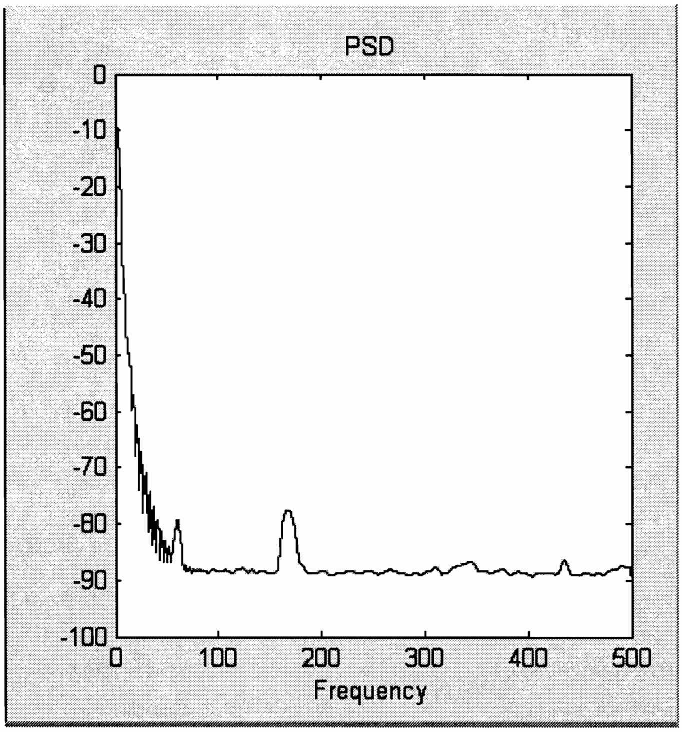

Figure 3.31: The spectral analysis of the sixth minute sucking of baby #87, seventh feeding

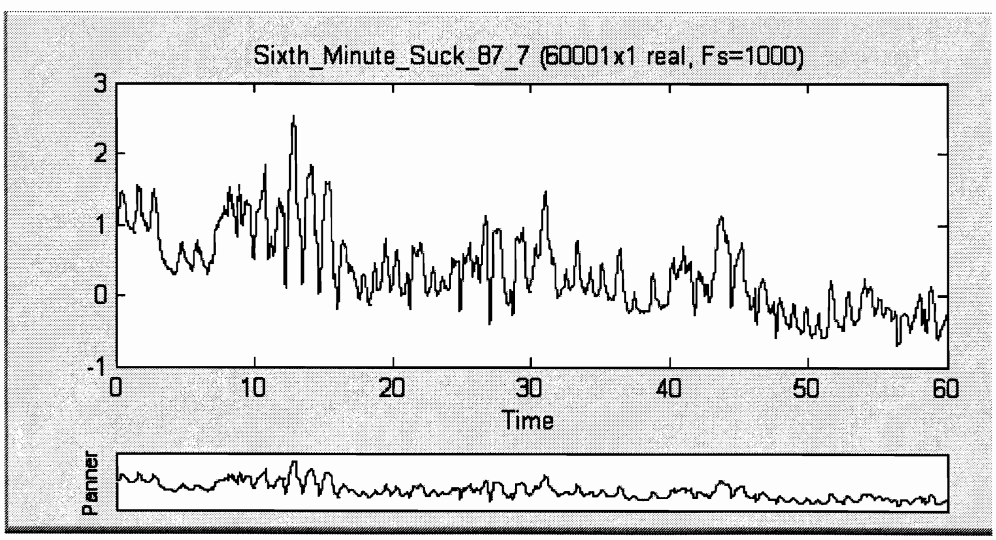

Figure 3.32: The sixth minute sucking of baby #87, seventh feeding

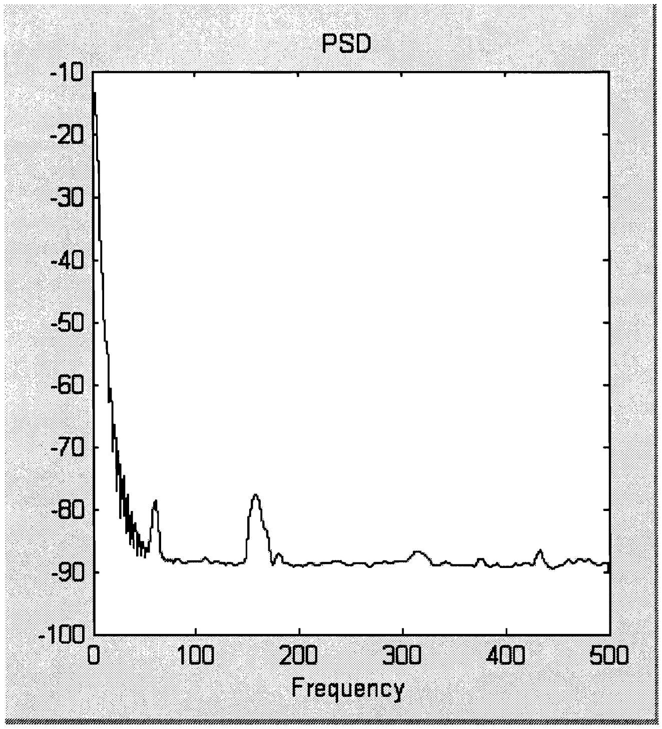

Figure 3.33: The spectral analysis of the seventh minute sucking of baby #87, seventh feeding

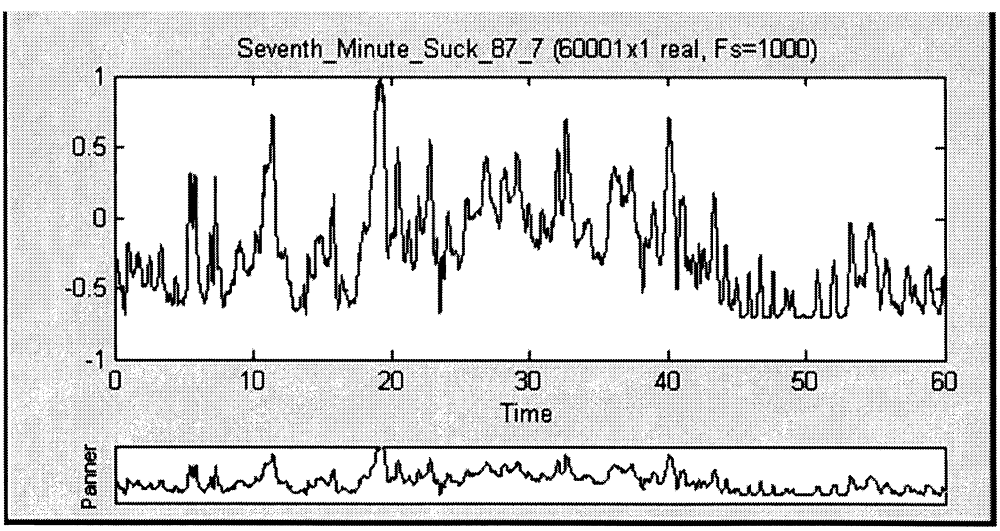

Figure 3.34: The seventh minute sucking for baby #87, seventh feeding

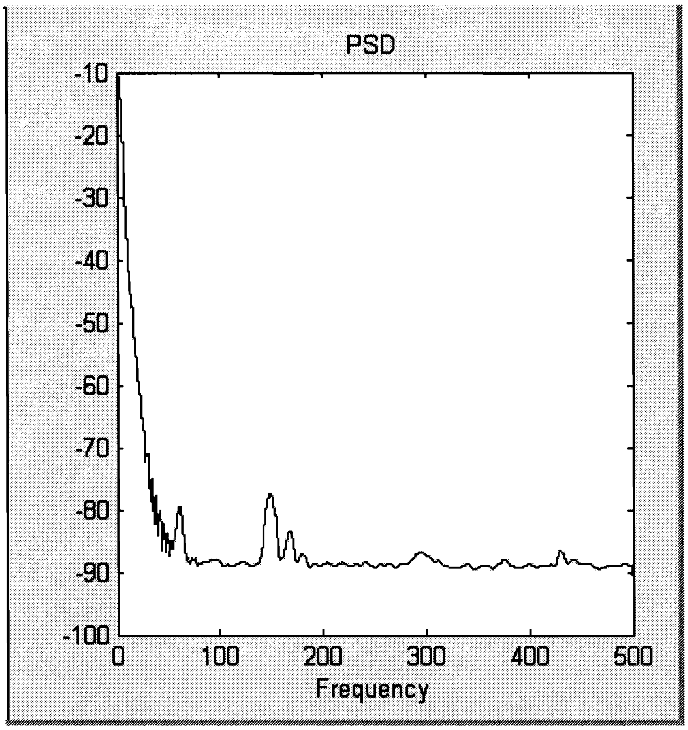

Figure 3.35: The spectral analysis of the eighth minute sucking of baby #87, seventh feeding

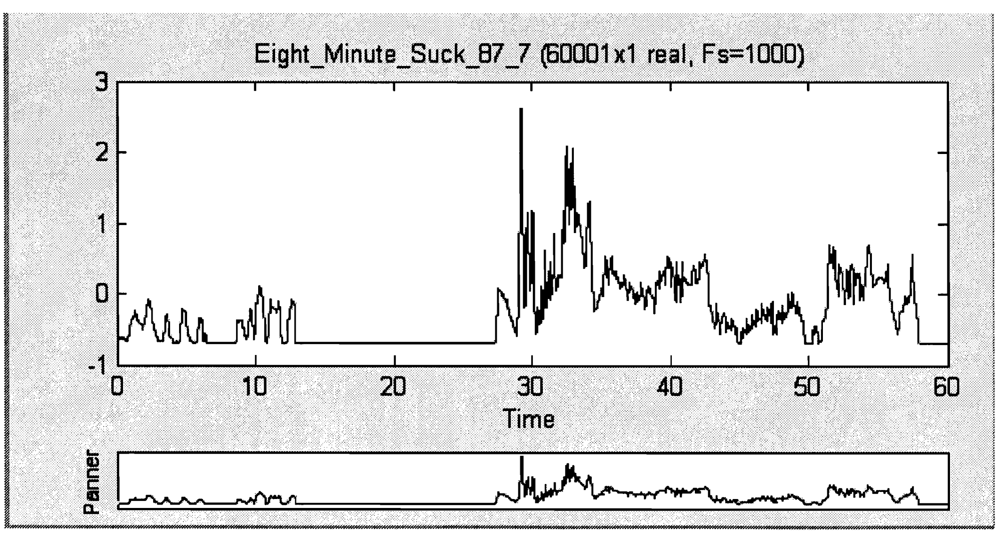

Figure 3.36: The eighth minute sucking of baby #87, seventh feeding

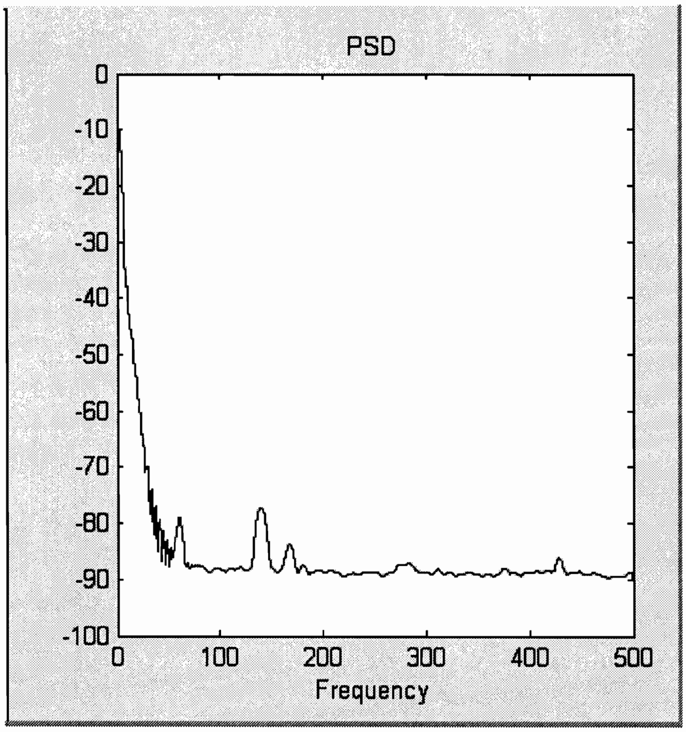

Figure 3.37: The spectral analysis of the ninth minute sucking of baby #87, seventh feeding

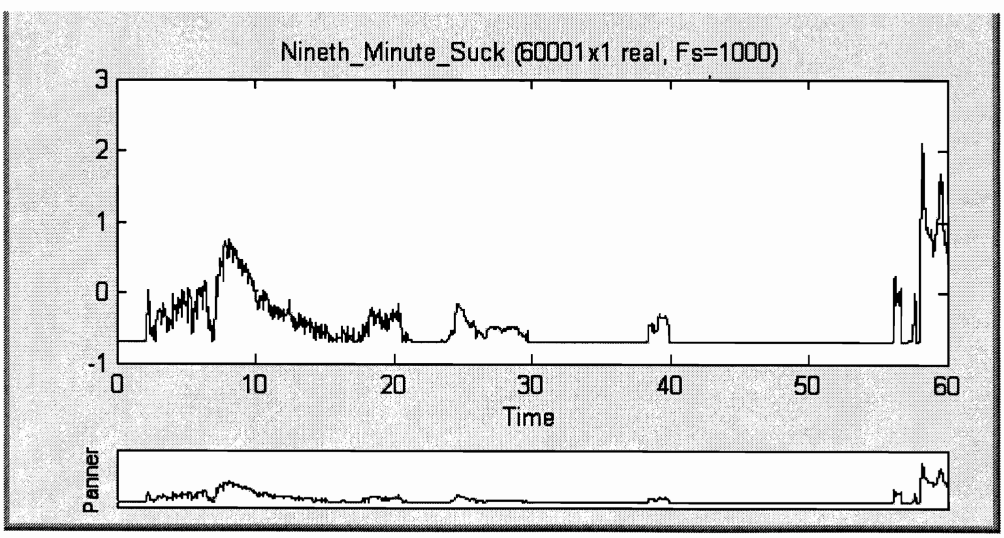

Figure 3.38: The ninth minute sucking of baby #87, seventh feeding

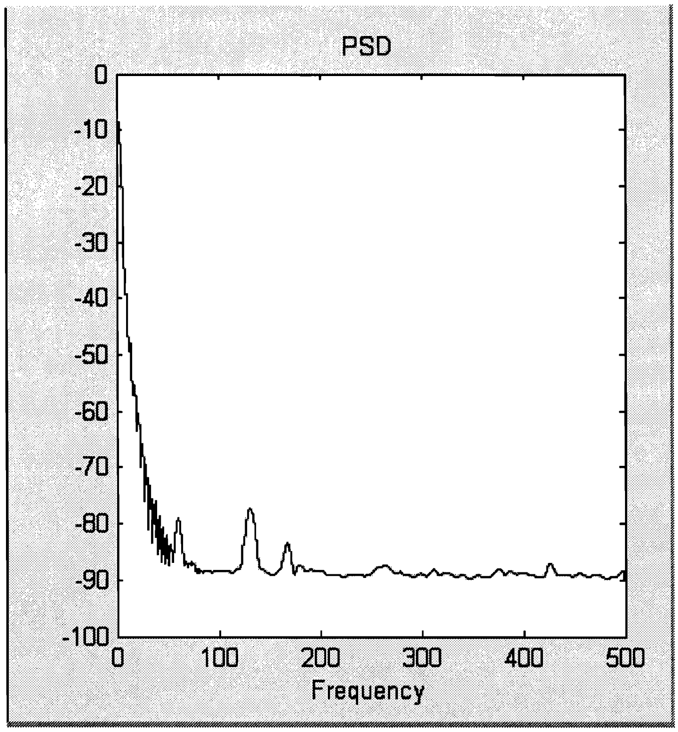

Figure 3.39: The spectral analysis of 10th minute sucking of baby #87, seventh feeding

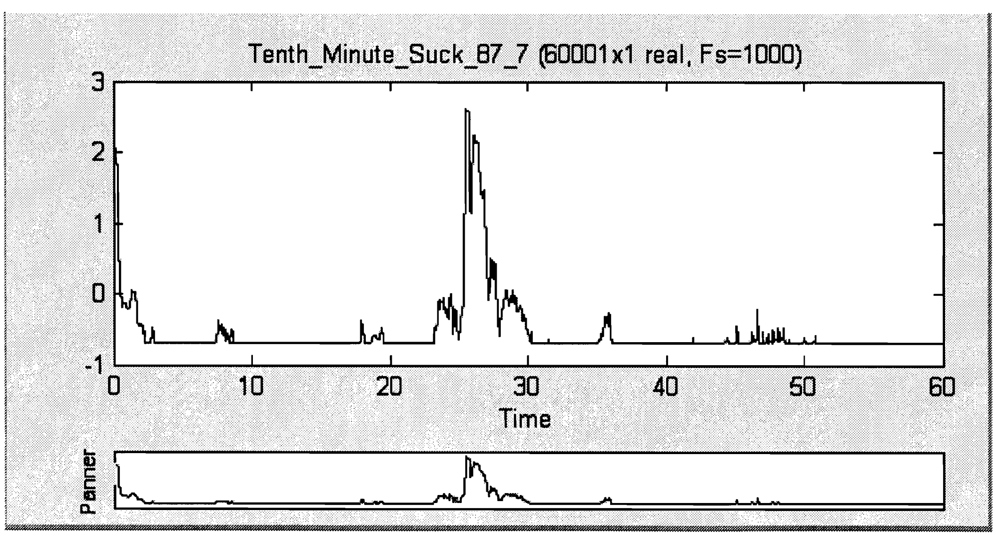

Figure 3.40: The 10th minute sucking of baby #87, seventh feeding

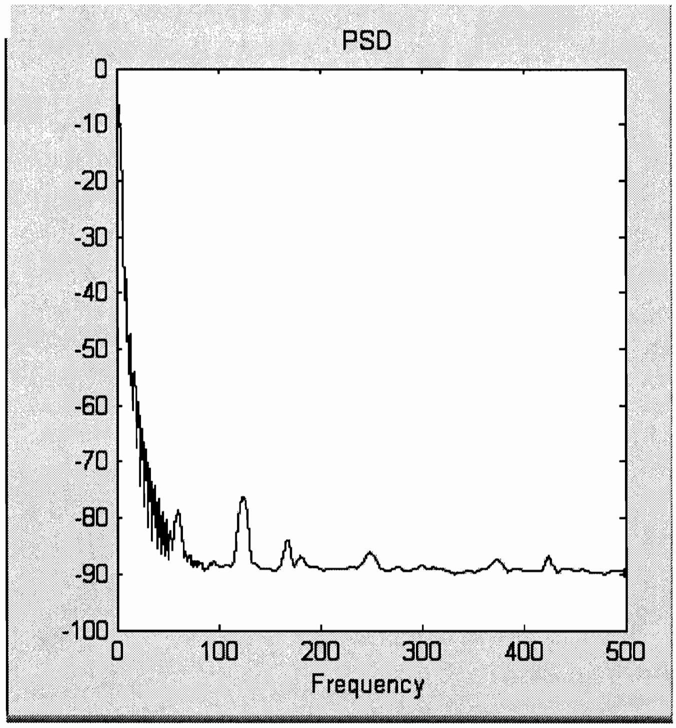

Figure 3.41: The spectral analysis of the 11th minute sucking of baby #87, seventh feeding

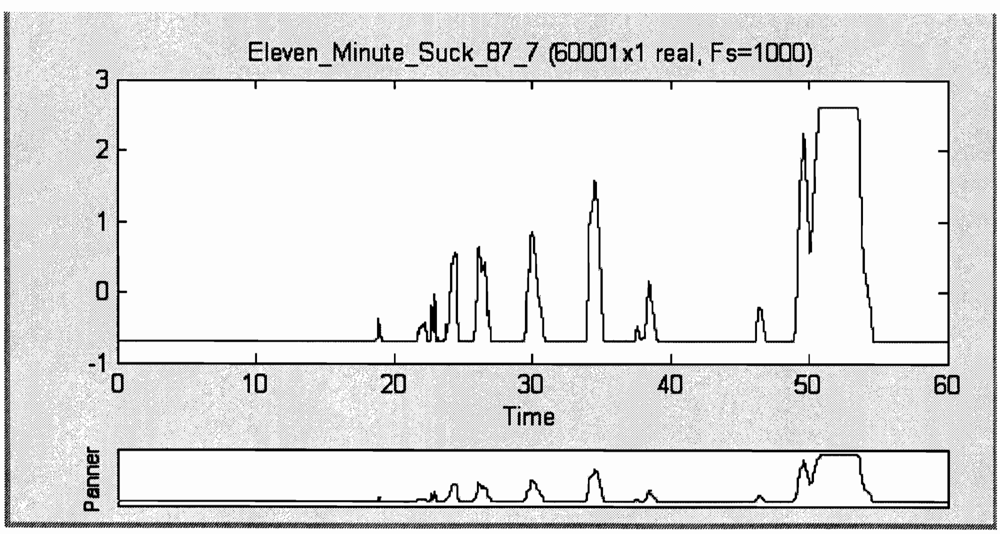

Figure 3.42: The 11th minute sucking of baby #87, seventh feeding

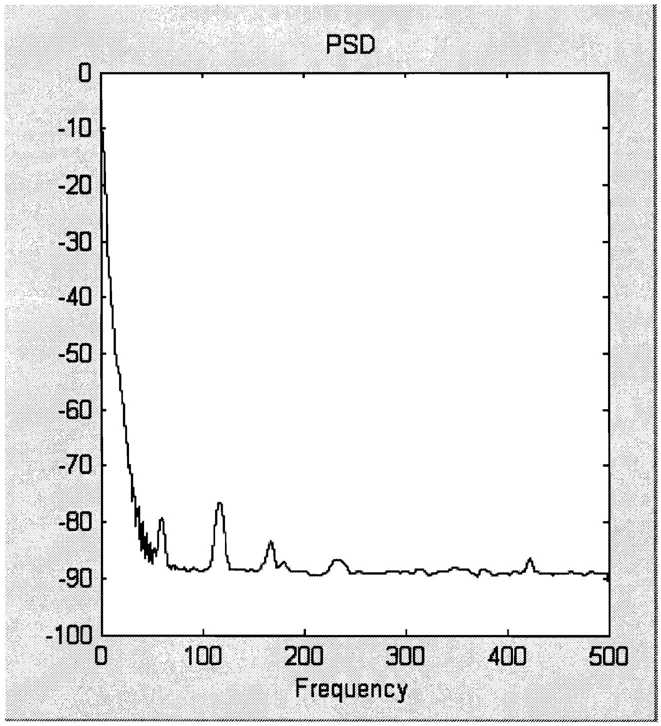

Figure 3.43: The spectral analysis of the 12th minute sucking of baby # 87, seventh feeding

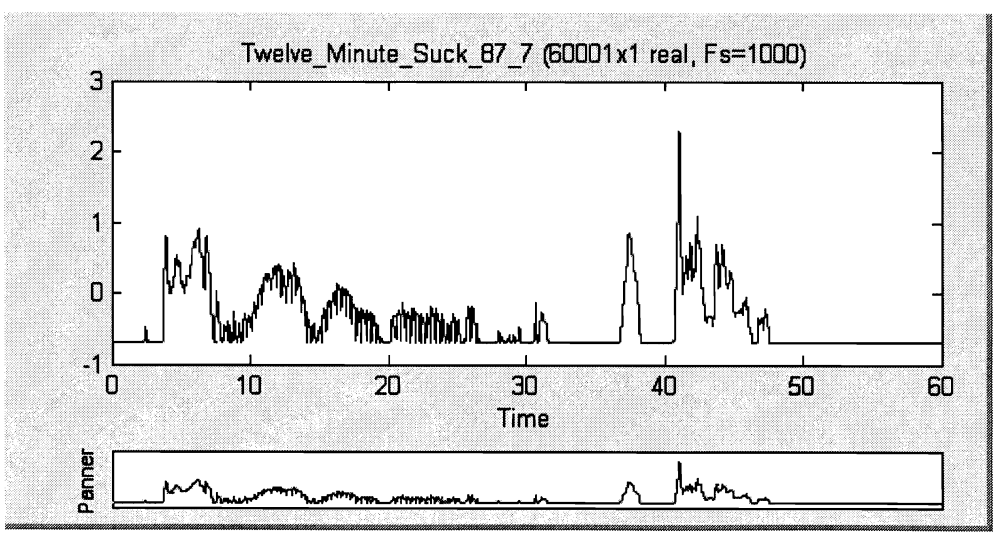

Figure 3.44: The 12th minute sucking for baby #87, seventh feeding

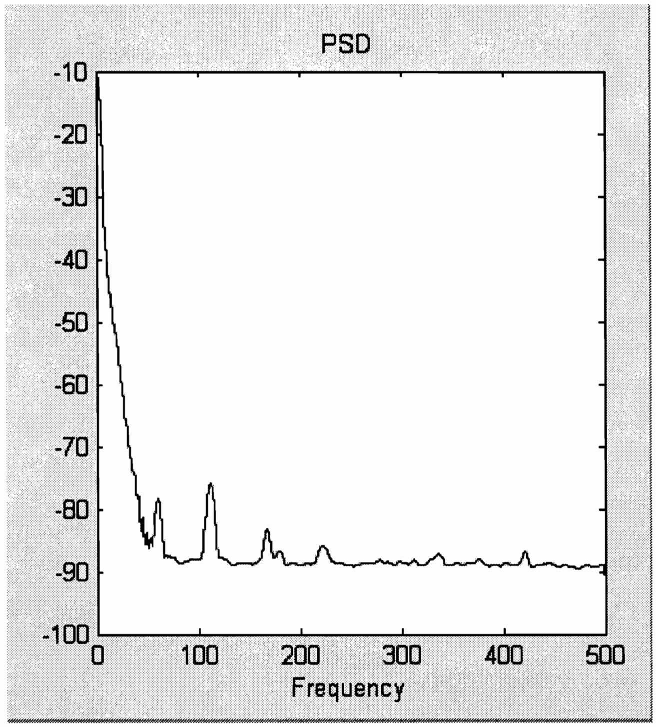

Figure 3.45: The spectral analysis of the 13th minute sucking of baby #87, seventh feeding

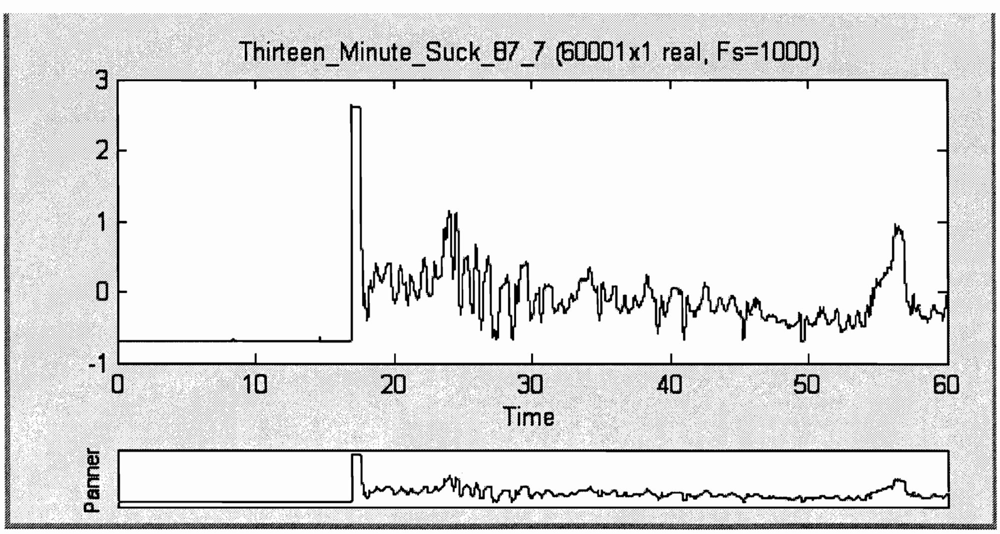

Figure 3.46: The 13th minute sucking for baby #87, seventh feeding

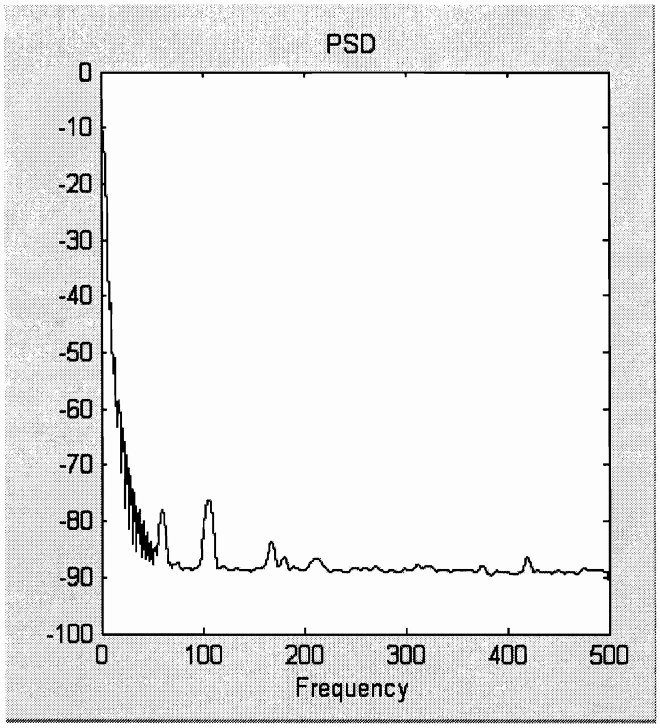

Figure 3.47: The spectral analysis of the 14th minute sucking of baby # 87, seventh feeding

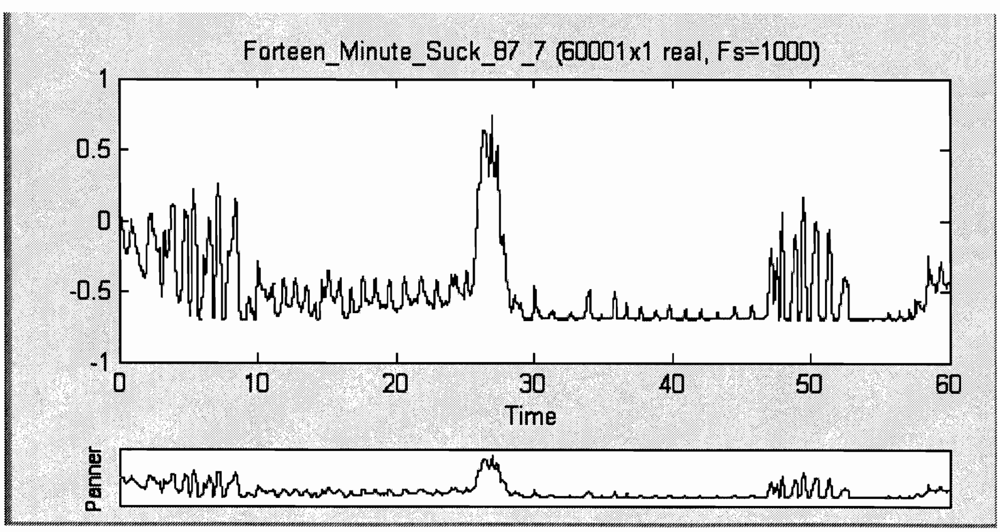

Figure 3.48: The 14th minute sucking of baby #87, seventh feeding

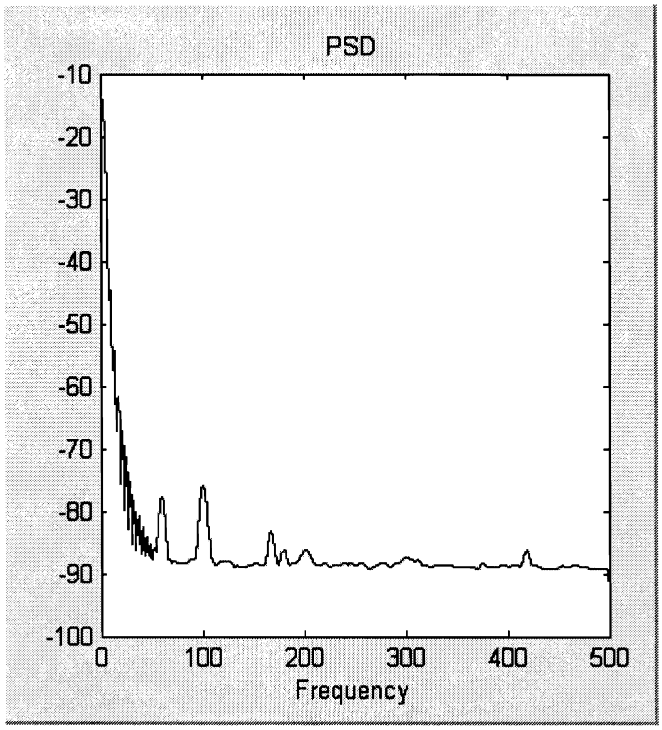

Figure 3.49: The spectral analysis of the 15th minute sucking of baby # 87, seventh feeding

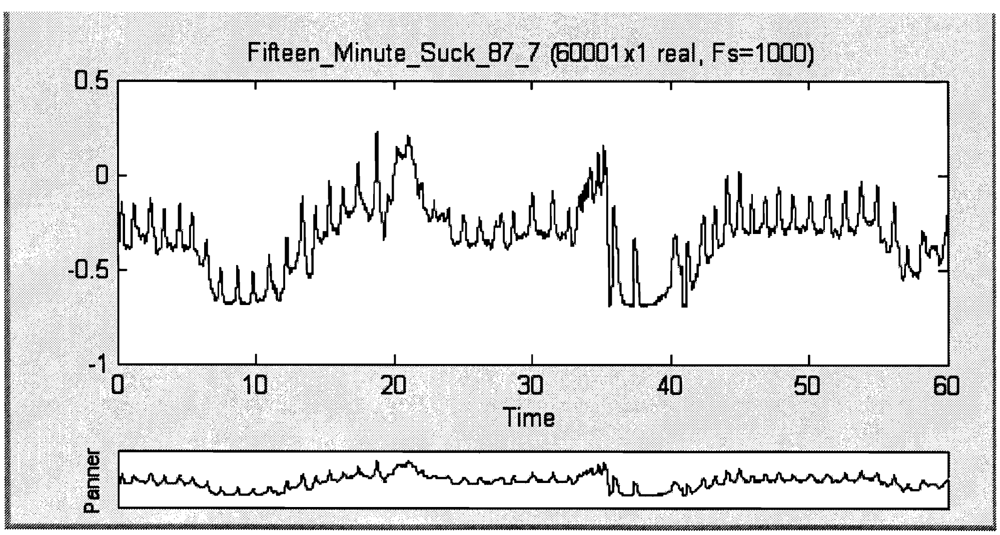

Figure 3.50: The 15th minute sucking of baby #87, seventh feeding

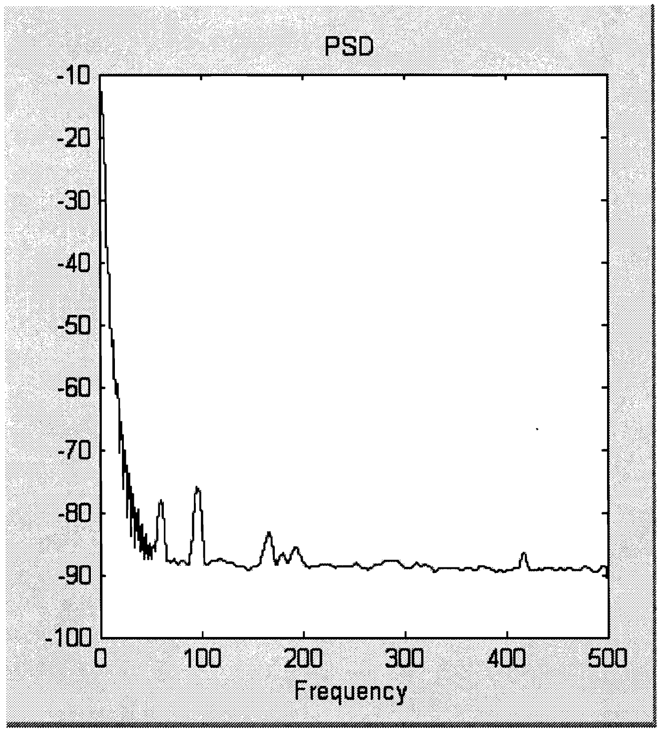

Figure 3.51: The spectral analysis of the 16th minute sucking of baby # 87, seventh feeding

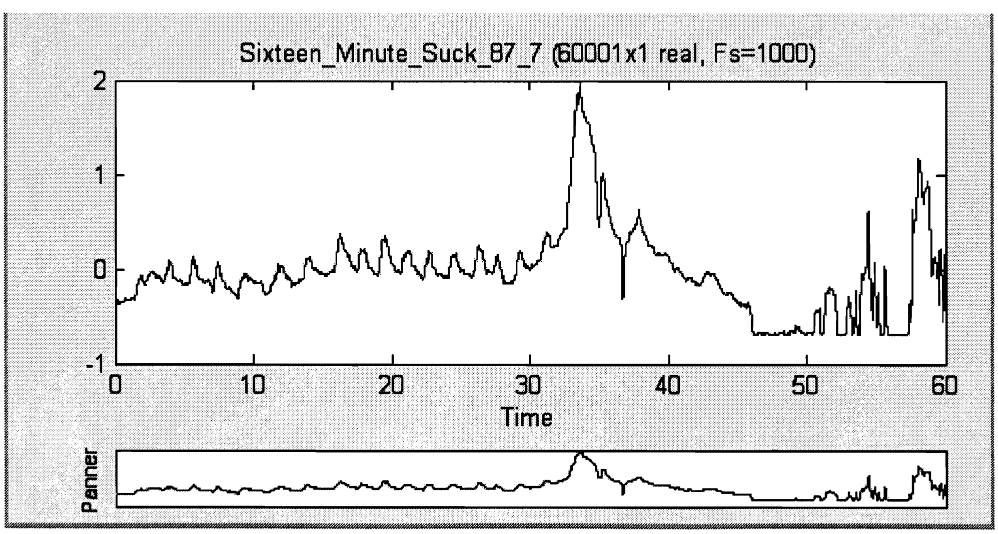

Figure 3.52: The 16th minute sucking of baby #87, seventh feeding

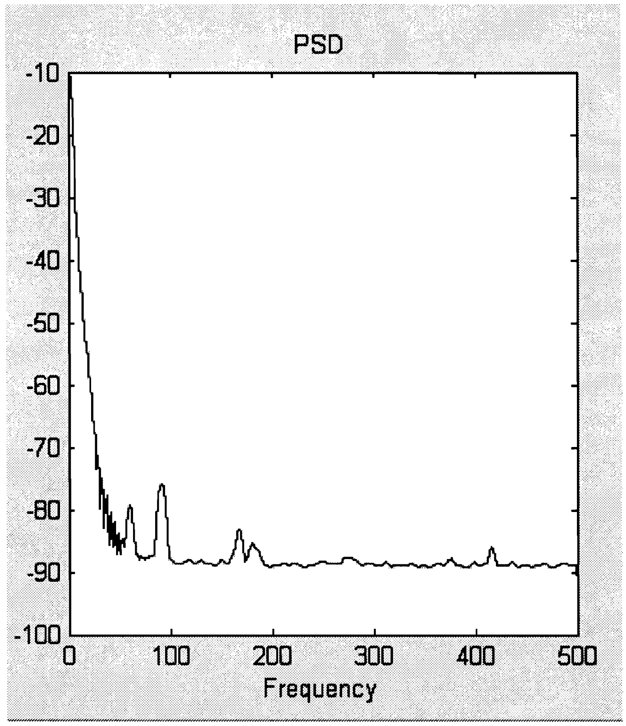

Figure 3.53: The spectral analysis of the17th minute sucking of baby #87, seventh feeding

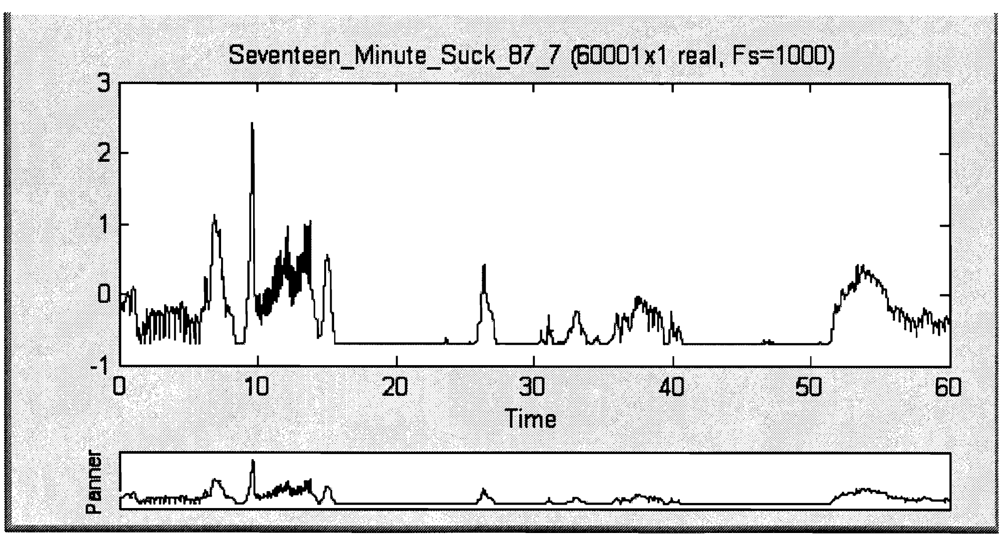

Figure 3.54: The17th minute sucking for baby # 87, seventh feeding

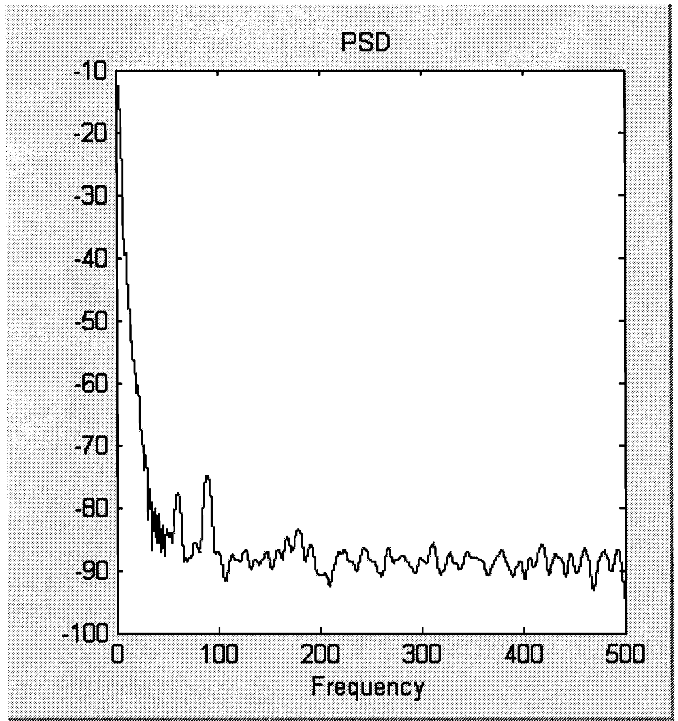

Figure 3.55: The spectral analysis of last minute sucking for baby #87, seventh feeding

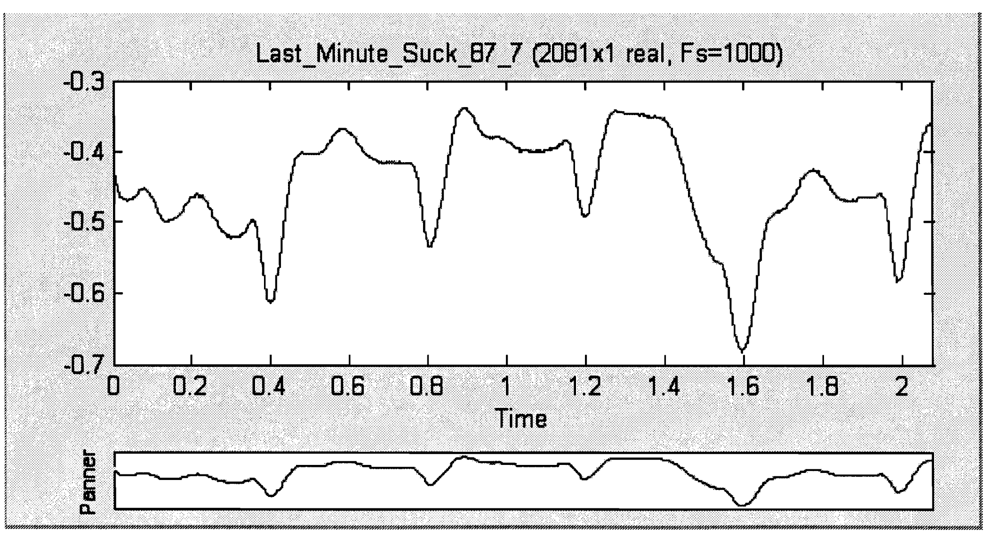

Figure 3.56: The last minute sucking of baby #87, seventh feeding

The Spectral Analysis of the Swallowing Waveform of Baby # 87, seventh feeding

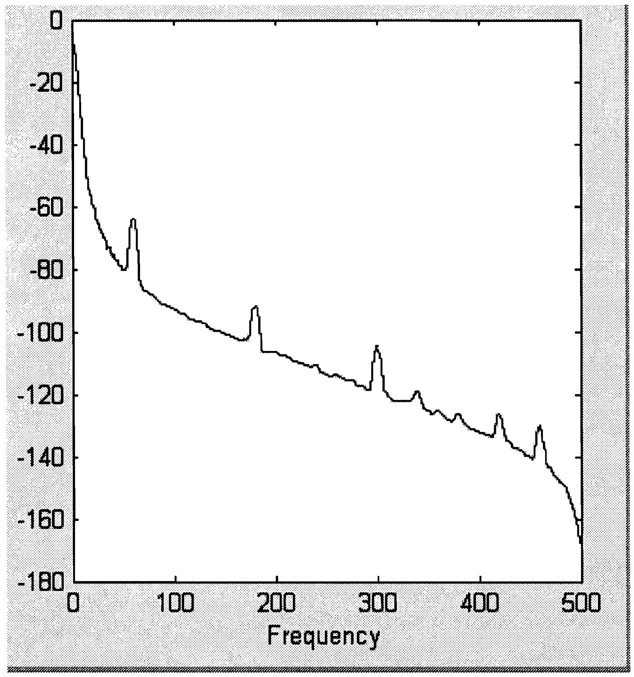

Figure 3.57: The spectral analysis of the first minute swallowing of baby # 87, seventh feeding

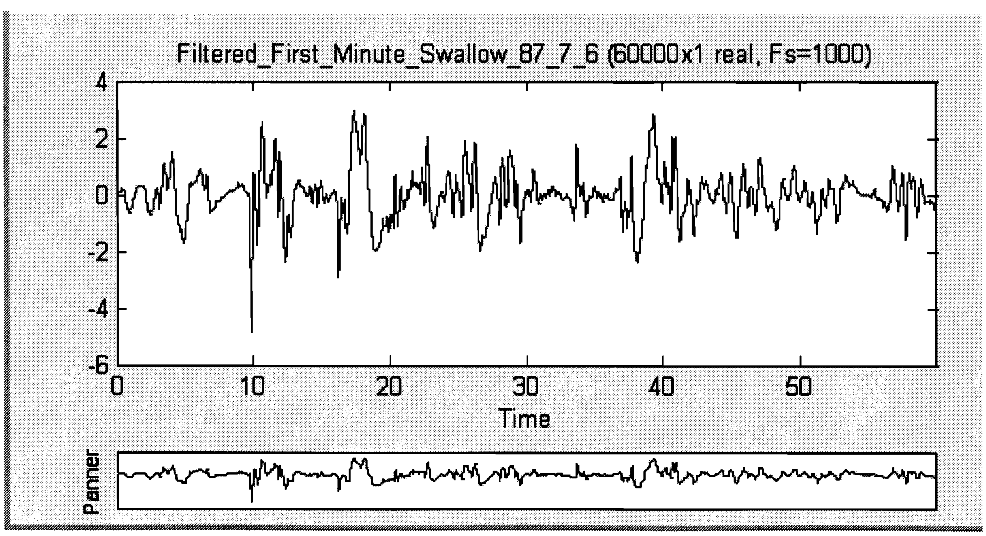

Figure 3.58: The first minute swallowing of baby # 87, seventh feeding

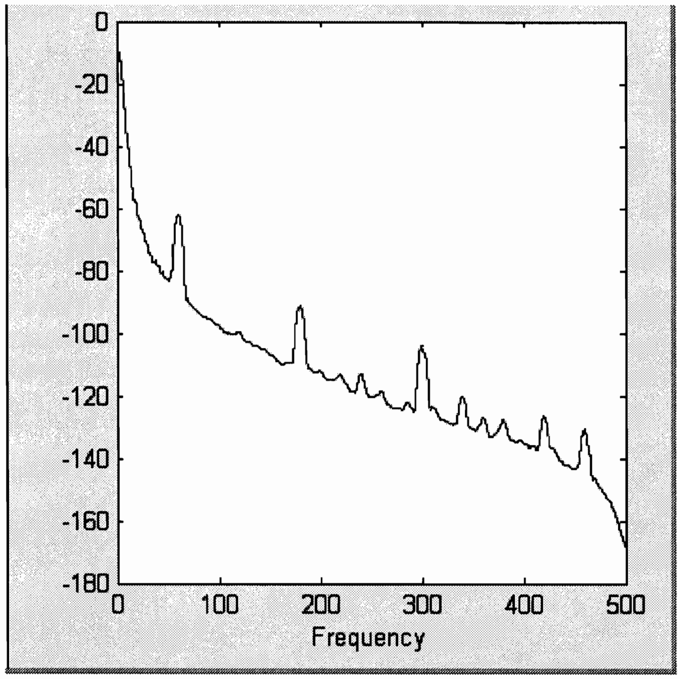

Figure 3.59: The spectral analysis of the second minute swallowing of baby #87, seventh feeding

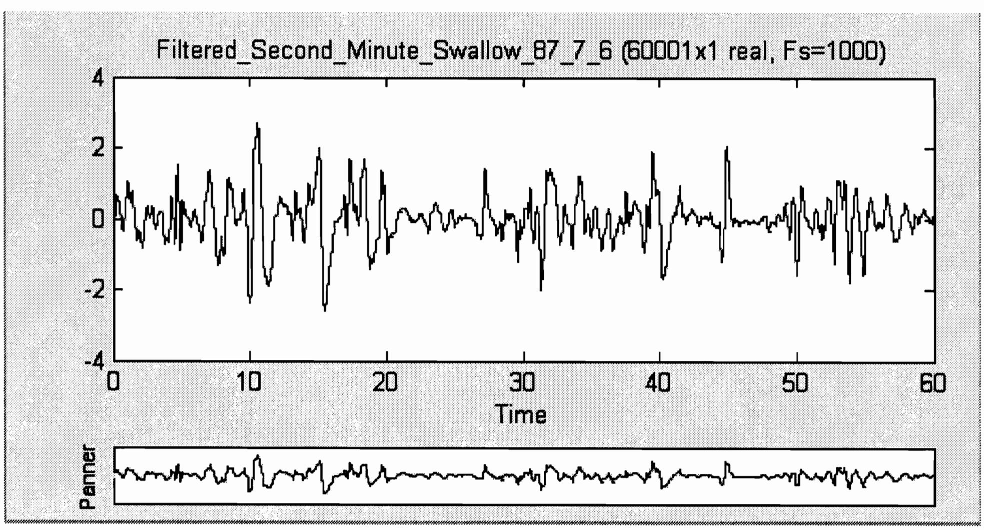

Figure 3.60: The second minute swallowing of baby #87, seventh feeding

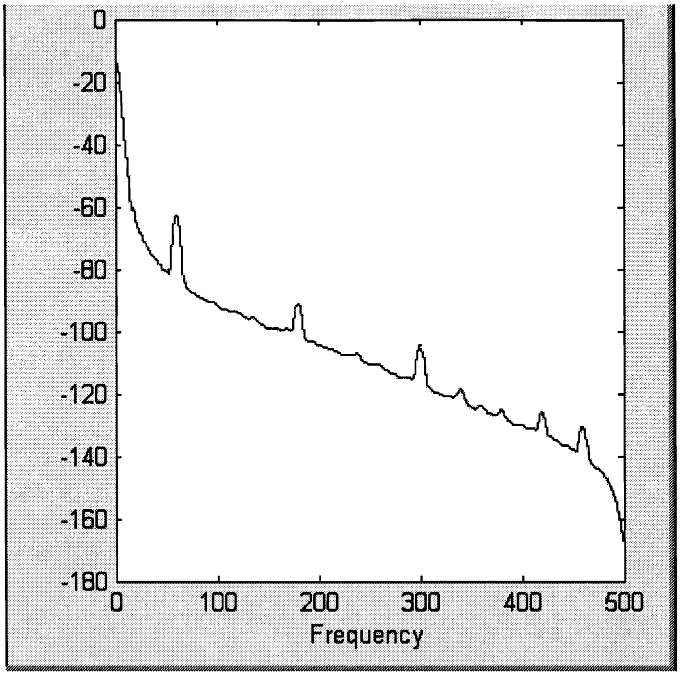

Figure 3.61: The spectral analysis of the third minute swallowing of baby # 87, seventh feeding

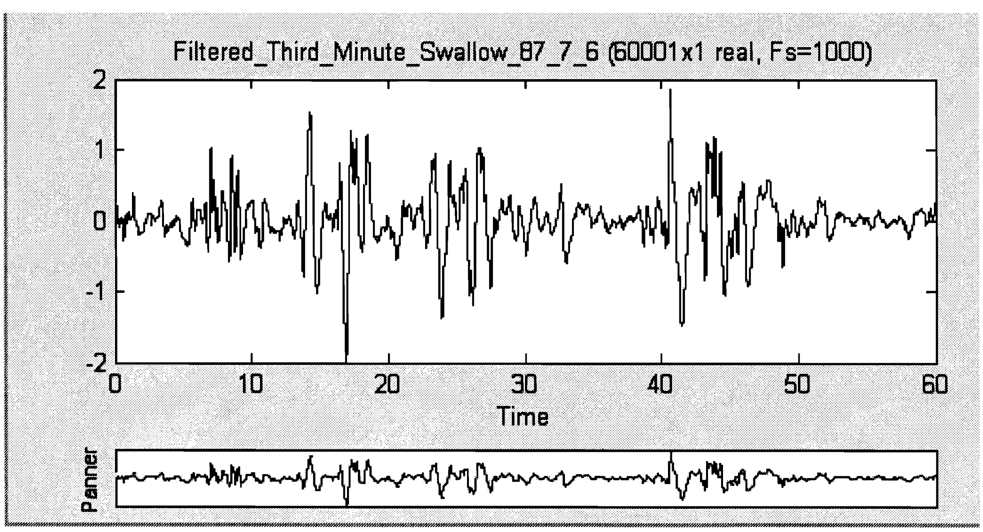

Figure 3.62: The third minute swallowing of baby # 87, seventh feeding

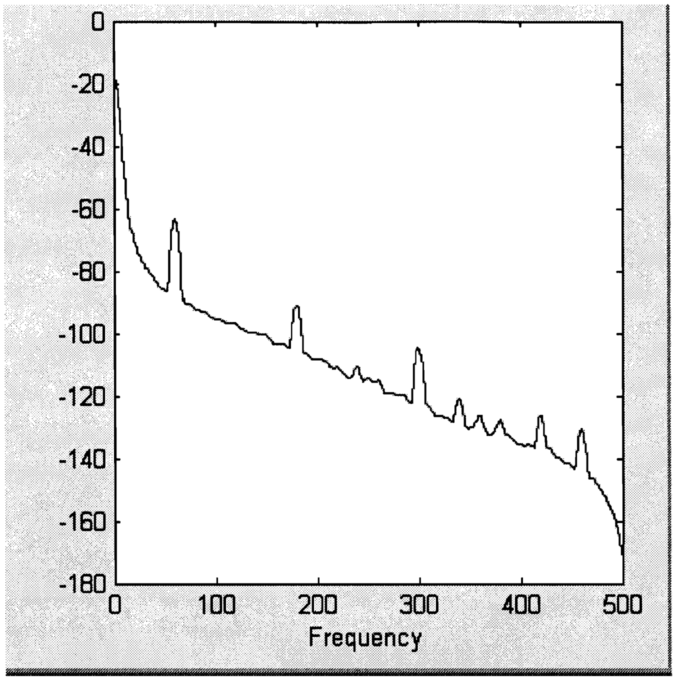

Figure 3.63: The spectral analysis of the forth minute swallowing of baby #87, seventh feeding

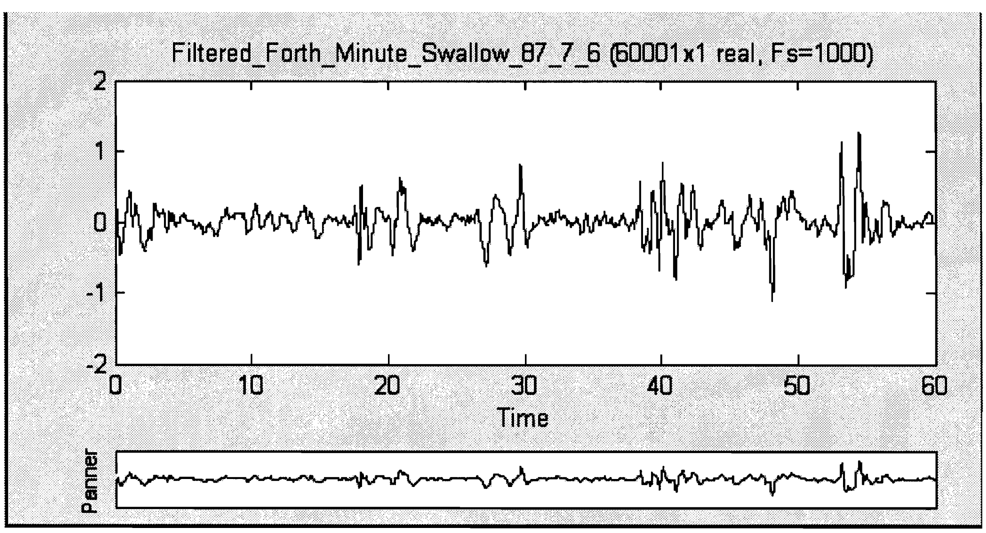

Figure 3.64: The forth minute swallowing of baby #87, seventh feeding

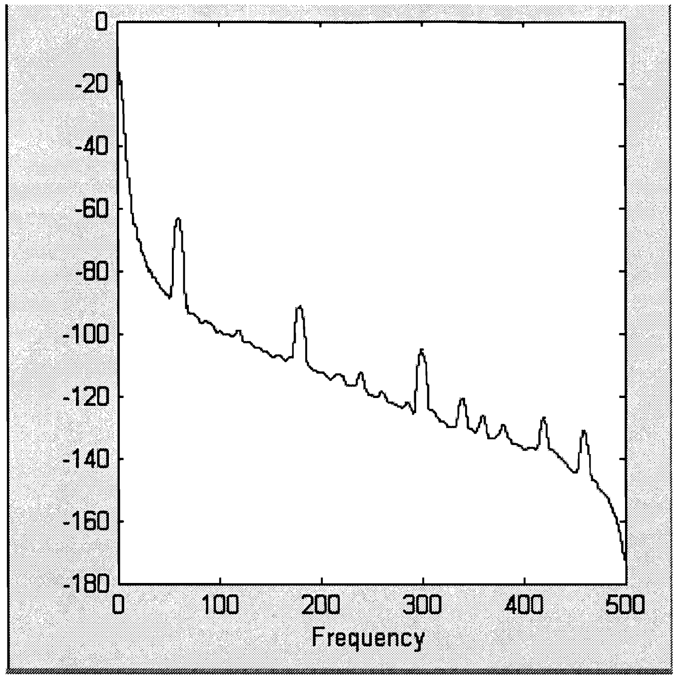

Figure 3.65: The spectral analysis of the fifth minute swallowing of baby #87, seventh feeding

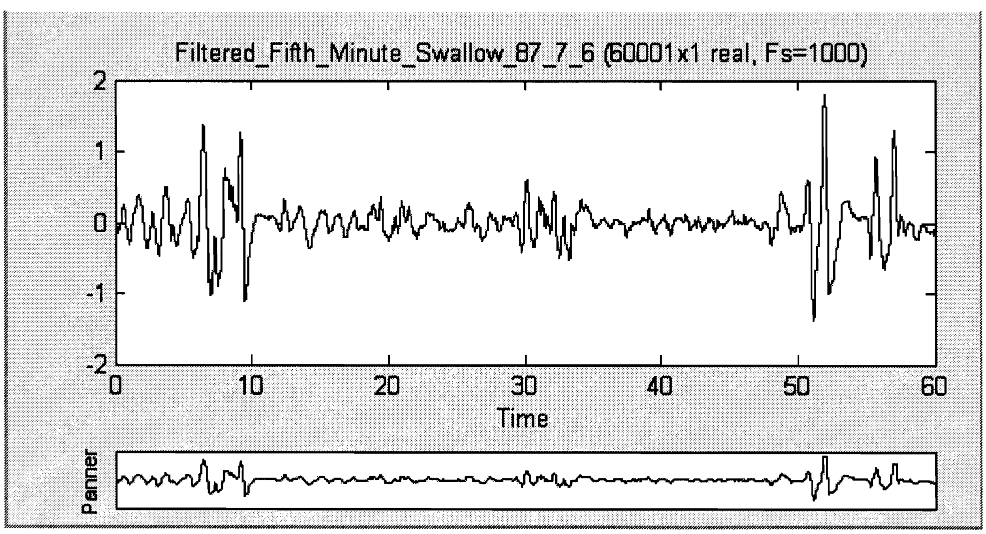

Figure 3.66: The fifth minute swallowing of baby #87, seventh feeding

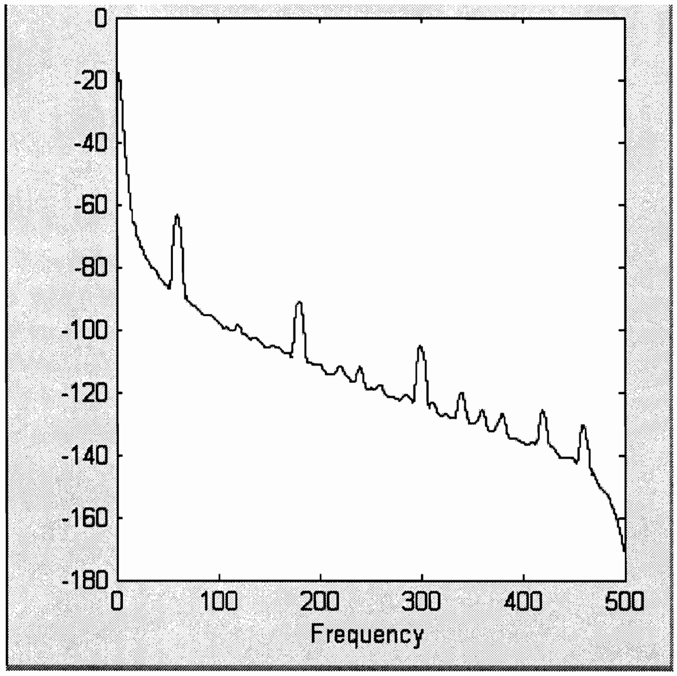

Figure 3.67: The spectral analysis of the sixth minute swallowing of baby #87, seventh feeding

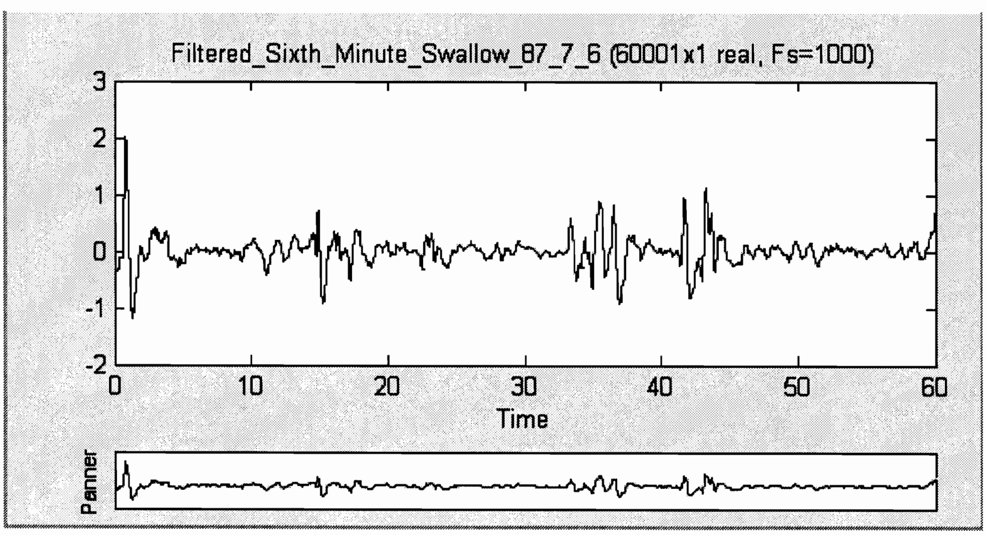

Figure 3.68: The sixth minute swallowing of baby #87, seventh feeding

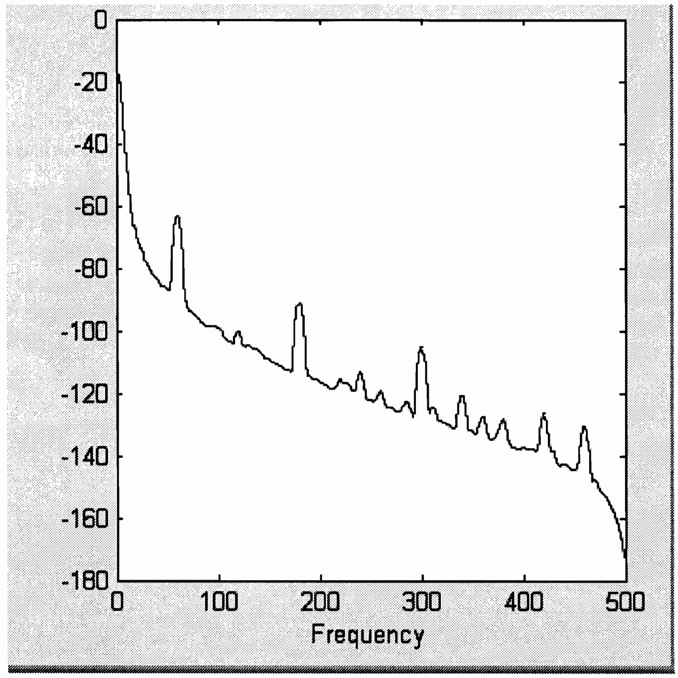

Figure 3.69: The spectral analysis of the seventh minute swallowing of baby # 87, seventh feeding

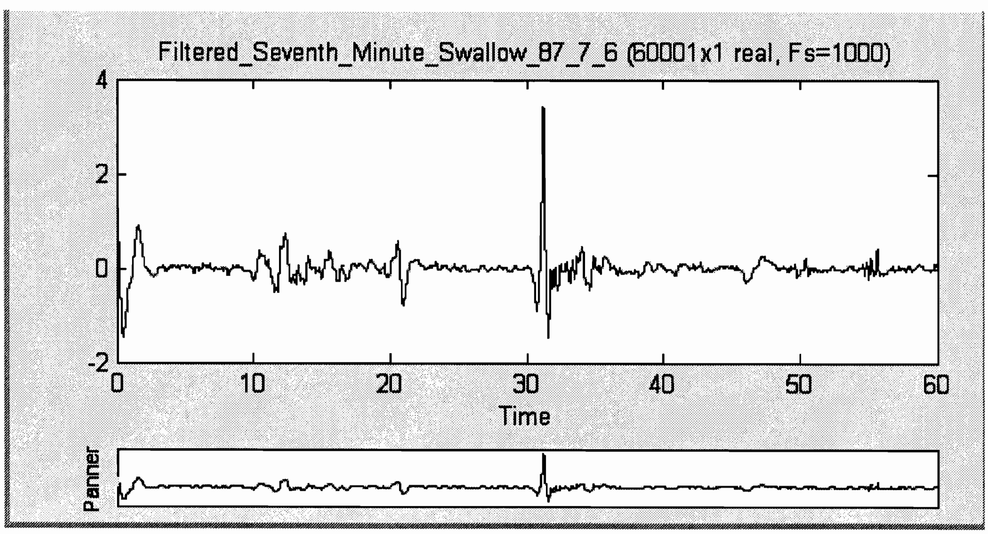

Figure 3.70: The seventh minute swallowing of baby #87, seventh feeding

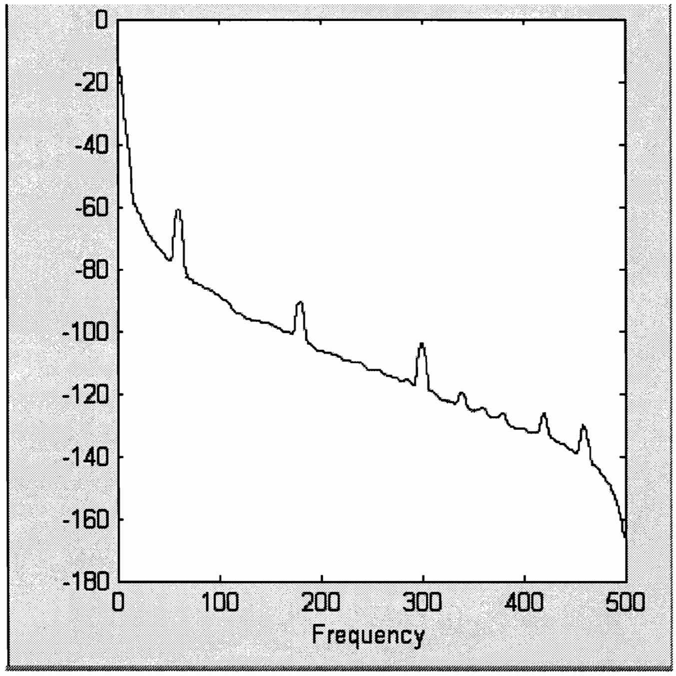

Figure 3.71: The spectral analysis of the eighth minute swallowing of baby #87, seventh feeding

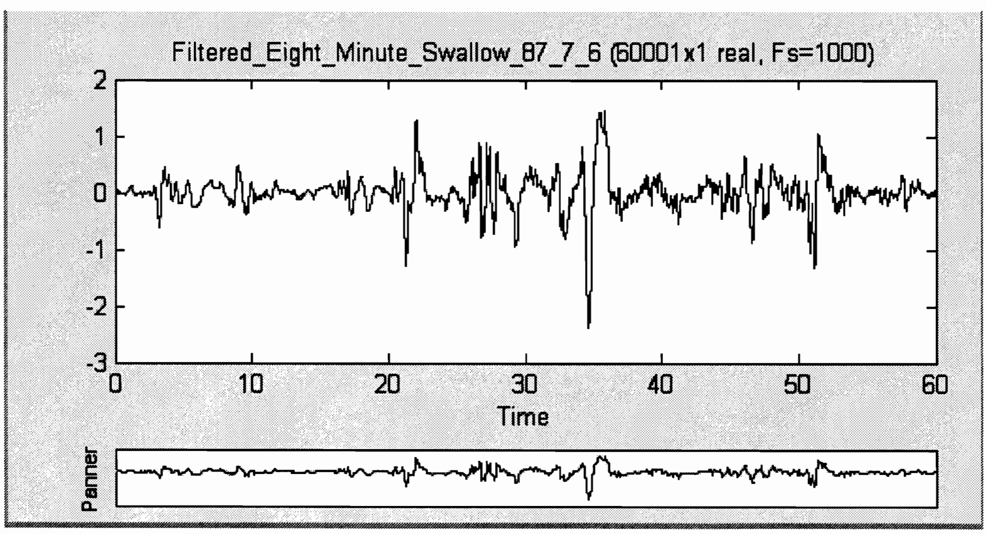

Figure 3.72: The eighth minute swallowing of baby # 87, seventh feeding

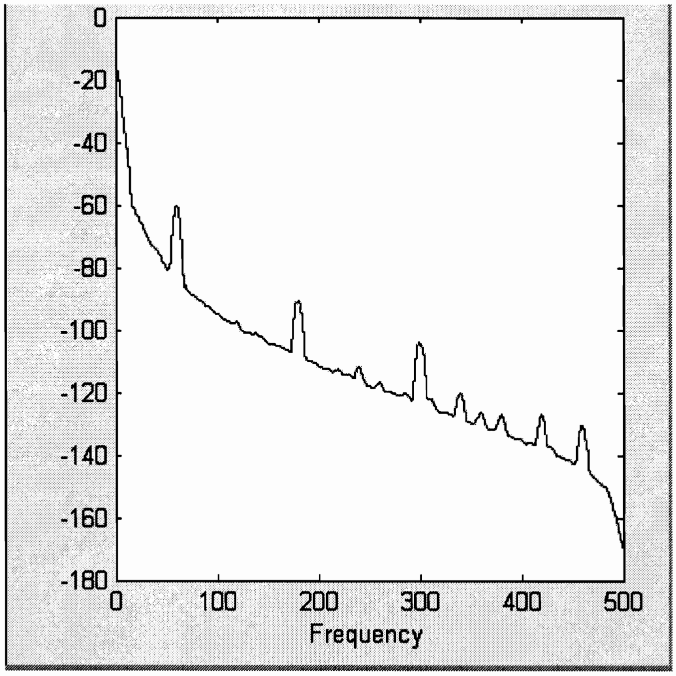

Figure 3.73: The spectral analysis of the ninth minute swallowing of baby #87, seventh feeding

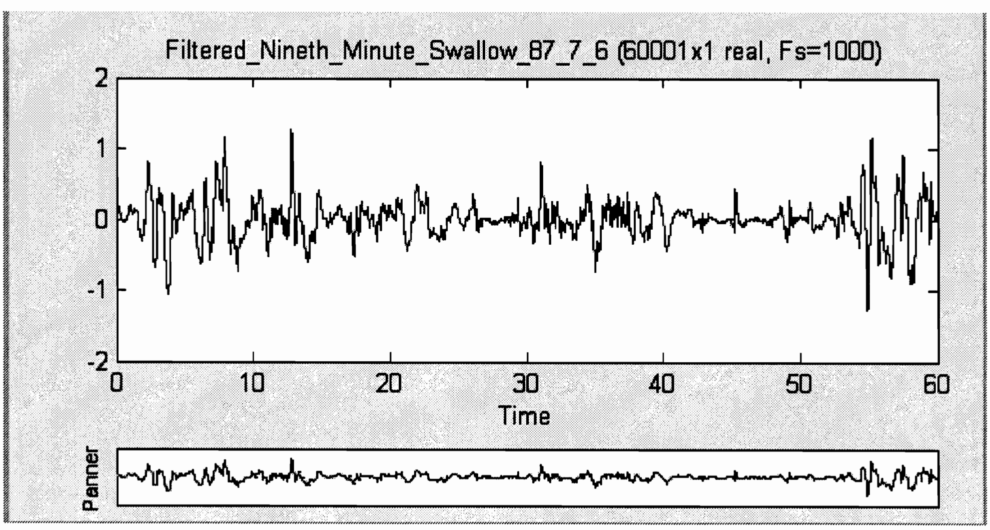

Figure 3.74: The ninth minute swallowing of baby # 87, seventh feeding

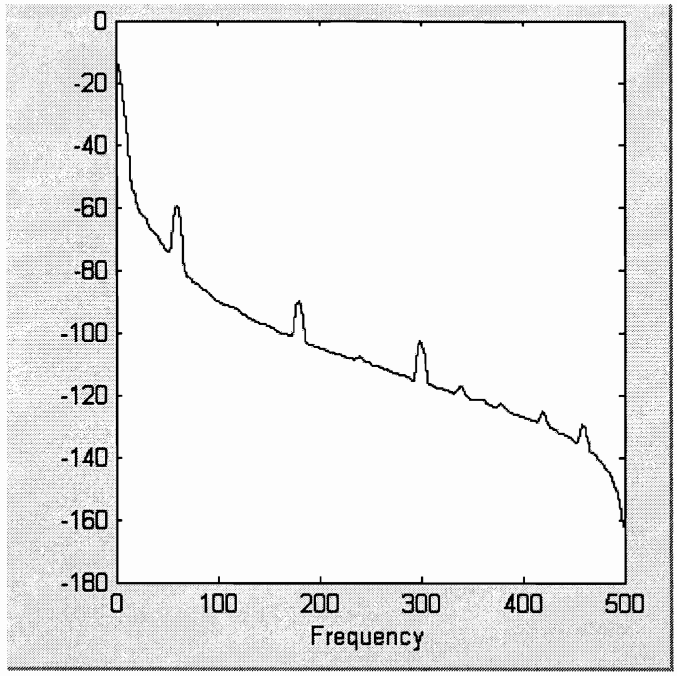

Figure 3.75: The spectral analysis of the10th minute swallowing of baby #87, seventh feeding

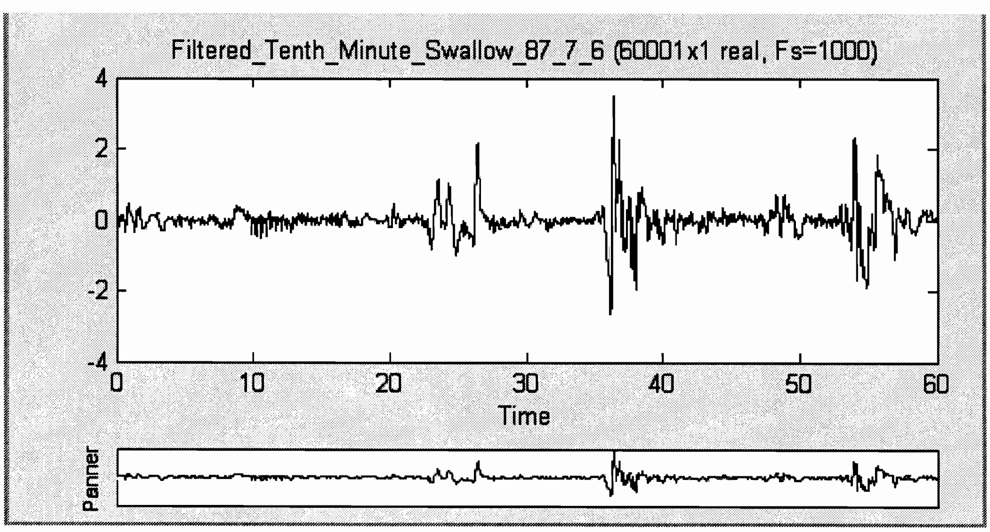

Figure 3.76: The 10th minute swallowing of baby #87, seventh feeding

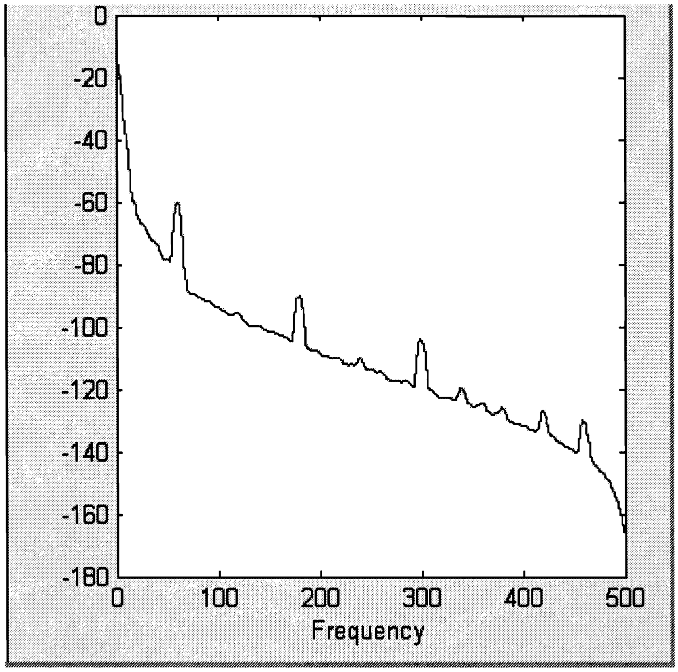

Figure 3.77: The spectral analysis of the11th minute swallowing of baby #87, seventh feeding

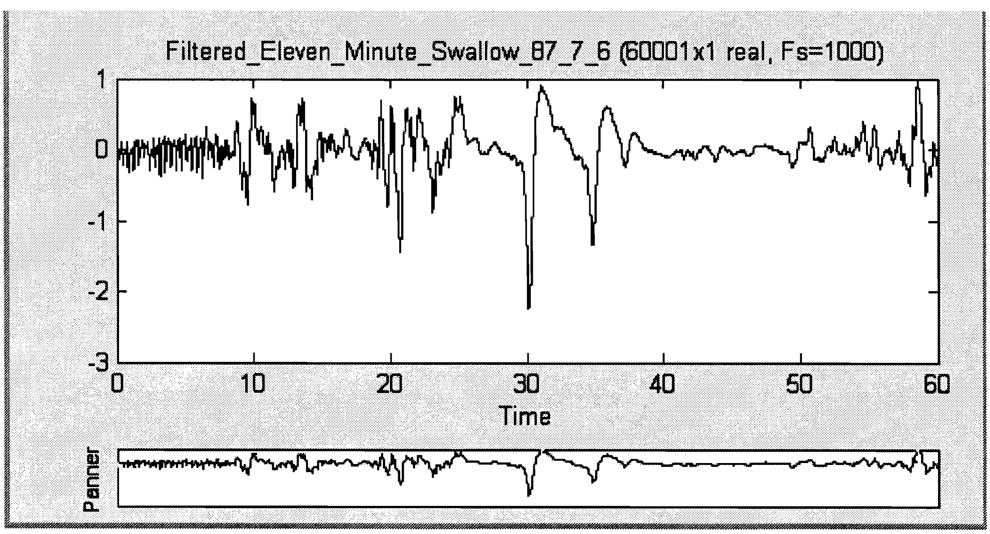

Figure 3.78: The11th minute swallowing for baby #87, seventh feeding

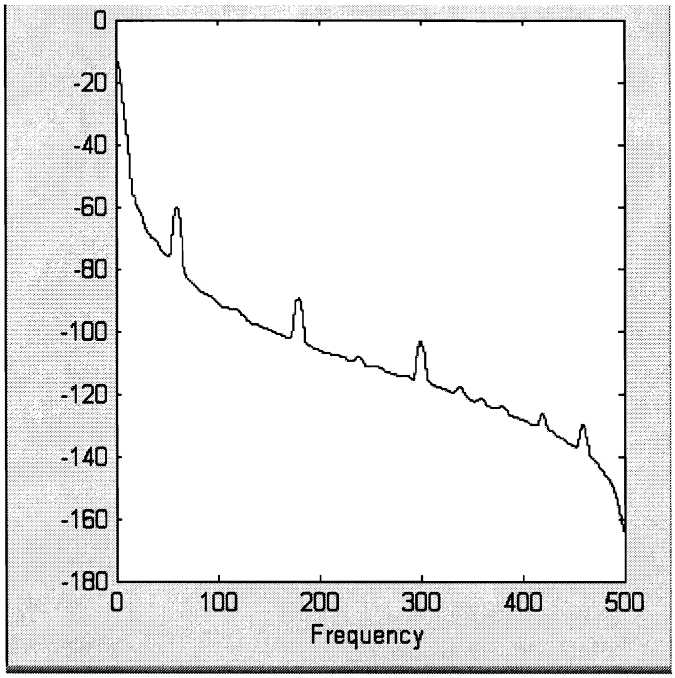

Figure 3.79: The spectral analysis of the12th minute swallowing of baby #87, seventh feeding

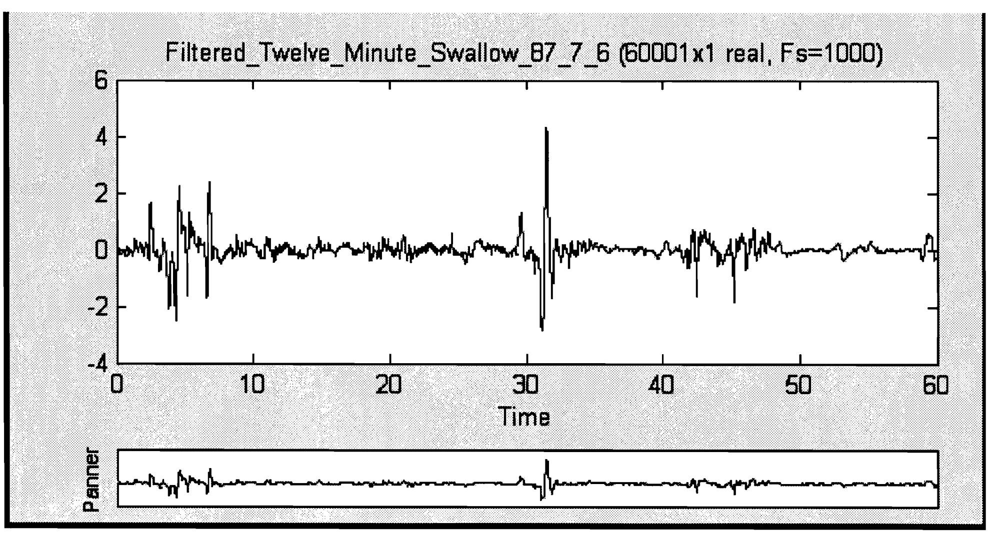

Figure 3.80: The12th minute swallowing of baby #87, seventh feeding

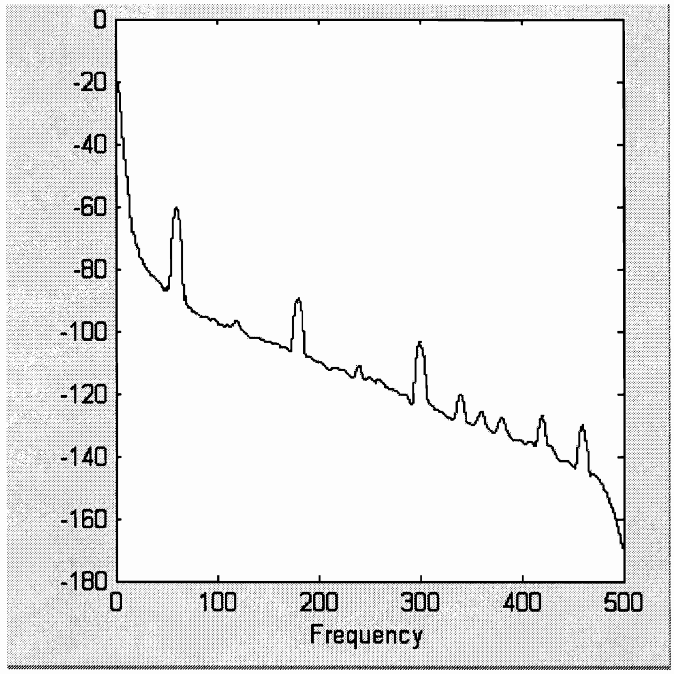

Figure 3.81: The spectral analysis of the13th minute swallowing of baby #87, seventh feeding

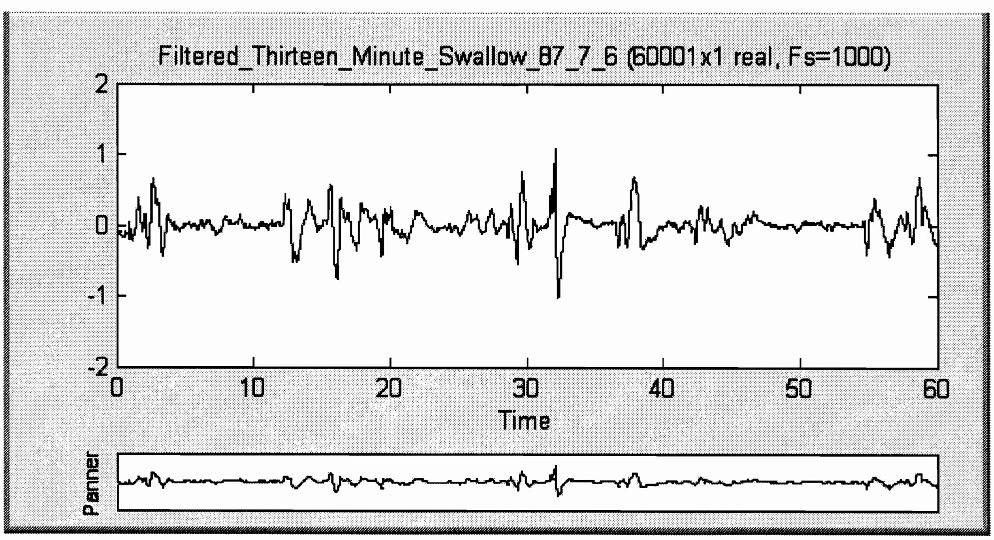

Figure 3.82: The 13th minute swallowing of baby #87, seventh feeding

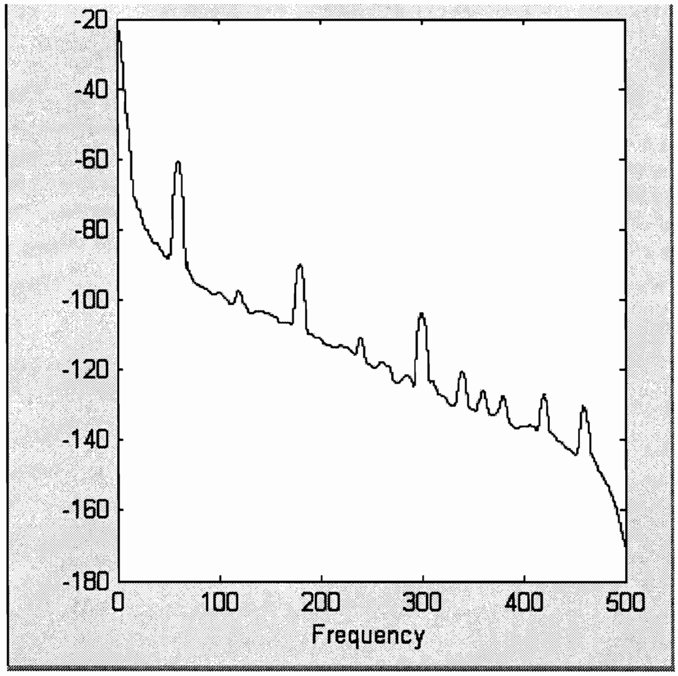

Figure 3.83: The spectral analysis of the14[th] minute swallowing of baby #87, seventh feeding

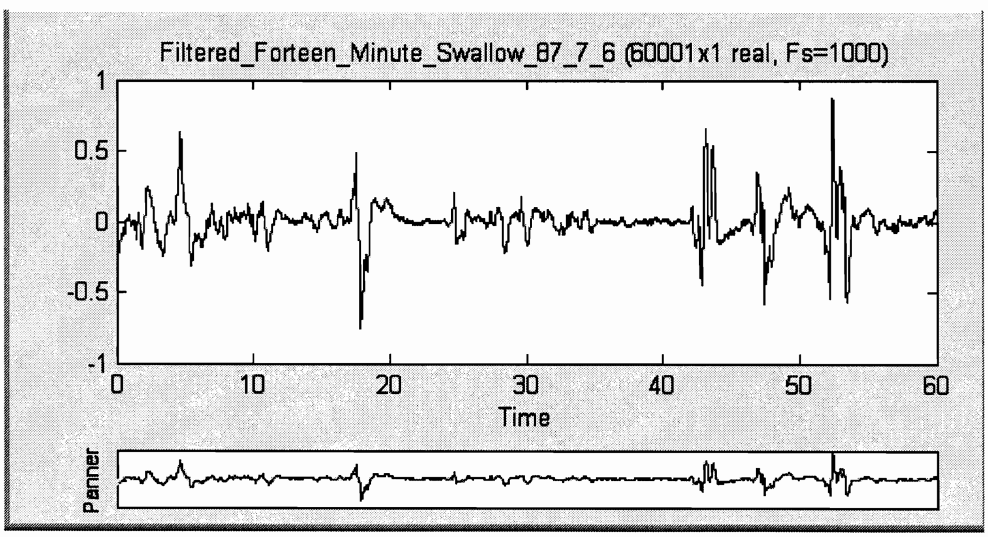

Figure 3.84: The13[th] minute swallowing of baby #87, seventh feeding

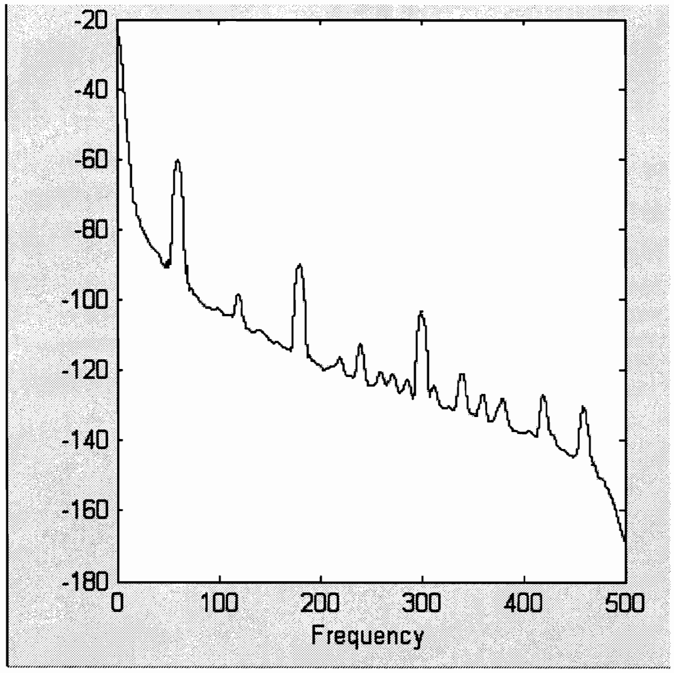

Figure 3.85: The spectral analysis of the15th minute swallowing of baby #87, seventh feeding

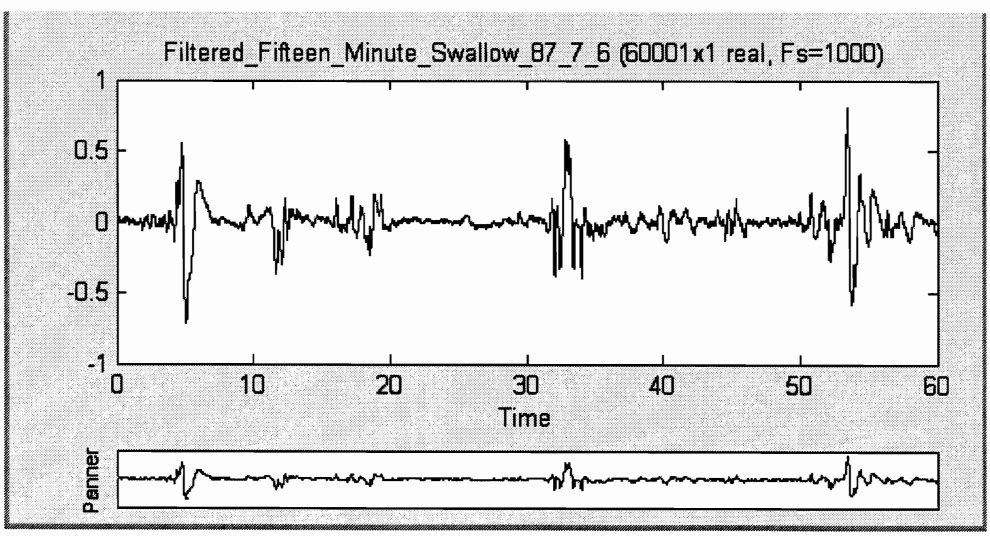

Figure 3.86: The15th minute swallowing of baby #87, seventh feeding

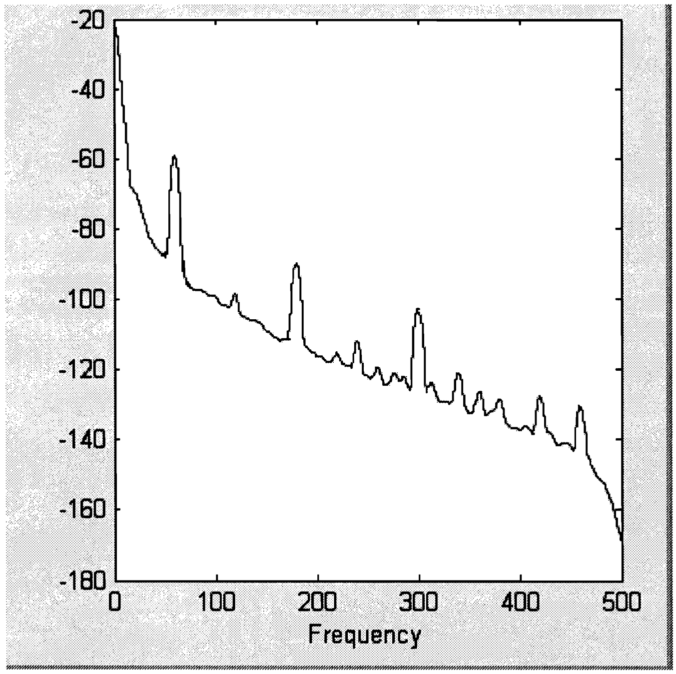

Figure 3.87: The spectral analysis of the16th minute swallowing of baby #87, seventh feeding

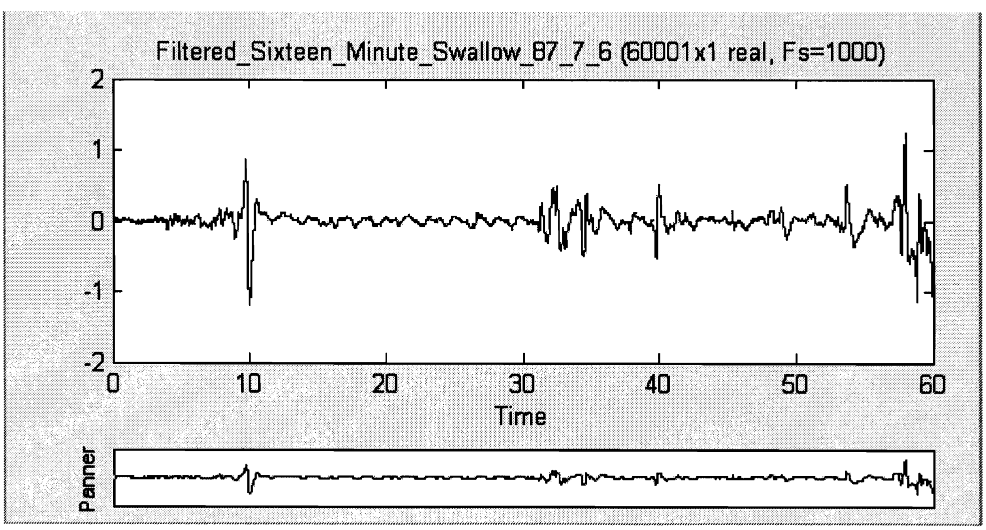

Figure 3.88: The16th minute swallowing of baby #87, seventh feeding

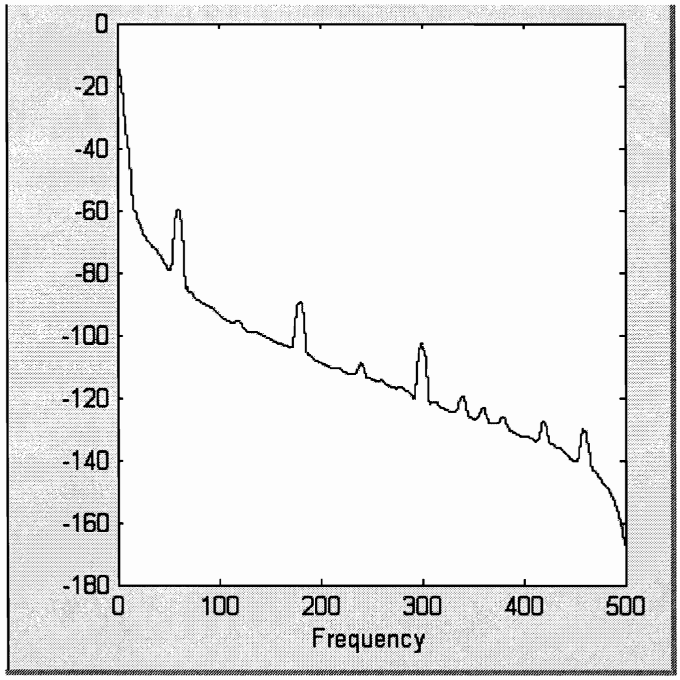

Figure 3.89: The spectral analysis of the17th minute swallowing of baby #87, seventh feeding

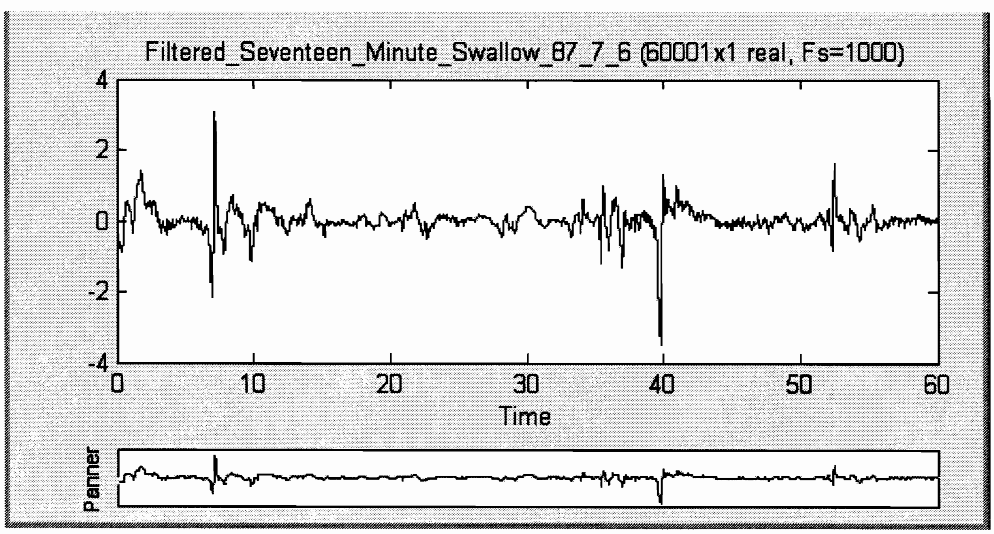

Figure 3.90: The17th minute swallowing of baby #87, seventh feeding

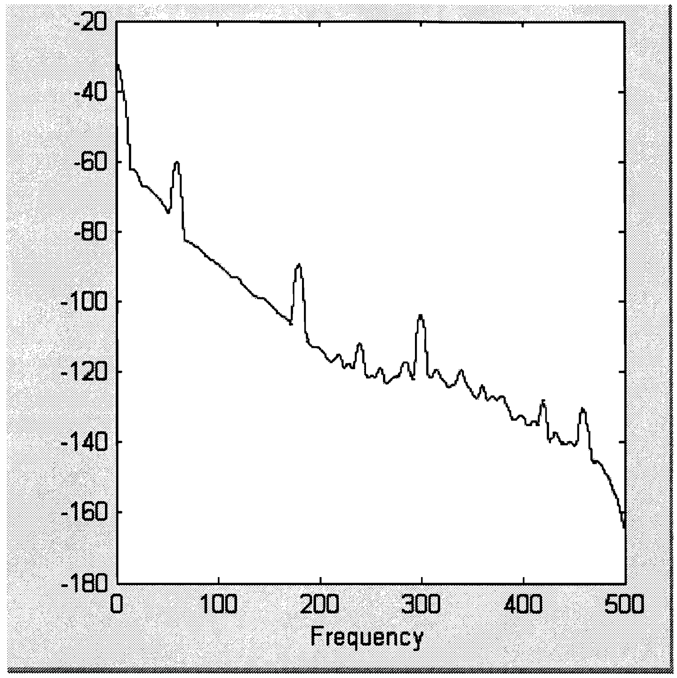

Figure 3.91: The spectral analysis of the last minute swallowing of baby # 87, seventh feeding

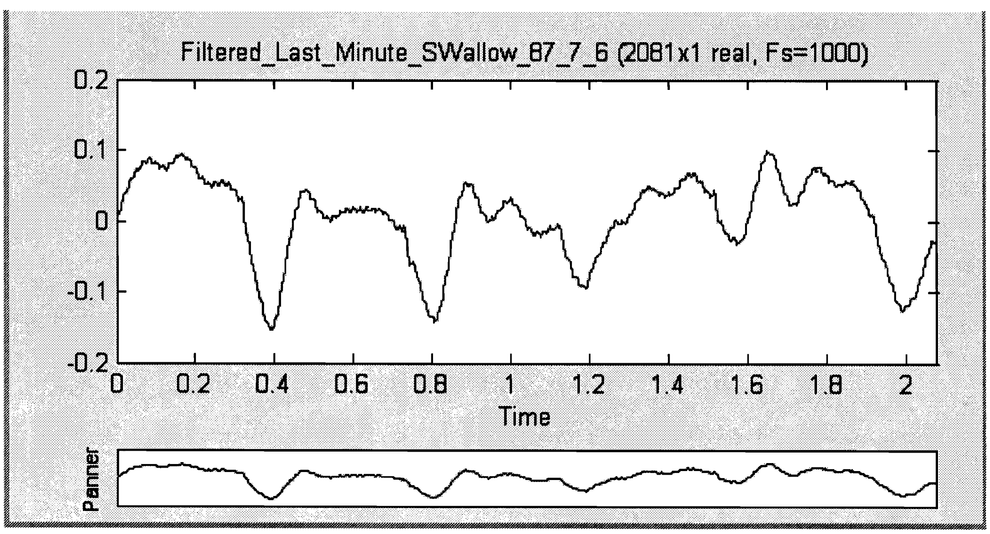

Figure 3.92: The last minute swallowing of baby #87, seventh feeding

The Spectral Analysis of Breathing Waveform of Baby # 81, 10^{th} feeding

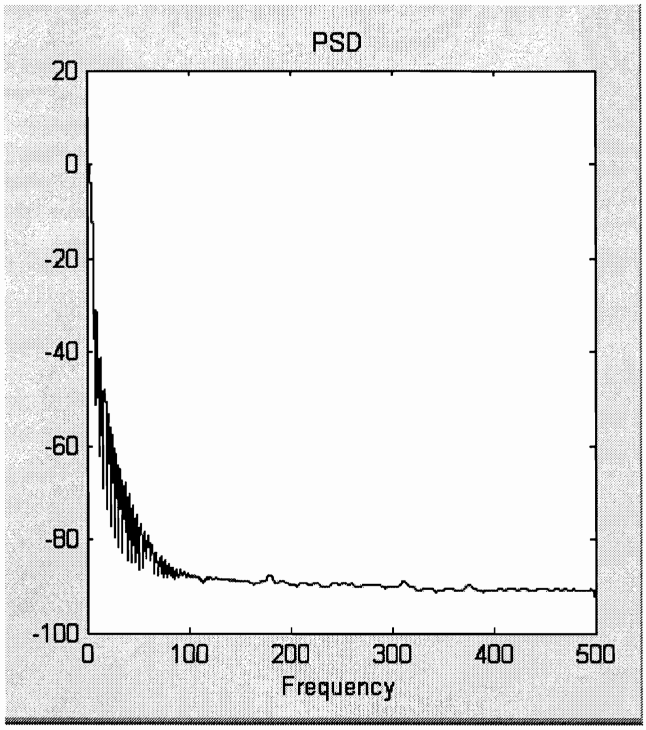

Figure 3.93: The spectral analysis of the first minute breathing of baby # 81, 10^{th} feeding

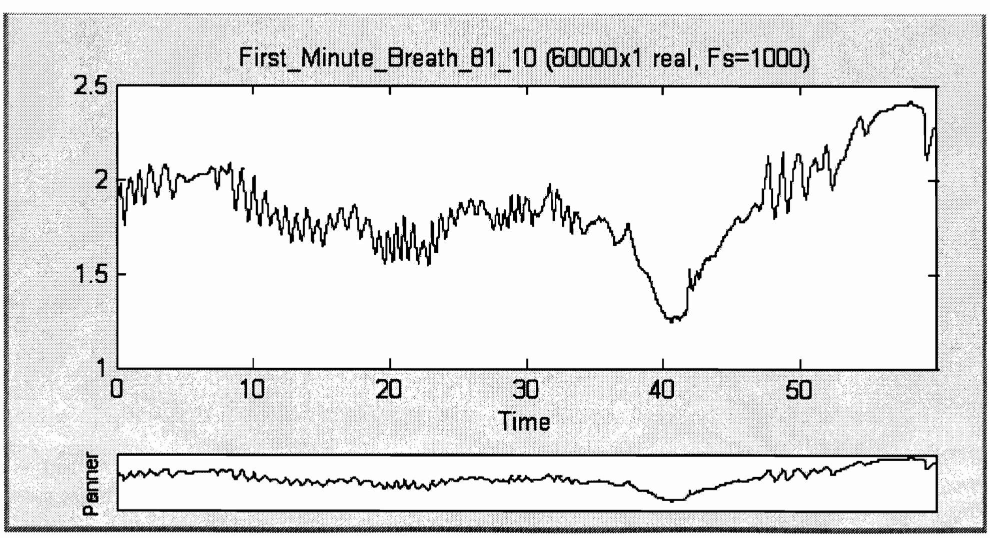

Figure 3.94: The first minute breathing of baby # 81, 10^{th} feeding

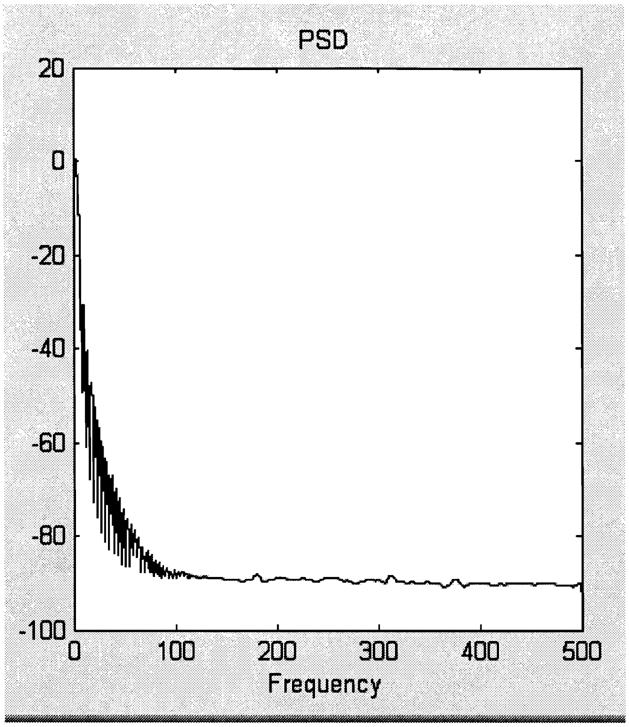

Figure 3.95: The spectral analysis of the second minute breathing of baby # 81, 10th feeding

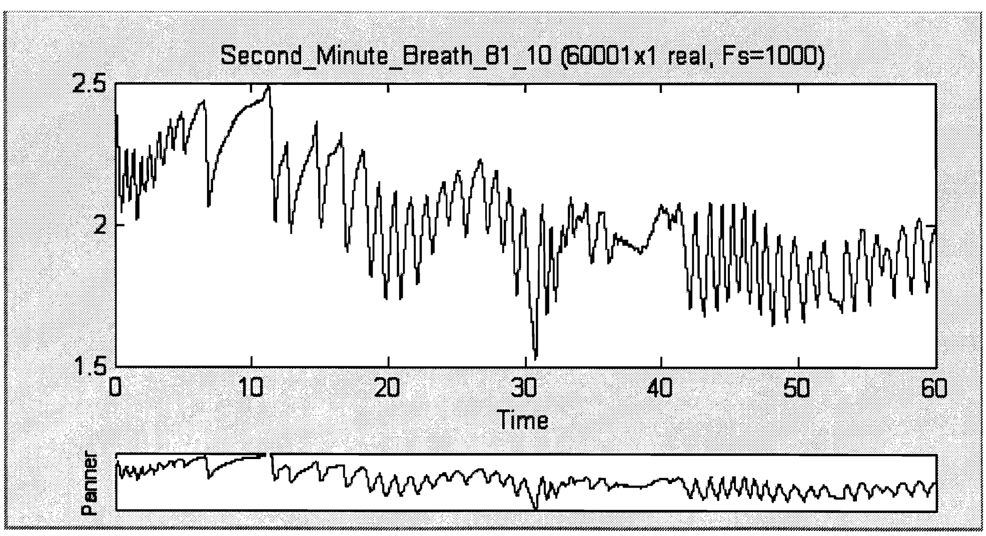

Figure 3.96: The second minute breathing of baby # 81, 10th feeding

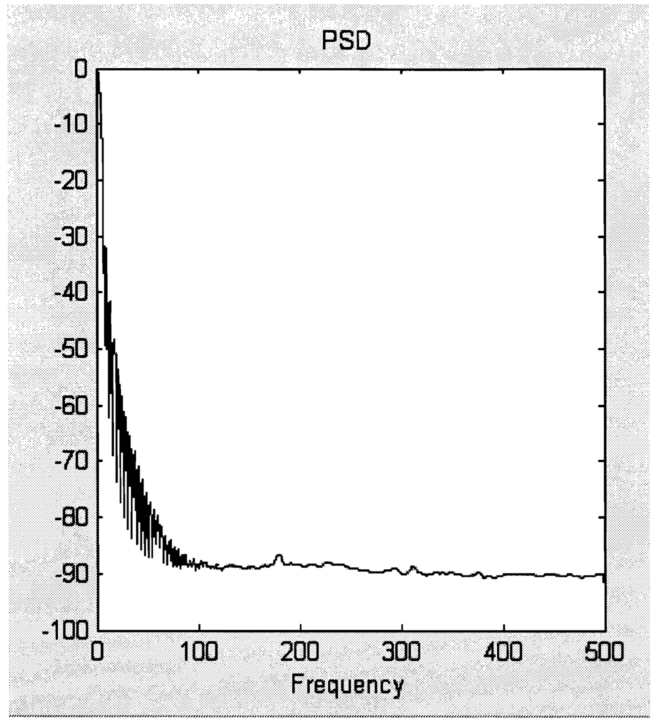

Figure 3.97: The spectral analysis of the third minute breathing of baby # 81, 10th feeding

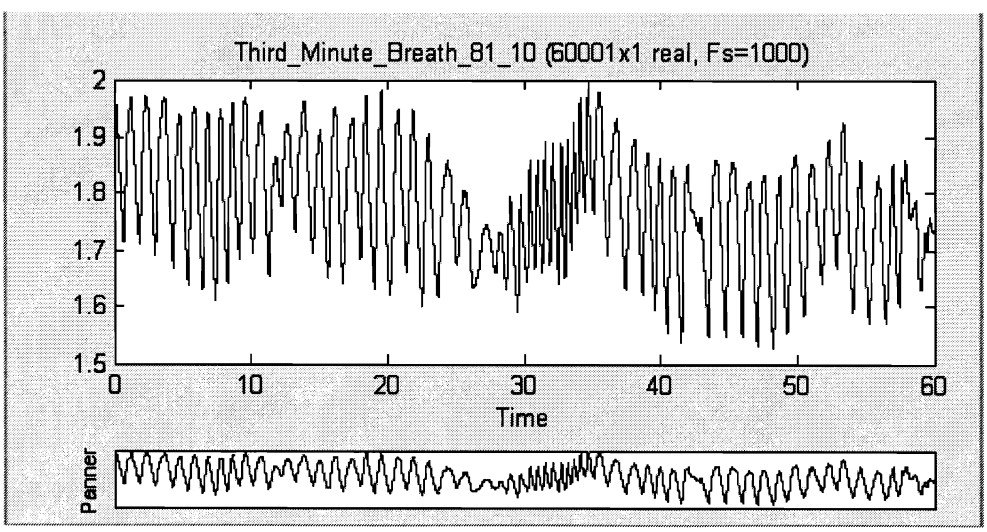

Figure 3.98: The third minute breathing of baby #81, 10th feeding

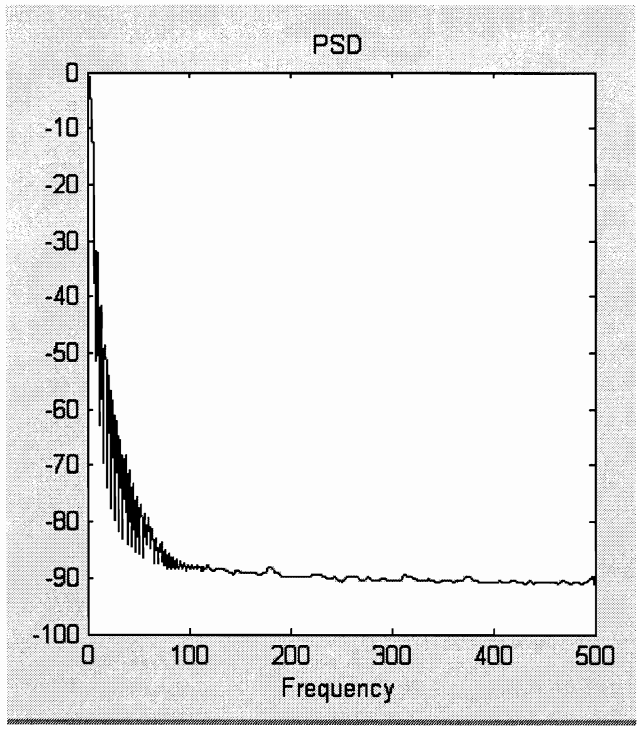

Figure 3.99: The spectral analysis of the forth minute breathing for baby #81, 10th feeding

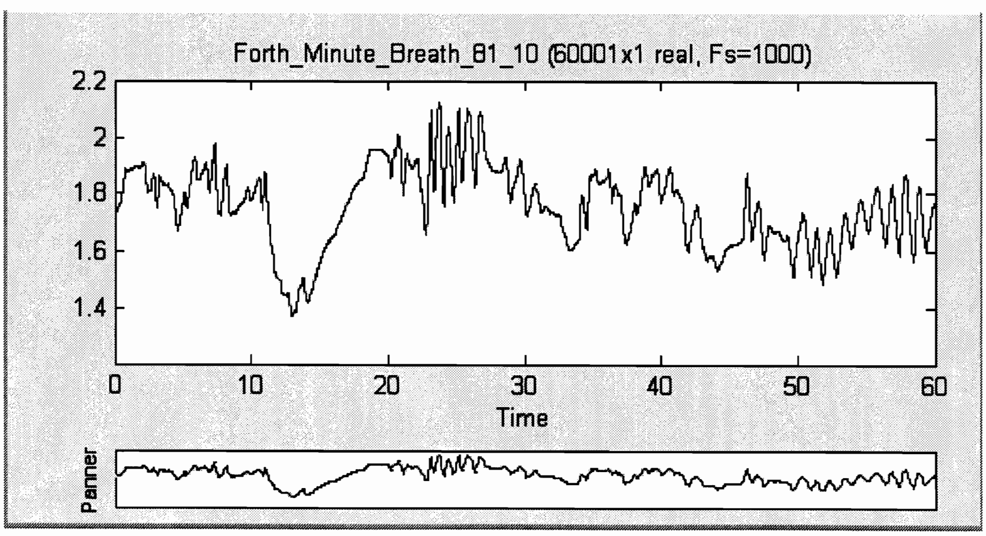

Figure 3.100: The forth minute breathing of baby # 81, 10th feeding

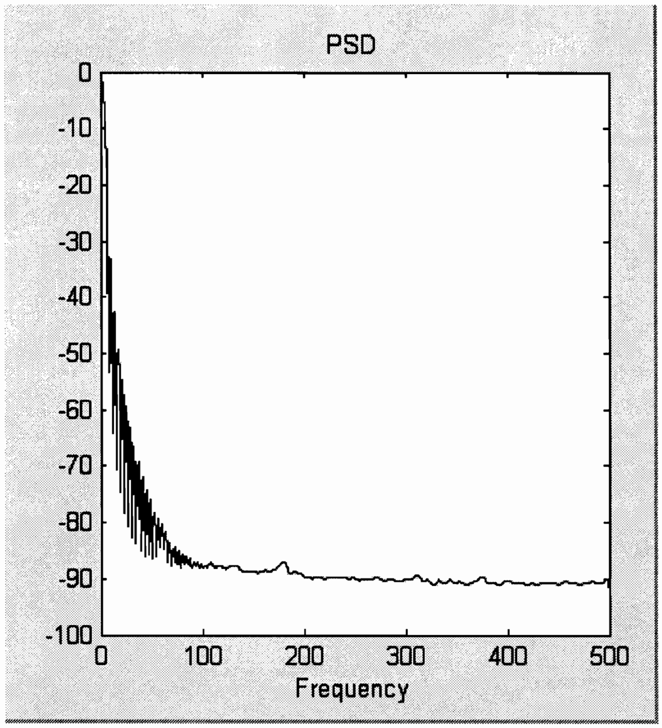

Figure 3.101: The spectral analysis of the fifth minute breathing for baby #81, 10th feeding

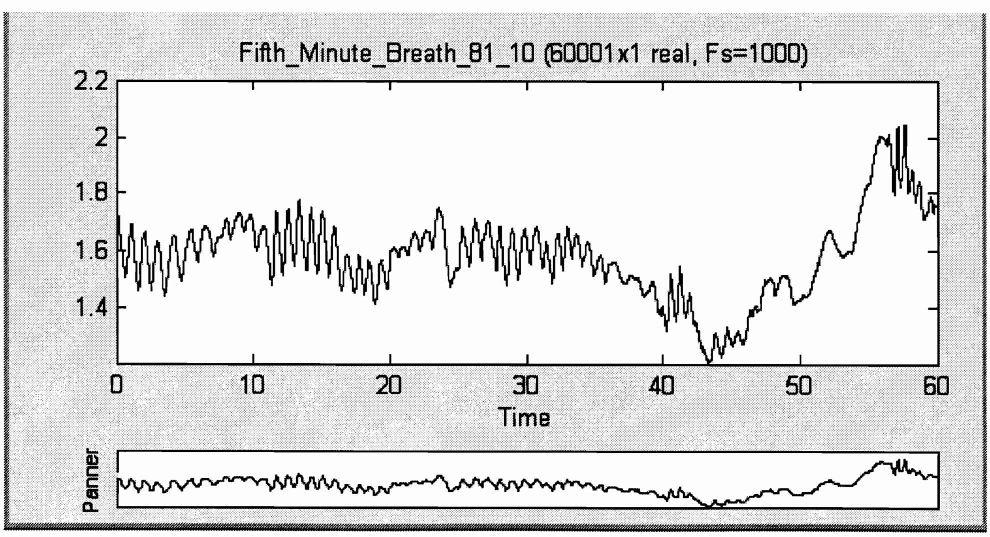

Figure 3.102: The fifth minute breathing of baby #81, 10th feeding

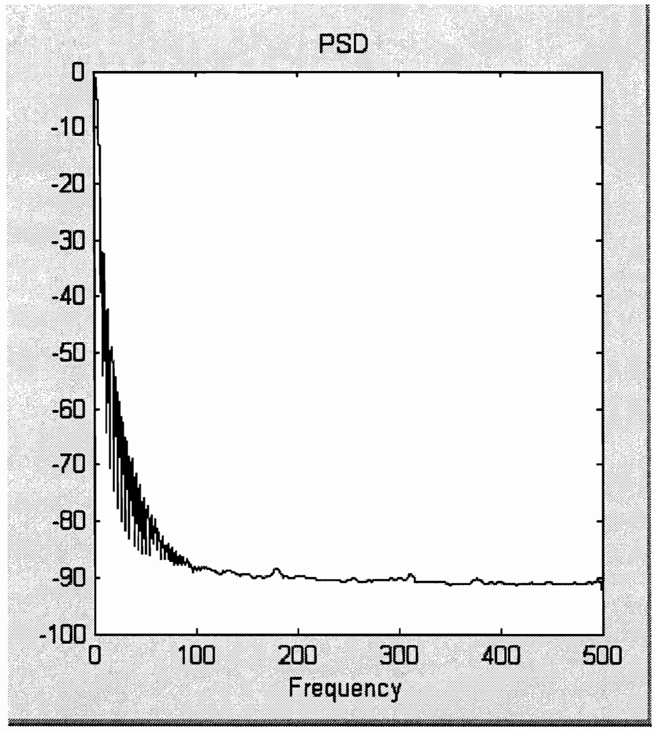

Figure 3.103: The spectral analysis of the sixth minute breathing of baby # 81, 10th feeding

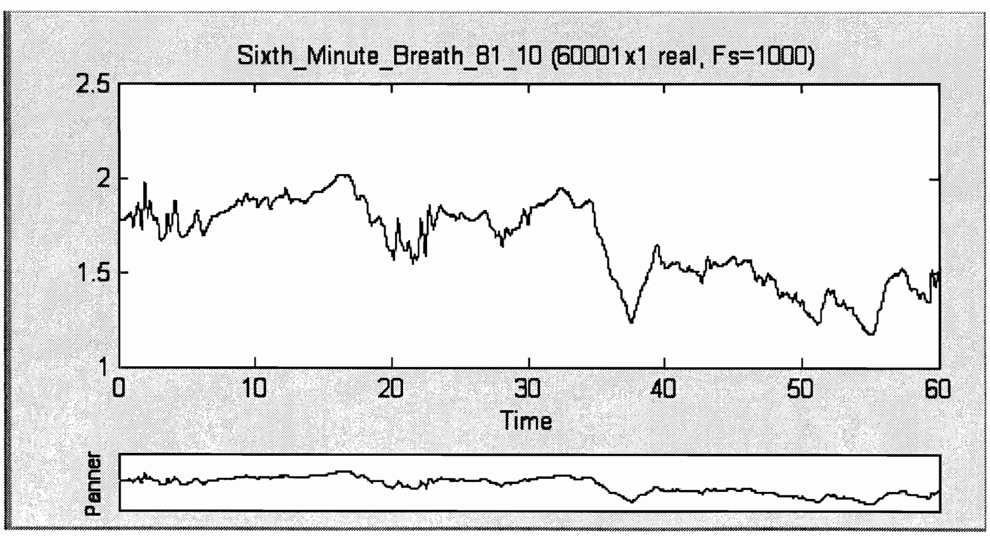

Figure 3.104: The sixth minute breathing of baby # 81, 10th feeding

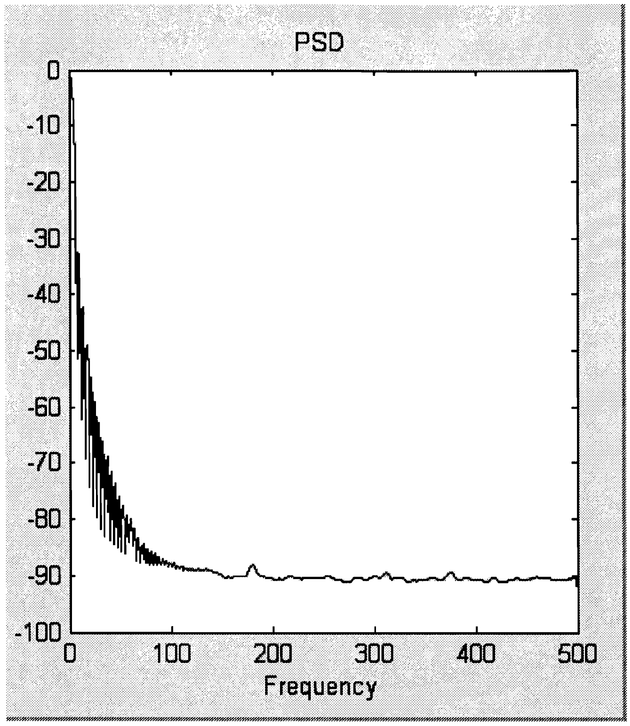

Figure 3.105: The spectral analysis of the seventh minute breathing of baby # 81, 10th feeding

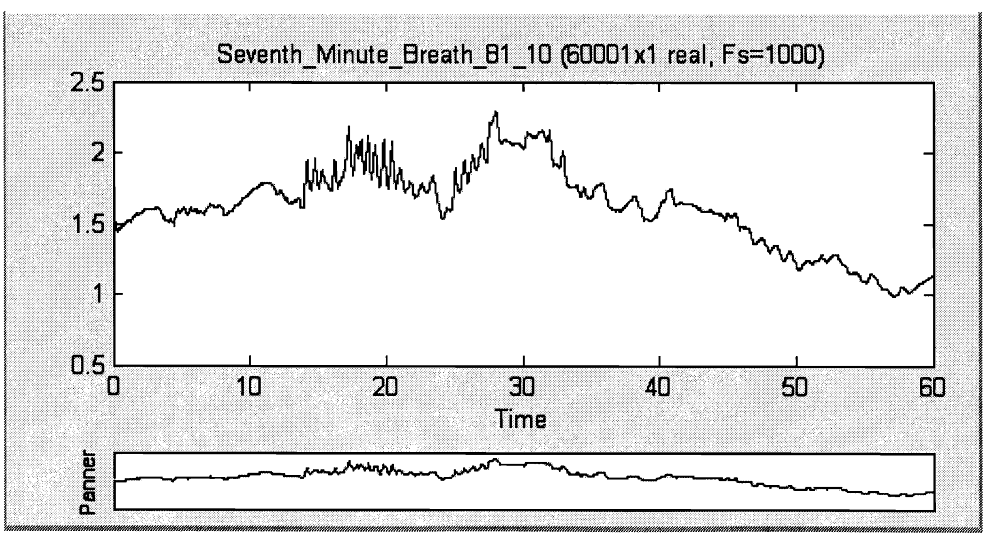

Figure 3.106: The seventh minute breathing of baby # 81, 10th feeding

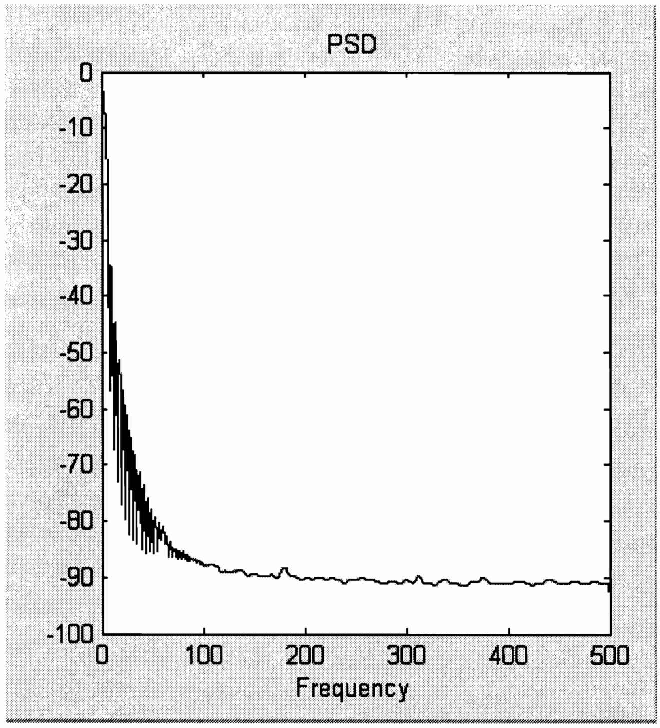

Figure 3.107: The spectral analysis of the eighth minute breathing of baby # 81, 10th feeding

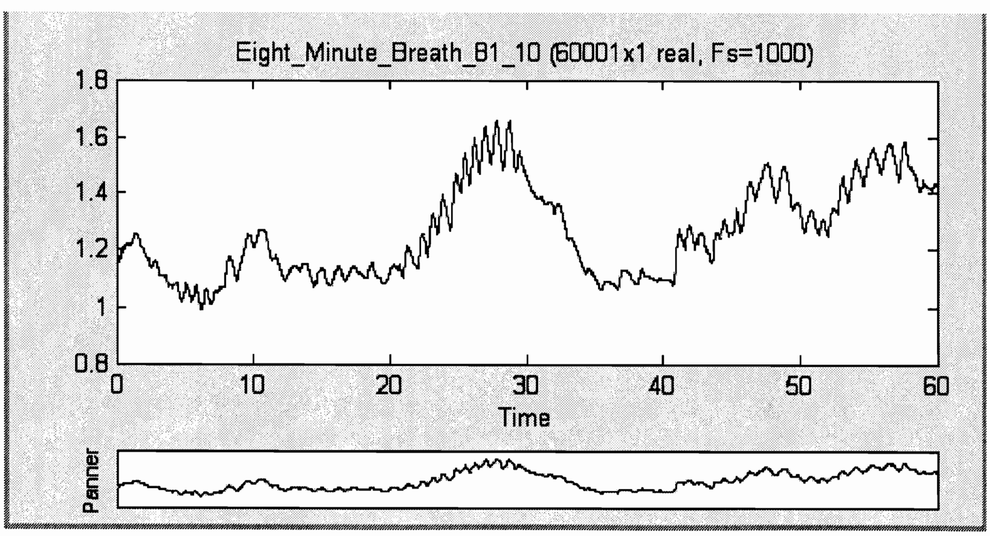

Figure 3.108: The eighth minute breathing of baby # 81, 10th feeding

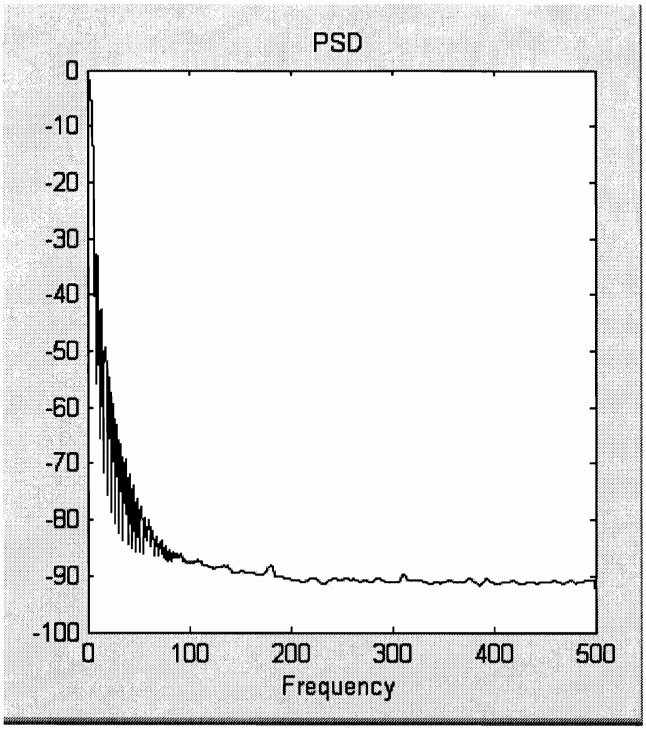

Figure 3.109: The spectral analysis of the ninth minute breathing of baby #81, 10th feeding

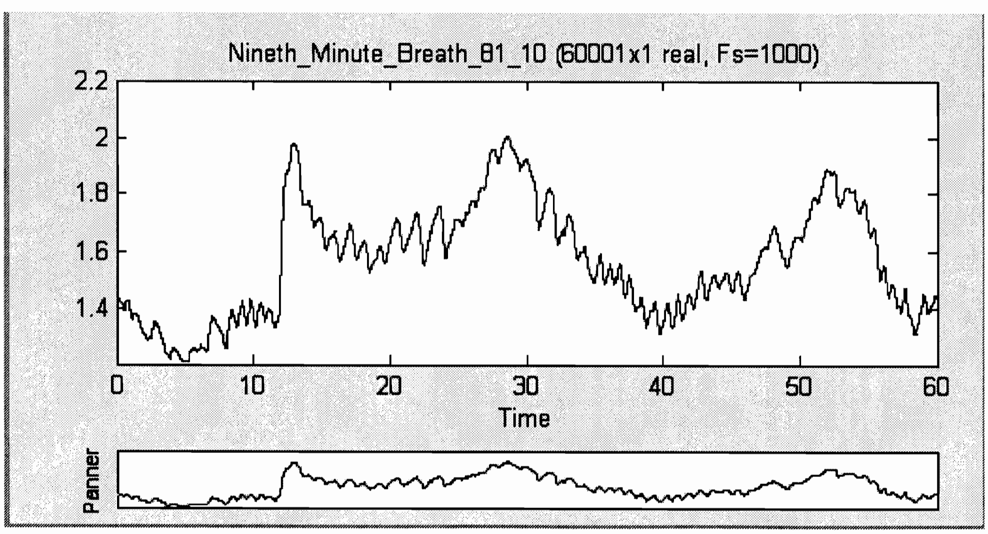

Figure 3.110: The ninth minute breathing of baby # 81, 10th feeding

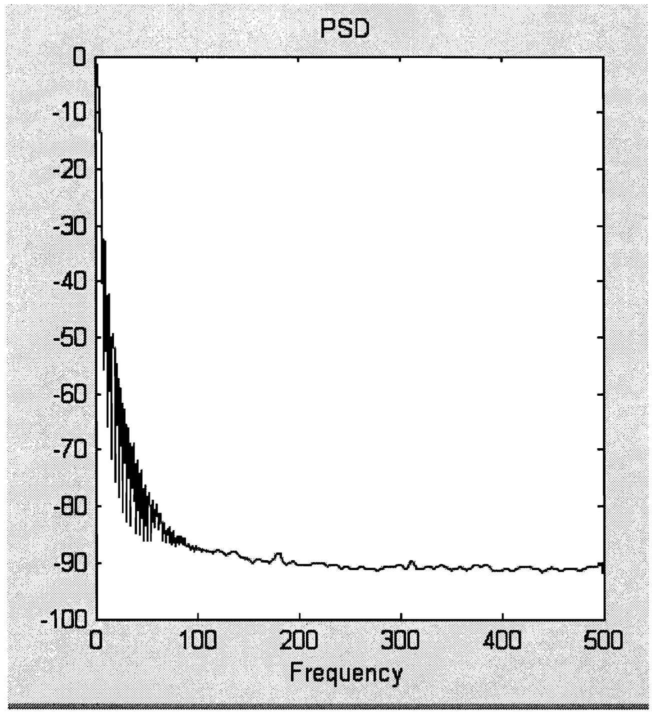

Figure 3.111: The spectral analysis of the10th minute breathing of baby # 81, 10th feeding

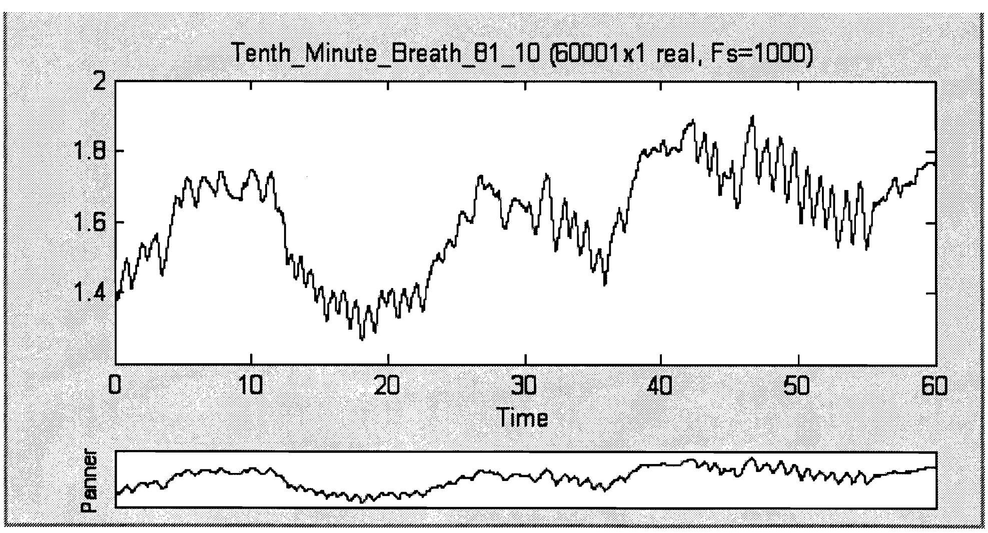

Figure 3.112: The 10th minute breathing of baby # 81, 10th feeding

The Spectral Analysis of the Sucking Waveform of Baby #81, 10th Feeding

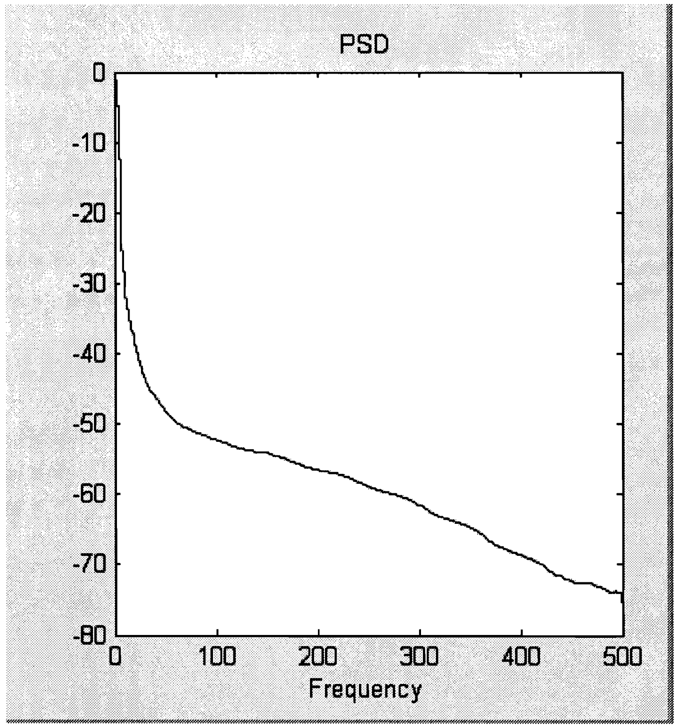

Figure 3.113: The spectral analysis of the first minute sucking of baby # 81, 10th feeding

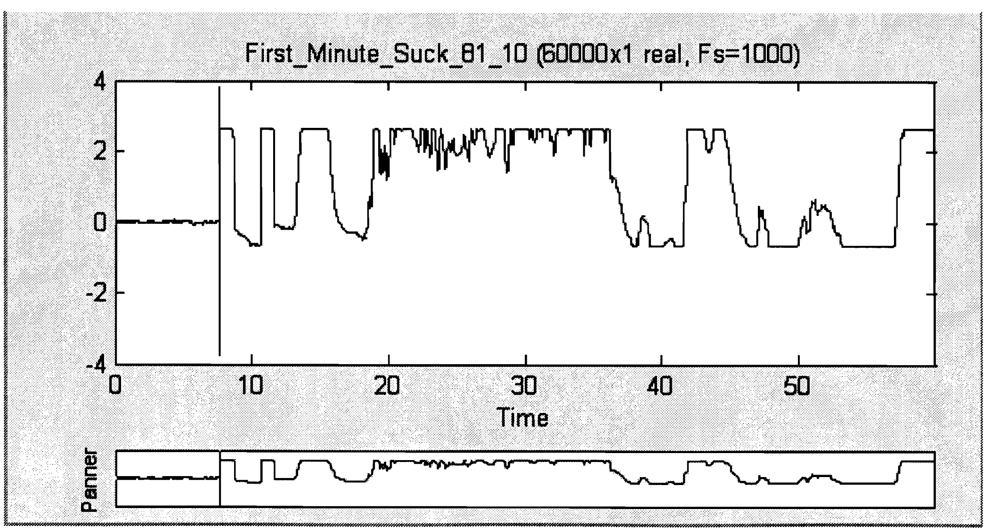

Figure 3.114: The first minute sucking of baby # 81, 10th feeding

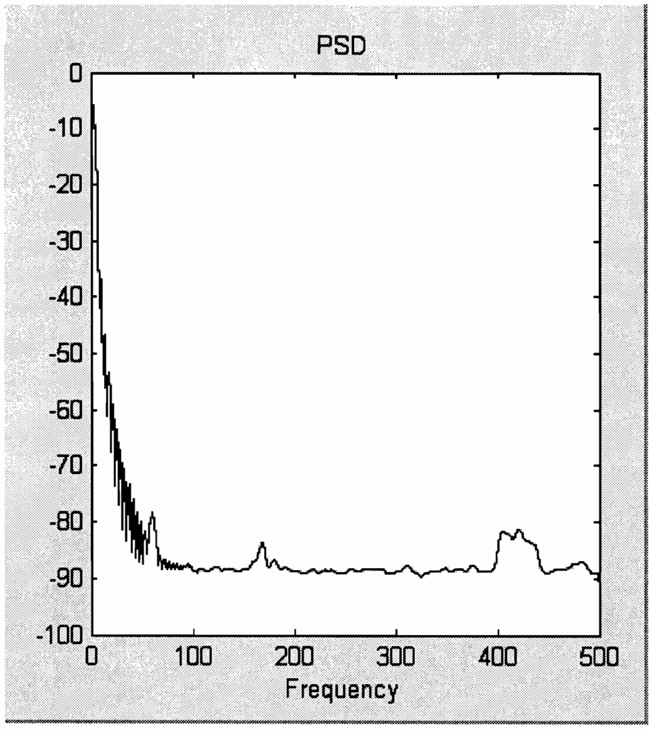

Figure 3.115: The spectral analysis of the second minute sucking of baby # 81, 10th feeding

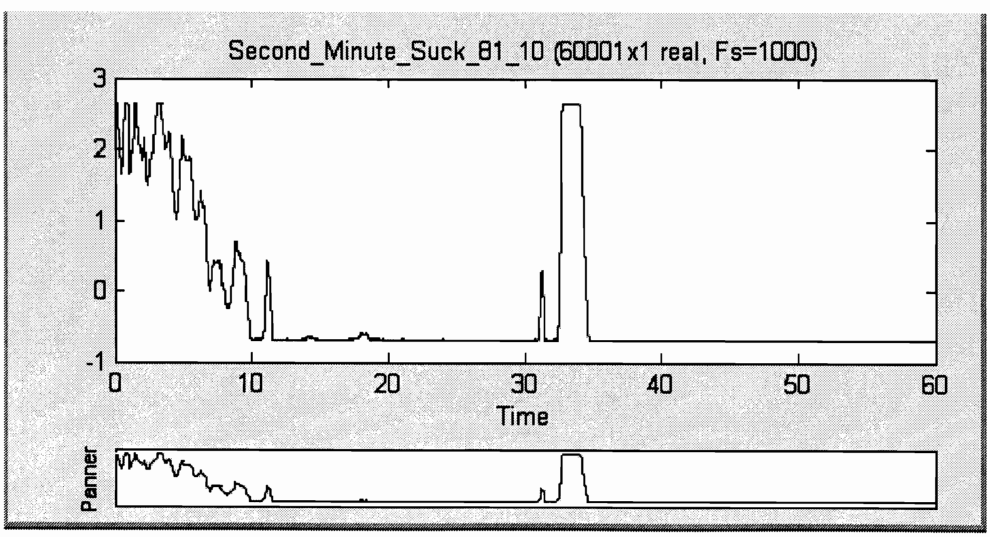

Figure 3.116: The second minute sucking of baby # 81, 10th feeding

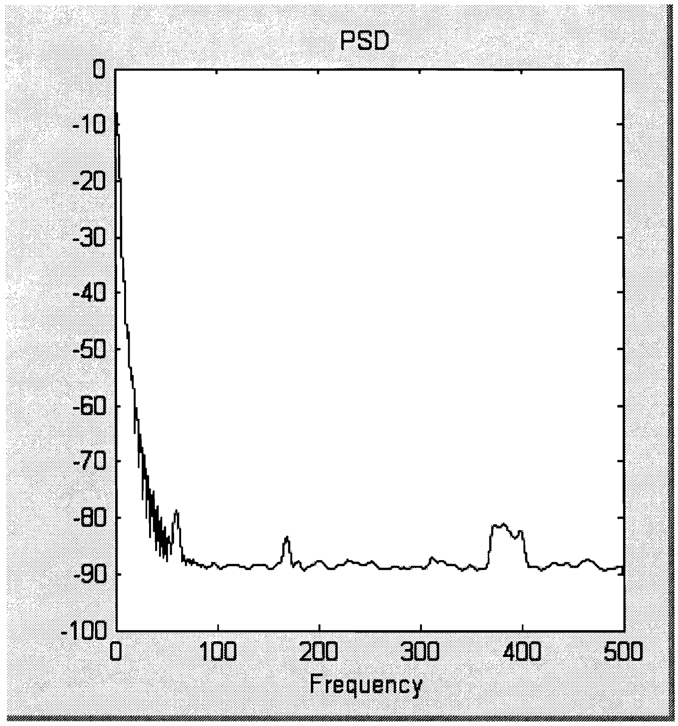

Figure 3.117: The spectral analysis of the third minute sucking of baby # 81, 10th feeding

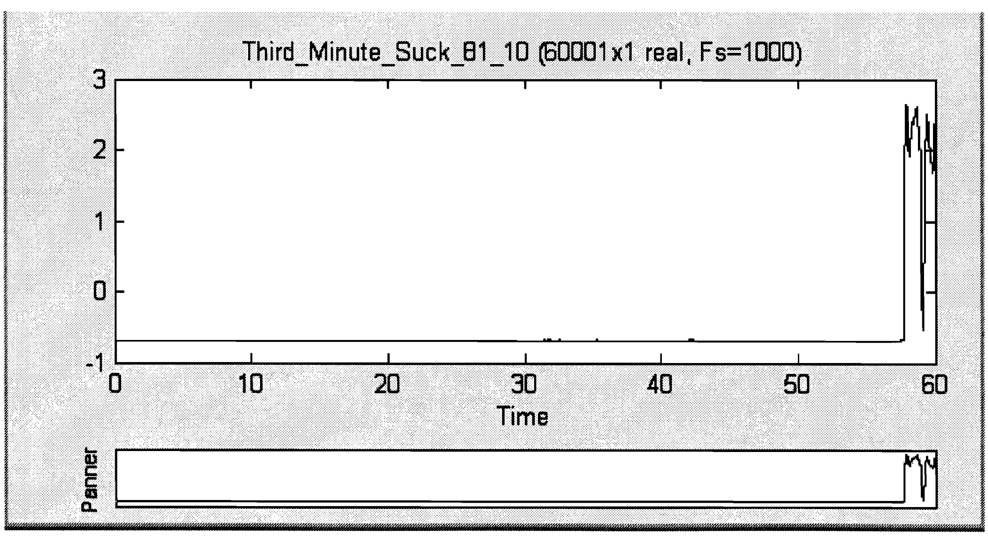

Figure 3.118: The third minute sucking of baby # 81, 10th feeding

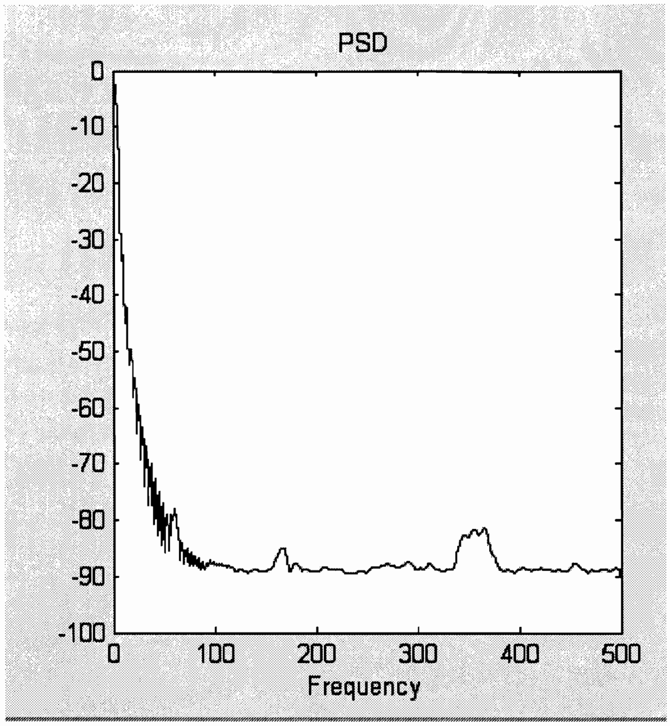

Figure 3.119: The spectral analysis of the forth minute sucking of baby # 81, 10th feeding

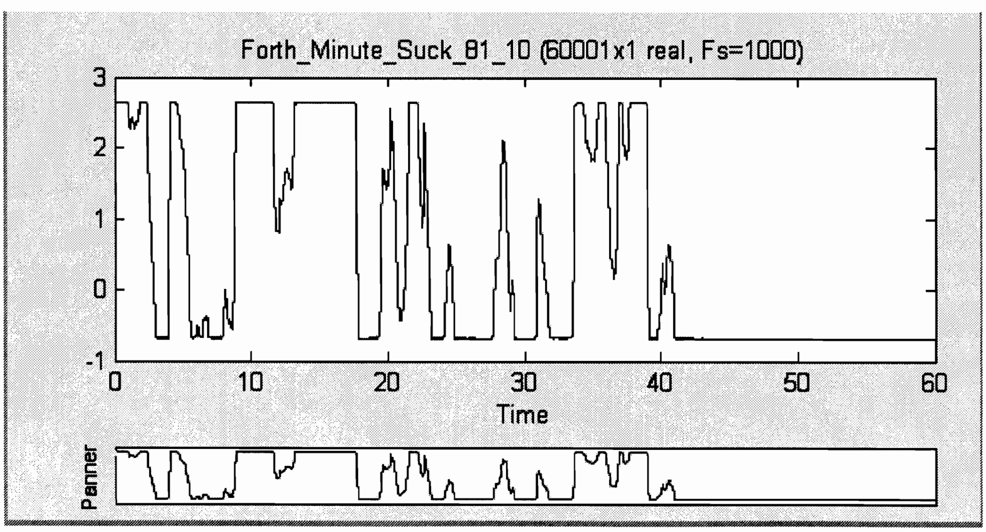

Figure 3.120: The forth minute sucking of baby # 81, 10th feeding

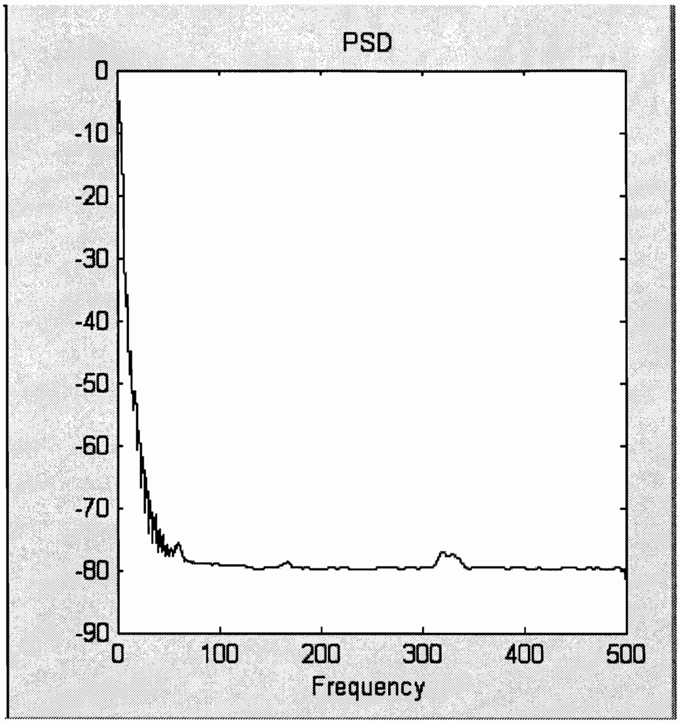

Figure 3.121: The spectral analysis of the fifth minute sucking of baby # 81, 10th feeding

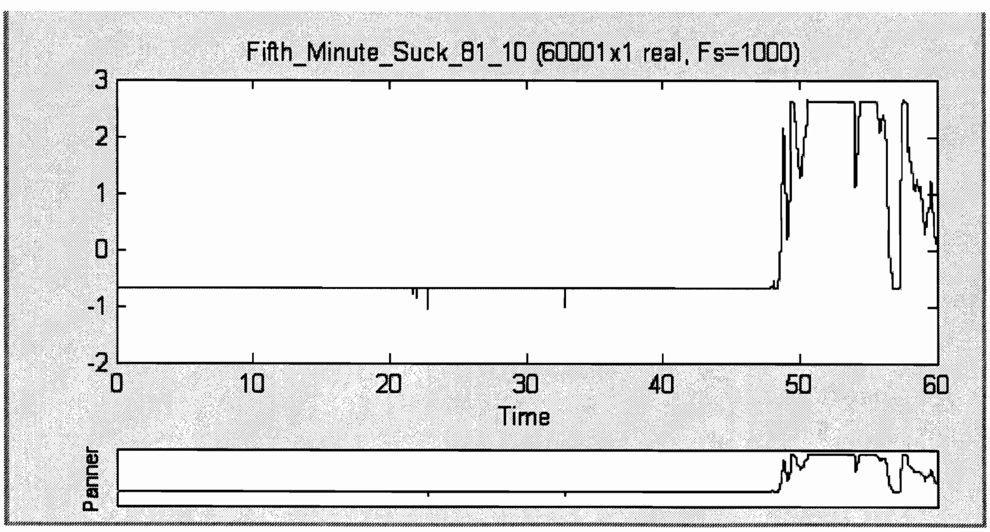

Figure 3.122: The fifth minute sucking for baby #81, 10th feeding

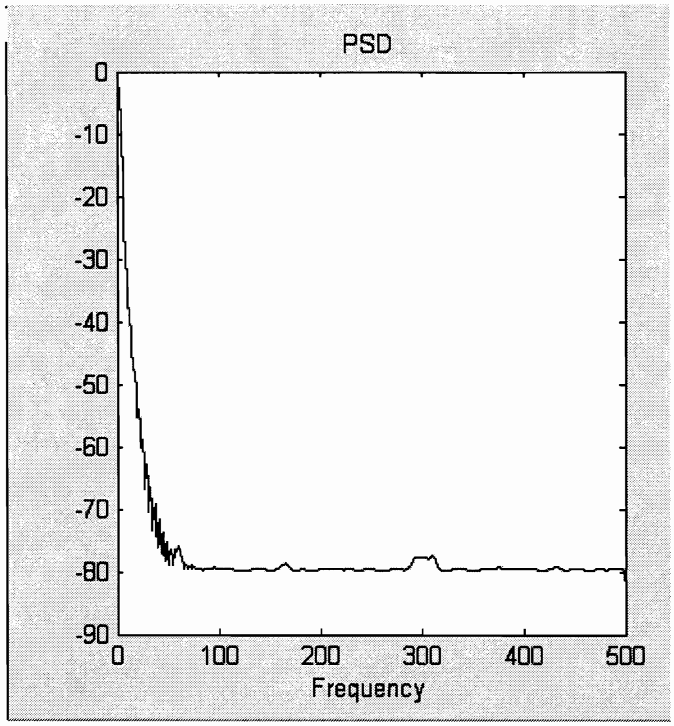

Figure 3.123: The spectral analysis of the sixth minute sucking of baby # 81, 10th feeding

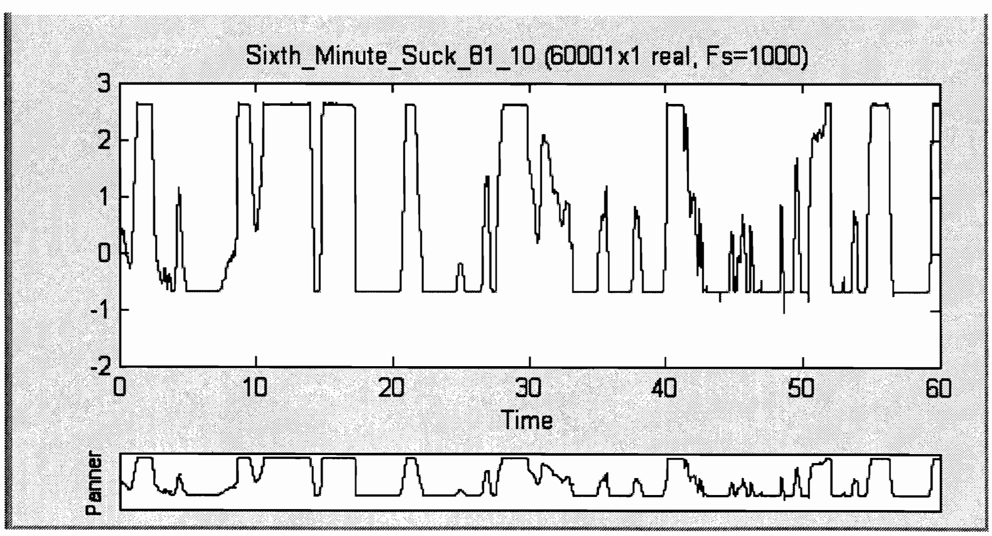

Figure 3.124: The sixth minute sucking of baby # 81, 10th feeding

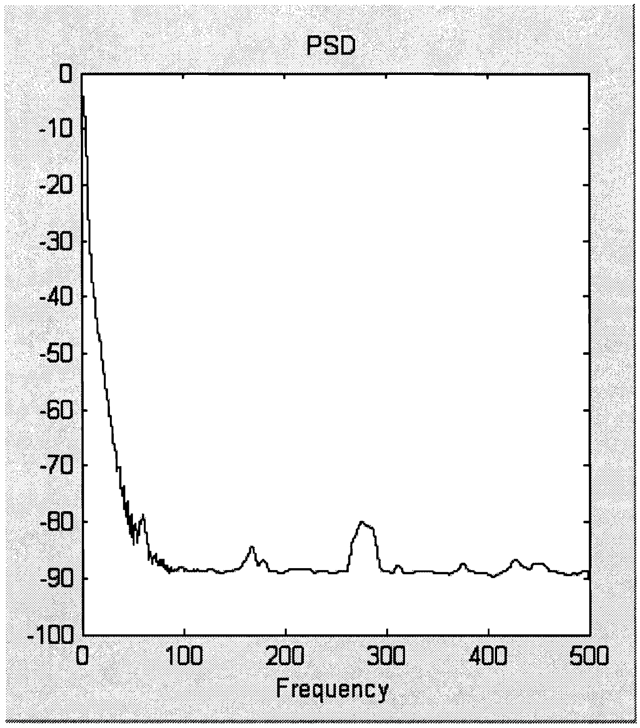

Figure 3.125: The spectral analysis of the seventh minute sucking of baby # 81, 10th feeding

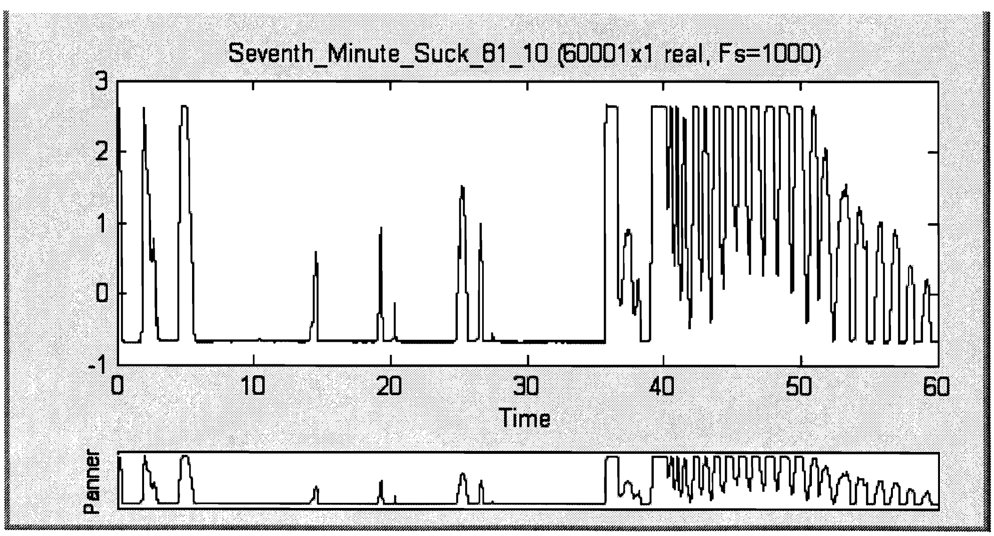

Figure 3.126: The seventh minute sucking for baby #81, 10th feeding

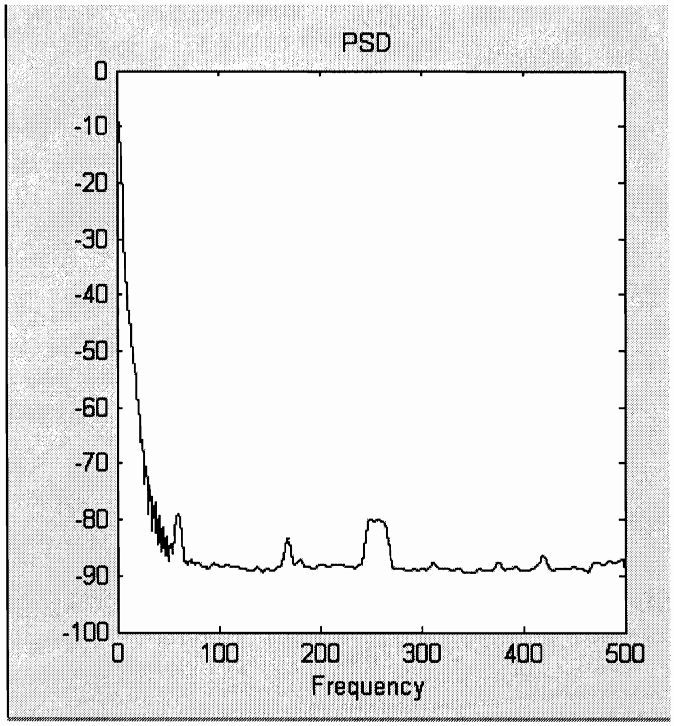

Figure 3.127: The spectral analysis of the eighth minute sucking of baby # 81, 10th feeding

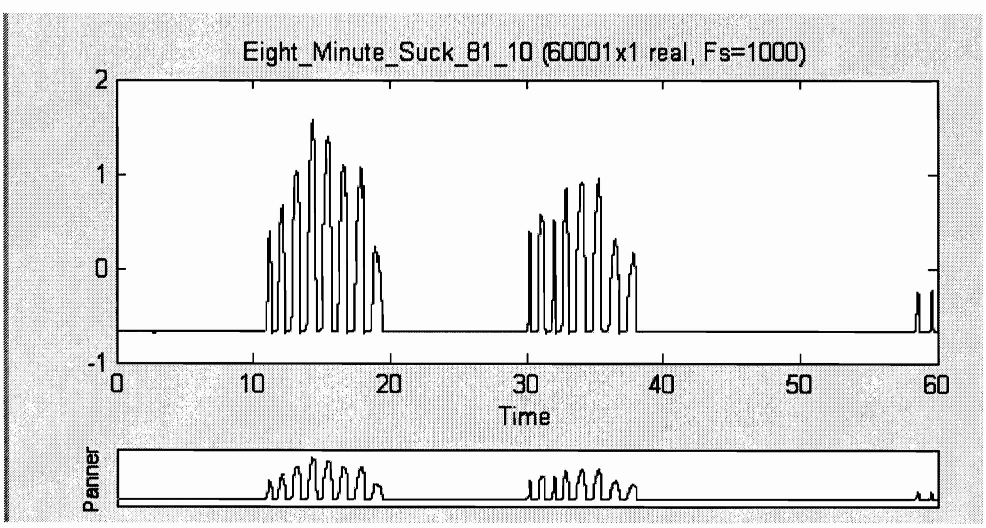

Figure 3.128: The eight minute sucking of baby # 81, 10th feeding

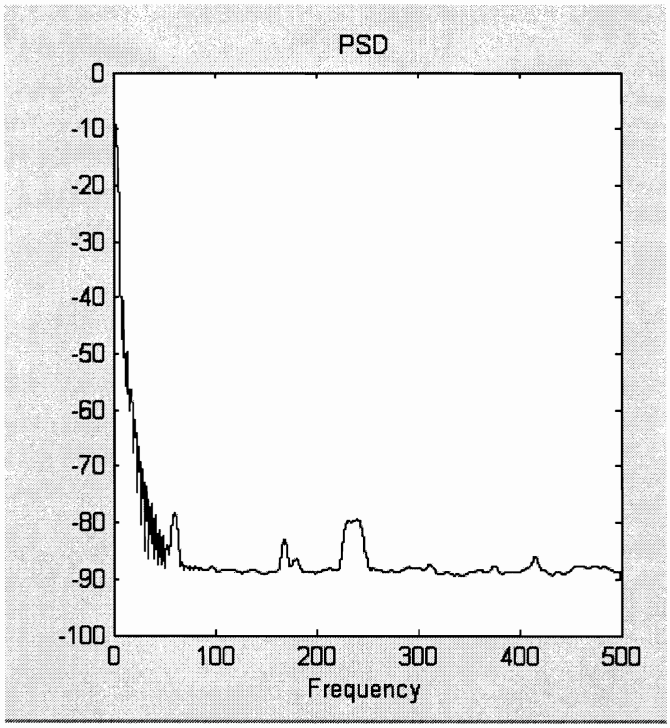

Figure 3.129: The spectral analysis of the ninth minute sucking of baby # 81, 10th feeding

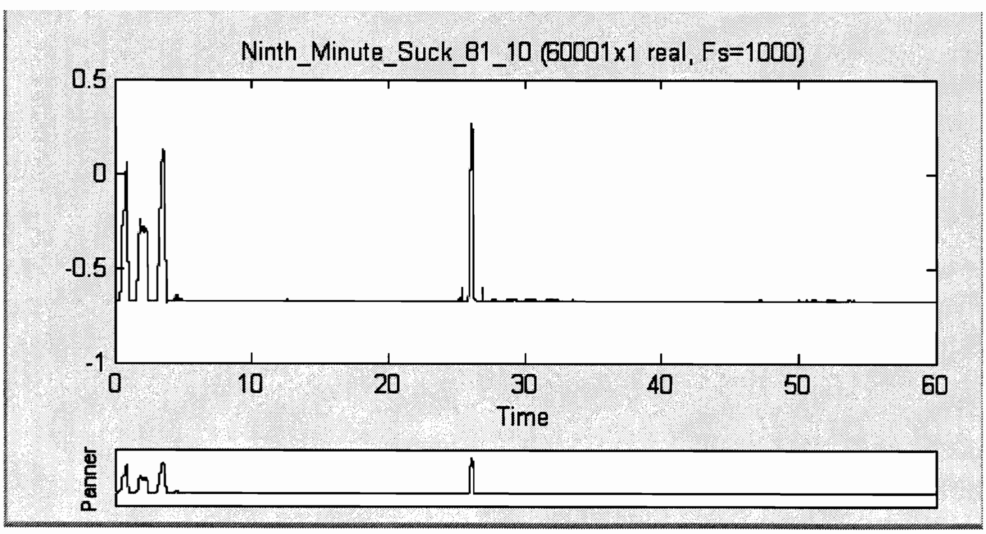

Figure 3.130: The ninth minute sucking of baby # 81, 10th feeding

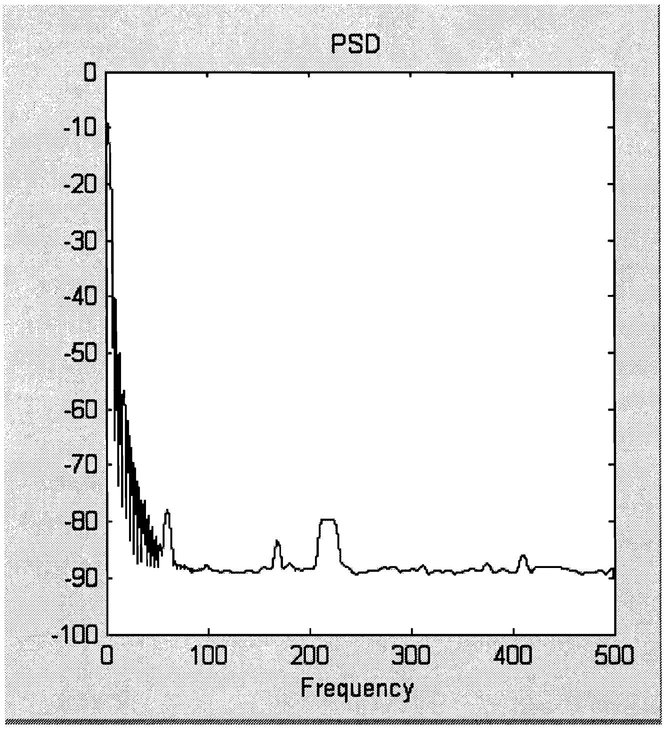

Figure 3.131: The spectral analysis of the10th minute sucking of baby # 81, 10th feeding

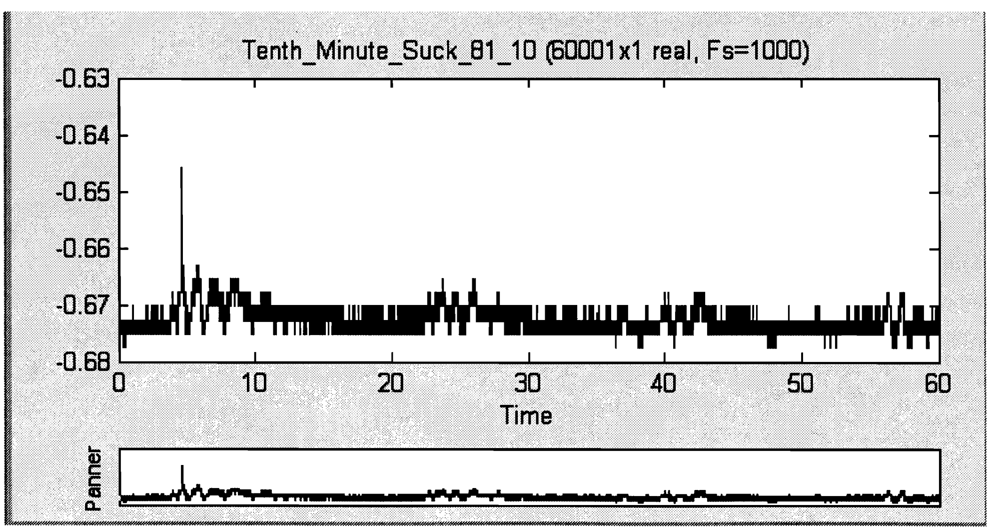

Figure 3.132: The 10th minute sucking of baby # 81, 10th feeding

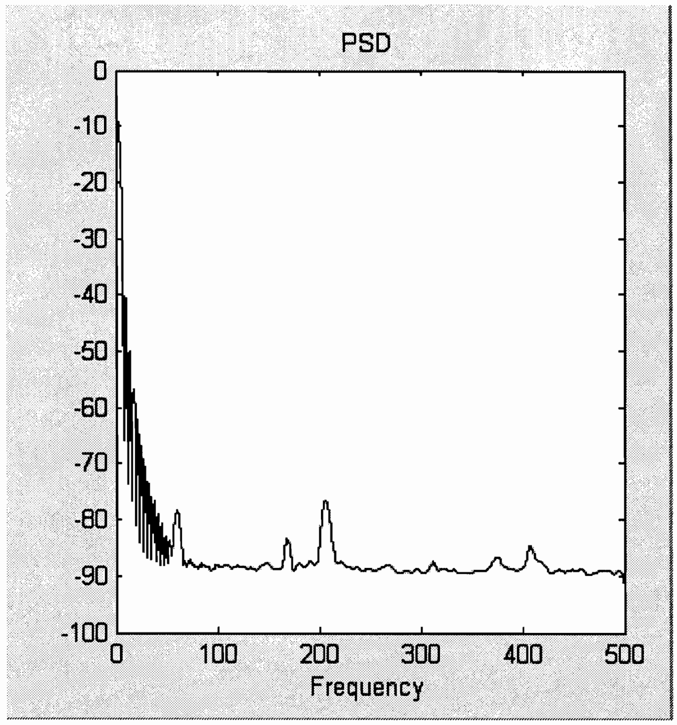

Figure 3.133: The spectral analysis of the last minute sucking of baby # 81, 10th feeding

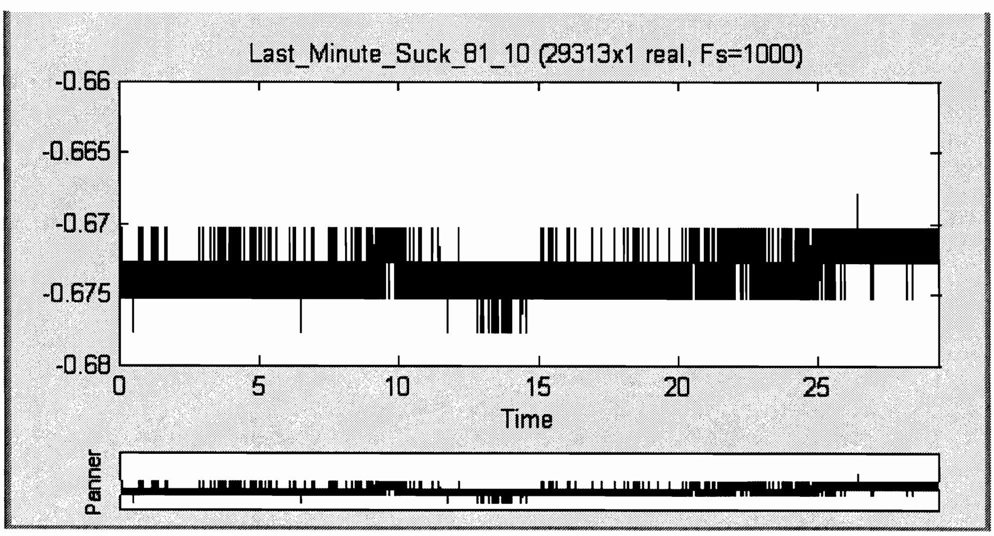

Figure 3.134: The last minute sucking of baby # 81, 10th feeding

The Spectral Analysis of the Swallowing Waveform of Baby #81, 10th Feeding

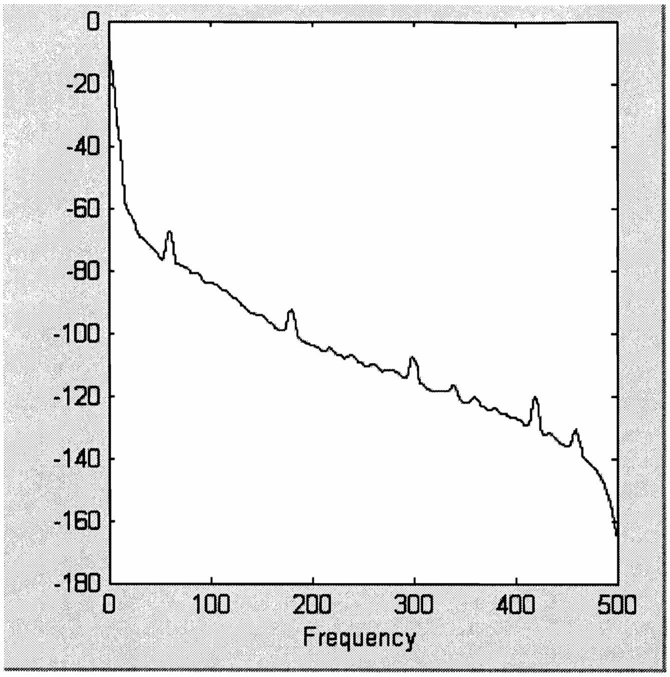

Figure 3.135: The spectral analysis of the first minute swallowing of baby # 81, 10^{th} feeding

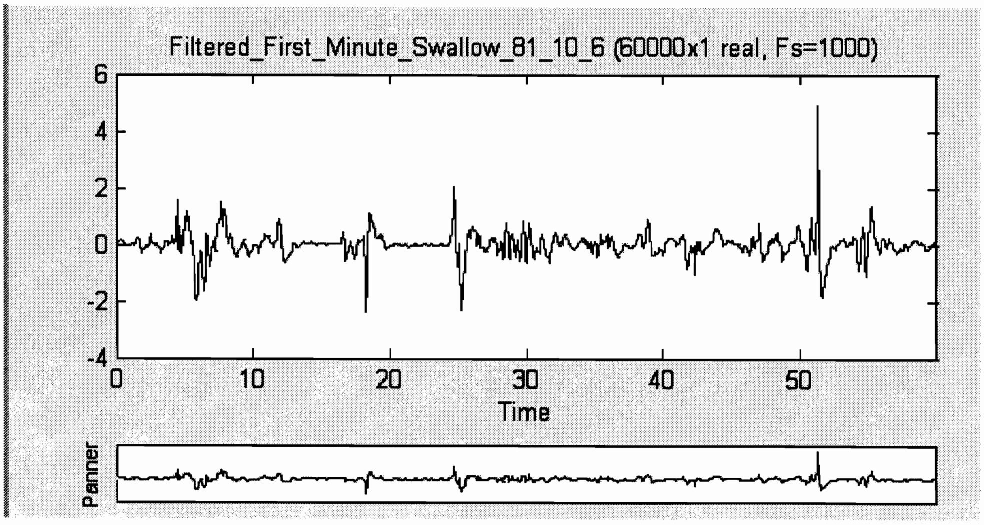

Figure 3.136: The first minute swallowing of baby # 81, 10^{th} feeding

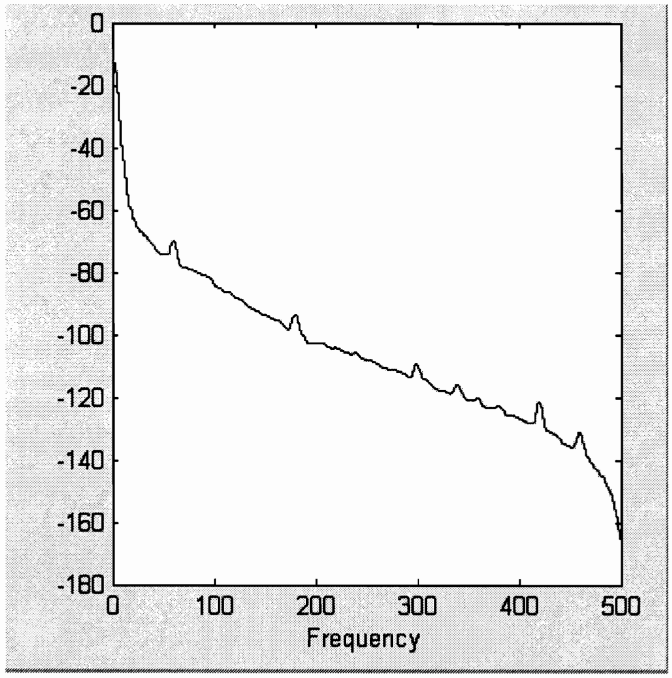

Figure 3.137: The spectral analysis of the second minute swallowing of baby # 81, 10th feeding

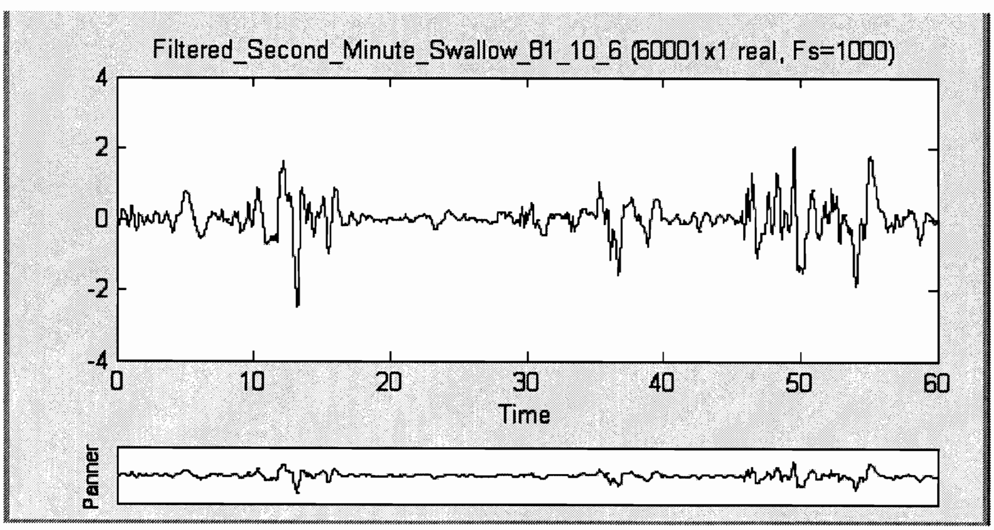

Figure 3.138: The second minute swallowing of baby #81, 10th feeding

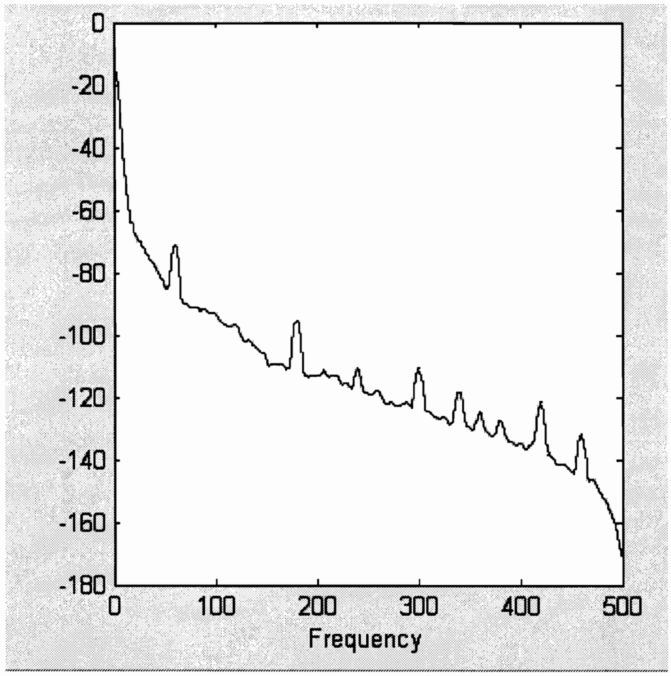

Figure 3.139: The spectral analysis of the third minute swallowing of baby #81, 10th feeding

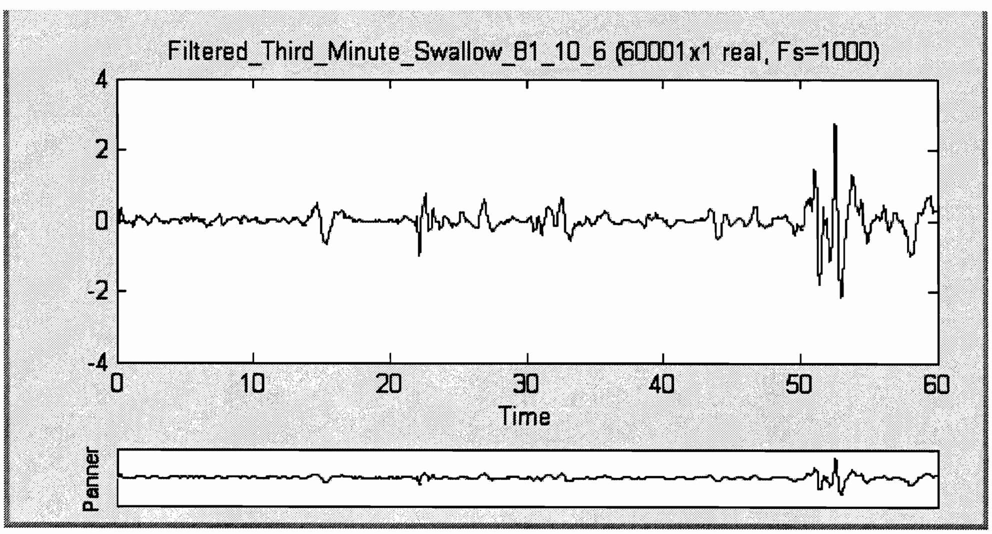

Figure 3.140: The third minute swallowing of baby #81, 10th feeding

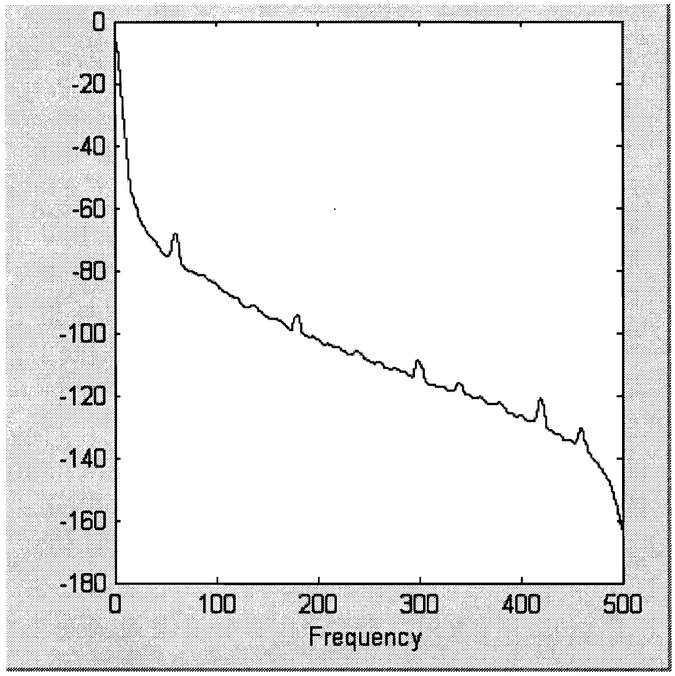

Figure 3.141: The spectral analysis of the forth minute swallowing of baby #81, 10th feeding

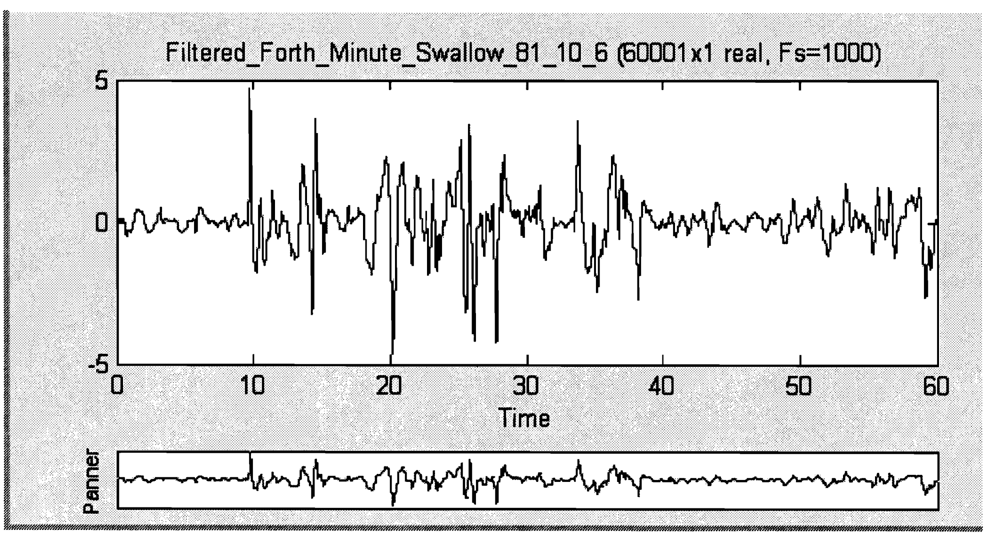

Figure 3.142: The forth minute swallowing of baby # 81, 10th feeding

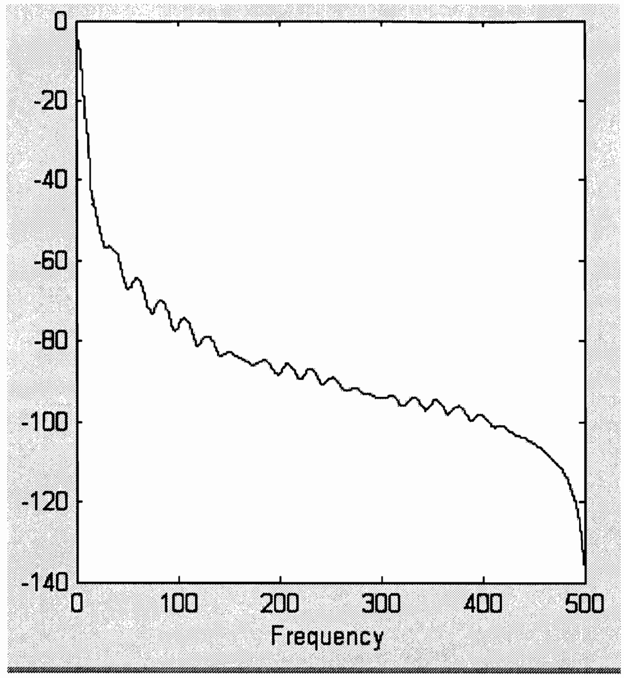

Figure 3.143: The spectral analysis of the fifth minute swallowing of baby # 81, 10th feeding

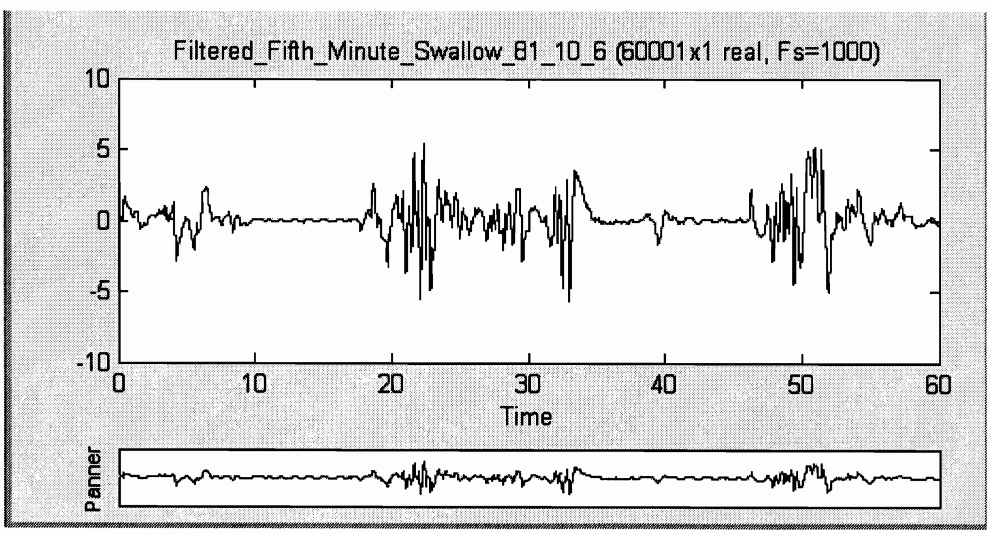

Figure 3.144: The fifth minute swallowing of baby # 81, 10th feeding

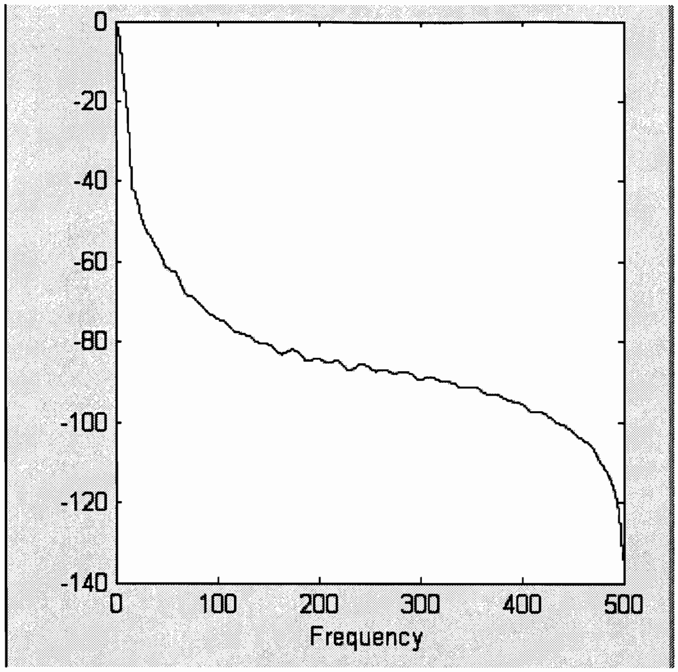

Figure 3.145: The spectral analysis of the sixth minute swallowing of baby # 81, 10th feeding

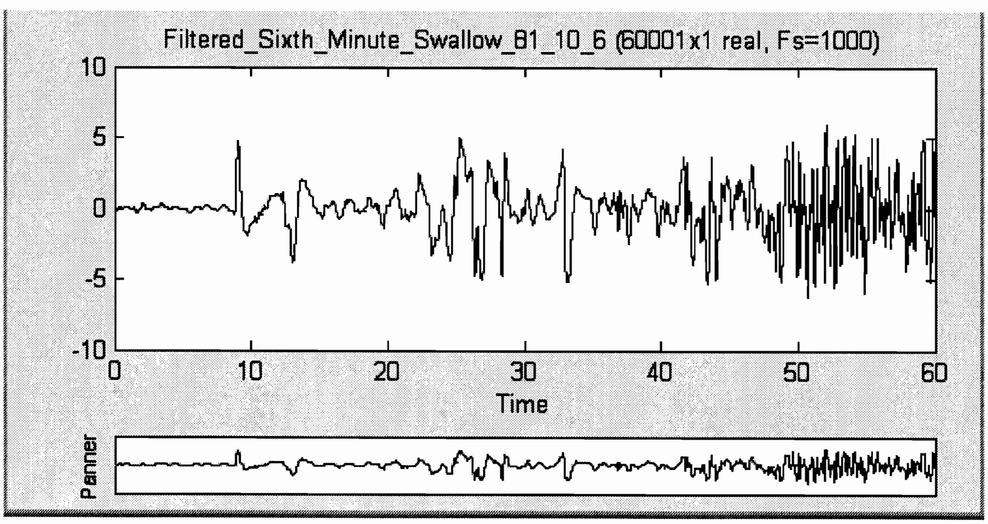

Figure 3.146: The sixth minute swallowing of baby # 81, 10th feeding

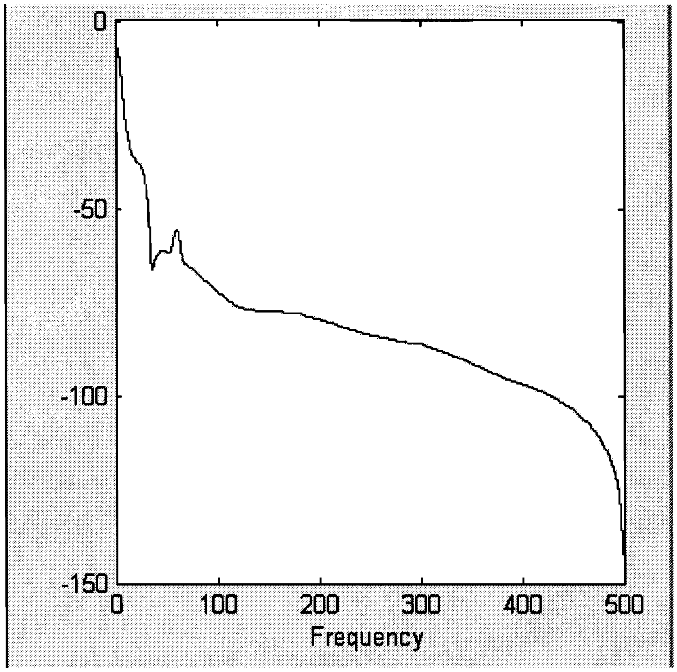

Figure 3.147: The spectral analysis of the seventh minute swallowing of baby # 81, 10^{th} feeding

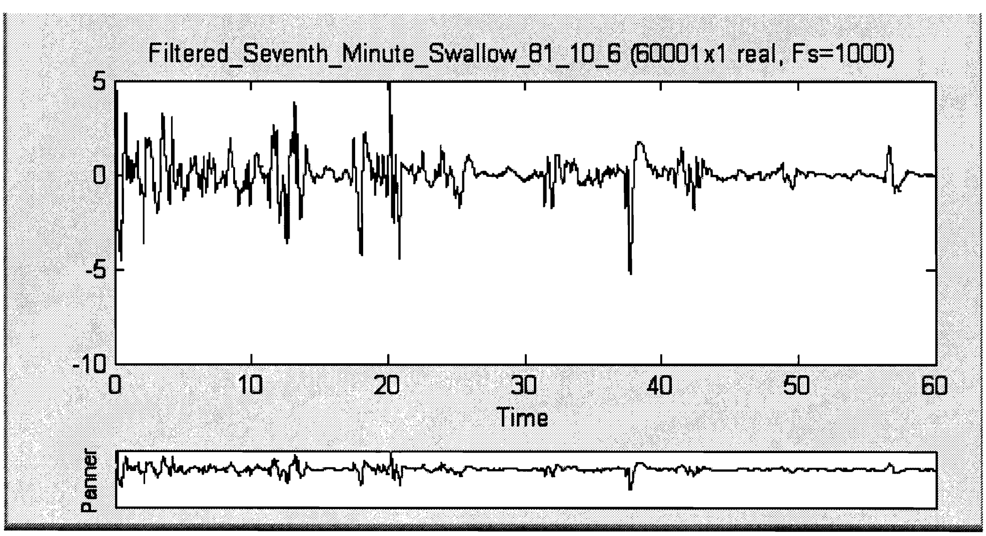

Figure 3.148: The seventh minute swallowing of baby # 81, 10^{th} feeding

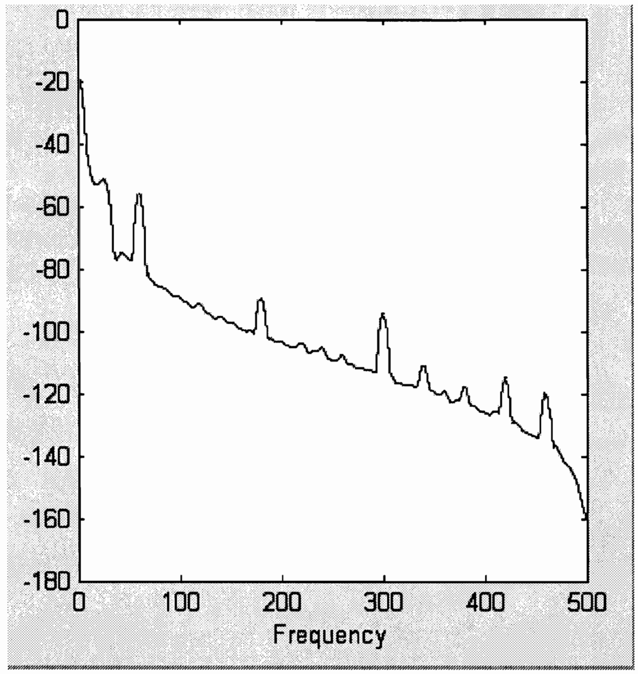

Figure 3.149: The spectral analysis of the eighth minute swallowing of baby #81, 10th feeding

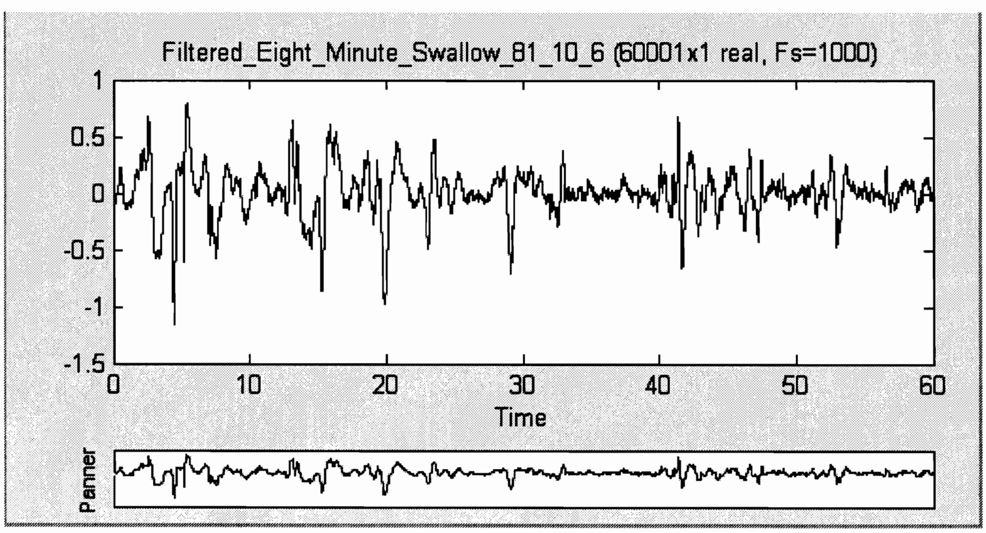

Figure 3.150: The eighth minute swallowing of baby # 81, 10th feeding

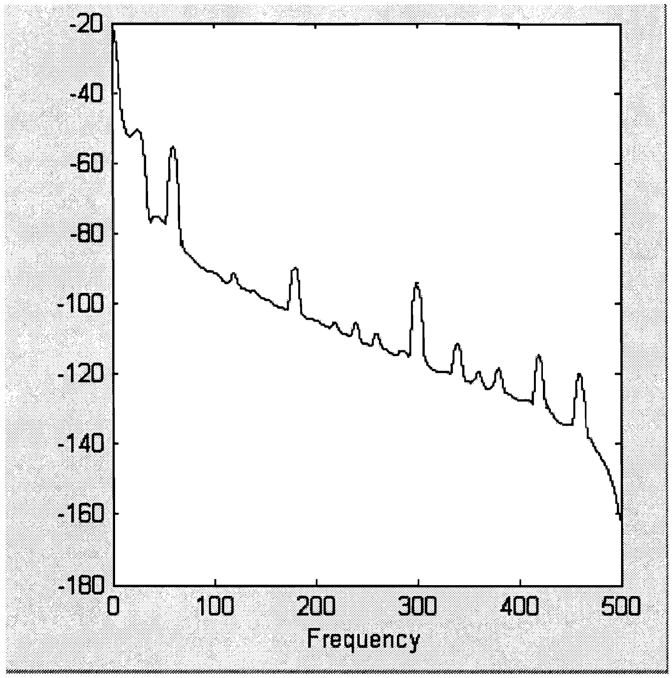

Figure 3.151: The spectral analysis of the ninth minute swallowing of baby # 81, 10th feeding

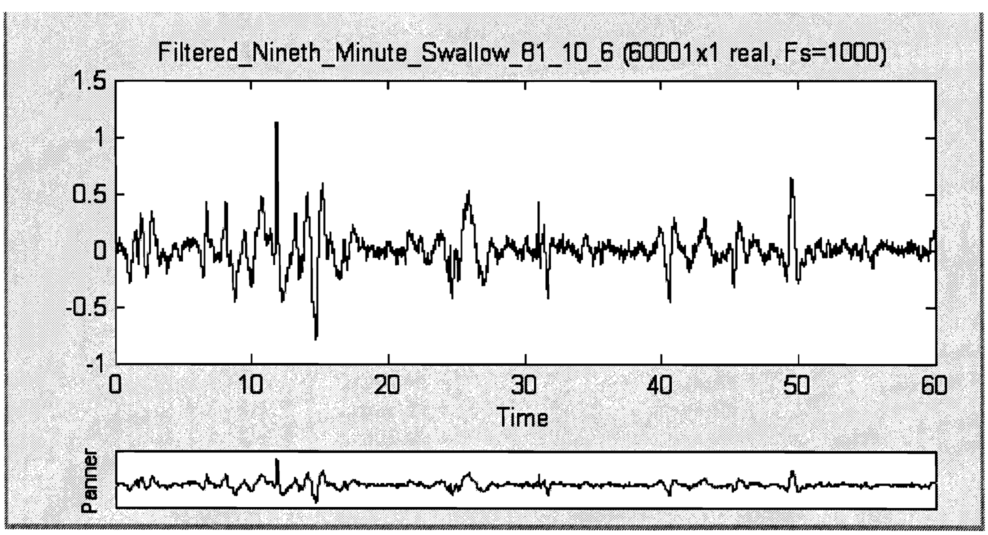

Figure 3.152: The ninth minute swallowing of baby # 81, 10th feeding

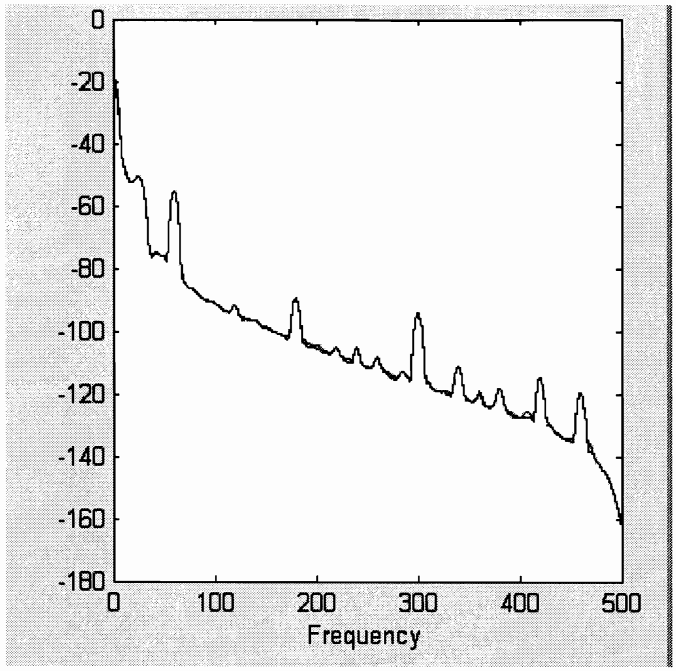

Figure 3.153: The spectral analysis of the10th minute swallowing of baby # 81, 10th feeding

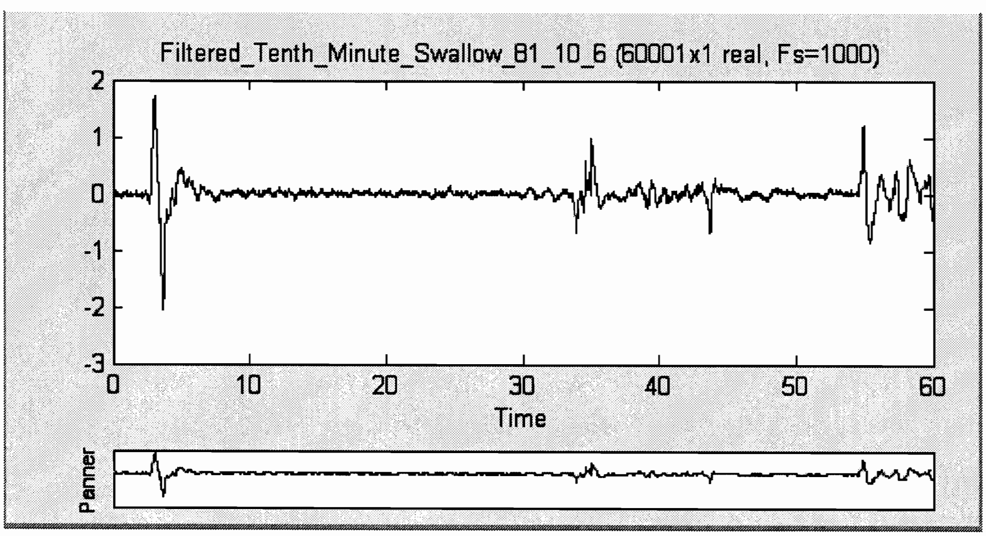

Figure 3.154: The 10th minute swallowing of baby #81, 10th feeding

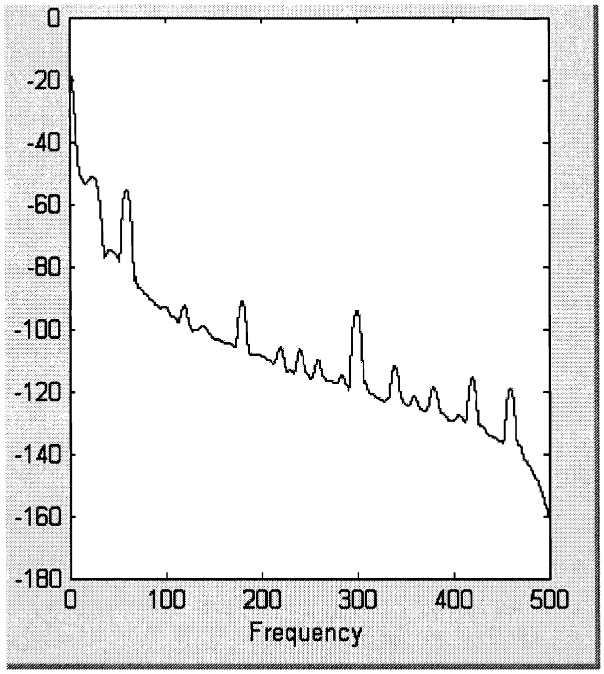

Figure 3.155: The spectral analysis of the 11th minute swallowing of baby # 81, 10th feeding

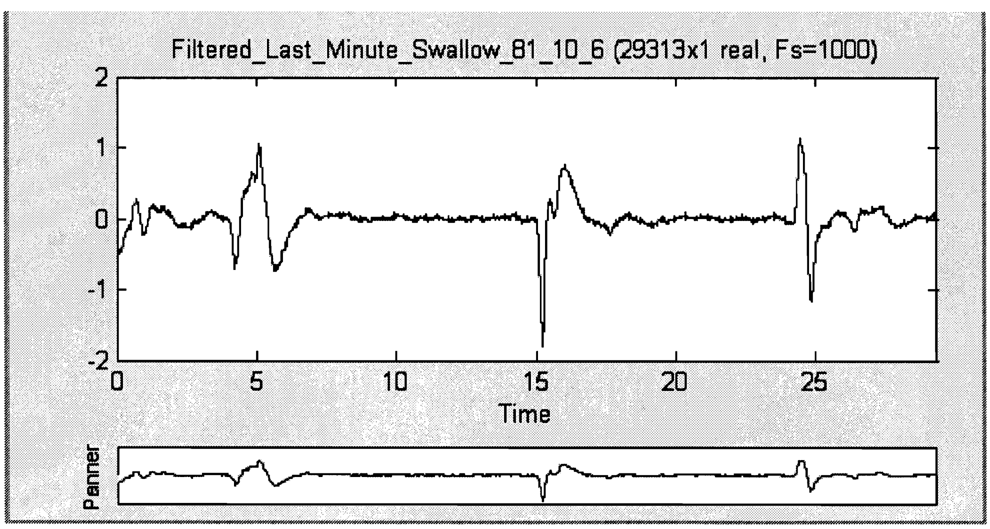

Figure 3.156: The 11th minute swallowing of baby # 81, 10th feeding

3.6. Conclusion

In this approach, an arbitrary window size of one minute was used to investigate the frequency content of each specific signal. The results showed that differences in waveform shape could not be adequately distinguished by examination of the frequency content. The results of spectral analysis for suck, swallow and breathing waveforms for both babies indicated that for a specific waveform, the shape of the signal differs from one minute to another while the frequency content does not change dramatically. For example, in baby #81's seventh and eighth minutes of sucking (Figures 3.125, 3.126, 3.127, 3.128), although the shape of the signals changes over the time, the frequency content of the signal remains fairly constant.

Because Welch method involves with averaging over frequency for the different segments, it is likely that the spectral content associated with the event of interest is hidden somewhere. In order to reveal the difference of frequency content, the size of the window needs to be reduced close to the actual duration of an event. Matching the window size to the actual duration of an event may reveal greater relationships between the shape of the signal and its frequency content.

Correlation and Matched Filtering

4.1. Introduction

In order to predict the appropriate time to introduce bottle-feeding to premature infants, heart rate, oxygen saturation, respiratory rate, sucking and swallowing activities are measured. These physiological measures are recorded directly into the Ponemah Data Acquisition System (PDAS). The objective of this work was to detect, identify and classify suck, swallow and respiratory waveforms independently and in relation to other waveforms. The goal was to look at each waveform and investigate how they change over time in order to determine whether a baby sucks, swallows and breaths in a well coordinated fashion.

In the first approach the integration of wavelet packet transform (for feature extraction) and neural networks (for classification) was investigated. As the results in chapter two show, the feature extraction method was not appropriate for this particular application. Because utilizing wavelet packet energy nodes did not describe each frame of a specific signal in a unique manner. Further, this resulted in the failure of classification using neural networks. According to the results of spectral analysis of all three signals in chapter three, the frequency content of these three signals are not tightly related to the shape of the signals in time domain. Therefore, at this point, the main question is," How can be a frame described in a unique manner?" In other words, "What is the ideal feature extraction method used to describe each frame uniquely?"

Feature extraction is the process of creating a representation or a transformation from the original data and is a special form of dimensionality reduction. Furthur, the best way to describe a frame is to eliminate this type of reduction and utilize that whole frame

itself as the parameters. Therefore, the best way for classification of a frame is to use the whole frame as parameters and feed it to NN. However, there are major problems in implementing a neural network to classify a frame using the whole frame as parameters. For example, frame size is a variable factor and may have a value up to 2000 samples while the implementation of a neural network with 2000 input size is very complicated and costly.

In this chapter, a whole new approach at using correlation and matched filtering in time domain is proposed.

4.2. Background

In this section the concept of correlation and matched filtering will be reviewed.

4.2.1. Correlation

Form a statistical point of view, cross-correlation (from now on correlation) is a measure of the relation and similarity between two or more random variables (Manolakis *et al* 2000). In signal processing, the correlation is defined as a measure of similarity between two signals (Proakis and Maqnolokis, 1996). This method is generally used to determine specification in an unrecognized signal by comparing it to a recognized one. In the signal processing literatures the correlation is mathematically described by the following equation.

$$y(\tau) = \int_{-\infty}^{+\infty} x_1(t) x_2(t+\tau) d\tau \qquad \text{Eq(4.1)}$$

Equation (4.1) defines the correlation $y(\tau)$ between two functions $x_1(t)$ and $x_2(t)$ as a function of the time shift τ . For any value of time shift τ , the two functions are multiplied and the result is integrated over infinity (Manolakis *et al* 2000, Baher 2001). This explanation differs from a convolution in that the shifted function is not inverted. Also one of the major consequences of this difference is that the correlation operation (unlike convolution) is not commutative.

In discrete time, assuming two real signal sequences $x(n)$ and $y(n)$ with finite energy, the correlation of $x(n)$ and $y(n)$ is a sequence $r_{xy}(l)$ which is defined as (Proakis and Manolakis, 1996; Bose and Rao, 1993) :

$$r_{xy}(l) = \sum_{n=-\infty}^{+\infty} x(n)y(n-l) \qquad l = 0,\pm1,\pm2,... \qquad \text{Eq (4.2)}$$

Equation (4.2) is equal to

$$r_{xy}(l) = \sum_{n=-\infty}^{+\infty} x(n+l)y(n) \qquad l = 0,\pm1,\pm2,... \qquad \text{Eq(4.3)}$$

The index l is the time shift or lag. Apparently, the computation of convolution and correlation are very similar. Convolutions involve folding a signal about the vertical axis, then shifting it, multiplying by another signal and summing over all values of the product sequence while correlation only involves shifting one signal, multiplying it by the other one and summing over all values of the product sequence.

In probability theory and statistics, correlation coefficient indicates the strength and direction of a linear relationship between two random variables (Ott and Longnecker, 2001). Two methods of calculating correlations are Spearman's Rank Correlation Coefficient and Pearson's or the Product-Moment Correlation Coefficient. The

correlation coefficient has a value between 0 and 1. If there is no relationship between the two random variables the correlation coefficient will be zero or very low. As the strength of the similarity increases the correlation coefficient gets closer to one therefore, a perfect fit will associate with a coefficient of one. For two random variables x and y with a size of N samples, the formula for computation of correlation using Pearson's method is (Ott and Longnecker, 2001):

$$r = \frac{N\sum xy - (\sum x)(\sum y)}{\sqrt{[N\sum x^2 - (\sum x)^2][N\sum y^2 - (\sum y)^2]}} \qquad \text{Eq (4.4)}$$

The correlation method is used extensively in pattern recognition and signal detection, especially the detection of signals buried in noise. Typical applications involve radar, sonar, ultrasound imaging, and other reflective ranging techniques (Proakis and Manolakis, 1996; Smith, 2003).

4.2.2. Matched Filtering Technique

. A matched filter is acquired by correlating a refrence waveform (template) with an unknown signal to investigate the presence of the template in the unknown signal. The occurrences of s in x are investigated by detecting peaks in $r_{sx}(l)$ (Smith 2003; Hippenstiel, 2002). To express this concept mathematically, an orthogonal projection concept is introduced.

The orthogonal projection (or simply projection) of $y \in C^N$ onto $x \in C^N$ is defined by

$$P_x(y) = \frac{<y, x>}{\|x\|^2} x \qquad \text{Eq(4.5)}$$

where $||x||^2$ is the length of the vector x and $<y,x>$ is the inner product of y and x (Smith 2003). The complex scalar $<y,x>/||x||^2$ is referred to as the coefficient of projection. Projecting one signal onto another indicates how much of the second signal is present in the first one. This technique can be used to determine whether a known signal is presented as a component of a more complicated signal. For example, consider a recorded signal *x(n)* which is believed to consist of a signal *s(n)* plus some additive measurement noise *e(n).* According to Equation (4.5) the projection of *s* onto *x* will be obtained using:

$$P_s(x) = \frac{<x, s>}{\|s\|^2} s = \frac{<s+e, s>}{\|s\|^2} = s + \frac{<e, s>}{\|s\|^2} s = s + \frac{N}{\|s\|^2} r_{se}(0) s \approx s \qquad \text{Eq(4.6)}$$

Since the projection of random, zero-mean noise *e* onto *s* is small with probability of one (Smith, 2003). The procedure is called matched filtering.

Matched filters are built directly on top of the correlation. The match filtering process incrementally slides the template over the unknown signal being processed while searching for a matching signal. Signals not correlated to the template will have a correlation coefficient close to zero. If a matching signal is detected, the correlation coefficient becomes closer to one with a maximum value of one for a perfect match (Smith, 2003; Hippenstiel, 2002)

4.3. Method

There were 97 babies enrolled in this study. For each baby several feedings were observed and physiological measurements were recorded using PDAS and Matlab based data acquisition system. However, due to the poor quality of swallowing signal for most of the babies, there were only two babies who had all three signals with an acceptable quality (baby #81, 10^{th} feeding and baby #87, seventh feeding).

The general system architecture is discussed in the following sections. The steps involved in this process are as follows:

- Data extraction and preprocessing
- Development of a prototype for each waveform (suck, swallow and breathing activities).
- Segmentation and matched filtering each specific waveform using the corresponding prototype.
- Analyzing the relationships between the signals.

4.3.1. Data Extraction and preprocessing

As mentioned in the chapter two, the digitized data from all channels were directly stored as one file on the resident hard disk drive by the system, therefore, the first step was to extract the data for each channel. The ultimate output of this task included three arrays: breathing data, swallowing data and sucking data (Figure (4.1)). These arrays can be saved separately as data files.

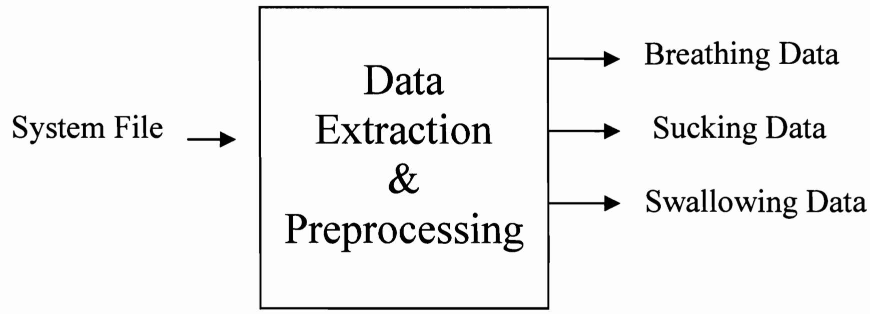

Figure 4.1: Data extraction and preprocessing task

Basically the breathing and sucking data had acceptable quality but due to the poor quality of swallowing signal, filtering was necessary to remove the noise.

4.3.1.1. Filtering Swallowing Signal

In order to measure a swallowing event during a baby's feeding, surface electromyography (EMG) was used. The contraction of the muscles involved with swallowing was detected by using two EMG electrodes placed on the skin overlying the muscles. The two bar electrodes were attached externally to either side of the left digastric muscle and the electrical potential that resulted from the generation and propagation of an action potential along muscle fiber was amplified (Pickler, 1999). Because EMG electrodes are very sensitive to movement the signal is subject to numerous technical problems. Such problems include signal interference like hum, signal acquisition problems like clipping or baseline drift, skin artifacts and many other kinds of interpretation problems (Webster, 1998). In order to reduce the effects of artifacts in this application , the swallowing signal was filtered using a seventh order Elliptic filter (Figure (4.2)).

Elliptic Filters

An elliptic filter or Cauer filter is a filter with equalized ripple (equiripple) in both the passband and the stopband. This is mainly because the elliptic filter has poles in the passband and zeros in the stopband. In fact, for the given values of ripple, no other type of filters with the same order can have a faster transition in gain between the pass band and the stop band (Proakis and Manolakis, 1996). The gain of a lowpass elliptic filter as a function of angular frequency ω can be obtained by:

$$G_n(\omega) = \frac{1}{\sqrt{1 + \varepsilon^2 R_n^2(\xi, \omega/\omega 0)}} \qquad \text{Eq(4.7)}$$

where ω_0 is the cutoff frequency, R_n is the *n*th-order elliptic rational function (also known as a Chebyshev rational function), ε is the ripple factor and ξ is the selectivity factor. The pass band ripple is determined by the value of the ripple factor while the combination of the ripple factor and the selectivity factor are used to specify the stop band ripple. In designing a point of view, an elliptic filter is characterized by four parameters: the passband edge frequency F_P (in HZ), the passband ripple R_p (in dB), the stopband attenuation R_s (in dB) and n which is the order of the filter.

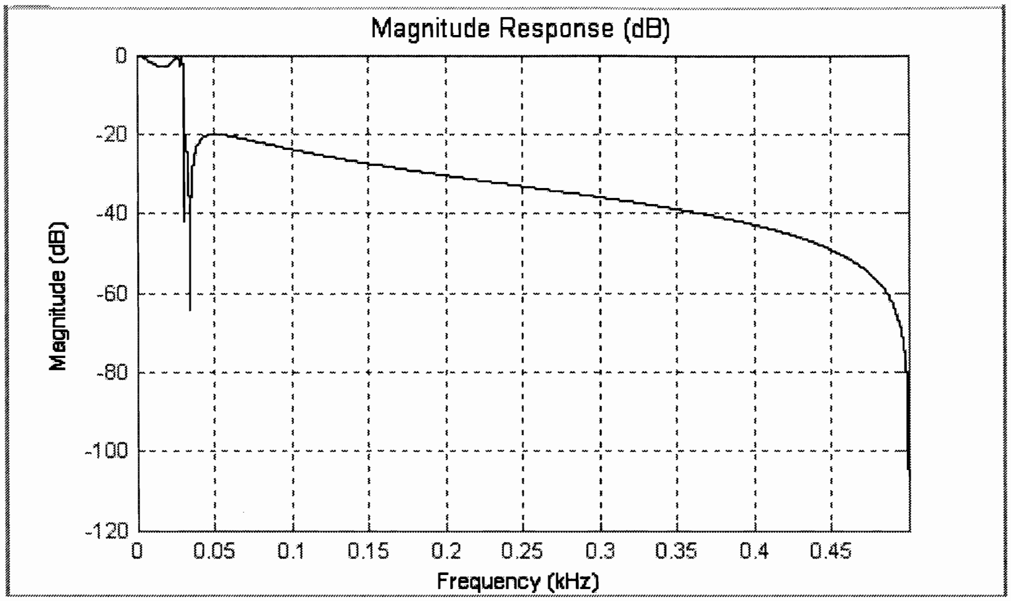

Figure 4.2: The seventh order elliptic filter used in this study.

Elliptic filters are equiripple in both the passband and stopband. This type of filter generally provides all filter requirements with the lowest order of any other type of filter. Given a filter order *n*, passband ripple *Rp* in decibels, and stopband ripple *Rs* in decibels, elliptic filters minimize transition width by:

$$|H(j\Omega)| = 10^{-R_P/20} \quad \text{at} \quad \Omega = 1 \qquad \text{Eq(4.8)}$$

In practical applications, this class of filters has better phase response characteristics than other type of filters (Proakis and Manolakis, 1996). This is one reason analog filters are more common in practice. Compared with the other filters, Butterworth and Chebyshev, Elliptic filters have narrow transition band (Lutovac, 2001). However, elliptic filter roll-off is not monotonic and eventually reaches an attenuation limit, called the stop-band floor. In this application, using Sptool in Matlab, a seventh order elliptic

filter with a R_P=3dB, R_s=20 dB and F_P=10 Hz was used to filter the swallowing signal. Figure (4.3) shows a portion of swallowing signal before and after filtering.

4.3.2. Development of a Prototype for each Waveform

In order to perform matched filtering to detect an activity in a specific waveform, a prototype (template) for each waveform had to be developed. The match filtering process incrementally slides the prototype over the unknown signal being processed while searching for a matching frame. Signals not correlated to the prototype will have in a correlation coefficient close to zero. If a matching frame is detected the correlation coefficient becomes closer one with a maximum value of one for a perfect match. In this study, in order to develop a prototype, several candidates of a representative activity were averaged. These candidates were selected by a subject expert. To decide how many patterns are necessary to develop the prototype a criterion named nipple time was applied. Nipple time is the time that the infant actually had the bottle in the mouth. In this study, 10% of the nipple time (calculated in seconds) was used as a criterion to develop the prototype.

For baby #87, having a nipple time of 9.15 minutes resulted in:

$$0.1 \times (9.15 \times 60) = 54.9 \approx 55 \text{ patterns}$$

Therefore, 55 representative patterns of a specific activity needed to be averaged to define the prototype for each specific activity. However, due to the unsatisfactory quality of the swallowing signal, only one representative pattern was selected to develop the prototype.

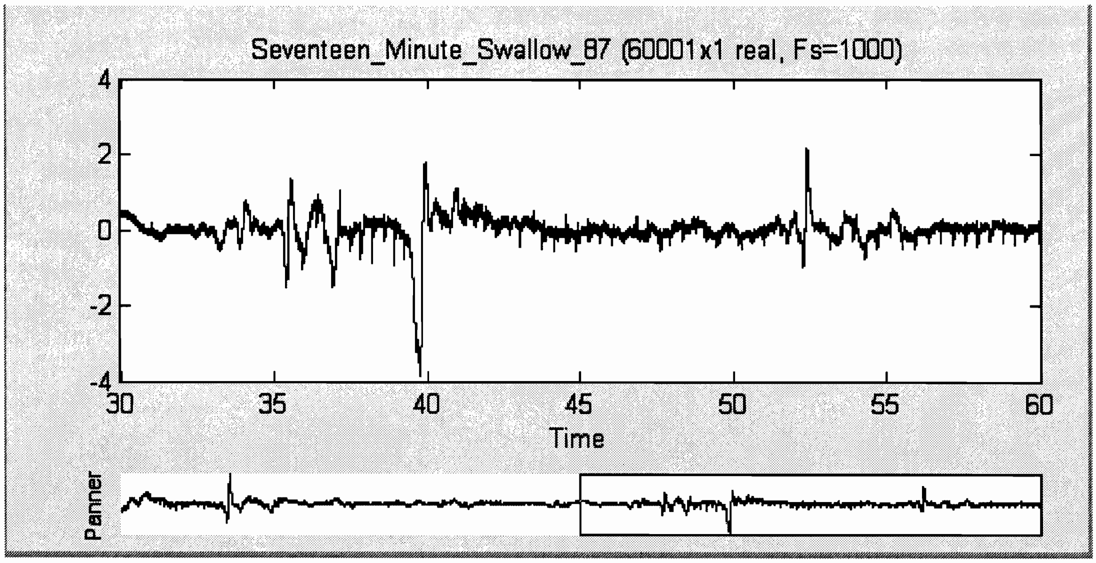

(a)

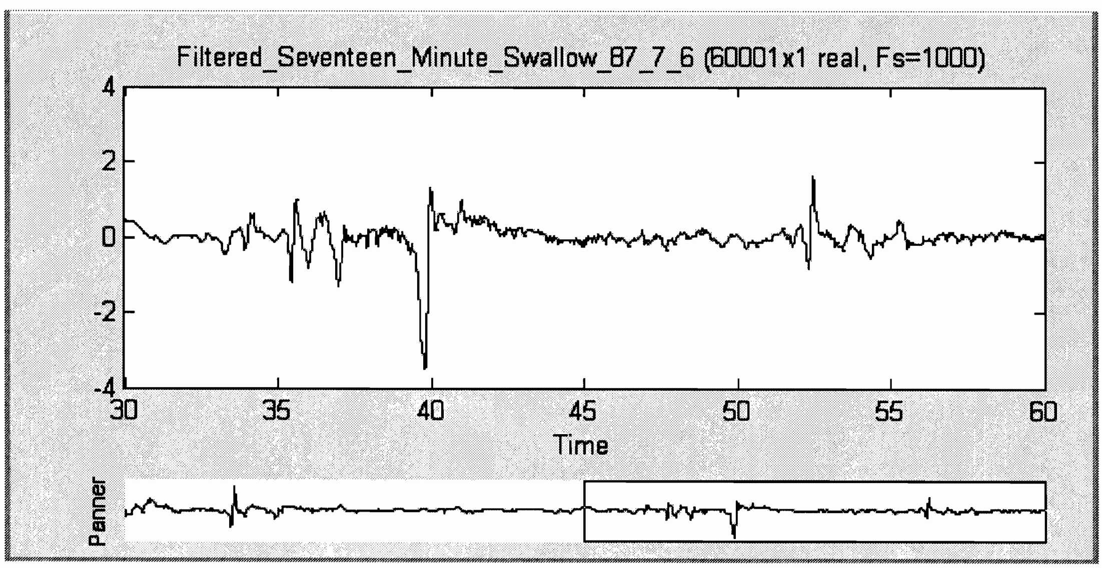

(b)

Figure 4.2: (a) A portion of swallowing signal before filtering. (b) The same portion of swallowing signal after filtering.

Baby #81 had a nipple time of 3.77 minutes. Picking up the 10% of nipple time resulted in :

$$0.1 \times (3.77 \times 60) = 22.62 \approx 23 \text{ patterns}$$

As a result, 23 candidate patterns of a specific activity were averaged to develop the prototype for each specific activity. Due to the poor quality of swallowing signal, only one pattern was selected as the candidate to define the prototype for swallowing signal. The user-defined functions *create_prototype_87_7* and *create_prototype_81_10* are used to implement the prototypes for baby #87 and baby #81 respectively. The corresponding m-files can be found in Appendix 2. The Figures (4.3), (4.4) and (4.5) represent the shape of the prototypes.

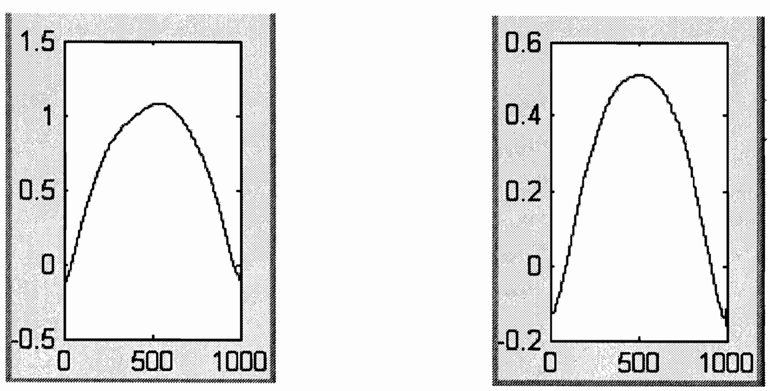

(a) (b)

Figure 4.3: (a) Sucking Prototype for baby # 81
(b) Sucking Prototype for baby # 87

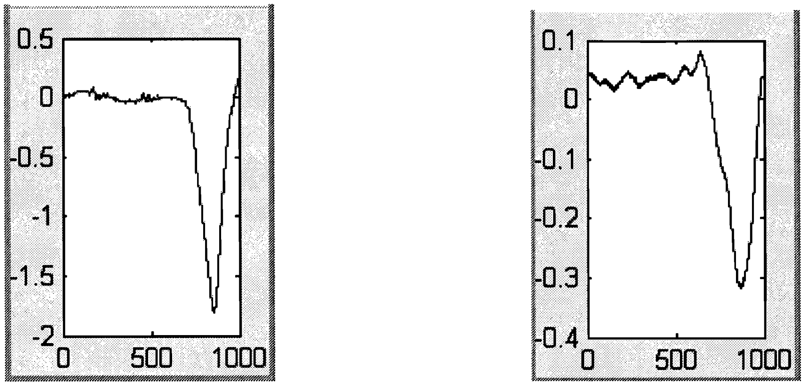

(a) (b)

Figure 4.4: (a) Swallowing Prototype for baby # 81
(b) Swallowing Prototype for baby # 87

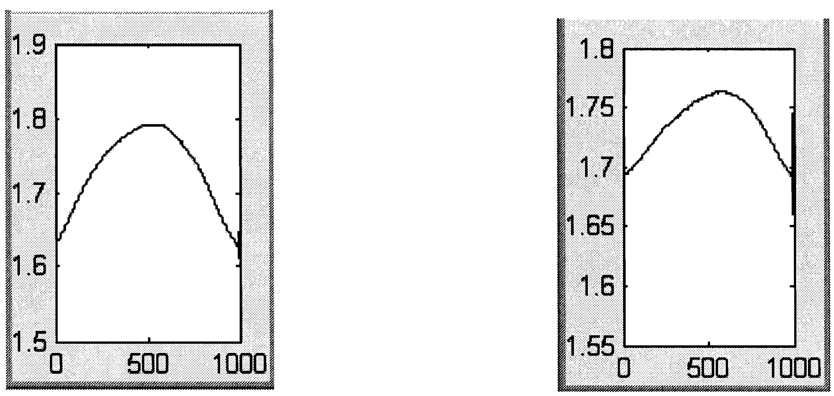

(a) (b)

Figure 4.5: (a) Breathing Prototype for baby # 81
(b) Breathing Prototype for baby # 87

4.3.3. Segmentation and Matched filtering

For each specific signal, the corresponding prototype is slid over the signal being processed while searching for a matching frame. The process of segmentation is the same as first approach (see section 2.4.2).

To perform the correlation, frames need to have the same size frames. In order to have the same size signals, resampling technique was applied. This task was performed

to change the sampling rate of all frames and make them the same size. In this study, all frames were resampled to have a length of 1000 samples. To perform this function in Matlab, a user-defined function named *resample-1000* was used. The m-file is available in Appendix 2. The following command in Matlab workspace can be used to perform the resampling task.

>> New_Signal = *resample_1000*(signal)

where the *New_Signal* is the same waveform but with a size of 1000 samples. Then the correlation between the prototype and the current frame, which is resampled to have a 1000 samples size, can be performed.

The whole signal was multiplied by a rectangular window which defined the current frame and the correlation between the current frame and the prototype was assessed. Frames that not correlated to the prototype will have a correlation coefficient close to zero. If a matching frame is detected, the correlation coefficient becomes closer one with a maximum value of one for a perfect match. In this study, for sucking and swallowing the goal was 85% correlation but for breathing this was decreased to 80%. For example, if the correlation coefficient of the current frame of breathing was 0.8 or higher, it was considered as a matching frame. The start time, the length of the current frame and the correlation coefficient was recorded in a matrix named occurrence matrix. The first row of this matrix indicated the start time of an activity, the second row corresponded to the length of an activity and the third row showed the correlation coefficient and can be interpreted as the level of certainty for that activity. Figure (4.6) shows the occurrence matrix of the sucking signal. Recalling that sampling rate is 1000

Hz, the first column of this matrix indicates: at the time of 85/1000=0.085 s there is 82% chance that a sucking incident has occurred and has lasted for about 1670/1000=1.67 s

Start time of an activity → row 1

Length of an activity → row 2

Level of Certainty → row 3

$$\begin{bmatrix} 85 & 1875 & 3040 & \ldots 20520 \ldots 58060 \\ 1670 & 990 & 560 & \ldots 520 \ldots 1010 \\ 0.82 & 0.9 & 0.93 & \ldots 0.89 \ldots 0.95 \end{bmatrix}$$

Figure 4.6: A typical occurrence matrix for sucking signal

This matrix was used to investigate the relationships between signals in the next step. The user-defined functions *scan_suck*, *scan_swallow* and *scan_breath* were implemented to perform this step with the corresponding m-files available in Appendix 2.

4.3.4. Analyzing the relationships between signals

In order to analyze the relationship between the three signals (suck, swallow and breathing), the corresponding occurrence matrices provided by the pervious step, were transformed into a binary stream. To perform this analysis, each minute of a specific signal was divided into consequent time slots and using the corresponding matrix the occurrence of that specific activity in different time slots was examined. The size of a time slot was 500 samples. The Table (4.1) shows the corresponding binary stream to the occurrence matrix of sucking shown in Figure (4.6).

Table 4.1: A typical binary stream

1-500	501-1000	1001-1500	1501-2000	2001-2500	2501-3000	3001-3500	…	20001-20500	20501-21000	…	58001-58500	58501-59000	59001-59500	59501-60000
0	1	1	1	1	1	1	…	0	1	…	1	1	0	0

At the end of a detection procedure for all three signals for a specific baby, the binary streams of all three signals were combined in a table named decision table. The decision table was used to determine whether suck, swallow and breathing had occurred in a coordinated fashion or not. Assuming Table (4.2) is the decision table for the first minute of feeding of a premature infant, this baby has been sucking for almost three seconds (third to eighth columns have the value of one in sucking row) without any swallowing incident (from third to eighth columns, swallowing has the value of zero in the binary stream). On the other hand, in the 59th second of feeding, the infant has been attempting to breathe and swallow at the same time (the last two columns have the value of 1 in swallow and breathing rows).

Table 4.2: A typical decision table

Time Slot	1-500	501-1000	1001-1500	1501-2000	2001-2500	2501-3000	3001-3500	…	58001-58500	58501-59000	59001-59500	59501-60000
Suck	0	1	1	1	1	1	1	…	1	1	0	0
Swallow	0	0	0	0	0	0	0	…	0	0	1	1
Breathing	1	1	1	0	0	1	0	…	1	0	1	1

By examining different minutes and different feedings for the same baby, it can be investigated whether the baby has reached the point of coordinating of suck, swallow and breathing processes. To perform this task, the user-defined function *transfer_to_one_zero* was implemented. The corresponding m-file is available in Appendix 2.

Actually, for both babies, the quality of signals in the selected samples was not acceptable for the entire feeding. For baby #81, the second, third, eight and ninth minutes were selected to be analyzed while acceptable data for baby # 81 were found in the third, forth, fifth, sixth, seventh, thirteenth and fourteenth minutes. Figure (4.7) shows the overall system architecture for this approach.

4.5. Evaluation

As was mentioned previously, due to the unsatisfactory quality of the swallowing signal for most of the babies enrolled in this research, the number of babies with reliable data was reduced to two babies (baby #81, 10th feeding and baby #87, seventh feeding).

The program was run for every minute of all three signals for each baby (suck, swallow and breathing) and the result of detection of each waveform were presented to the subject expert for evaluation. The outcome of evaluation was expressed as the *agreements* and *disagreements* between the system and the subject expert for each minute. In other words, if the subject expert accepted a pattern as an activity while the system rejected it or vise versa, this would be a *disagreement*. But if both the system and the subject expert agree with a pattern as an activity, this would be an *agreement*.

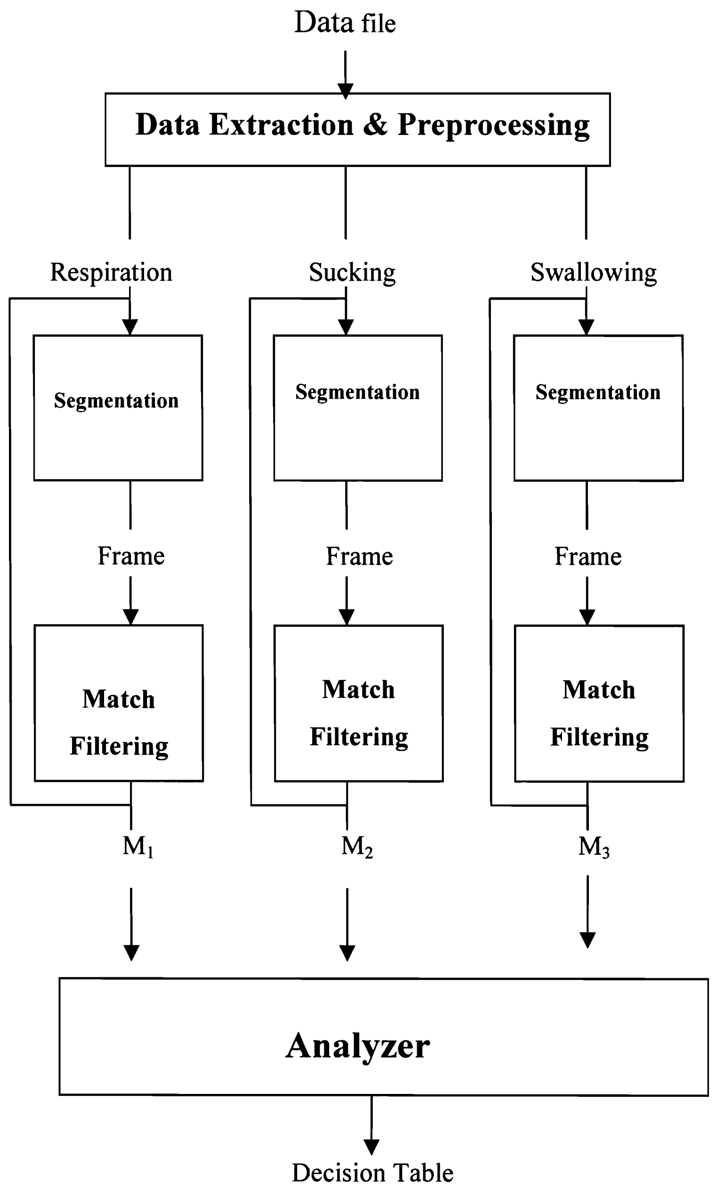

Figure 4.7: The overall system architecture of third approach where M_i is corresponding occurrence matrix

4.6. Results

The results of this study are shown in following sections. In first section, the results of detection of every minute of suck, swallow and breathing waveforms of baby #87, seventh feeding and baby #81, 10th feeding and the evaluation of detection are presented. In the second section, the result of combining the binary streams of all three signals in a decision table and analyzing the relationship of these signals are shown.

4.6.1. Result of Detection

In this section, the results of detection of every minute of suck, swallow and breathing waveforms of baby #87, seventh feeding is presented. For simplicity, the occurrence matrices are shown in form of a table.

The Detection of Sucking for Baby #87, Seventh Feeding

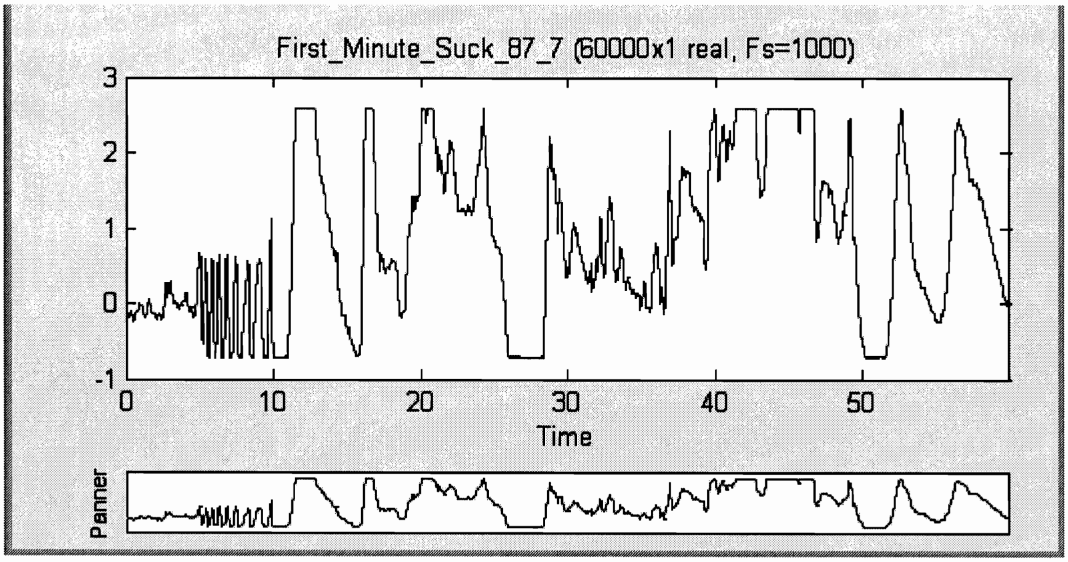

Figure 4.8: The first minute of sucking of baby #87, seventh feeding

Table 4.3: The analysis of the first minute of sucking of Baby #87, seventh feeding

Time Slot	Length	Level of Certainty	Time Slot	Length	Level of Certainty
561	820	0.95413	30081	860	0.94639
3801	540	0.89294	31981	500	0.90033
4661	580	0.88677	32501	780	0.96116
5581	520	0.91018	33321	600	0.92284
6581	500	0.9032	34941	500	0.86386
7141	580	0.91227	35501	1100	0.88231
7781	800	0.91499	36661	500	0.89166
8601	760	0.97393	37301	1540	0.87254
9541	500	0.89808	39501	840	0.93032
15721	1820	0.87918	40341	500	0.93477
17781	660	0.85952	41061	1960	0.86429
19641	1860	0.88612	46821	1600	0.95856
21561	1000	0.94357	48821	640	0.89002
23381	1640	0.88174	51861	1740	0.94823
28181	1900	0.86103	55861	1740	0.87341

Table 4.4: The evaluation of the first minute of sucking of baby #87, seventh feeding

Agreement(s)	Disagreement(s)
26	6

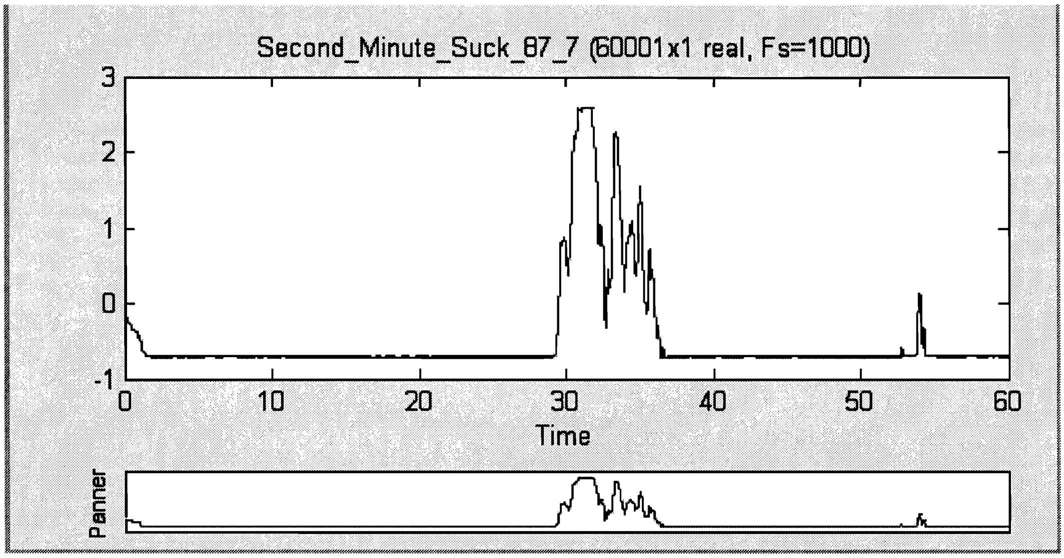

Figure 4.9: The second minute of sucking of baby #87, seventh feeding

Table 4.5: The analysis of the second minute of sucking of baby #87,seventh feeding

Time Slot	Length	Level of Certainty
29481	700	0.90113
30321	1880	0.8987
32941	1080	0.93863
34021	720	0.88684
34761	540	0.9221
35401	740	0.88039
53701	520	0.9438

Table 4.6: The evaluation of the second minute of sucking of baby #87, seventh feeding

Agreement(s)	Disagreement(s)
5	1

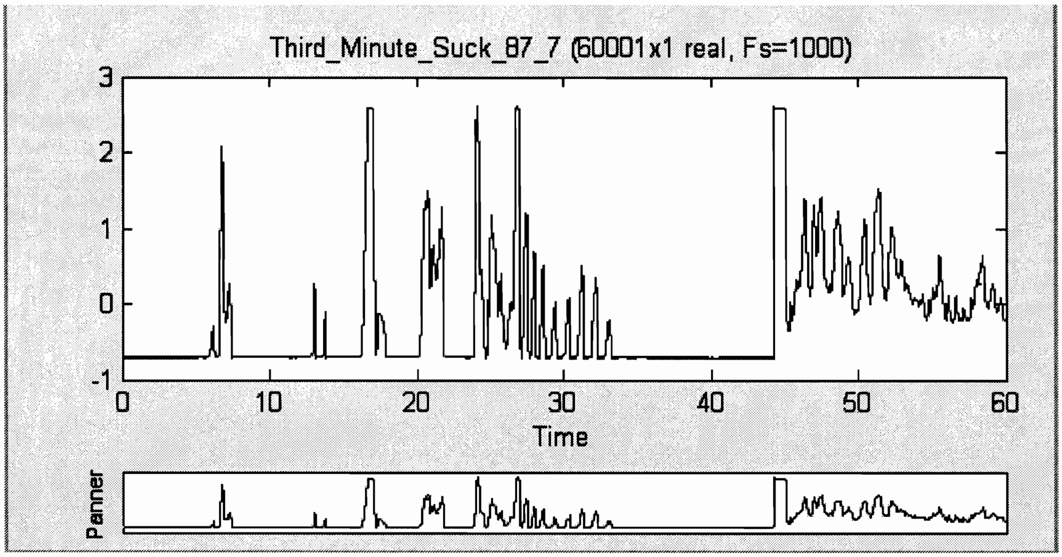

Figure 4.10: The third minute of sucking for baby #87, seventh feeding

Table 4.7: The analysis of the third minute of sucking of baby #87,seventh feeding

Time Slot	Length	Level of Certainty	Time Slot	Length	Level of Certainty
5881	500	0.89248	30021	560	0.88909
6521	500	0.8996	30921	560	0.8933
16201	1220	0.91703	31801	660	0.88215
20281	760	0.93606	32781	600	0.87932
23701	980	0.85756	43981	1440	0.88683
24761	860	0.9266	45961	820	0.89494
26501	700	0.90468	47141	660	0.93402
27201	500	0.92069	53661	520	0.93646
27741	500	0.90414	55201	660	0.89146
28321	520	0.89647	57761	1060	0.85024
29041	660	0.87146	58861	520	0.93365

Table 4.8: The evaluation of the third minute of sucking of baby #87, seventh feeding

Agreement(s)	Disagreement(s)
22	6

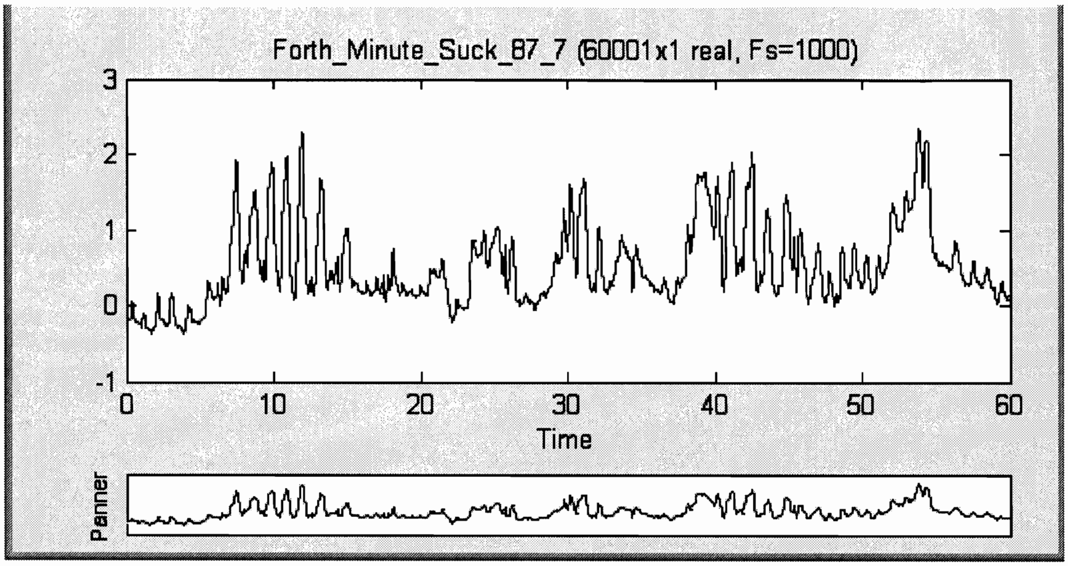

Figure4.11: The forth minute of sucking of baby #87, seventh feeding

Table 4.9: The analysis of the forth minute of sucking of baby #87, seventh feeding

Time Slot	Length	Level of Certainty	Time Slot	Length	Level of Certainty	Time Slot	Length	Level of Certainty
141	500	0.85942	18561	520	0.91667	44481	980	0.94299
921	500	0.91609	20221	1860	0.88121	45461	860	0.9339
1901	500	0.85808	23361	520	0.90301	46321	820	0.91914
2741	740	0.89074	24021	500	0.85794	47561	1240	0.92669
3941	680	0.87811	24581	1100	0.94244	48401	500	0.90135
5361	500	0.89589	25861	740	0.94619	49061	560	0.88892
6841	1140	0.8995	26841	600	0.92234	50001	900	0.95956
8121	1100	0.91025	29521	520	0.93119	50901	620	0.93095
9321	1020	0.91647	30501	1080	0.93636	51761	520	0.88702
10381	900	0.96121	31821	720	0.91388	52761	780	0.86509
11381	1040	0.91085	33021	1500	0.9476	53261	500	0.8668
12701	1020	0.92146	36241	700	0.89882	55881	1580	0.88584
14021	500	0.85897	38341	1720	0.95192	57281	960	0.88233
14541	780	0.99086	40561	1060	0.91785	58081	540	0.89697
16081	500	0.8914	41801	1180	0.90068	59161	800	0.87084
16761	520	0.89345	43121	520	0.90845	44481	700	0.94299

Table 4.10: The evaluation of the forth minute of sucking of baby #87, seventh feeding

Agreement(s)	Disagreement(s)
41	7

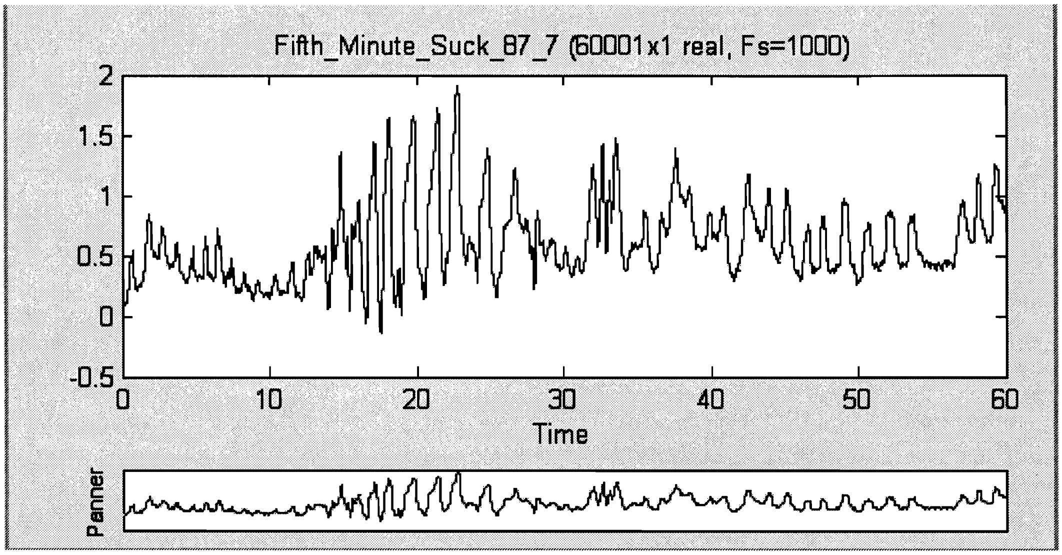

Figure 4.12: The fifth minute of sucking of baby #87, seventh feeding

Table 4.11: The analysis of the fifth minute of sucking of baby #87, seventh feeding

Time Slot	Length	Level of Certainty	Time Slot	Length	Level of Certainty	Time Slot	Length	Level of Certainty
281	800	0.89121	20521	1440	0.92734	41881	1600	0.86326
1481	720	0.8988	22021	1340	0.91688	43541	780	0.91324
2341	840	0.8733	23361	720	0.88983	44561	1240	0.86795
3421	600	0.85852	24101	1200	0.96173	46081	940	0.90905
5401	520	0.89378	26221	980	0.87533	47201	900	0.90203
6121	880	0.8978	28741	900	0.92894	48521	1240	0.87421
8041	500	0.85637	29781	800	0.8912	50081	1200	0.88209
8841	820	0.89851	30601	680	0.92522	51461	1520	0.86845
9981	820	0.92115	31501	940	0.93257	53201	1020	0.90739
11061	860	0.90165	32841	1340	0.85948	55221	500	0.85284
12361	500	0.91308	35201	740	0.87286	56441	1400	0.88105
14501	720	0.86743	36441	620	0.86977	57861	620	0.96765
15381	1120	0.91391	37081	1220	0.85199	58941	980	0.85571
16521	1020	0.96115	38301	500	0.88981			
17581	960	0.95888	39641	560	0.92196			
18861	1600	0.90809	40401	880	0.90415			

Table 4.12: The evaluation of the fifth minute of sucking of baby #87, seventh feeding

Agreement(s)	Disagreement(s)
39	8

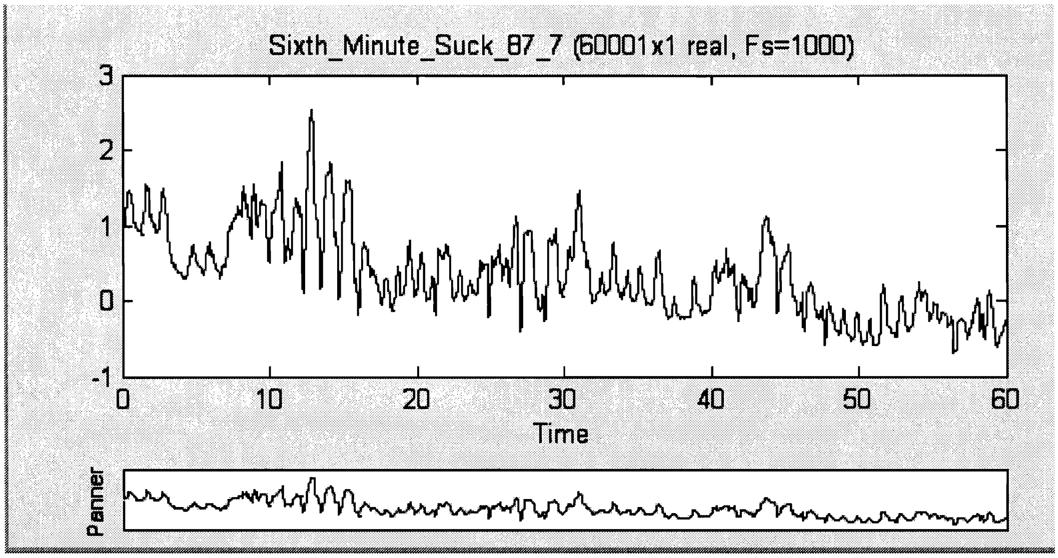

Figure 4.13: The sixth minute of sucking of baby #87, seventh feeding

Table 4.13: The analysis of the sixth minute of sucking of baby #87, seventh feeding

Time Slot	Length	Level of Certainty	Time Slot	Length	Level of Certainty	Time Slot	Length	Level of Certainty
61	900	0.94181	20781	500	0.88202	40001	560	0.91077
1281	900	0.87328	21281	200	0.86525	41861	800	0.89866
2301	960	0.89395	22521	800	0.87068	42921	1760	0.93629
4201	1380	0.88624	23981	1000	0.89289	44681	840	0.87817
5581	740	0.87555	25301	540	0.87954	46261	1020	0.94271
8681	500	0.86704	25841	500	0.86898	47661	880	0.88823
9181	600	0.89942	26341	680	0.9193	48641	720	0.88771
9921	1240	0.89584	27041	1180	0.95599	49501	820	0.88728
11341	1000	0.93375	28641	1340	0.92143	50441	620	0.87463
12341	900	0.9372	29981	2000	0.89367	51261	940	0.86084
13381	1400	0.94755	32261	600	0.88163	52461	920	0.91478
14781	1000	0.99359	32921	920	0.86568	53501	1480	0.91444
16081	820	0.93556	34041	580	0.88434	55421	660	0.96368
17541	780	0.92698	34761	880	0.86616	56521	960	0.90213
18401	660	0.89136	35861	1180	0.88301	57541	780	0.85433
19081	800	0.93022	37101	800	0.87059	58481	880	0.94592
19921	740	0.93653	38521	720	0.88491			

Table 4.14: The evaluation of the sixth minute of sucking of baby #87, seventh feeding

Agreement(s)	Disagreement(s)
50	1

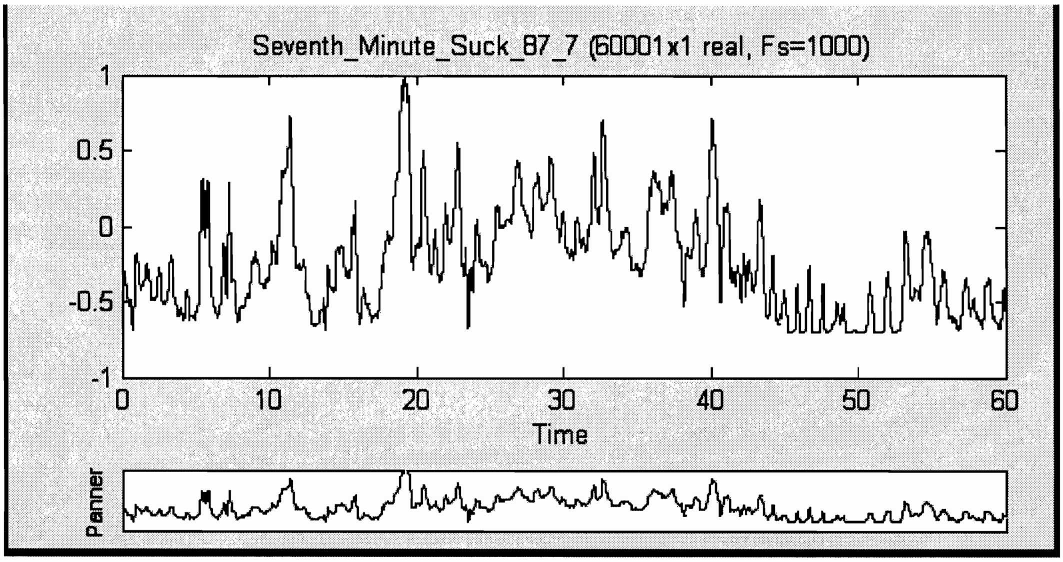

Figure 4.14: The seventh minute of sucking of baby #87, seventh feeding

Table 4.15: The analysis of the seventh minute sucking of baby #87, seventh feeding

Time Slot	Length	Level of Certainty	Time Slot	Length	Level of Certainty	Time Slot	Length	Level of Certainty
761	560	0.88809	21741	500	0.86943	40761	620	0.93699
1321	720	0.9063	22321	920	0.87753	42361	520	.9545
2281	520	0.87061	23841	580	0.89672	42941	860	0.93926
2941	800	0.85994	25281	500	0.90323	43901	680	0.87317
4141	500	0.90921	26321	1220	0.87371	44621	700	0.85497
4841	1660	0.86751	27821	840	0.89779	45621	500	0.88677
6641	500	0.8943	28761	860	0.87649	46381	620	0.89762
8461	1260	0.8737	29721	500	0.96471	47341	500	0.86006
10001	500	0.90379	30721	540	0.90827	48321	500	0.85599
10501	1380	0.92206	31761	660	0.86242	50501	700	0.8961
13281	560	0.86614	32421	640	0.94033	51601	840	0.89726
14321	1080	0.88732	33401	1420	0.86455	52861	880	0.89289
15441	640	0.9116	35641	1300	0.88881	54021	1420	0.91031
16081	900	0.89624	37001	740	0.92234	55441	700	0.954
18221	1820	0.88144	38581	880	0.8952	56921	780	0.93606
20961	620	0.91514	39541	1220	0.96888	58341	1000	0.89823

Table 4.16: The evaluation of the seventh minute of sucking of baby #87, seventh feeding

Agreement(s)	Disagreement(s)
47	2

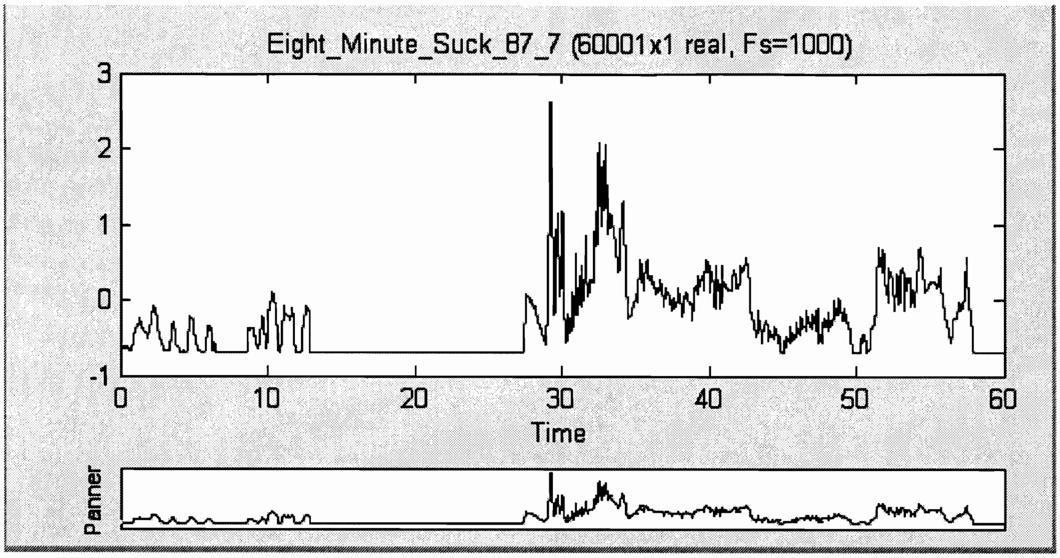

Figure 4.15: The eighth minute of sucking of baby #87, seventh feeding

Table 4.17: The analysis of the eighth minute of sucking of baby #87, seventh feeding

Time Slot	Length	Level of Certainty	Time Slot	Length	Level of Certainty
821	1080	0.92757	33101	500	0.89078
1921	760	0.981	33801	680	0.91524
3181	880	0.86079	35101	500	0.85898
4381	980	0.89041	36441	520	0.8774
5721	580	0.94706	37701	500	0.8528
8481	920	0.90505	41481	500	0.91082
9401	500	0.91808	41981	880	0.85063
9901	820	0.97857	50161	620	0.85414
10721	1300	0.93462	51221	940	0.89505
12141	980	0.89728	53901	900	0.91275
27101	1840	0.88747	54821	740	0.97662
28981	540	0.93191	57201	520	0.85022

Table 4.18: The evaluation of the eighth minute of sucking of Baby #87, seventh feeding

Agreement(s)	Disagreement(s)
17	7

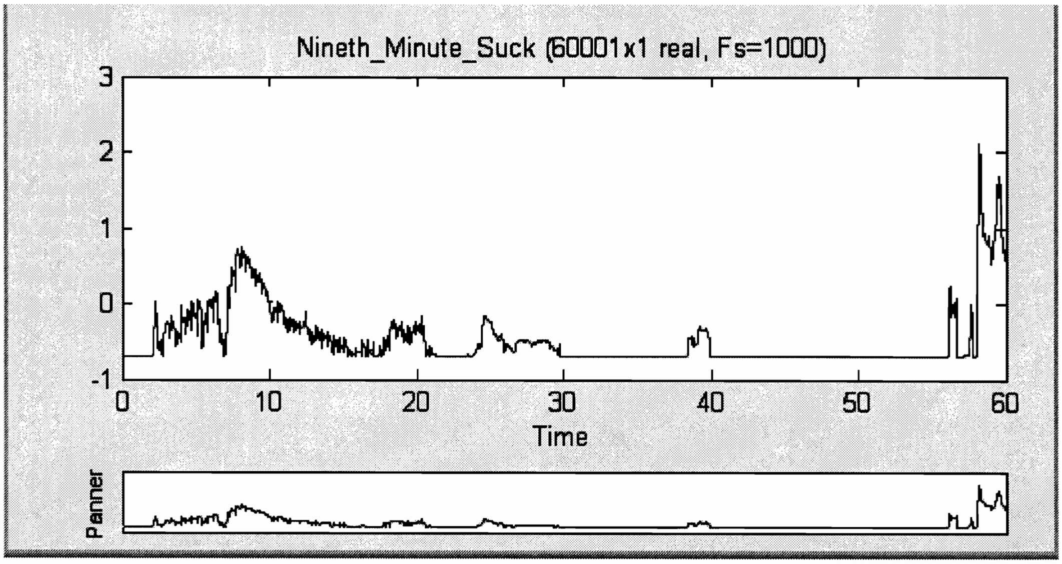

Figure 4.16: The ninth minute of sucking of baby #87, seventh feeding

Table 4.19: The analysis of the ninth minute of sucking of baby #87, seventh feeding

Time Slot	Length	Level of Certainty
2021	500	0.8972
2681	1120	0.8563
5381	1540	0.8719
19521	1200	0.8581
24121	1540	0.8762
26721	1180	0.8967
38881	1200	0.9086
55861	1080	0.8766
57401	520	0.8879
59021	960	0.8787

Table 4.20: The evaluation of the ninth minute of sucking of Baby #87, seventh feeding

Agreement(s)	Disagreement(s)
5	5

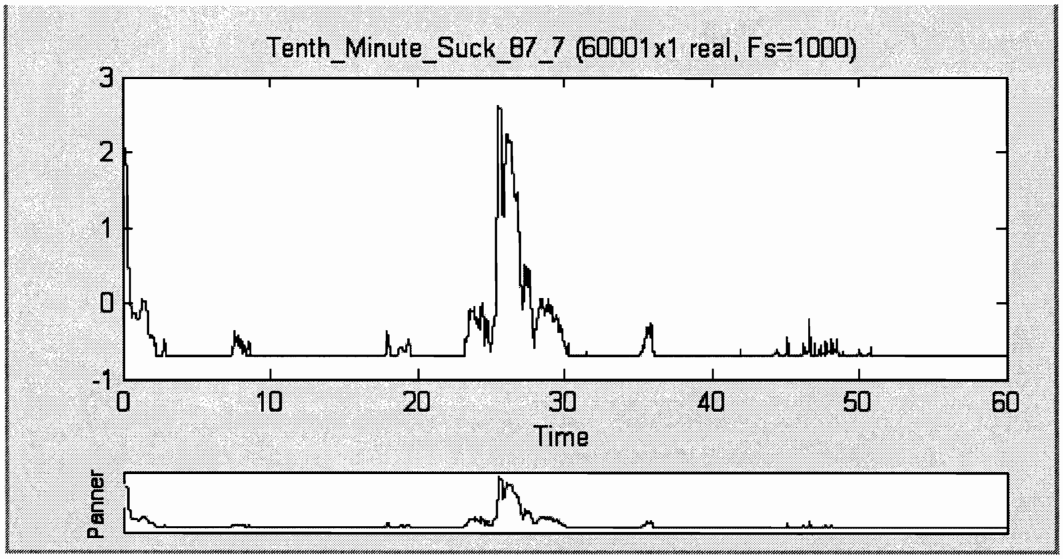

Figure 4.17: The 10th minute of sucking of baby #87, seventh feeding

Table 4.21: The analysis of the 10th minute of sucking of baby #87, seventh feeding

Time Slot	Length	Level of Certainty
1001	860	0.9152
17721	500	0.8702
19121	500	0.8647
23341	900	0.8831
25381	540	0.9413
25921	680	0.9066
27841	1980	0.8558
35081	1220	0.8767
1001	860	0.9152

Table 4.22: The evaluation of the 10th minute of sucking of baby #87, seventh feeding

Agreement(s)	Disagreement(s)
6	2

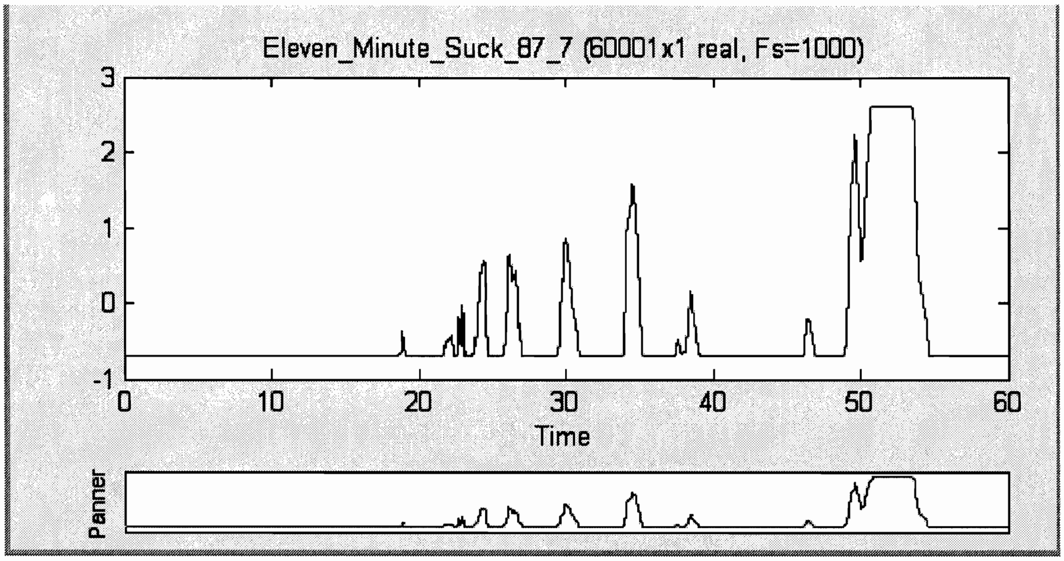

Figure 4.18: The 11th minute of sucking of baby #87, seventh feeding

Table 4.23: The analysis of the 11th minute of sucking of Baby #87, seventh feeding

Time Slot	Length	Level of Certainty
18661	500	0.8676
21581	1040	0.9273
23681	1240	0.8697
25521	1780	0.8876
29241	1780	0.9108
33681	1740	0.9417
37301	720	0.8763
38041	1000	0.9373
45961	1160	0.8910
49081	1100	0.9379

Table 4.24: The evaluation of the 11th minute of sucking of baby #87, seventh feeding

Agreement(s)	Disagreement(s)
9	2

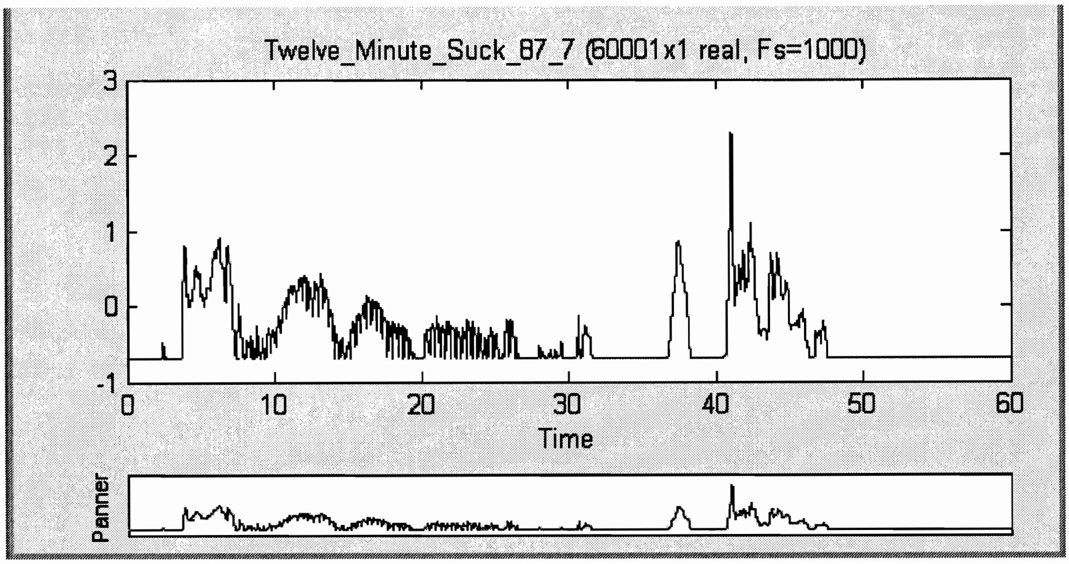

Figure 4.19: The 12th minute of sucking of baby #87, seventh feeding

Table 4.25: The analysis of the 12th minute of sucking of baby #87,seventh feeding

Time Slot	Length	Level of Certainty	Time Slot	Length	Level of Certainty
3681	540	0.8717	40781	600	0.8846
4301	840	0.9431	42001	820	0.8950
5541	1220	0.9428	43021	500	0.9088
10901	660	0.8941	43521	500	0.8837
24441	500	0.8647	44521	500	0.9129
30801	940	0.9263	46481	1380	0.8765
36701	1700	0.9726			

Table 4.26: The evaluation of the 12th minute of sucking of baby #87, seventh feeding

Agreement(s)	Disagreement(s)
11	3

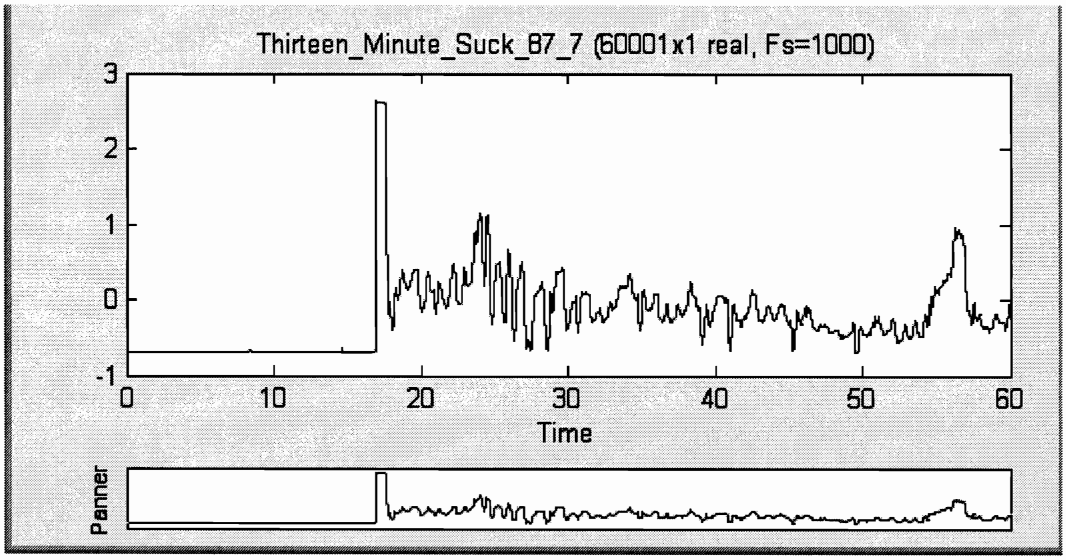

Figure 4.20: The 13th minute of sucking of baby #87, seventh feeding

Table 4.27: The analysis of the 13th minute of sucking of baby #87, seventh feeding

Time Slot	Length	Level of Certainty	Time Slot	Length	Level of Certainty
16581	1500	0.8761	35621	700	0.8863
18441	720	0.8701	36461	560	0.8974
19181	760	0.9148	37201	560	0.8963
20081	1000	0.9145	37761	1320	0.8771
21741	900	0.8965	39181	500	0.8764
22761	500	0.8649	39681	1400	0.8674
23401	980	0.9107	42041	1100	0.8950
24801	960	0.9544	43241	840	0.9272
25761	500	0.9326	44101	800	0.9741
26301	940	0.9687	45761	1000	0.9019
27401	1300	0.9550	47221	500	0.8580
28701	1340	0.8836	50301	1300	0.9010
30041	680	0.9345	51721	620	0.8888
30721	940	0.9350	52621	620	0.9042
31761	680	0.9156	53281	620	0.8774
33021	1880	0.8930	55581	1760	0.8918
34941	520	0.8695	58601	1160	0.8898

Table 4.28: The evaluation of the 13th minute of sucking of baby #87, seventh feeding

Agreement(s)	Disagreement(s)
31	3

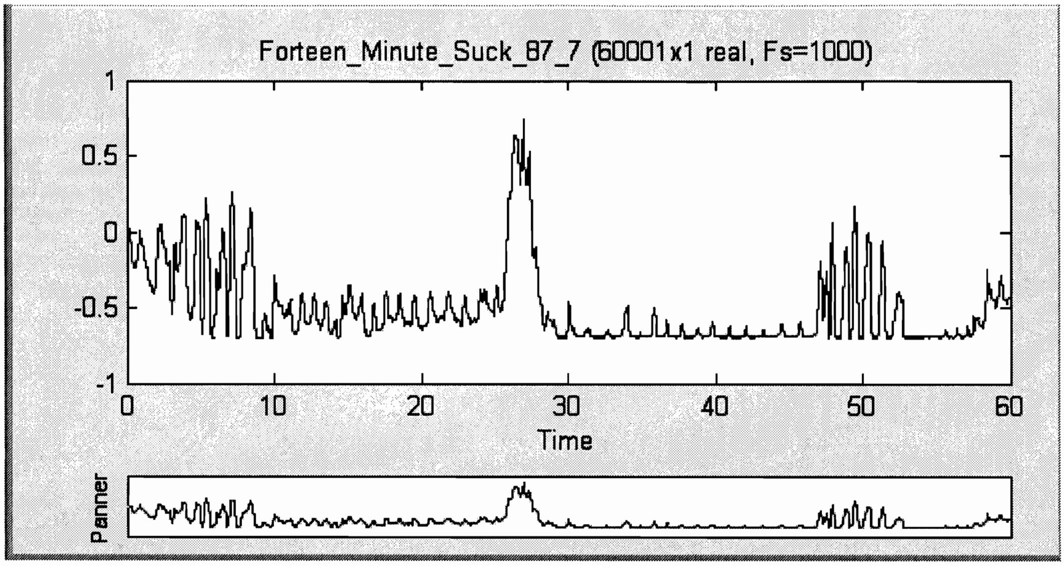

Figure 4.21: The 14th minute of sucking of baby #87, seventh feeding

Table 4.29: The analysis of the 14th minute of sucking of baby #87, seventh feeding

Time Slot	Length	Level of Certainty	Time Slot	Length	Level of Certainty
461	1040	0.8901	21441	940	0.8721
1681	1480	0.9110	22661	720	0.8904
3421	800	0.8974	23661	1280	0.8548
4381	780	0.9384	25681	1980	0.8530
5161	520	0.9856	28381	500	0.8586
6201	620	0.9101	30861	920	0.8589
6841	620	0.9795	33621	720	0.8911
7521	1440	0.9026	35581	580	0.9064
9021	760	0.8573	39561	500	0.8559
11561	660	0.8838	44241	540	0.8608
12361	720	0.8675	45501	520	0.8653
13141	720	0.8976	46881	500	0.9302
14781	720	0.8958	47701	540	0.9148
15541	700	0.8637	48461	760	0.8991
16521	540	0.8802	49221	500	0.9880
17361	540	0.8897	49881	940	0.9061
18221	660	0.8611	50981	740	0.8928
19201	740	0.8814	51841	1220	0.8943
20261	880	0.8605	59041	700	0.9140

Table 4.30: The evaluation of the 14th minute of sucking of baby #87, seventh feeding

Agreement(s)	Disagreement(s)
38	0

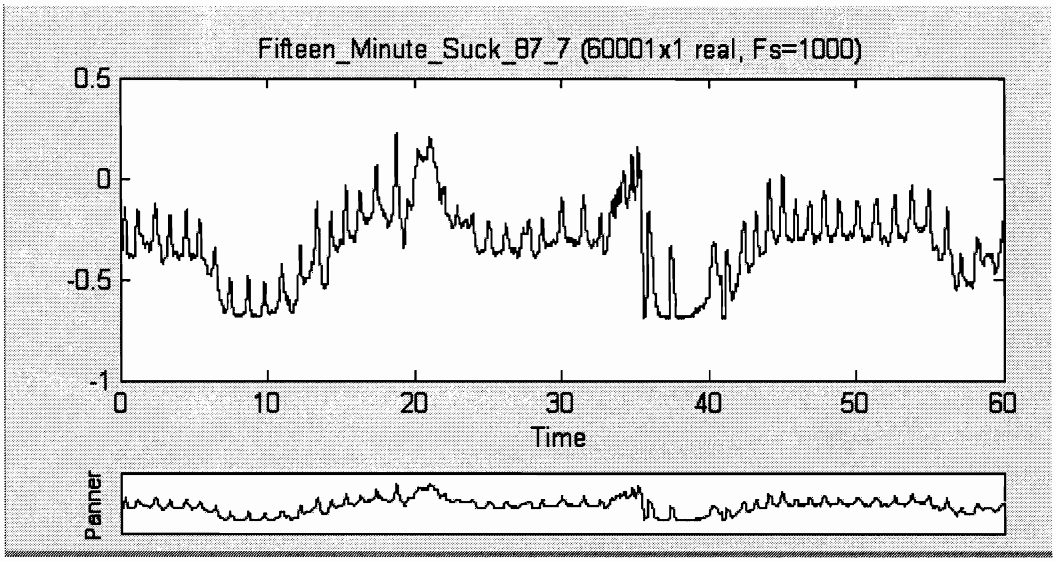

Figure 4.22: The 15th minute of sucking of baby #87, seventh feeding

Table 4.31: The analysis of the 15th minute of sucking of baby #87, seventh feeding

Time Slot	Length	Level of Certainty	Time Slot	Length	Level of Certainty	Time Slot	Length	Level of Certainty
41	600	0.8855	17061	720	0.8616	41961	840	0.8791
921	660	0.8541	18401	760	0.8615	42981	560	0.8977
1981	940	0.8690	19801	1940	0.8610	43781	760	0.8874
3101	600	0.9008	23241	500	0.8974	44701	700	0.9172
4181	660	0.8793	24721	740	0.8869	45661	520	0.8673
5141	540	0.8913	25841	860	0.8971	46481	760	0.8787
6141	540	0.8962	27001	1320	0.9013	47501	720	0.9141
7141	640	0.8561	28441	540	0.8981	48601	580	0.8674
8421	520	0.8729	29641	820	0.8793	49721	880	0.8842
9541	560	0.8669	31181	700	0.8784	50921	920	0.9010
10641	720	0.8851	32401	540	0.9003	52261	760	0.8766
11981	540	0.8942	33981	500	0.9386	53461	680	0.8934
12881	920	0.8571	35001	500	0.8884	54621	620	0.8866
14081	500	0.8532	35601	900	0.8908	55861	600	0.8785
15101	520	0.9262	37161	720	0.8791	57921	780	0.8799
16061	580	0.8748	39681	1460	0.8977			

Table 4.32: The evaluation of the 15th minute of sucking of baby #87, seventh feeding

Agreement(s)	Disagreement(s)
47	0

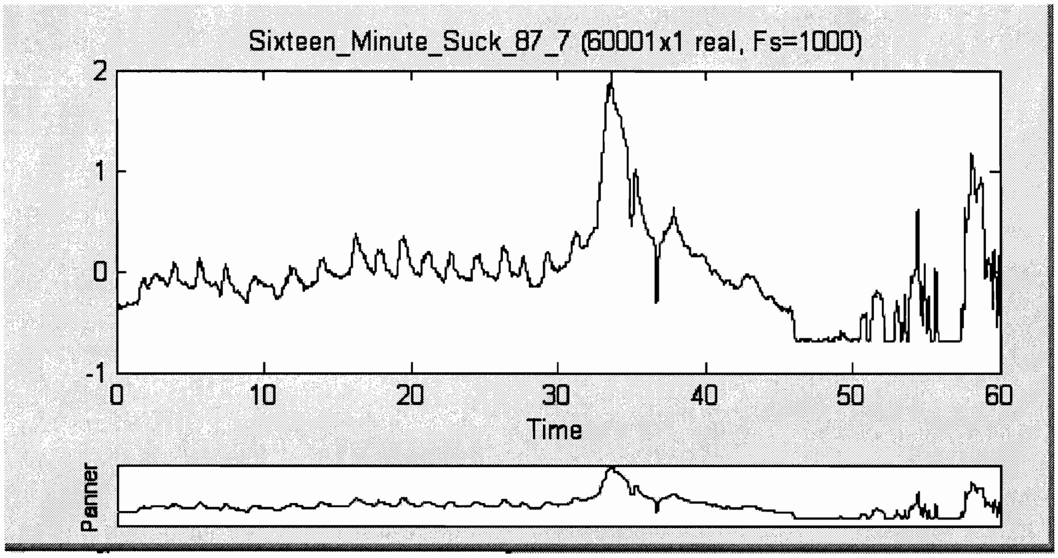

Figure 4.23: The 16th minute of sucking of baby #87, seventh feeding

Table 4.33: The analysis of the 16th minute of sucking of baby #87, seventh feeding

Time Slot	Length	Level of Certainty	Time Slot	Length	Level of Certainty
1541	720	0.8888	25761	1320	0.9161
2321	760	0.9510	27261	860	0.9194
3401	1180	0.8621	28821	1220	0.8566
5221	1040	0.8886	30801	1040	0.8815
6961	1160	0.8698	32881	1820	0.8951
9101	600	0.8725	34961	880	0.8677
11161	1740	0.9362	36861	1900	0.9192
13581	840	0.9053	40461	500	0.8985
15541	1860	0.8811	41301	500	0.8700
17461	960	0.9642	42201	1700	0.9720
18801	1620	0.8885	50341	880	0.9000
20521	1400	0.9271	51221	1000	0.9337
22181	1260	0.8941	52701	700	0.9077
23981	1240	0.8930	57401	1800	0.9080

Table 4.34: The evaluation of the 16th minute of sucking of baby #87, seventh feeding

Agreement(s)	Disagreement(s)
28	0

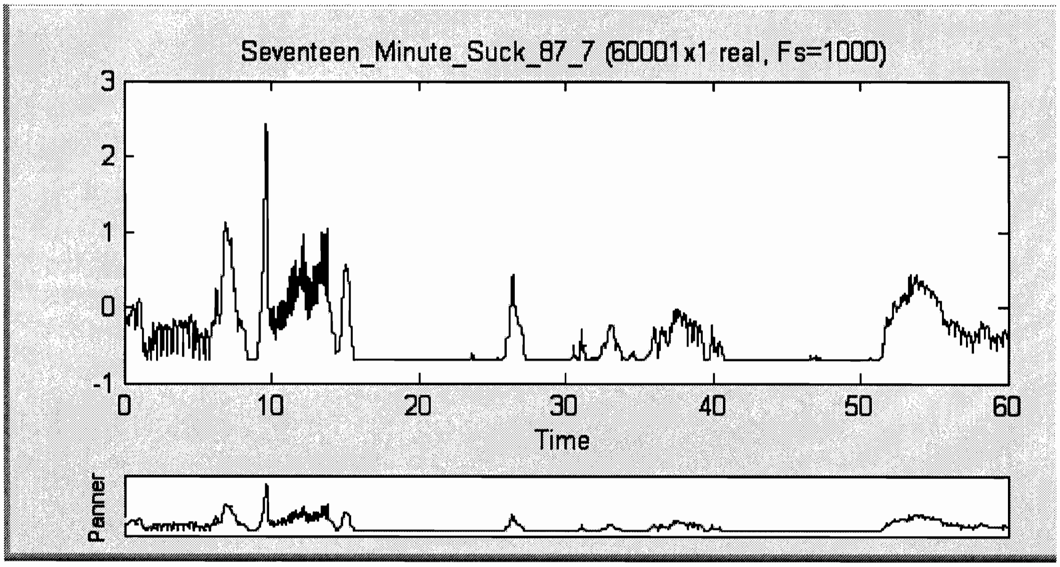

Figure 4.24: The 17th minute of sucking of baby #87, seventh feeding

Table 4.35: The analysis of the 17th minute of sucking of baby #87,seventh feeding

Time Slot	Length	Level of Certainty
281	580	0.8926
6361	1440	0.9234
9301	600	0.8707
14441	1280	0.9104
25601	1900	0.8662
32181	1840	0.8825
35761	560	0.9200
36321	660	0.8955
40261	500	0.8668
53501	540	0.9218

Table 4.36: The evaluation of the 17th minute of sucking of baby #87, seventh feeding

Agreement(s)	Disagreement(s)
5	0

The Detection of Swallowing for Baby #87, 7^{th} feeding

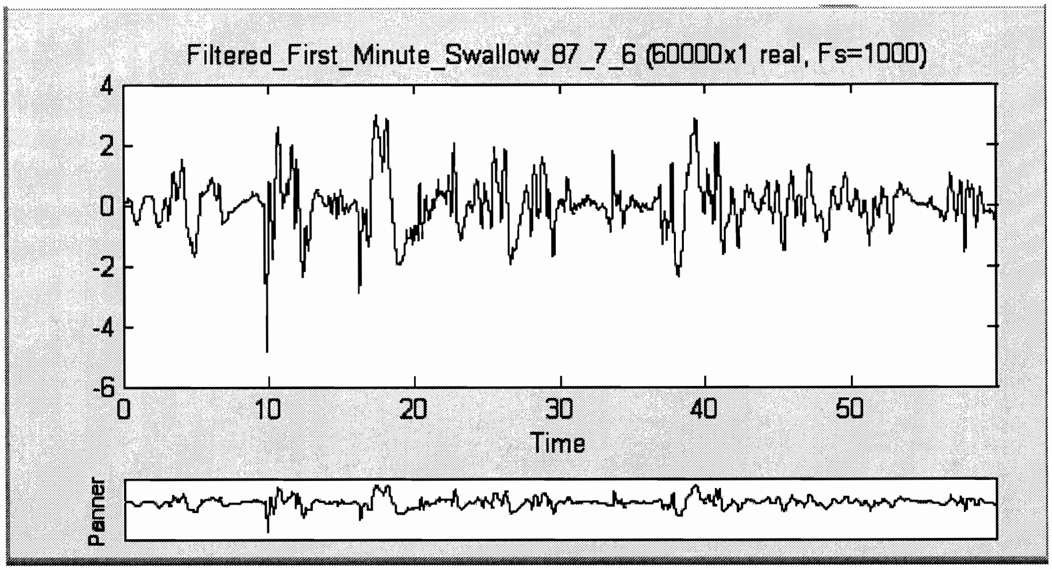

Figure 4.25: The first minute of swallowing of baby #87, seventh feeding

Table 4.37: The analysis of the first minute of swallowing of baby #87, seventh feeding

Time Slot	Length	Level of Certainty
5341	920	0.85295
8401	1660	0.86063
11101	1420	0.85259
14781	1720	0.882
36221	1000	0.85259
43801	1840	0.86742

Table 4.38: The evaluation of the first minute of swallowing of baby #87, seventh feeding

Agreement(s)	Disagreement(s)
4	2

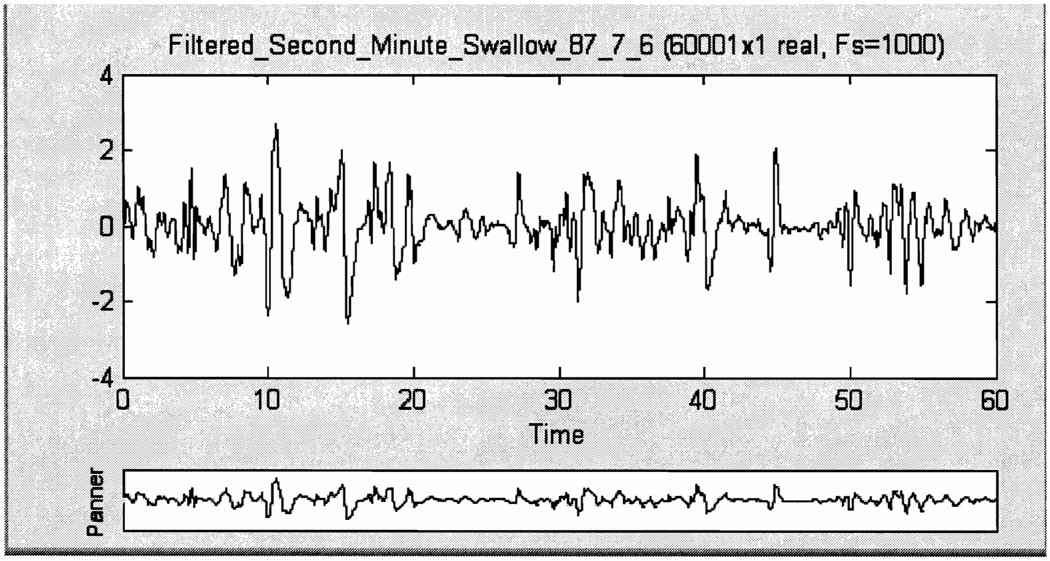

Figure 4.26: The second minute of swallowing of baby #87, seventh feeding

Table 4.39: The analysis of the second minute of swallowing of baby #87, seventh feeding

Time Slot	Length	Level of Certainty
5161	1500	0.88011
8701	1520	0.94063
11981	1320	0.88641
13961	1840	0.85802
25221	1880	0.90901
28641	1160	0.88173
37481	1600	0.90849
43121	1660	0.90637
48841	1400	0.85522
52841	1160	0.89846

Table 4.40: The evaluation of the second minute of swallowing of baby #87, seventh feeding

Agreement(s)	Disagreement(s)
5	5

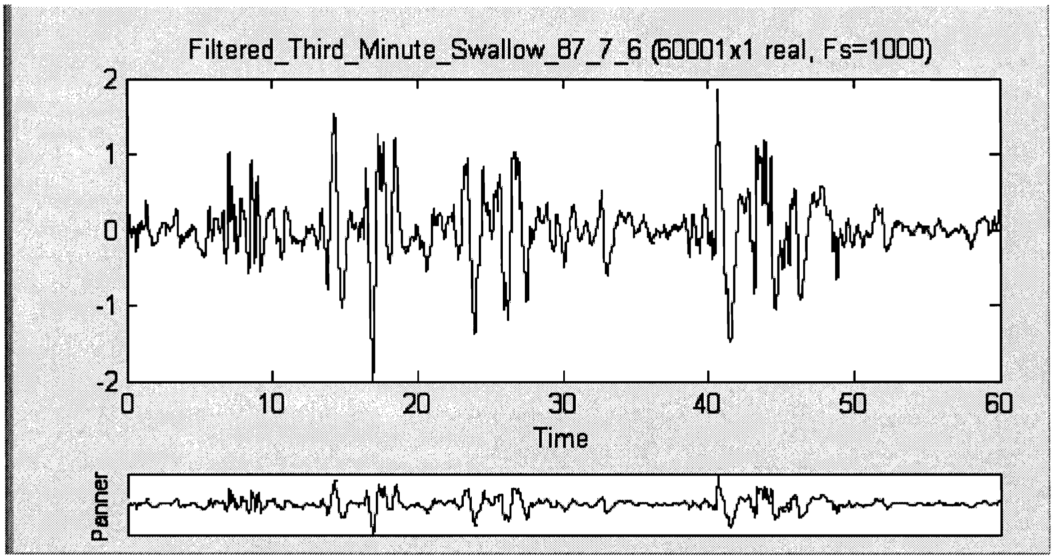

Figure 4.27: The third minute of swallowing of baby #87, seventh feeding

Table 4.41: The analysis of the third minute of swallowing of baby #87, seventh feeding

Time Slot	Length	Level of Certainty
5961	1020	0.85351
12441	1540	0.88039
15461	1640	0.95311
24421	1960	0.85469
42021	1300	0.88716

Table 4.42: The evaluation of the third minute of swallowing of baby #87, seventh feeding

Agreement(s)	Disagreement(s)
5	1

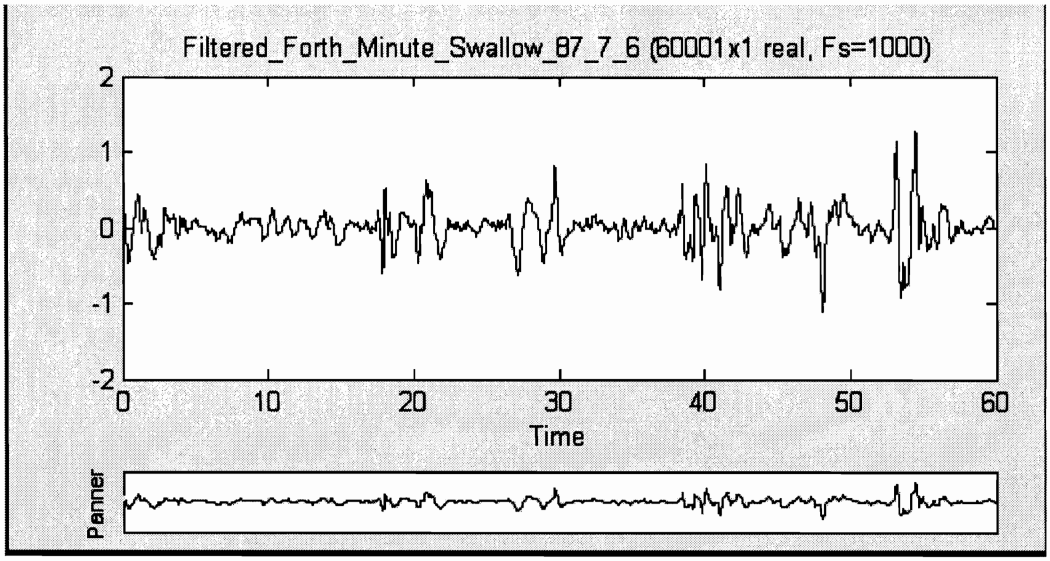

Figure 4.28: The forth minute of swallowing of baby #87, seventh feeding

Table 4.43: The analysis of the forth minute of swallowing of baby #87, seventh feeding

Time Slot	Length	Level of Certainty
16941	1060	0.91632
25421	1920	0.85788
46561	1800	0.86602

Table 4.44: The evaluation of the forth minute of swallowing of baby #87, seventh feeding

Agreement(s)	Disagreement(s)
2	1

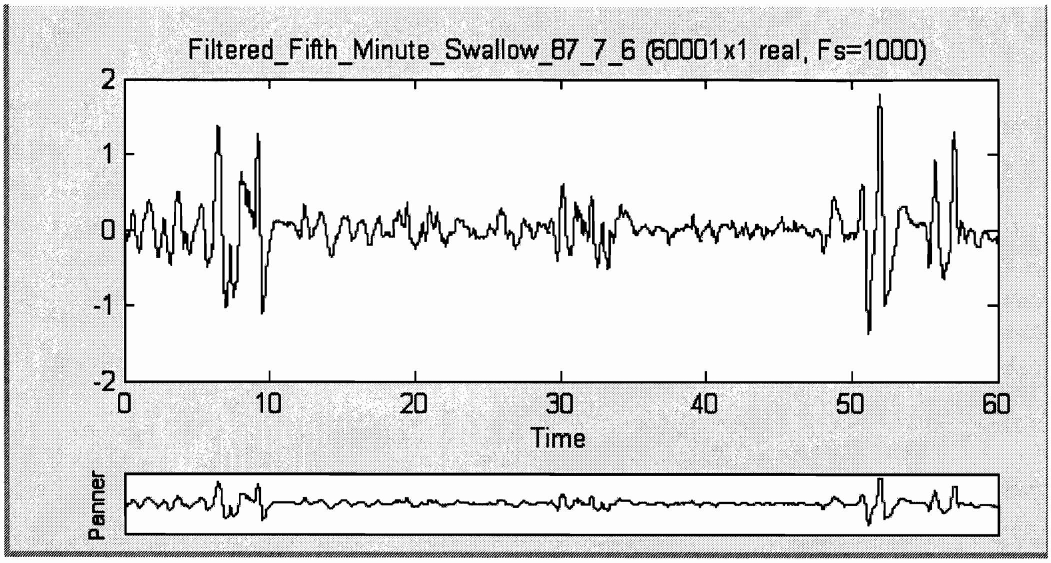

Figure4.29: The fifth minute of swallowing of baby #87, seventh feeding

Table 4.45: The analysis of the fifth minute of swallowing of baby #87, seventh feeding

Time Slot	Length	Level of Certainty
8061	1780	0.8519
49661	1760	0.89986
53901	1620	0.92786

Table 4.46: The evaluation of the fifth minute of swallowing of baby #87, seventh feeding

Agreement(s)	Disagreement(s)
2	1

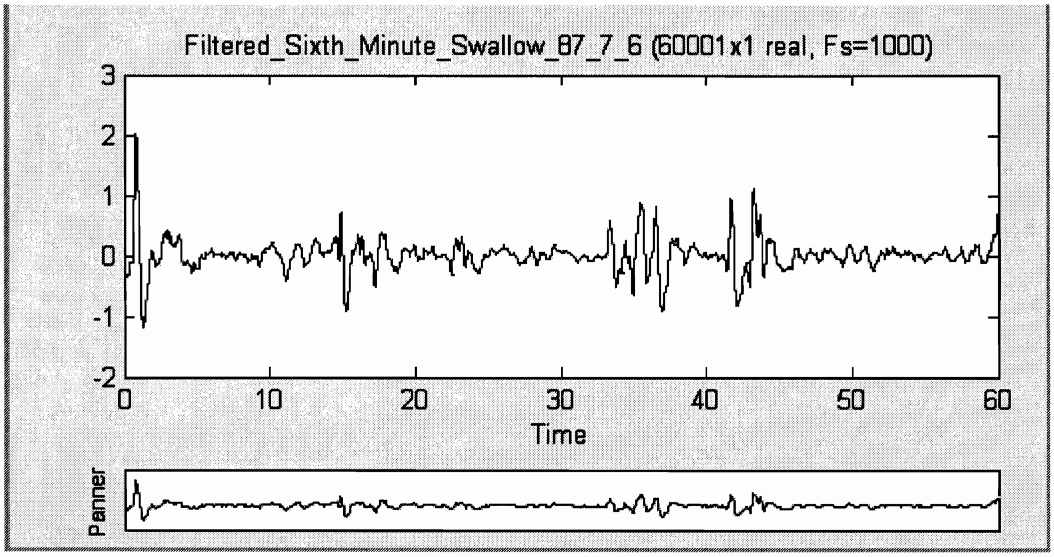

Figure 4.30: The sixth minute of swallowing of baby #87, seventh feeding

Table 4.47: The analysis of the sixth minute of swallowing of baby #87, seventh feeding

Time Slot	Length	Level of Certainty
13701	1820	0.90396
16381	1000	0.89961

Table 4.48: The evaluation of the sixth minute of swallowing of baby #87, seventh feeding

Agreement(s)	Disagreement(s)
2	2

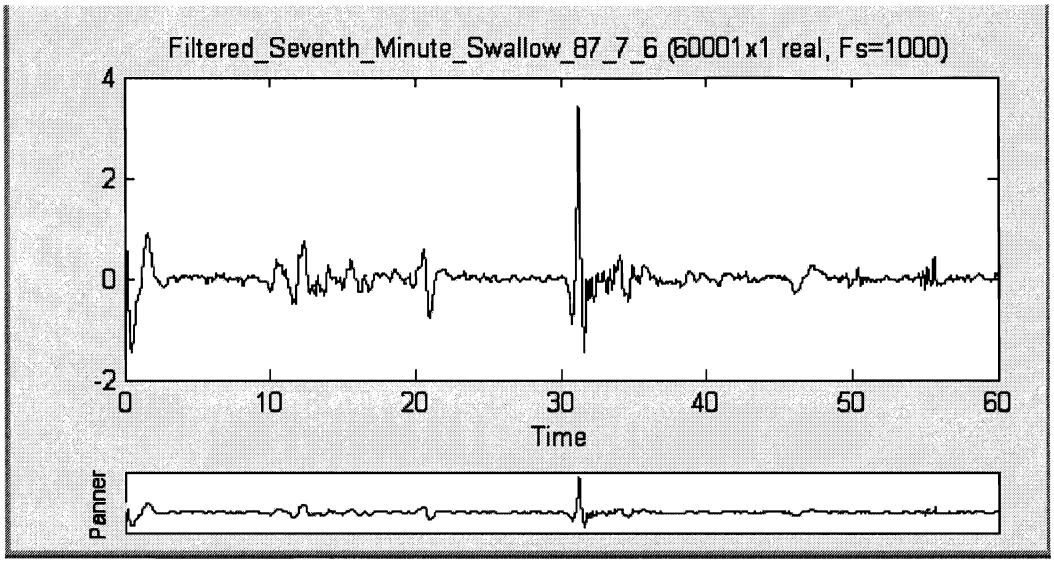

Figure 4.31: The seventh minute of swallowing of baby #87, seventh feeding

Table 4.49: The analysis of the seventh minute of swallowing of baby #87, seventh feeding

Time Slot	Length	Level of Certainty
20021	1040	0.8505
29461	1480	0.94726

Table4.50: The evaluation of the seventh minute of swallowing of baby #87, seventh feeding

Agreement(s)	Disagreement(s)
1	1

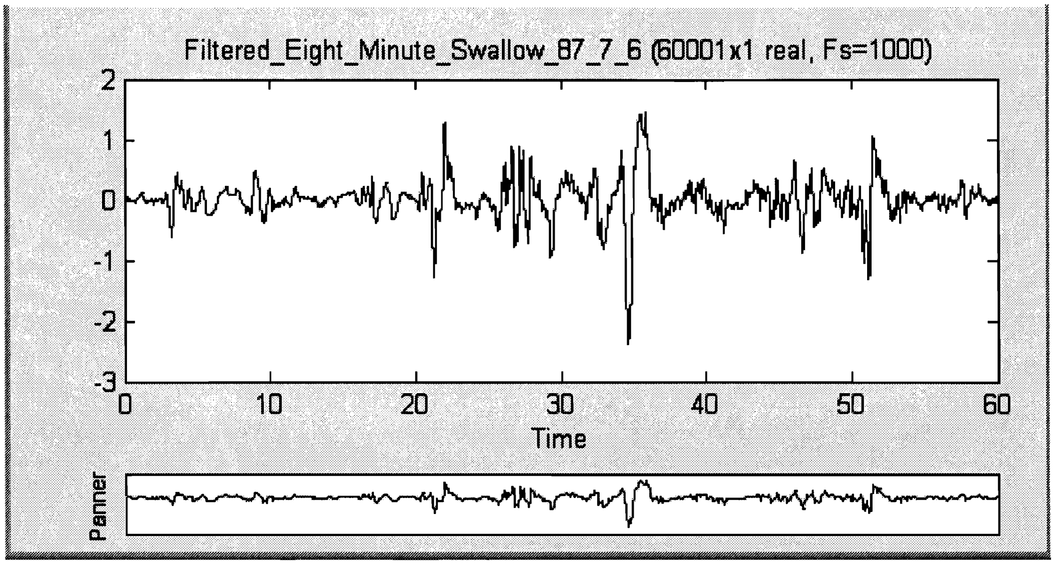

Figure4.32: The eighth minute of swallowing of baby #87, seventh feeding

Table 4.51: The analysis of the eighth minute swallowing of baby #87, seventh feeding

Time Slot	Length	Level of Certainty
1801	1660	0.91507
19941	1580	0.87061
28101	1480	0.87101
33181	1720	0.93779
35241	1180	0.85264
49801	1220	0.88704

Table 4.52: The evaluation of the eighth minute of swallowing of baby #87, seventh feeding

Agreement(s)	Disagreement(s)
3	1

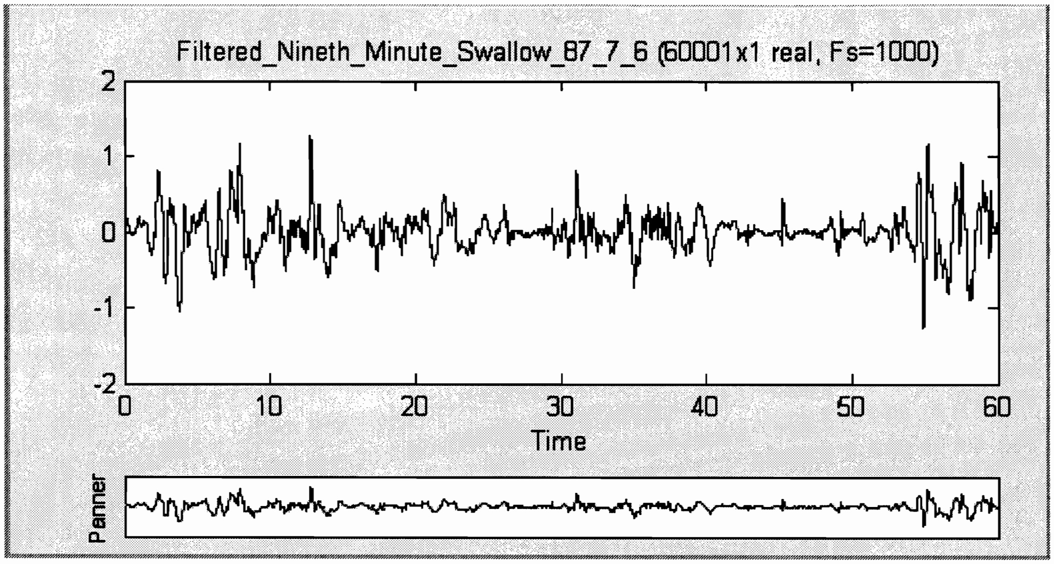

Figure 4.33: The ninth minute of swallowing of baby #87, seventh feeding

Due to the poor quality of this minute, it was not analyzed.

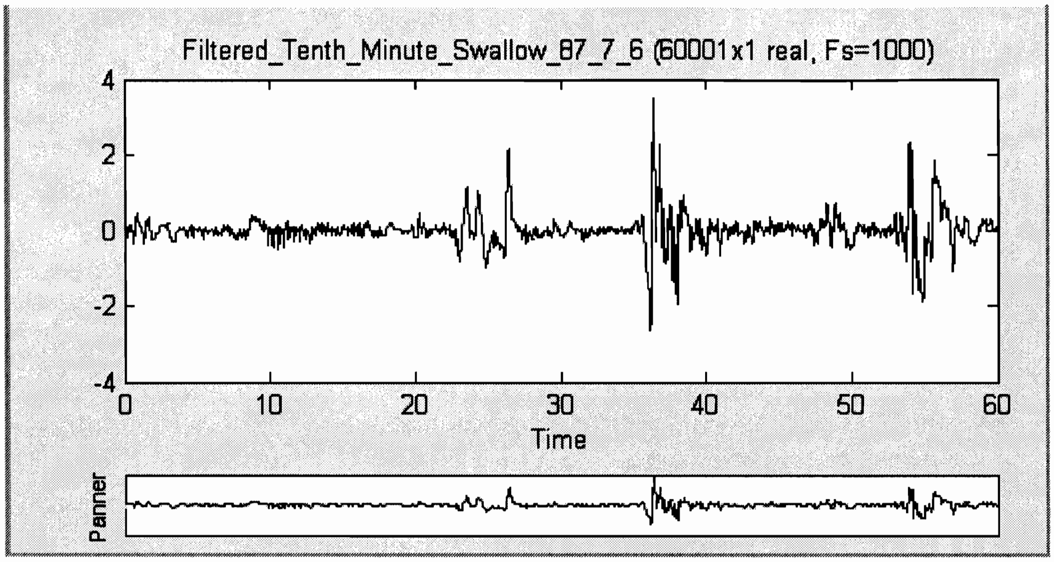

Figure 4.34: The 10th minute of swallowing of baby #87, seventh feeding

Table 4.53: The analysis of the 10th minute of swallowing of baby #87, seventh feeding

Time Slot	Length	Level of Certainty
21641	1600	0.93302
34621	1680	0.90965
40101	1000	0.89174
56021	1080	0.89758

Table 4.54: The evaluation of the 10th minute of swallowing of baby #87, seventh feeding

Agreement(s)	Disagreement(s)
3	2

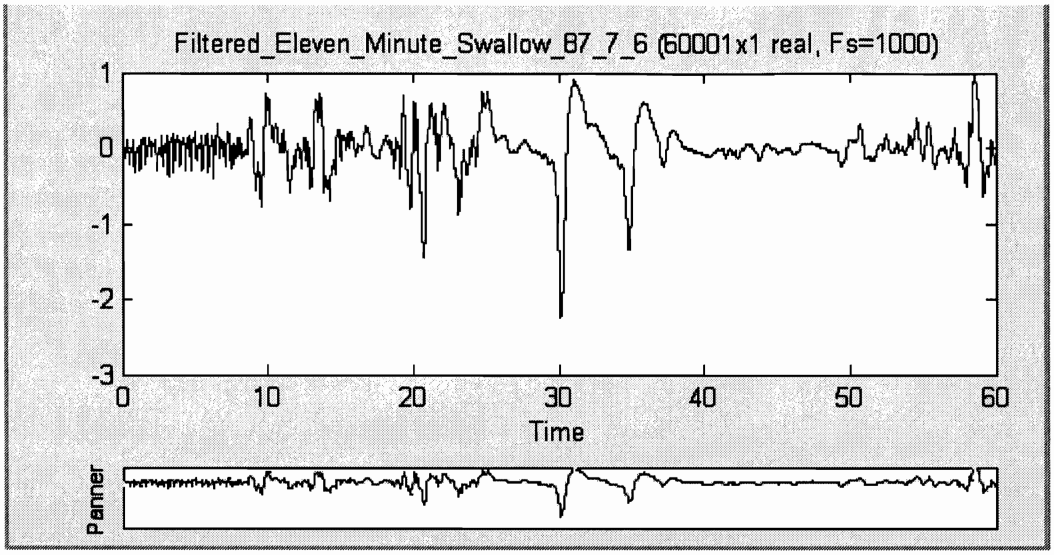

Figure 4.35: The 11th minute of swallowing of baby #87, seventh feeding

Table 4.55: The analysis of the 11th minute of swallowing of baby #87, seventh feeding

Time Slot	Length	Level of Certainty
10621	1000	0.86748
28761	1600	0.91573
33361	1660	0.9082

Table 4.56: The evaluation of the 11th minute of swallowing of baby #87, seventh feeding

Agreement(s)	Disagreement(s)
2	1

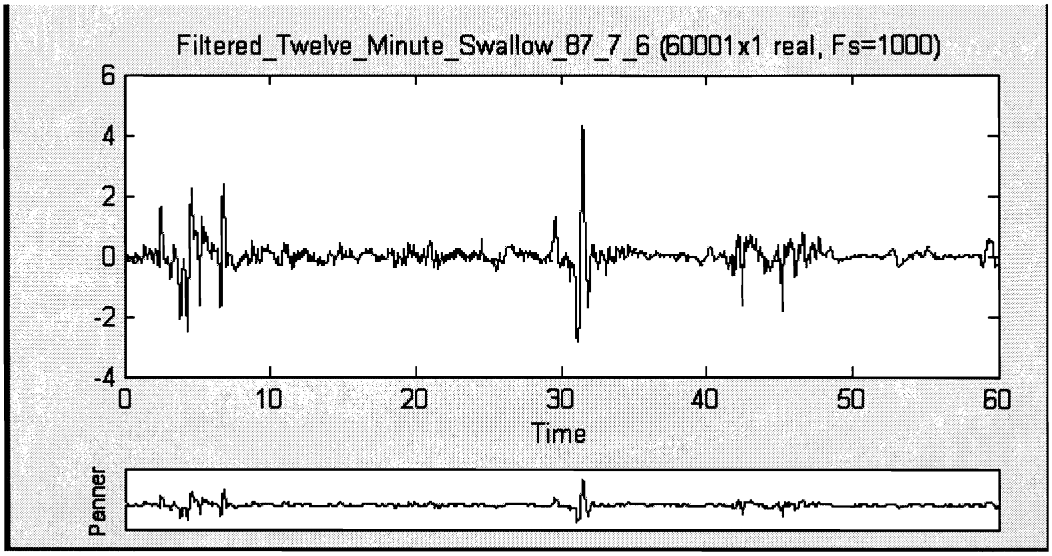

Figure 4.36: The 12th minute of swallowing of baby #87, seventh feeding

Table 4.57: The analysis of the 12th minute of swallowing of baby #87, seventh feeding

Time Slot	Length	Level of Certainty
2641	1400	0.90503
5721	1000	0.93521
29821	1560	0.92805

Table 4.58: The evaluation of the 12th minute of swallowing of Baby #87, seventh feeding

Agreement(s)	Disagreement(s)
3	0

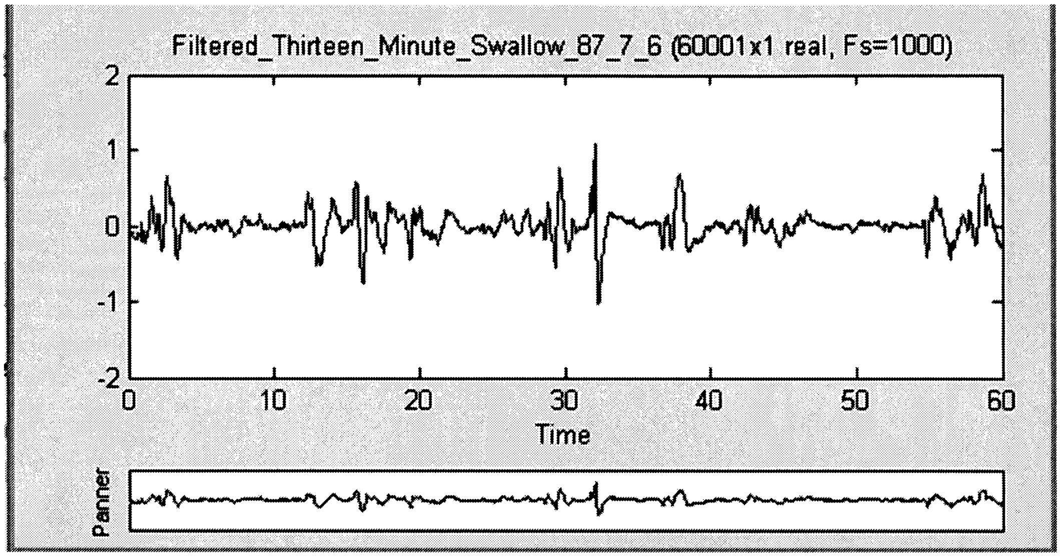

Figure 4.37: The 13th minute of swallowing of baby #87, seventh feeding

Table 4.59: The analysis of the 13th minute of swallowing of baby #87, seventh feeding

Time Slot	Length	Level of Certainty
14501	1840	0.88659
27961	1540	0.86197
31281	1260	0.85103

Table 4.60: The evaluation of the 13th minute of swallowing of baby #87, seventh feeding

Agreement(s)	Disagreement(s)
3	0

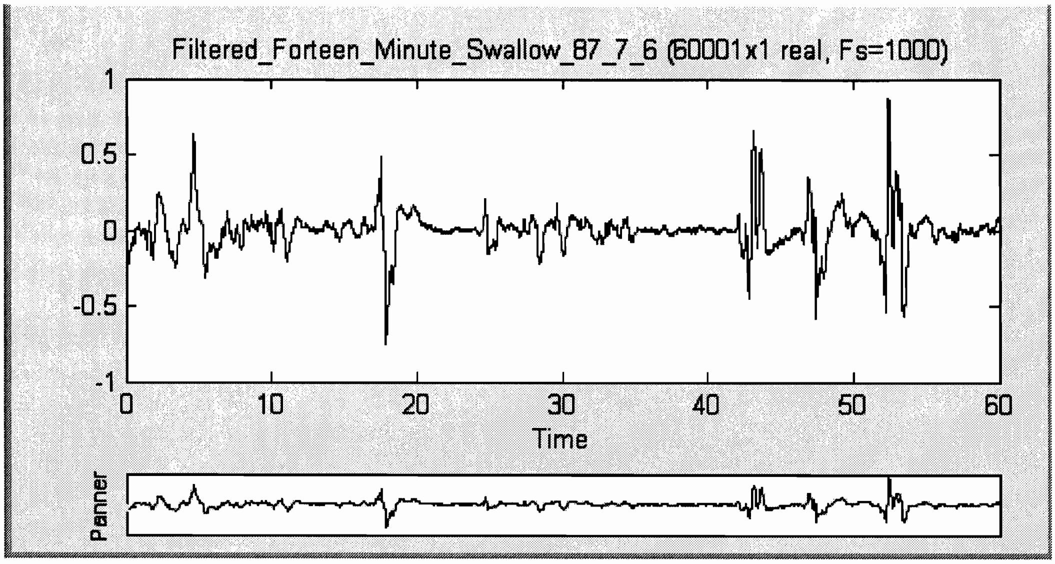

Figure 4.38: The 14th minute of swallowing of baby #87, seventh feeding

Table 4.61: The analysis of the 14th minute of swallowing of baby #87, seventh feeding

Time Slot	Length	Level of Certainty
16361	1820	0.89655

Table 4.62: The evaluation of the 14th minute of swallowing of baby #87, seventh feeding

Agreement(s)	Disagreement(s)
2	1

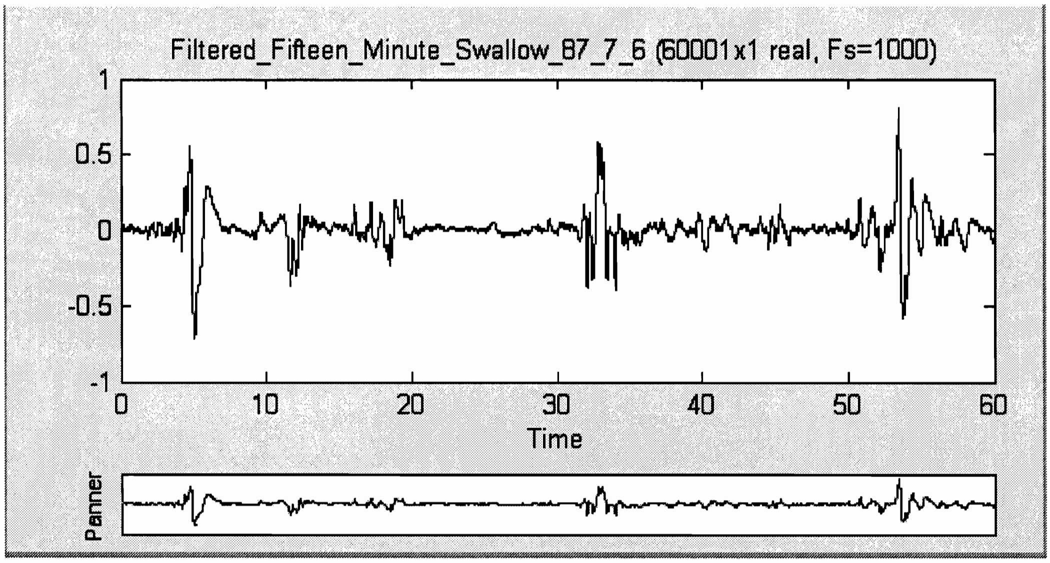

Figure 4.39: The 15th minute of swallowing of baby #87, seventh feeding

Table 4.63: The analysis of the 15th minute of swallowing of baby #87, seventh feeding

Time Slot	Length	Level of Certainty
3781	1520	0.85883

Table 4.64: The evaluation of the 15th minute of swallowing of baby #87, seventh feeding

Agreement(s)	Disagreement(s)
2	1

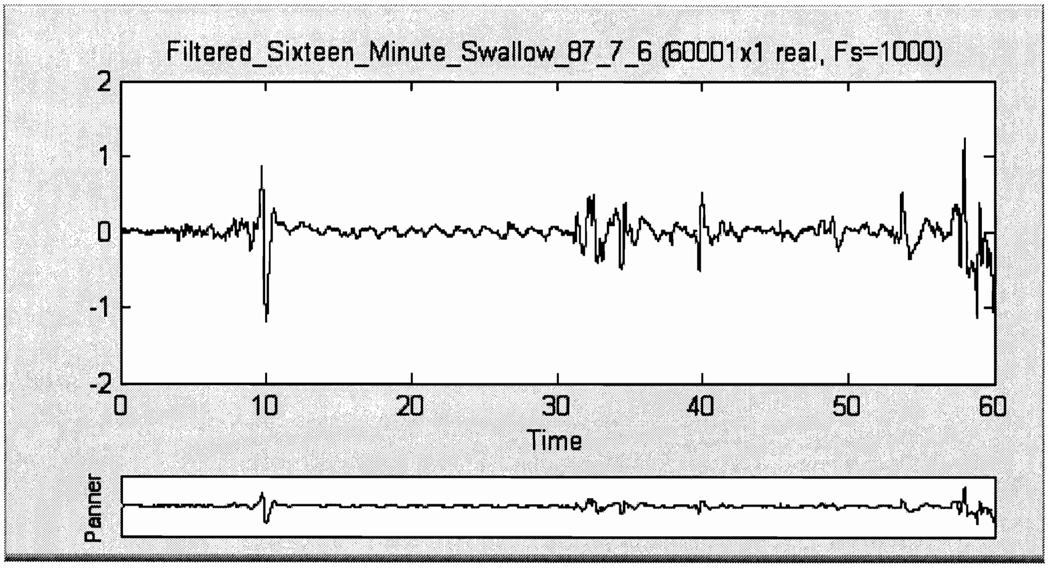

Figure 4.50: The 16th minute of swallowing of baby #87, seventh feeding

Table 4.65: The analysis of the 16th minute of swallowing of baby #87, seventh feeding

Time Slot	Length	Level of Certainty
8821	1400	0.85099
33401	1260	0.9176
38901	1000	0.94232

Table 4.66: The evaluation of the 16th minute of swallowing of baby #87, seventh feeding

Agreement(s)	Disagreement(s)
3	0

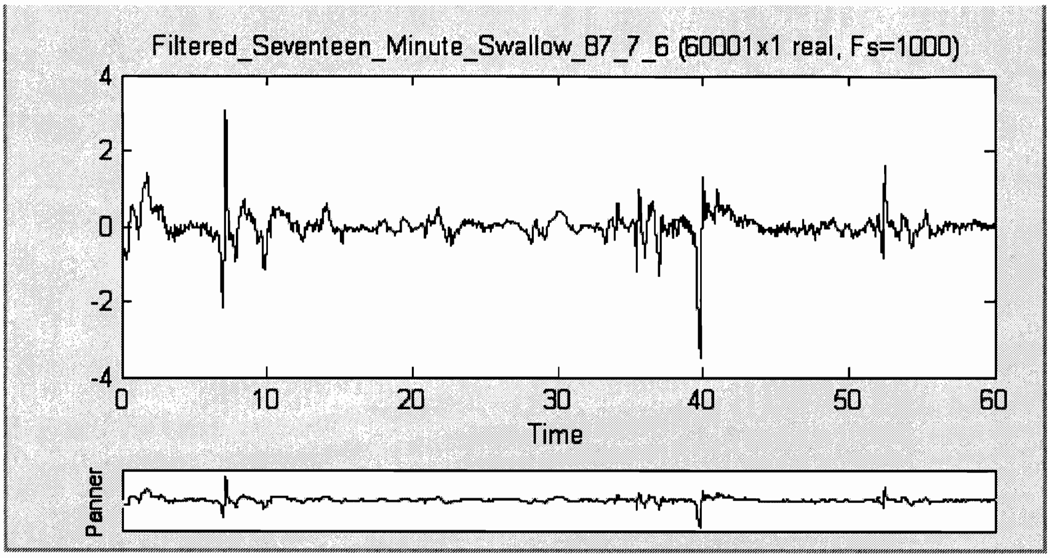

Figure 4.51: The 17th minute of swallowing of baby #87, seventh feeding

Table 4.67: The analysis of the 17th minute of swallowing of baby #87, seventh feeding

Time Slot	Length	Level of Certainty
5841	1240	0.92418
38501	1440	0.96082

Table 4.68: The evaluation of the 17th minute of swallowing of baby #87, seventh feeding

Agreement(s)	Disagreement(s)
2	0

The Detection of Breathing for Baby #87, Seventh Feeding

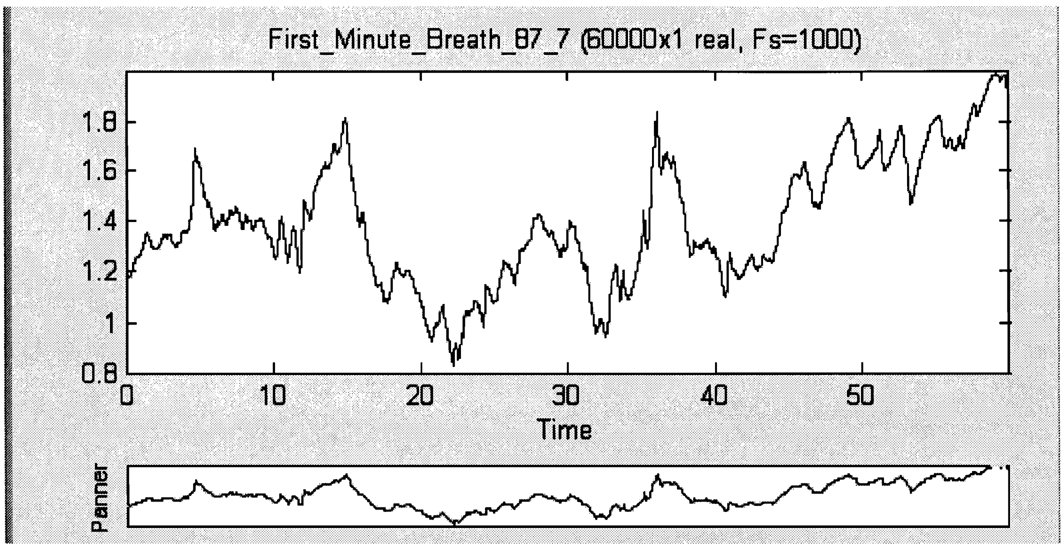

Figure 4.52: The first minute of breathing of baby #87, seventh feeding

Table 4.69: The analysis of the first minute of breathing of baby #87, seventh feeding

Time Slot	Length	Level of Certainty	Time Slot	Length	Level of Certainty
701	1440	0.83604	31921	700	0.86215
2141	1200	0.91421	32801	880	0.92925
4081	1560	0.82073	34881	620	0.8669
6701	1260	0.88737	35621	860	0.90064
8521	1040	0.92081	38981	880	0.82305
10061	960	0.88965	40781	540	0.82526
11021	640	0.95373	41841	1180	0.88365
13641	1880	0.83387	44921	1720	0.87451
17881	1020	0.80651	48161	1540	0.9356
20621	1500	0.89366	50081	1700	0.811
22181	440	0.81312	51781	1380	0.93478
22801	1540	0.87262	54181	1580	0.94797
25201	1300	0.90004	57181	760	0.81513
27181	1660	0.89373	58101	1880	0.80025
29401	1780	0.85905			

Table 4.70: The evaluation of the first minute of breathing of baby #87, seventh feeding

Agreement(s)	Disagreement(s)
29	0

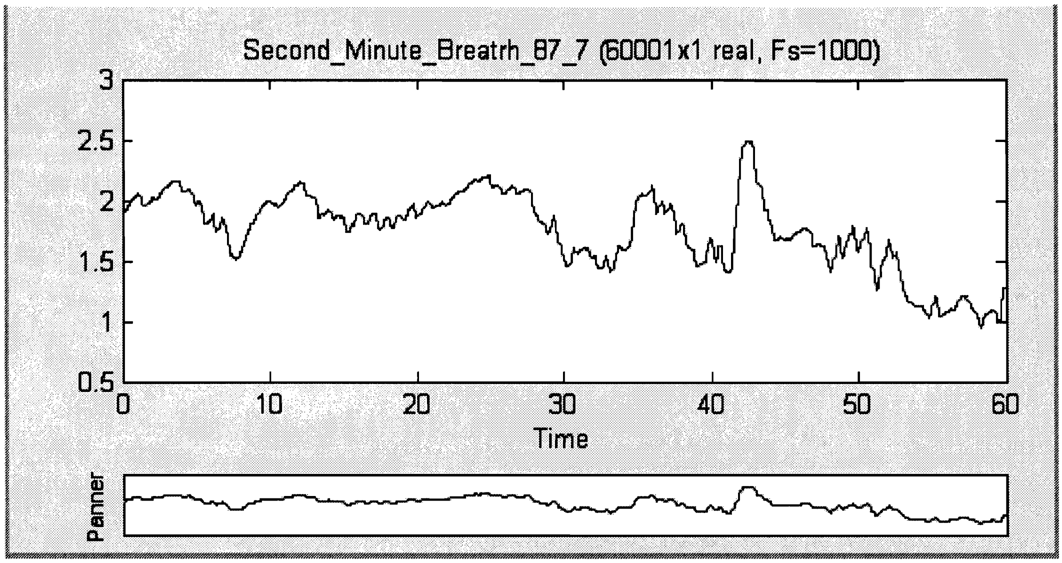

Figure 4.53: The second minute of breathing of baby #87, seventh feeding

Table 4.71: The analysis of the second minute of breathing of baby #87, seventh feeding

Time Slot	Length	Level of Certainty	Time Slot	Length	Level of Certainty
161	1540	0.90215	28881	780	0.90868
2681	1580	0.92279	30221	1920	0.81156
5601	800	0.89597	32481	760	0.84593
6401	720	0.93083	34681	1800	0.84742
9221	1460	0.83878	36861	740	0.88218
11081	1600	0.92833	37661	700	0.88652
13341	1080	0.87346	39461	980	0.89463
15401	1320	0.87588	41681	1620	0.92438
16721	660	0.82314	45321	1700	0.88239
17501	860	0.94713	48261	780	0.87839
18401	800	0.8409	49041	960	0.9361
19201	840	0.96351	50021	840	0.91426
20261	1020	0.87225	51221	1760	0.92179
23341	2000	0.80268	54701	960	0.88217
25881	1040	0.90779	56301	1540	0.94797
26921	920	0.84232	58301	1300	0.93048

Table 4.72: The evaluation of the second minute of breathing of baby #87, seventh feeding

Agreement(s)	Disagreement(s)
32	0

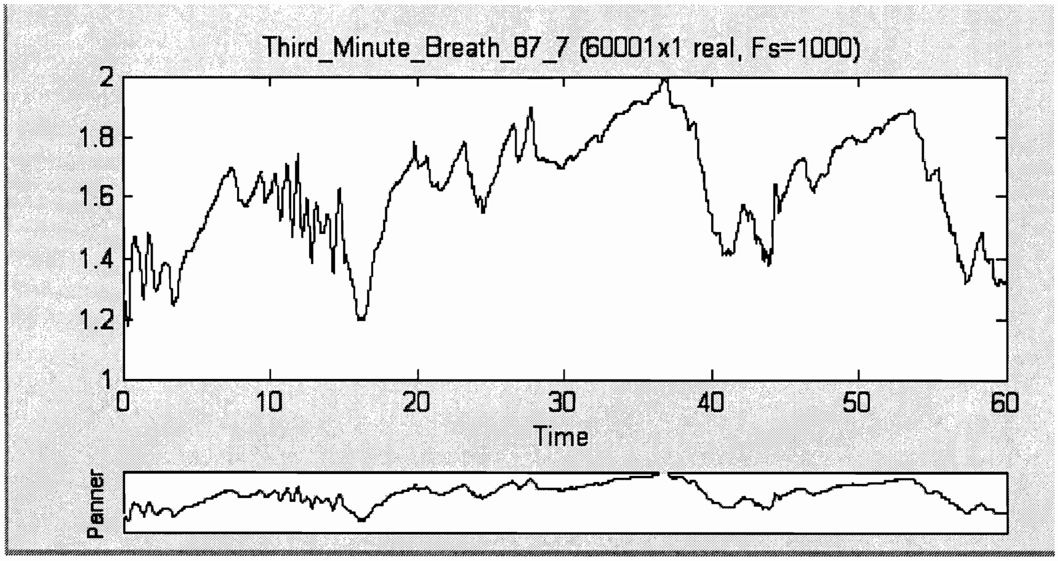

Figure 4.54: The third minute of breathing of baby #87, seventh feeding

Table 4.73: The analysis of the third minute of breathing of baby #87, seventh feeding

Time Slot	Length	Level of Certainty	Time Slot	Length	Level of Certainty
261	22121	0.88946	22121	1620	0.88946
1501	25441	0.94417	25441	1680	0.94417
2201	27141	0.93372	27141	1040	0.93372
6341	31501	0.92874	31501	1020	0.92874
8441	34561	0.84551	34561	1020	0.84551
9901	35601	0.88198	35601	1940	0.88198
10661	41441	0.95934	41441	1720	0.95934
11521	44121	0.96778	44121	560	0.96778
12161	45161	0.94024	45161	1600	0.94024
12821	48921	0.88598	48921	1040	0.88598
13521	50621	0.85795	50621	1020	0.85795
14261	54741	0.95158	54741	900	0.95158
19221	57321	0.80023	57321	1840	0.80023

Table 4.74: The evaluation of the third minute of breathing of baby #87, seventh feeding

Agreement(s)	Disagreement(s)
26	1

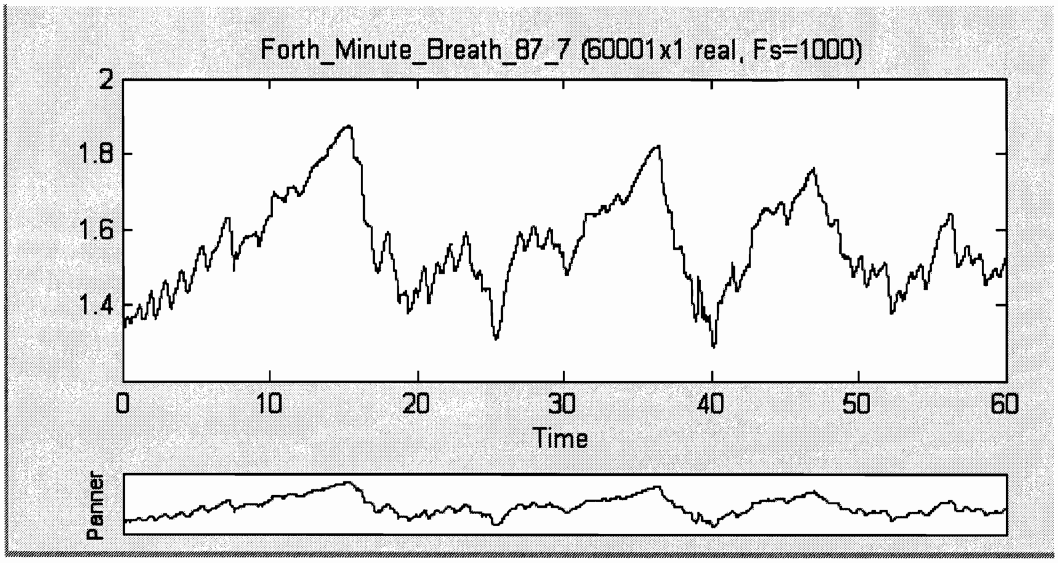

Figure 4.55: The forth minute of breathing of baby #87, seventh feeding

Table 4.75: The analysis of the forth minute of breathing of baby #87, seventh feeding

Time Slot	Length	Level of Certainty	Time Slot	Length	Level of Certainty
521	1040	0.8321	0.8706	0.8989	0.8521
1561	700	0.9158	0.8759	0.8047	0.8212
2341	1020	0.9386	0.8726	0.8737	0.9111
3441	1040	0.9307	0.8744	0.8164	0.9053
4721	1200	0.9013	0.8909	0.8309	
5941	1820	0.8753	0.8706	0.8989	0.8521
10981	1100	0.8824	0.8759	0.8047	0.8212
14221	1680	0.8388	0.8726	0.8737	0.9111
17201	1540	0.8665	0.8744	0.8164	0.9053
19641	1320	0.8195	0.8909	0.8309	
21001	800	0.8035	0.8706	0.8989	0.8521
21801	820	0.9436	0.8759	0.8047	0.8212
22661	1180	0.9407	0.8726	0.8737	0.9111
26541	940	0.8930	0.8744	0.8164	0.9053
27481	880	0.9456			

Table 4.76: The evaluation of the forth minute of breathing of baby #87, seventh feeding

Agreement(s)	Disagreement(s)
29	0

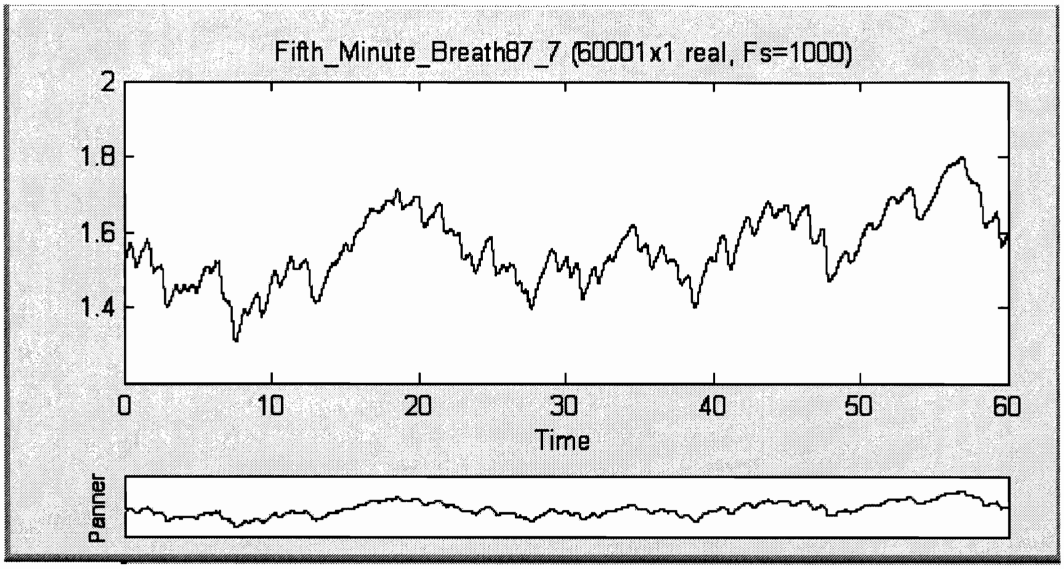

Figure 4.56: The fifth minute of breathing of baby #87, seventh feeding

Table 4.77: The analysis of the fifth minute of breathing of baby #87, seventh feeding

Time Slot	Length	Level of Certainty	Time Slot	Length	Level of Certainty
1	820	0.9050	31421	940	0.9102
841	1200	0.9470	33521	1640	0.8771
4861	1900	0.8243	35881	1160	0.9165
8341	1120	0.9179	39921	1400	0.8577
9741	940	0.8887	41681	1240	0.8886
10761	1040	0.8403	43121	1180	0.9136
11801	840	0.8232	44301	1040	0.8079
16361	960	0.8103	45381	1420	0.9100
18081	880	0.8110	46881	840	0.8551
19121	1200	0.8142	48401	1060	0.9170
20401	1520	0.8605	50061	940	0.8232
23781	1720	0.9044	51581	1020	0.8180
28281	1460	0.8704	52661	1120	0.9225
30281	800	0.8275	56221	1080	0.8531

Table 4.78: The evaluation of the fifth minute of breathing of baby #87, seventh feeding

Agreement(s)	Disagreement(s)
28	0

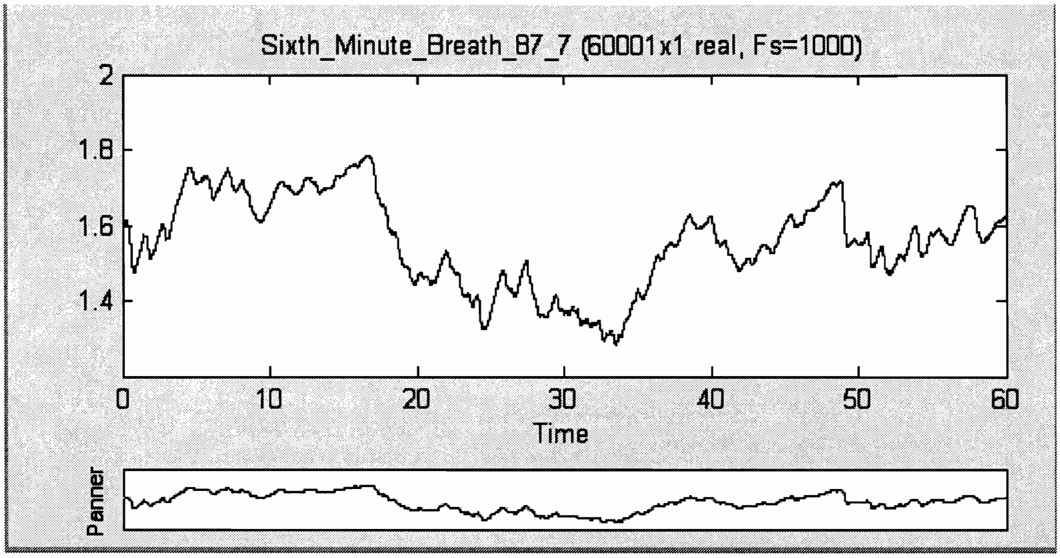

Figure4.57: The sixth minute of breathing of baby #87, seventh feeding

Table 4.79: The analysis of the sixth minute of breathing of baby #87, seventh feeding

Time Slot	Length	Level of Certainty	Time Slot	Length	Level of Certainty
861	1220	0.8901	32621	920	0.8637
2201	940	0.9190	37921	1260	0.8671
3881	1360	0.8485	39281	1100	0.8692
6241	1580	0.8671	41881	1020	0.8252
10261	960	0.8193	43061	1080	0.9017
11841	1620	0.8097	44801	1140	0.8701
15941	1260	0.8364	49181	960	0.8353
21121	1660	0.8547	50901	1080	0.9066
24941	1760	0.8490	52981	1500	0.8845
26721	1220	0.9493	54701	1220	0.8272
28741	1340	0.8358	56621	1600	0.9268

Table 4.80: The evaluation of the sixth minute of breathing of baby #87, seventh feeding

Agreement(s)	Disagreement(s)
21	3

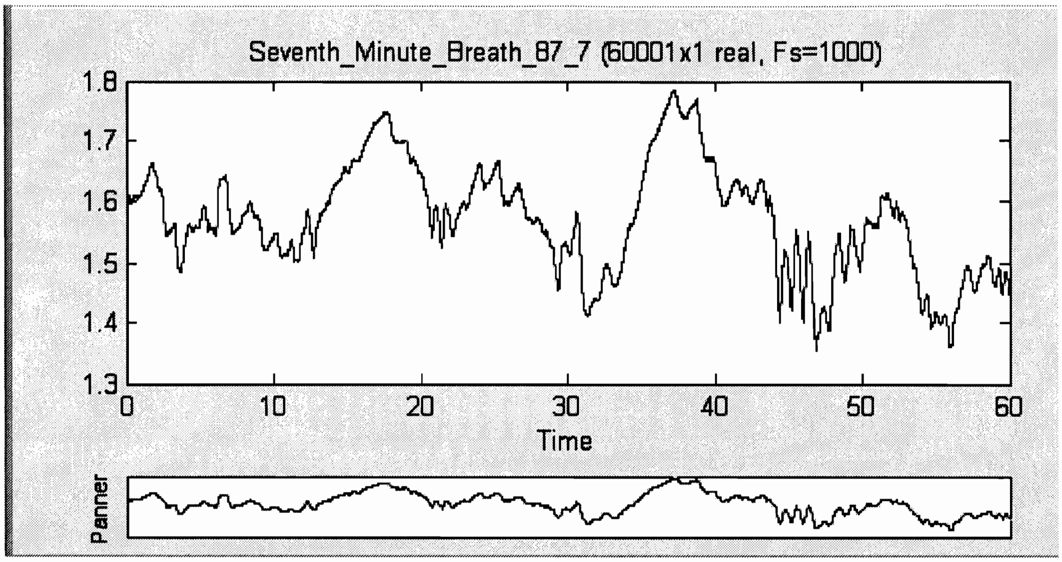

Figure 4.58: The seventh minute of breathing of baby #87, seventh feeding

Table 4.81: The analysis of the seventh minute of breathing for baby #87, seventh feeding

Time Slot	Length	Level of Certainty	Time Slot	Length	Level of Certainty
781	1780	0.8493	36381	1520	0.8216
4641	1020	0.8238	38021	1100	0.8271
5821	1460	0.8910	40921	1040	0.9486
7321	1980	0.8032	42501	1140	0.9390
9441	1120	0.9177	44341	920	0.9197
11601	1200	0.9286	45261	600	0.8966
17021	1040	0.9018	45941	840	0.9451
20681	740	0.8168	46881	940	0.8778
21421	720	0.8293	47901	960	0.9393
23361	1100	0.8901	48861	860	0.9032
24541	1120	0.8807	50961	1260	0.8776
25901	1320	0.8604	56481	1240	0.8930
29241	1960	0.8133	57761	1280	
32061	1240	0.8686			

Table 4.82: The evaluation of the seventh minute of breathing of baby #87, seventh feeding

Agreement(s)	Disagreement(s)
27	1

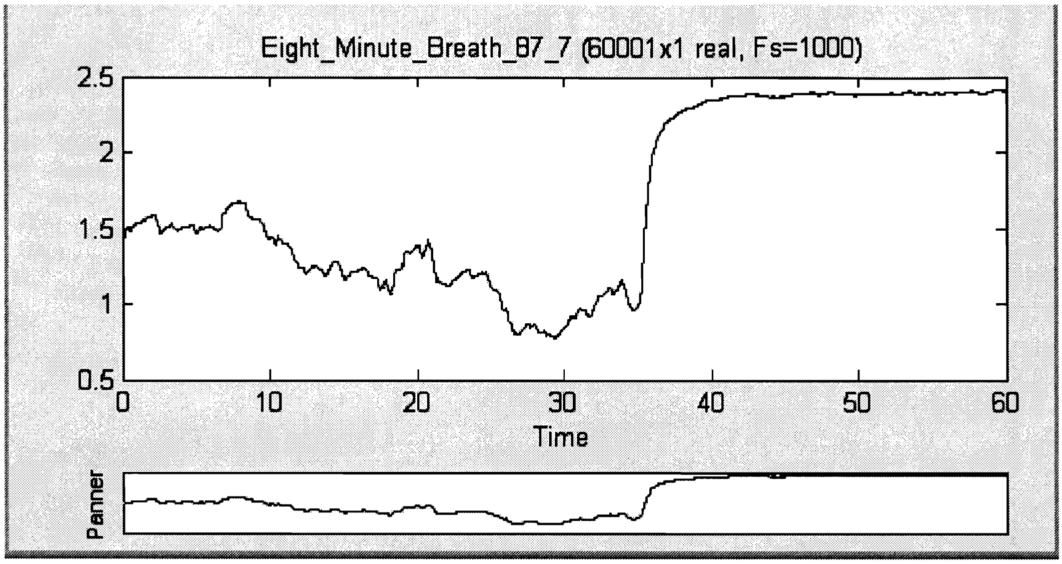

Figure 4.59: The eighth minute of breathing of baby #87, seventh feeding

Due to the poor quality of this minute, it was not analyzed.

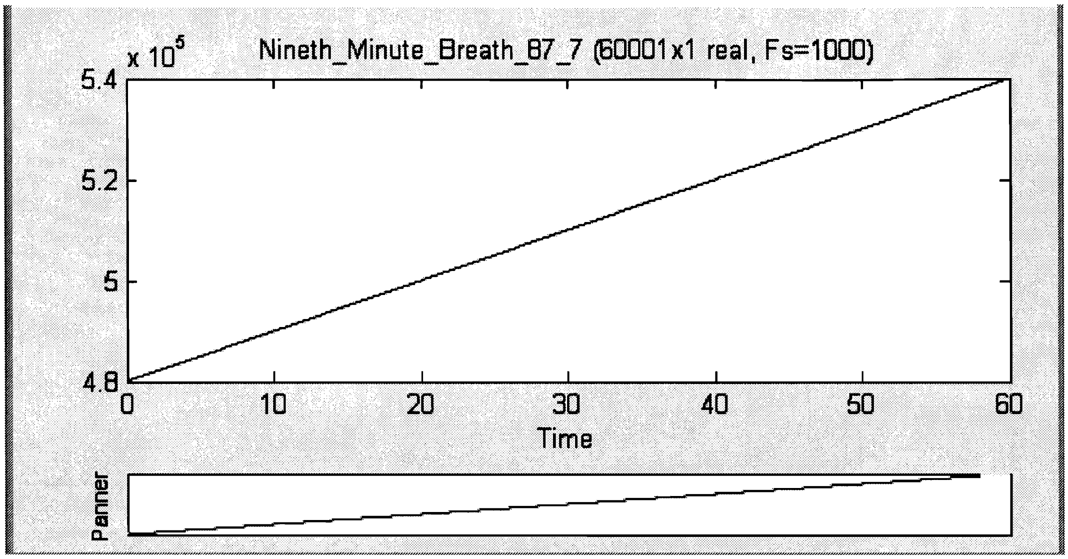

Figure 4.60: The ninth minute of breathing of baby #87, seventh feeding

Due to the unsatisfactory quality of this minute, it was not analyzed.

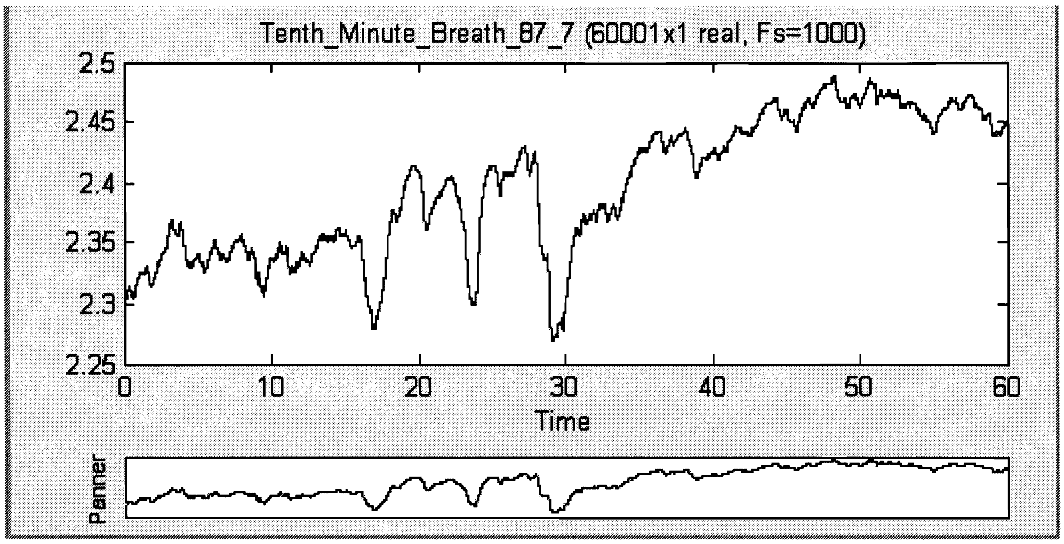

Figure 4.61: The 10th minute of breathing of baby #87, seventh feeding

Due to the unsatisfactory quality of this minute, it was not analyzed.

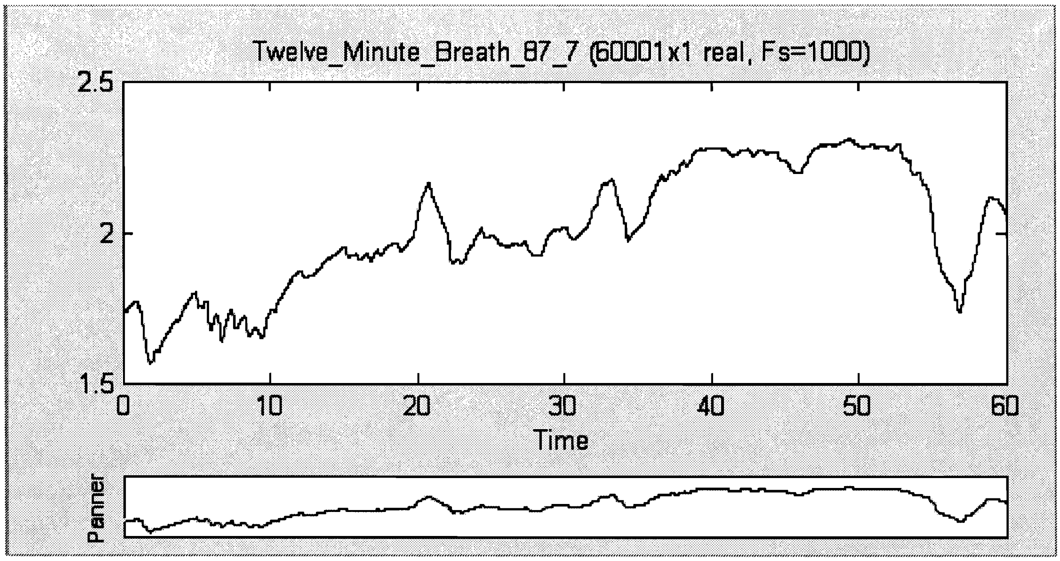

Figure 4.62: The 12th minute of breathing of baby #87, seventh feeding

Due to the unsatisfactory quality of this minute, it was not analyzed.

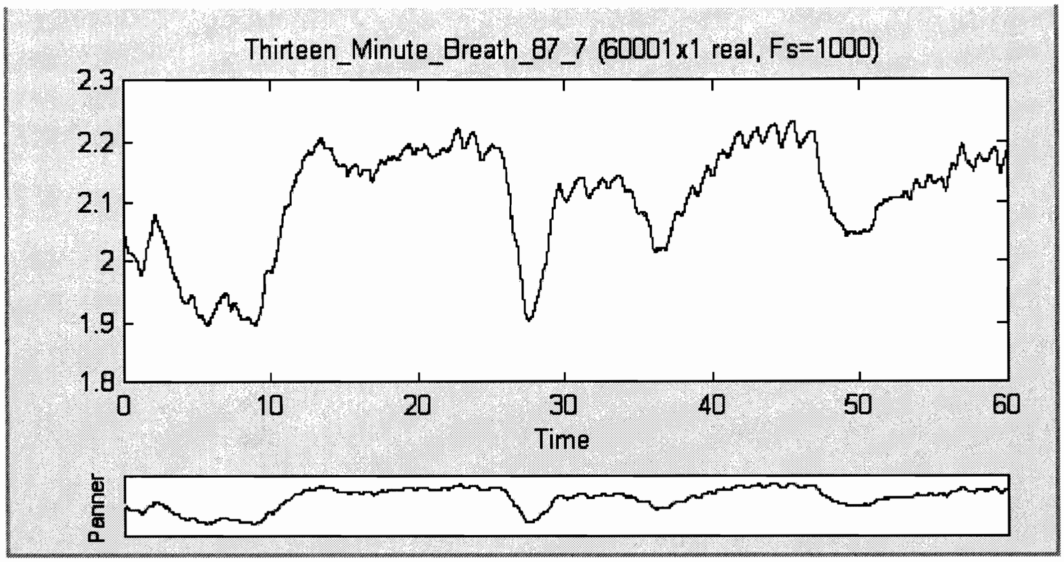

Figure 4.63: The 13th minute of breathing of baby #87, seventh feeding

Table 4.83: The analysis of the 13th minute of breathing of baby #87, seventh feeding

Time Slot	Length	Level of Certainty	Time Slot	Length	Level of Certainty
1281	1860	0.8188	38141	960	0.8135
6281	1080	0.9012	39181	960	0.8114
12821	1020	0.9312	40201	980	0.8039
15181	980	0.9187	41321	1020	0.9582
18781	1020	0.8903	42481	980	0.9559
19861	1020	0.8014	43601	1080	0.9231
22201	1040	0.9512	44821	1140	0.9230
23241	980	0.9498	46101	1140	0.8597
24701	1020	0.8115	53401	980	0.8013
29141	1020	0.8832	56441	1020	0.8751
30521	1080	0.8993	57681	980	0.8037
31981	1020	0.8707	58661	940	0.8036
33061	1020	0.9503			

Table 4.84: The evaluation of the 13th minute of breathing of baby #87, seventh feeding

Agreement(s)	Disagreement(s)
25	2

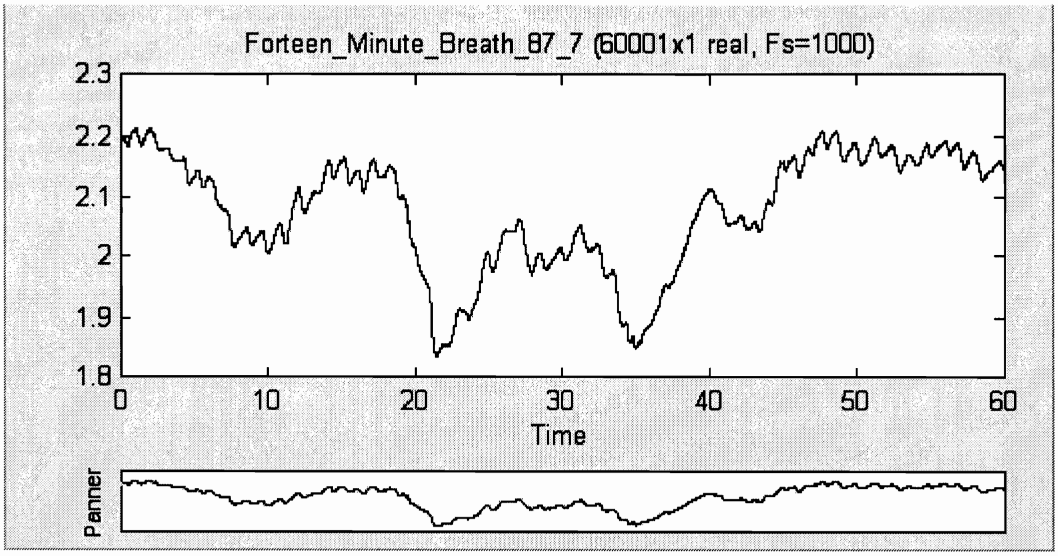

Figure 4.64: The 14th minute of breathing of baby #87, seventh feeding

Table 4.85: The analysis of the 14th minute of breathing of baby #87, seventh feeding

Time Slot	Length	Level of Certainty	Time Slot	Length	Level of Certainty
481	980	0.9577	29261	1020	0.9064
1481	1020	0.9520	30461	1400	0.8426
4621	1020	0.9219	39521	1040	0.9592
7921	1040	0.9227	41521	1020	0.8425
8961	980	0.9352	42541	980	0.8044
10201	1100	0.9137	45101	1020	0.8871
11481	1120	0.8988	47061	1040	0.9388
13561	1020	0.8872	48101	940	0.8376
14581	960	0.9307	49261	1080	0.9259
15541	980	0.9199	50681	1080	0.9128
16621	1020	0.9347	51761	980	0.9115
17781	1020	0.9363	53041	1020	0.9027
22681	1020	0.8434	54161	1020	0.8782
24401	1020	0.8842	55301	1020	0.8770
26501	1040	0.8555	57321	1100	0.9243
27941	1040	0.9433			

Table 4.86: The evaluation of the 14th minute of breathing of baby #87, seventh feeding

Agreement(s)	Disagreement(s)
31	4

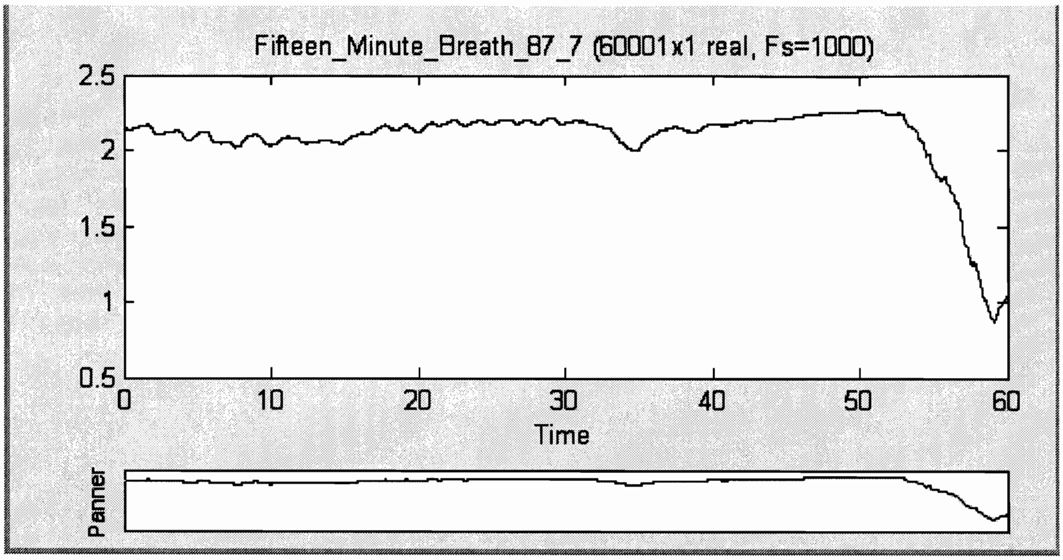

Figure 4.65: The 15th minute of breathing of baby #87, seventh feeding

Due to the unsatisfactory quality of this minute, it was not analyzed.

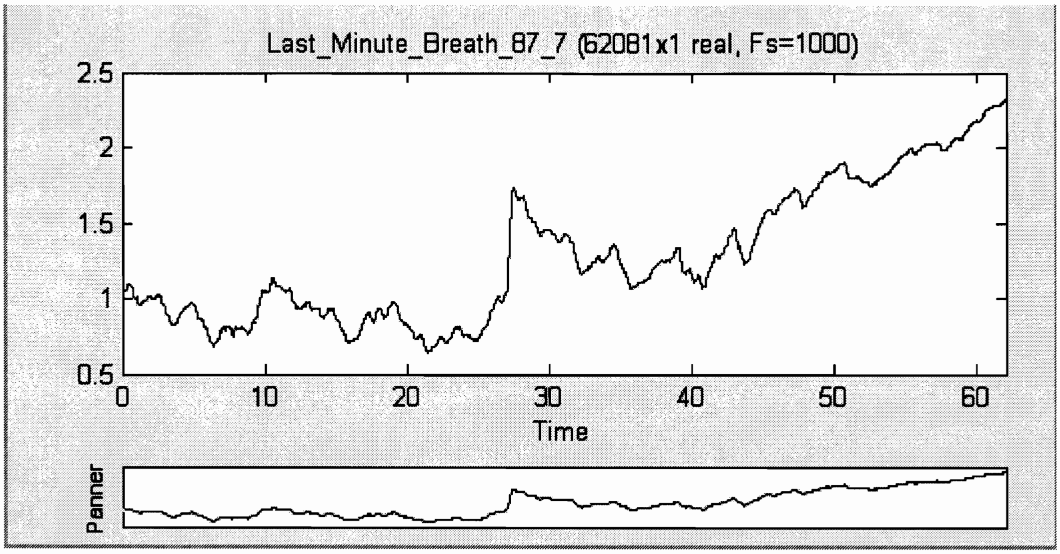

Figure 4.66: The last minute of breathing of baby #87, seventh feeding

Due to the unsatisfactory quality of this minute, it was not analyzed.

<u>The Detection of Sucking of Baby #81, 10th Feeding</u>

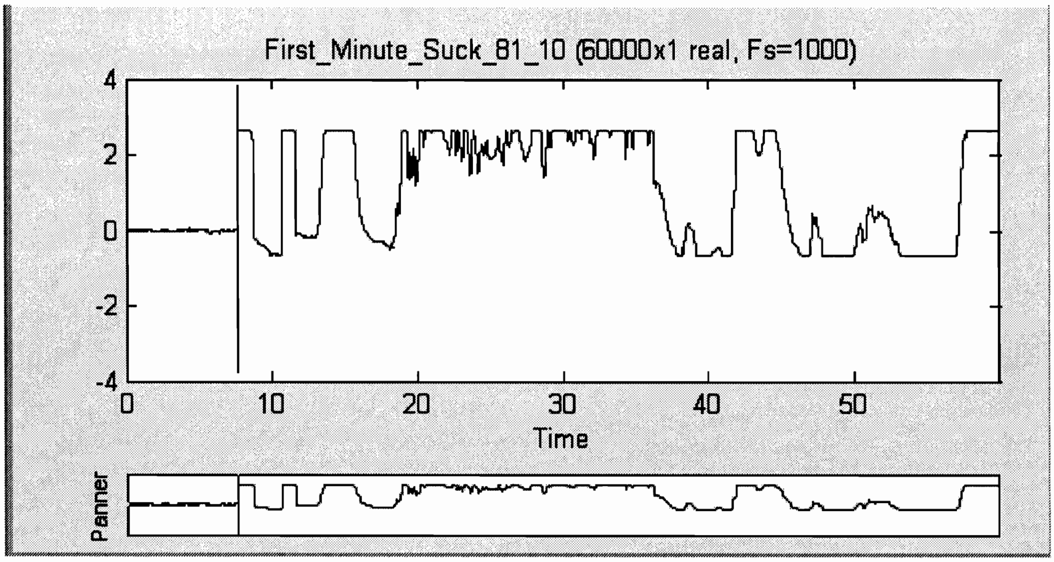

Figure 4.67: The first minute of sucking of baby #81, 10^{th} feeding

Due to the unsatisfactory quality of this minute, it was not analyzed.

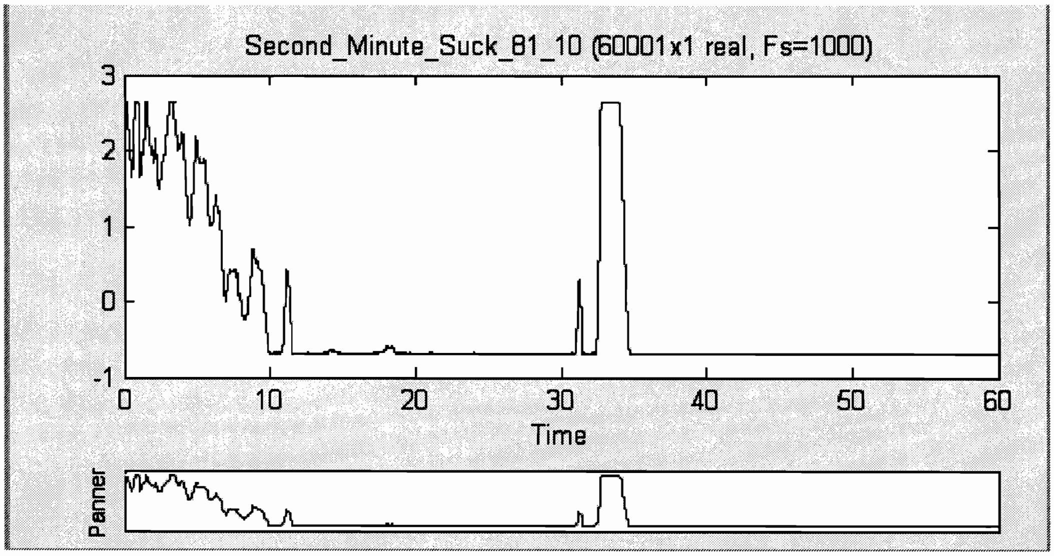

Figure4.68: The second minute of mucking of baby #81, 10th feeding

Table 4.87: The analysis of the second minute of sucking of baby #81,10th feeding

Time Slot	Length	Level of Certainty
501	660	0.9358
1281	520	0.8849
2341	1940	0.8777
4381	1620	0.9198
6001	620	0.8738
6881	1180	0.9214
8181	1740	0.9340
10741	900	0.8982
17541	1300	0.8591
30981	580	0.9137
32461	1940	0.8703

Table4.88: The Evaluation of the second minute of sucking of baby #81, 10th feeding

Agreement(s)	Disagreement(s)
8	2

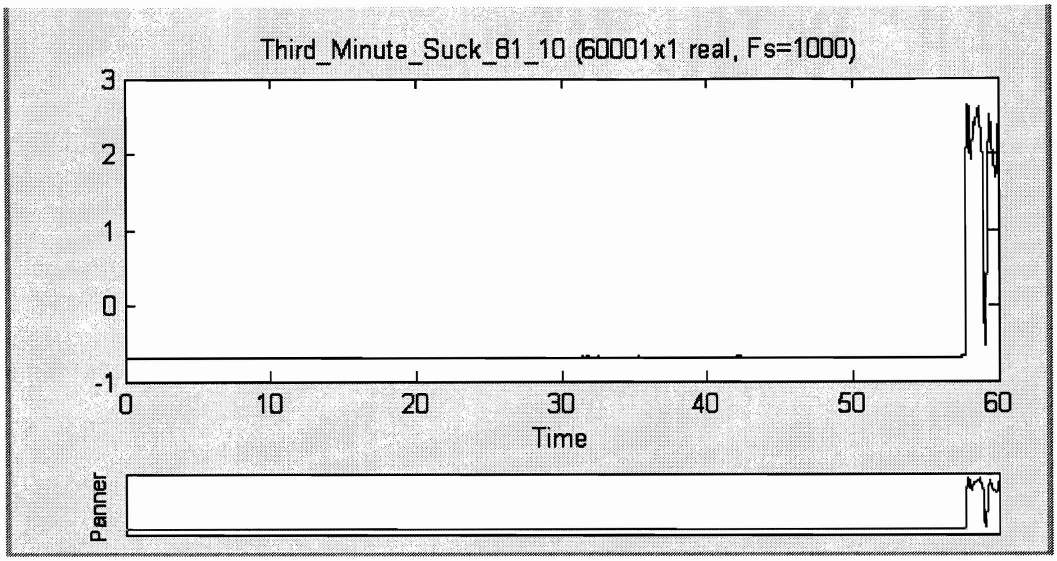

Figure 4.69: The third minute of sucking of baby #81, 10th feeding

Table 4.89: The Analysis of the third minute of sucking of baby #81, 10th feeding

Time Slot	Length	Level of Certainty
57481	1720	0.8885
59201	500	0.8701

Table 4.90: The evaluation of the third minute of sucking of baby #81, 10th feeding

Agreement(s)	Disagreement(s)
2	0

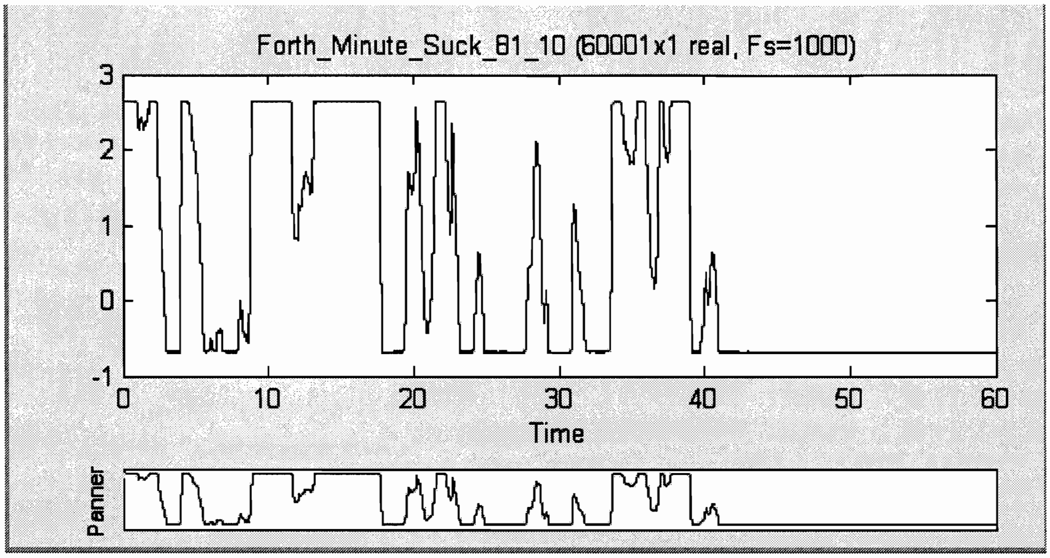

Figure 4.70: The forth minute of sucking of baby #81, 10th feeding

Table 4.91: The analysis of the forth minute of sucking of baby #81, 10th feeding

Time Slot	Length	Level of Certainty
3681	1800	0.9172
6241	740	0.9037
7861	500	0.8654
12281	680	0.9424
19201	1740	0.9498
21221	1400	0.9537
23961	1080	0.9060
27481	1920	0.8628
30781	720	0.8781
34981	1300	0.8887
36781	680	0.8763
39521	1840	0.8856

Table 4.92: The evaluation of the forth minute of sucking of baby #81, 10th feeding

Agreement(s)	Disagreement(s)
6	6

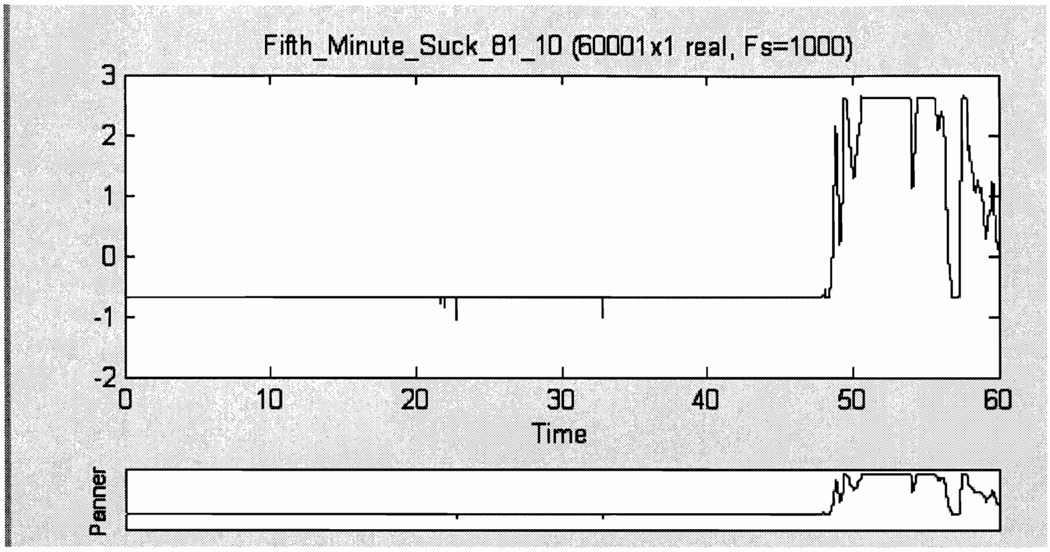

Figure4.71: The fifth minute of sucking of baby #81, 10th feeding

Table 4.93: The analysis of the fifth minute of sucking of baby #81,10th feeding

Time Slot	Length	Level of Certainty
48521	660	0.8852
49201	760	0.8959
54181	1800	0.8694
57321	820	0.8657
59081	880	0.8741

Table 4.94: The evaluation of the fifth minute of sucking of baby #81, 10th feeding

Agreement(s)	Disagreement(s)
4	1

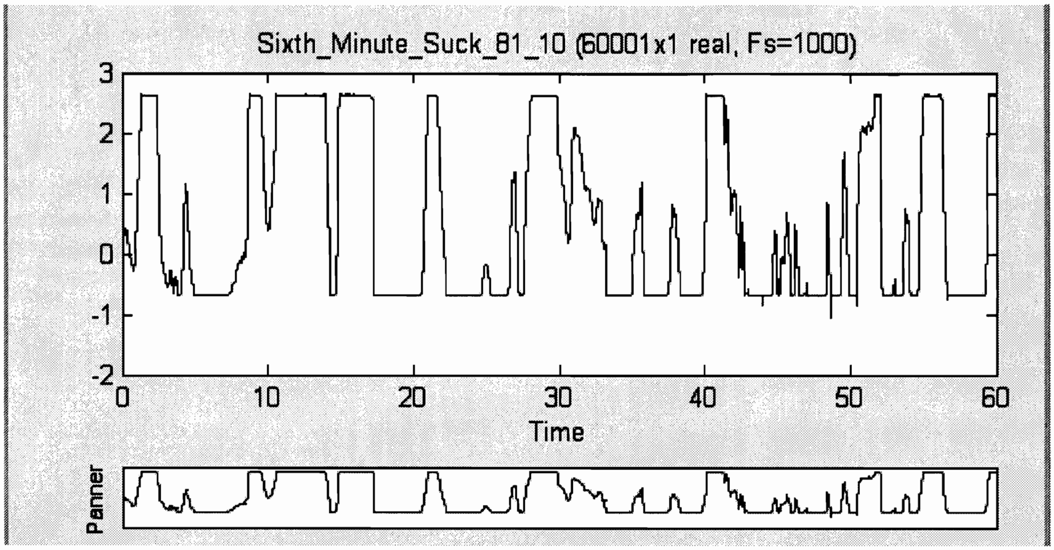

Figure 4.72: The sixth minute of sucking of baby #81, 10th feeding

Table 4.95: The analysis of the sixth minute of sucking of baby #81, 10th feeding

Time Slot	Length	Level of Certainty
1	500	0.9022
921	1760	0.9399
3941	940	0.8673
8321	1760	0.9337
20521	1700	0.9736
24521	960	0.9094
26421	980	0.8967
30661	1280	0.8921
32421	680	0.9097
34861	1240	0.8829
37361	1140	0.8983
39881	1900	0.8707
41781	1900	0.8757
44541	500	0.9039
45121	500	0.8658
49221	920	0.8981
53501	780	0.8849
54621	720	0.8874

Table 4.96: The evaluation of the sixth minute of sucking of baby #81, 10th feeding

Agreement(s)	Disagreement(s)
9	9

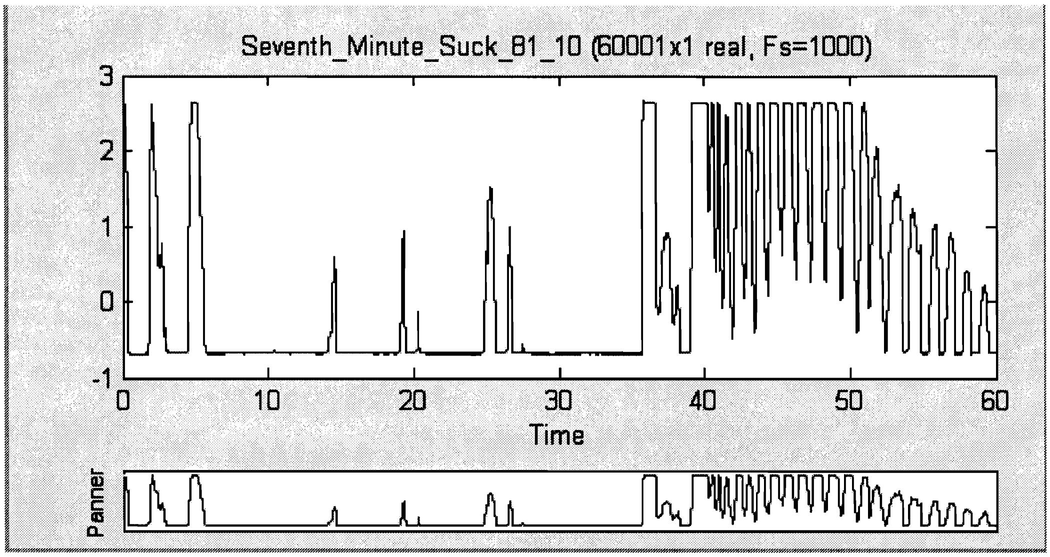

Figure 4.73: The seventh minute of sucking of baby #81, 10th feeding

Table 4.97: The analysis of the seventh minute of sucking of baby #81, 10th feeding

Time Slot	Length	Level of Certainty	Time Slot	Length	Level of Certainty
1701	860	0.8836	44401	800	0.9383
4121	1800	0.8933	45281	1020	0.9433
14261	500	0.8840	46301	920	0.9565
19001	500	0.8601	47241	1080	0.9598
24681	1200	0.8985	48321	1000	0.9527
26361	540	0.8945	49341	1120	0.9613
35501	1520	0.8860	50521	880	0.9642
37021	720	0.9671	51401	800	0.9950
37861	540	0.8892	52341	1580	0.9398
40741	500	0.8582	53921	1020	0.9035
41281	500	0.9464	55241	1060	0.8855
41941	880	0.9260	56401	960	0.9063
42821	500	0.9750	57541	940	0.8977
43401	1000	0.9078	58681	1020	0.9075

Table 4.98: The evaluation of the seventh minute of sucking of baby #81, 10th feeding

Agreement(s)	Disagreement(s)
30	2

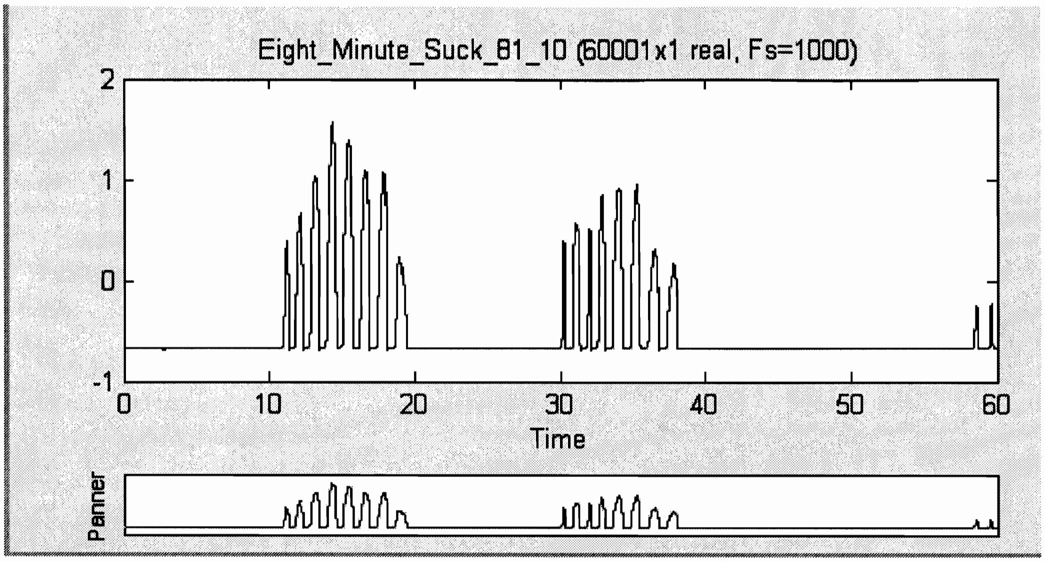

Figure 4.74: The eighth minute of sucking of baby #81, 10th feeding

Table 4.99: The analysis of the eighth minute of sucking of baby #81, 10th feeding

Time Slot	Length	Level of Certainty
10921	500	0.9013
11661	820	0.8926
12641	1040	0.8917
13781	1040	0.9154
14901	1020	0.9377
16081	1020	0.9051
17301	1040	0.9036
18481	1180	0.9041
30721	820	0.8974
32501	760	0.9008
33441	1120	0.8969
34701	1000	0.8937
35861	1200	0.8940
37181	1140	0.8909

Table 4.100: The evaluation of the eighth minute of sucking for baby #81, 10th feeding

Agreement(s)	Disagreement(s)
14	0

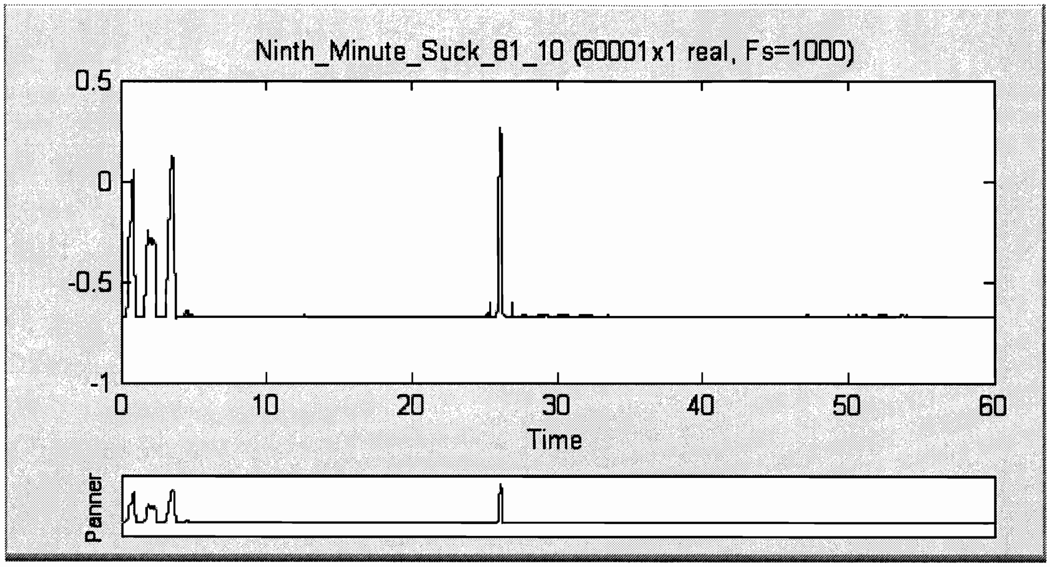

Figure 4.75: The ninth minute of sucking of baby #81, 10th feeding

Table 4.101: The analysis of the ninth minute of sucking of baby #81, 10th feeding

Time Slot	Length	Level of Certainty
321	840	0.8800
1401	1320	0.8852
3021	900	0.9017
25781	620	0.8917
29921	1000	0.8554

Table 4.102: The evaluation of the ninth minute of sucking of baby #81, 10th feeding

Agreement(s)	Disagreement(s)
4	1

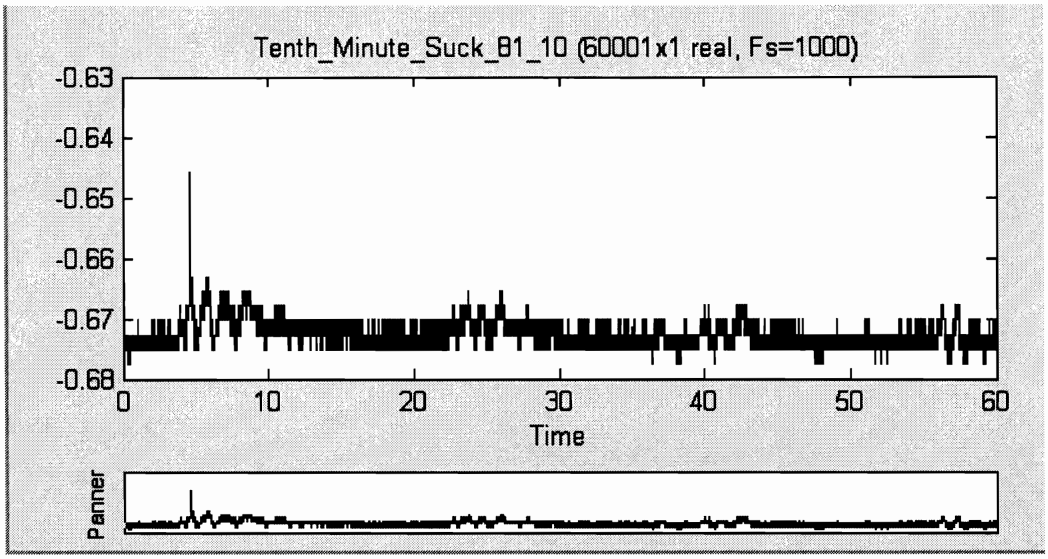

(a)

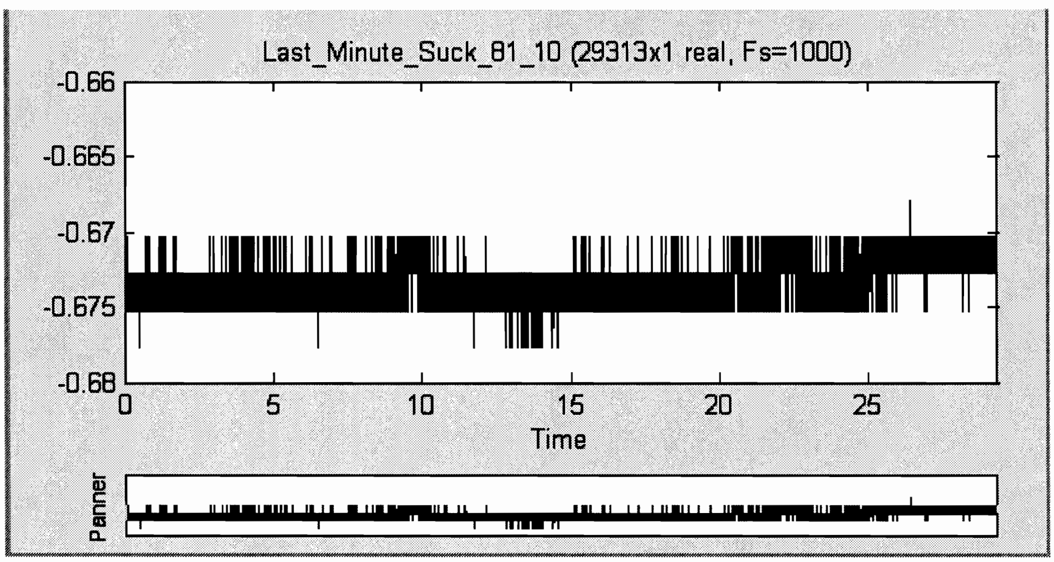

(b)

Figure 4.76: (a) The 10^{th} minute of sucking of baby #81, 10^{th} feeding. (b) The last minute of sucking of baby #81, 10^{th} feeding. These two minutes are not analyzed due to the poor quality of the signals

The Detection of the Swallowing Signal for Baby #81, 10th Feeding

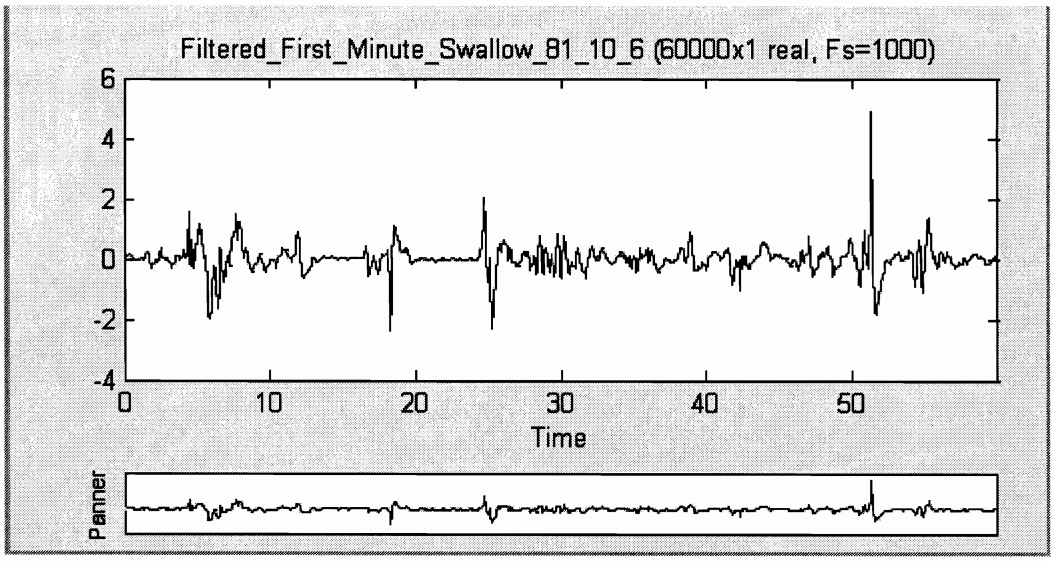

Figure 4.78: The first minute of swallowing for baby #81, 10th feeding

Table 4.103: The analysis of the first minute of swallowing of baby #81,10th feeding

Time Slot	Length	Level of Certainty
4241	1900	0.8535
17041	1460	0.8742
40301	1780	0.9376
52781	1800	0.9266

Table 4.104: The evaluation of the first minute of swallowing of baby #81, 10th feeding

Agreement(s)	Disagreement(s)
3	1

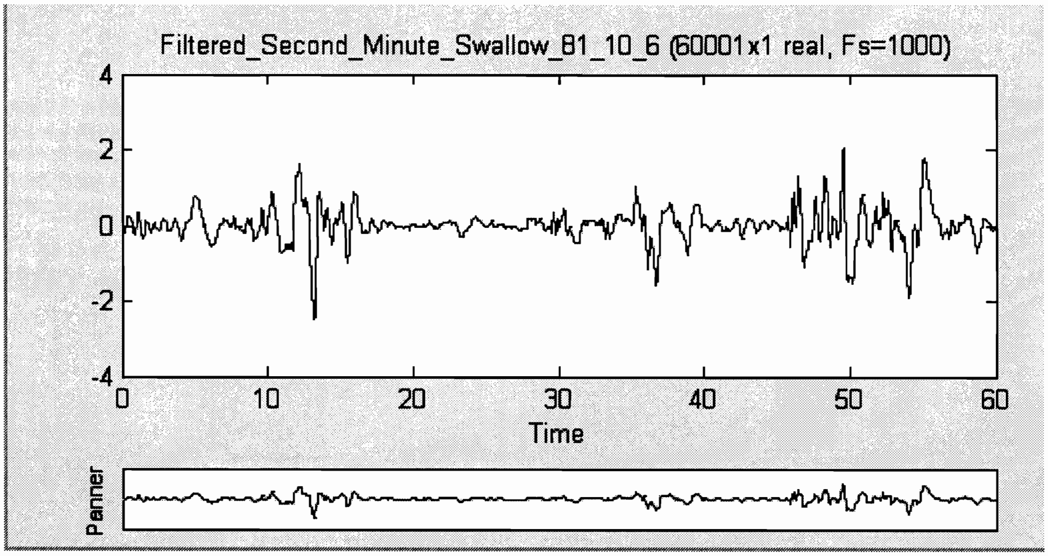

Figure 4.79: The second minute of swallowing of baby #81, 10th feeding

Table 4.105: The analysis of the second minute of swallowing of baby #81, 10th feeding

Time Slot	Length	Level of Certainty
54401	1920	0.8707

Table 4.106: The evaluation of the second minute of swallowing of baby #81, 10th feeding

Agreement(s)	Disagreement(s)
1	0

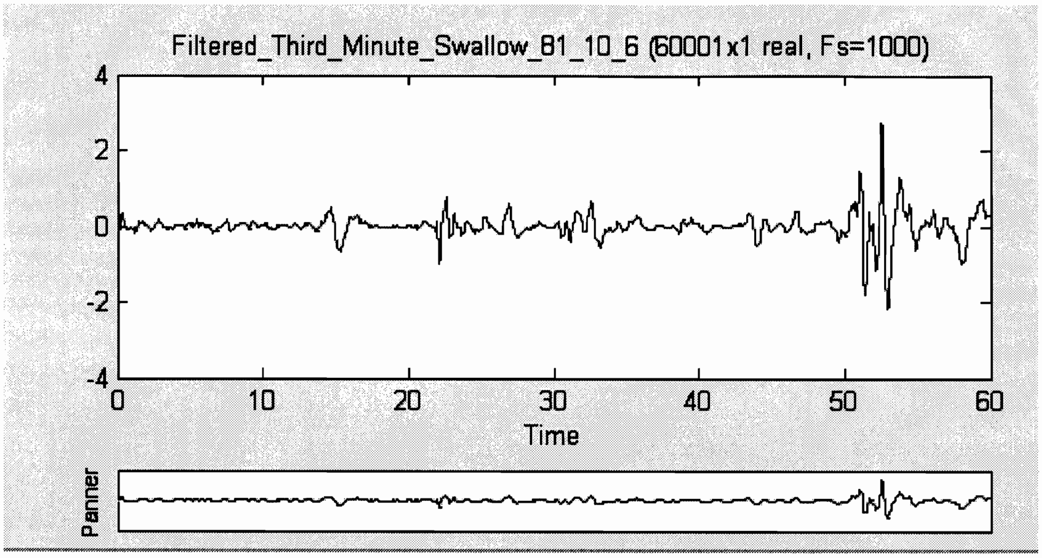

Figure 4.80: The third minute of swallowing of baby #81, 10th feeding

Table 4.107: The analysis of the third minute of swallowing of baby #81,10th feeding

Time Slot	Length	Level of Certainty
20601	1820	0.8890

Table 4.108: Evaluation of the Third Minute of Swallowing for Baby #81, 10th feeding

Agreement(s)	Disagreement(s)
1	0

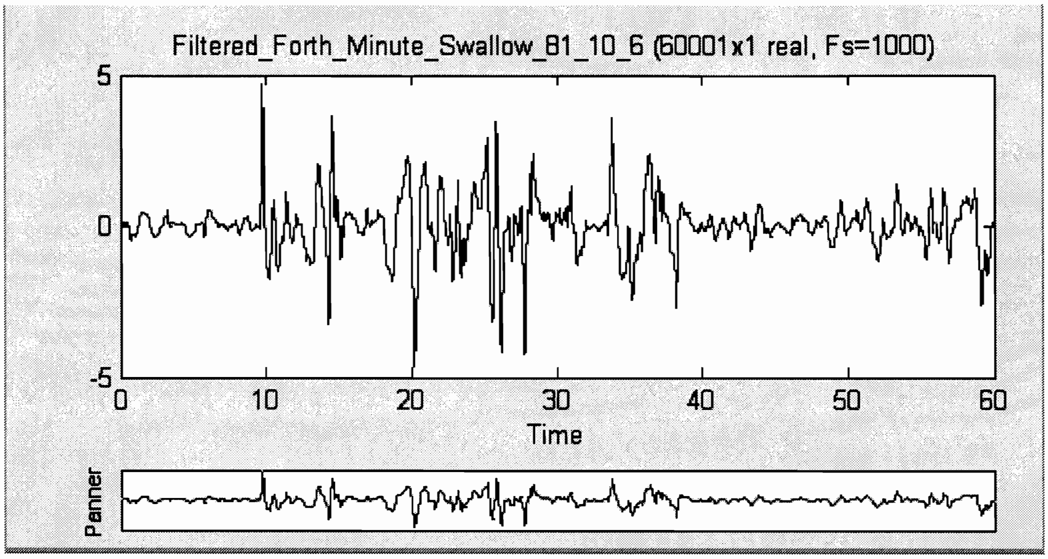

Figure 4.81: The forth minute of swallowing of baby #81, 10th feeding

Table 4.109: The analysis of the forth minute of swallowing of baby #81,10th feeding

Time Slot	Length	Level of Certainty
13361	1100	0.8812
18921	1540	0.8617
24061	1780	0.8814
26361	1700	0.9277
28841	1080	0.8734
42021	1620	0.8822
53861	1760	0.8728
57641	1800	0.8633

Table 4.110: The evaluation of the forth minute of swallowing of baby #81, 10th feeding

Agreement(s)	Disagreement(s)
4	4

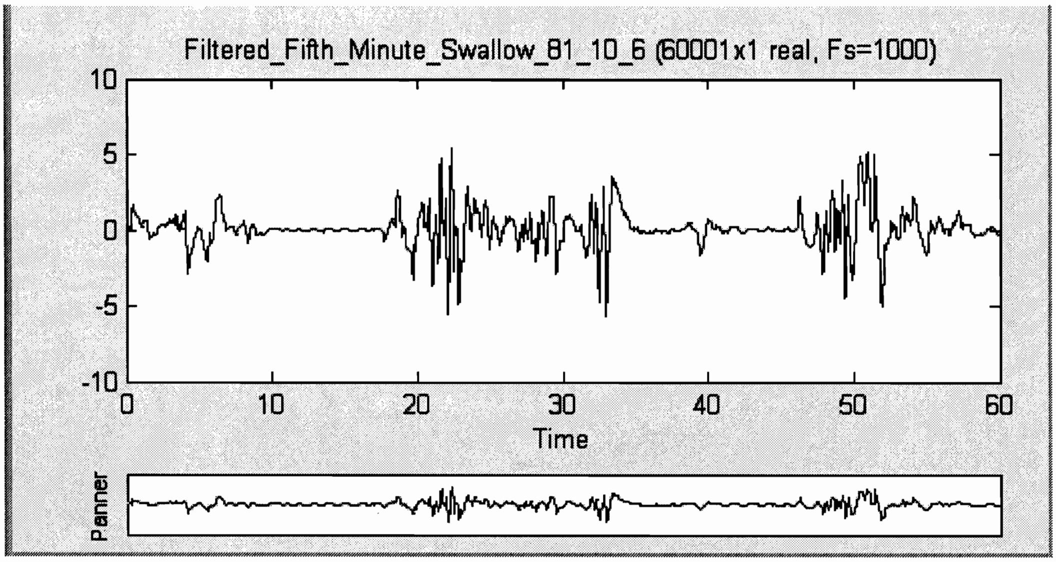

Figure 4.82: The fifth minute of swallowing of baby #81, 10th feeding

Table 4.111: The analysis of the fifth minute of swallowing of baby #81,10th feeding

Time Slot	Length	Level of Certainty
16341	1680	0.9675
19961	1300	0.9033
25941	1220	0.8594
30081	1840	0.8717
37961	1820	0.8696

Table 4.112: The evaluation of the fifth minute of swallowing of baby #81, 10th feeding

Agreement(s)	Disagreement(s)
3	2

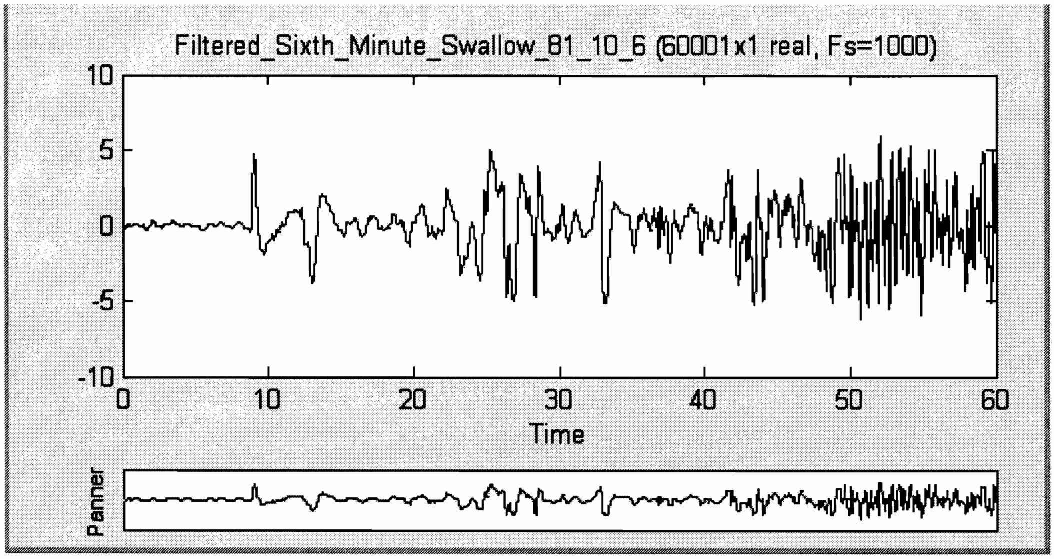

Figure 4.83: The sixth minute of swallowing of baby #81, 10^{th} feeding

Due to the poor quality of the signal, this minute was not analyzed.

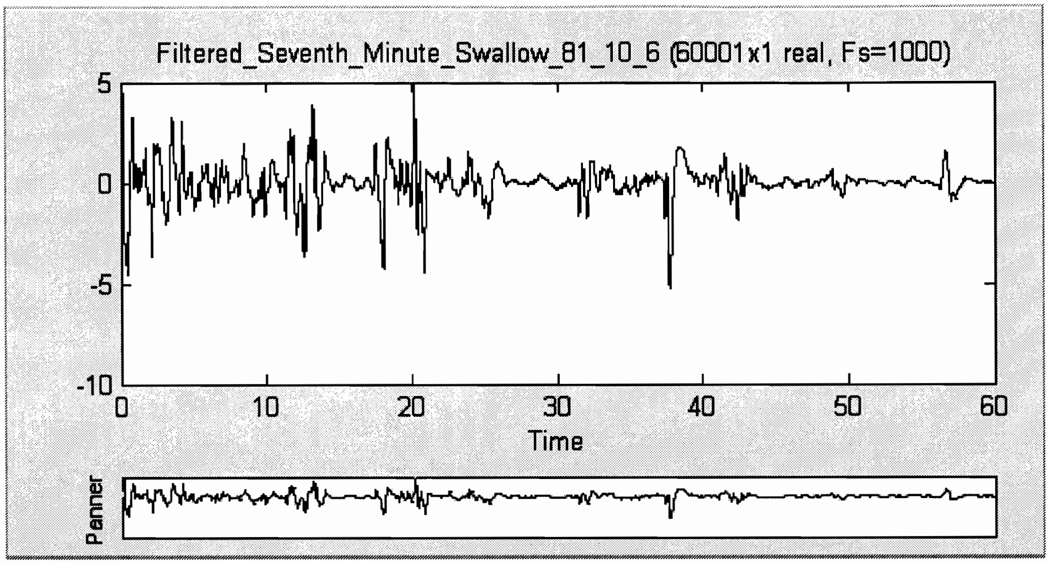

Figure 4.84: The seventh minute of swallowing of baby #81, 10th feeding

Table 4.113: The analysis of the seventh minute of swallowing of baby #81,10th feeding

Time Slot	Length	Level of Certainty
10481	1000	0.8657
16461	1780	0.8957
21021	1140	0.8546
30461	1260	0.9044
36301	1760	0.9315
40161	1060	0.8555

Table 4.114: The evaluation of the seventh minute of swallowing for baby #81, 10th feeding

Agreement(s)	Disagreement(s)
3	3

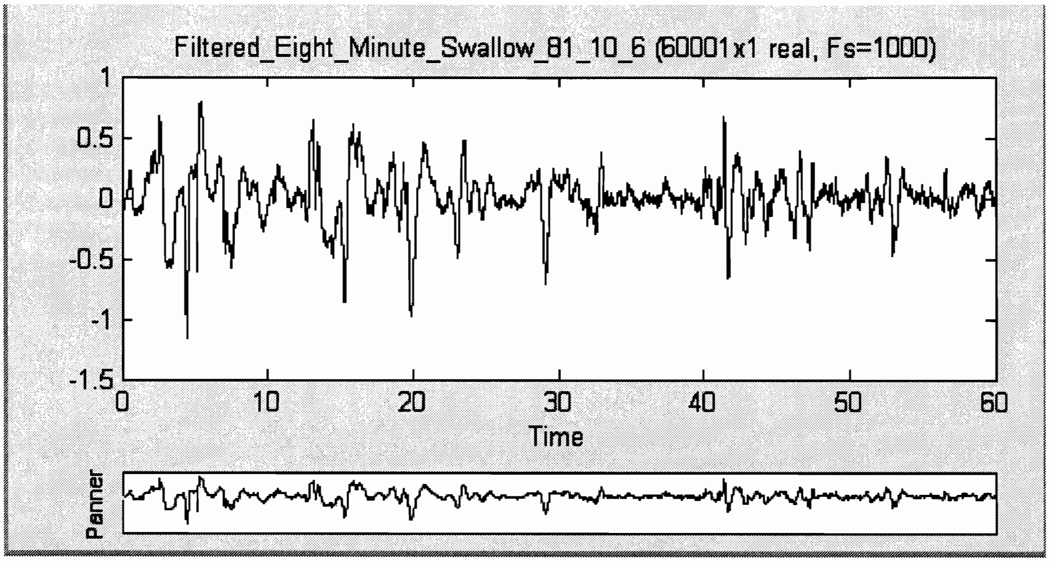

Figure 4.85: The eighth minute of swallowing for baby #81, 10th feeding

Table 4.115: The analysis of the eighth minute of swallowing of baby #81, 10th feeding

Time Slot	Length	Level of Certainty
3541	1100	0.8922
18241	1940	0.8643
21601	1740	0.9022
27661	1720	0.8988

Table 4.116: The evaluation of the eighth minute of swallowing of Baby #81, 10th feeding

Agreement(s)	Disagreement(s)
3	3

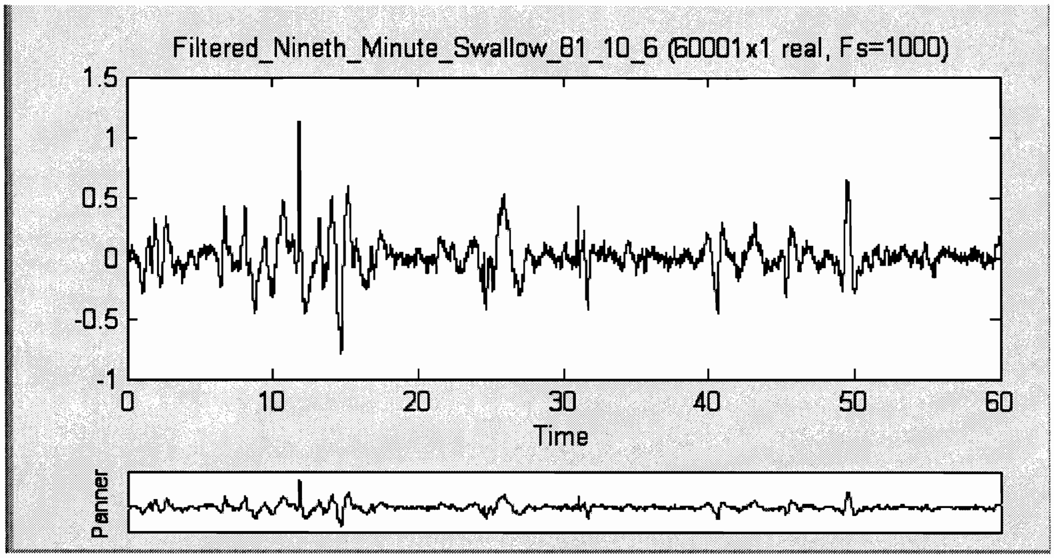

Figure 4.86: The ninth minute of swallowing of baby #81, 10th feeding

Table 4.117: The analysis of the ninth minute of swallowing of baby #81, 10th feeding

Time Slot	Length	Level of Certainty
0	0	0

Table 4.118: The evaluation of the ninth minute of swallowing for baby #81, 10th feeding

Agreement(s)	Disagreement(s)
0	0

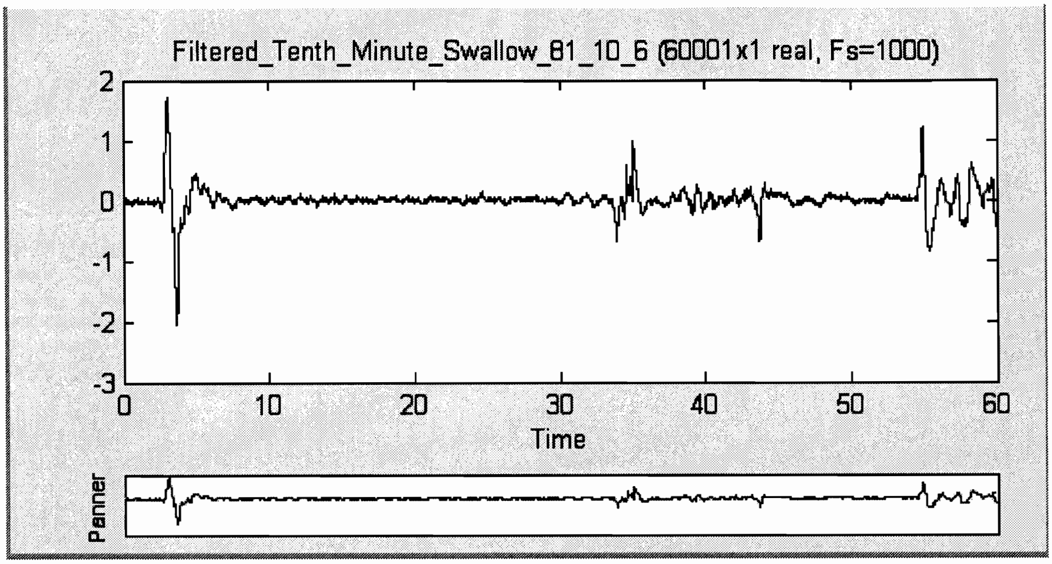

Figure4.87: The 10th minute of swallowing of baby #81, 10th feeding

Table 4.119: The analysis of the 10th minute of swallowing of baby #81,10th feeding

Time Slot	Length	Level of Certainty
32501	1680	0.9421
42341	1660	0.9240

Table 4.120: The evaluation of the 10th minute of swallowing of baby #81, 10th feeding

Agreement(s)	Disagreement(s)
0	2

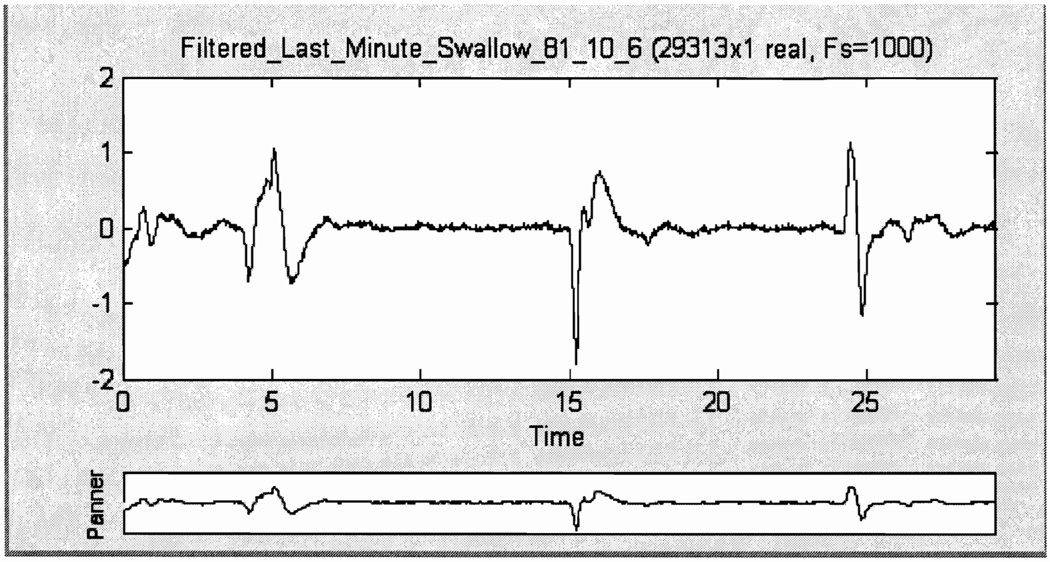

Figure 4.88: The last minute of swallowing of baby #81, 10th feeding

Table 4.121: The analysis of the last minute of swallowing of baby #81,10th feeding

Time Slot	Length	Level of Certainty
2841	1660	0.9646
13821	1660	0.9890

Table 4.122: The evaluation of the last minute of swallowing of baby #81, 10th feeding

Agreement(s)	Disagreement(s)
2	0

The Detection of Breathing Signal for Baby # 81, 10th Feeding

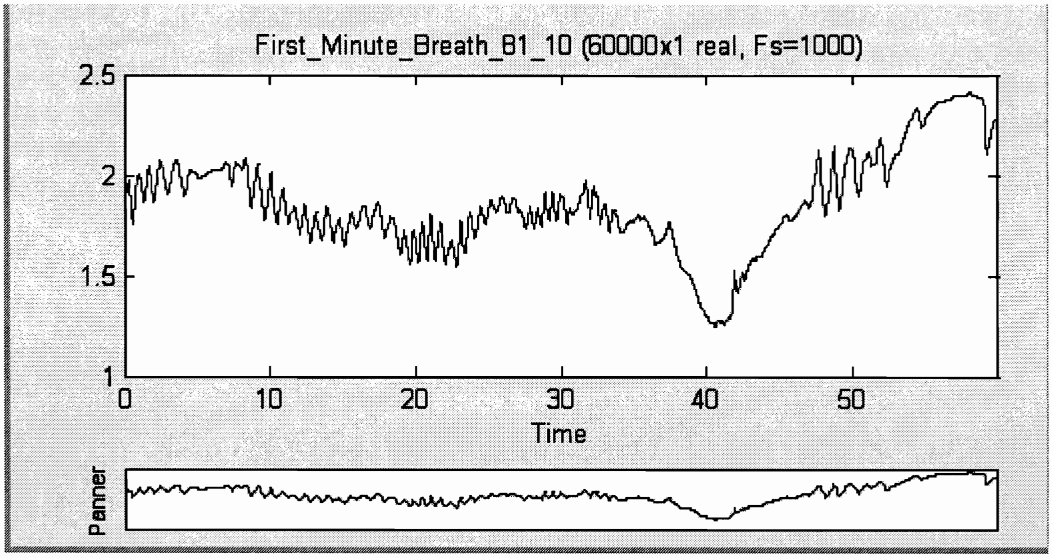

Figure 4.89: The first minute of breathing of baby #81, 10th feeding

Table 4.123: The analysis of first minute of breathing of baby #81,10th feeding

Time Slot	Length	Level of Certainty	Time Slot	Length	Level of Certainty	Time Slot	Length	Level of Certainty
621	840	0.9236	16861	1000	0.9764	29661	820	0.9329
1461	520	0.8277	17881	940	0.9827	31121	980	0.8942
2021	1040	0.9345	18901	720	0.8648	32661	720	0.8784
3081	980	0.9922	19621	580	0.8703	33381	680	0.8304
4261	960	0.8125	20201	580	0.8983	34281	1980	0.8079
6441	1020	0.8384	20781	540	0.9048	36481	1740	0.8695
8641	1040	0.9275	21341	720	0.9420	46261	900	0.8295
9681	700	0.9342	22061	780	0.9377	47161	940	0.9565
10441	860	0.9529	22841	580	0.8449	48181	1020	0.9105
11981	840	0.8965	23421	720	0.8816	49221	1240	0.9801
12821	680	0.8963	24161	700	0.8396	50581	860	0.8264
13521	840	0.9483	25501	940	0.9061	51481	840	0.9189
14361	720	0.9013	27561	640	0.8092	53761	1160	0.9037
15181	880	0.8793	28621	600	0.8155	57501	1020	0.8673
16061	760	0.9073						

Table 4.124: The evaluation of the first minute of breathing of baby #81, 10th feeding

Agreement(s)	Disagreement(s)
39	4

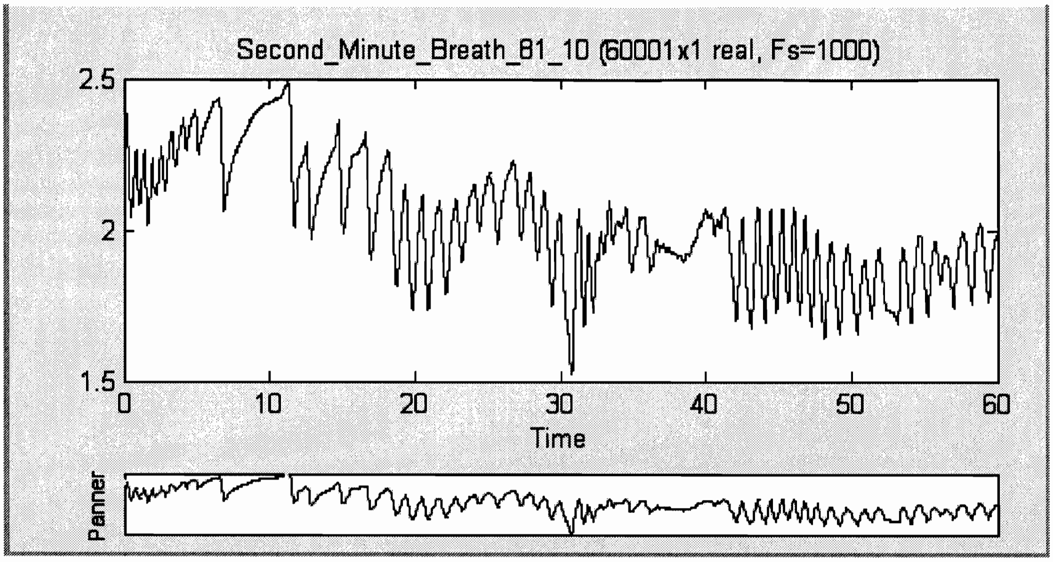

Figure 4.90: The Second Minute of Breathing for Baby #81, 10^{th} feeding

Table 4.125: Analysis of the Second Minute of Breathing for Baby #81,10^{th} feeding

Time Slot	Length	Level of Certainty	Time Slot	Length	Level of Certainty	Time Slot	Length	Level of Certainty
481	660	0.8740	23421	1120	0.9674	44041	820	0.9167
1141	480	0.8487	24541	1080	0.9857	44881	720	0.9397
2221	680	0.8536	25701	1740	0.9673	45641	800	0.9392
2901	700	0.8397	27441	840	0.9652	46461	700	0.9536
3621	740	0.8287	28361	1040	0.9403	47201	900	0.9412
4361	820	0.8823	29441	980	0.9753	48121	1040	0.9495
5181	1820	0.8424	30821	920	0.9082	49181	1160	0.9600
11641	1380	0.9298	31741	440	0.8578	50381	1060	0.9478
13321	1900	0.8107	33041	660	0.8677	51441	880	0.9806
15221	1840	0.8894	34881	1480	0.9484	53081	1060	0.9038
17061	1700	0.9630	39421	1320	0.8758	54141	1040	0.9907
18761	1020	0.9794	40921	780	0.8256	55281	920	0.9370
19861	1120	0.9612	42001	1140	0.8721	56921	1420	0.9611
21001	1160	0.9885	43141	860	0.9554	58341	920	0.9878
22241	1100	0.9621						

Table 4.126: Evaluation of the Second Minute of Breathing for Baby #81, 10^{th}

Agreement(s)	Disagreement(s)
43	3

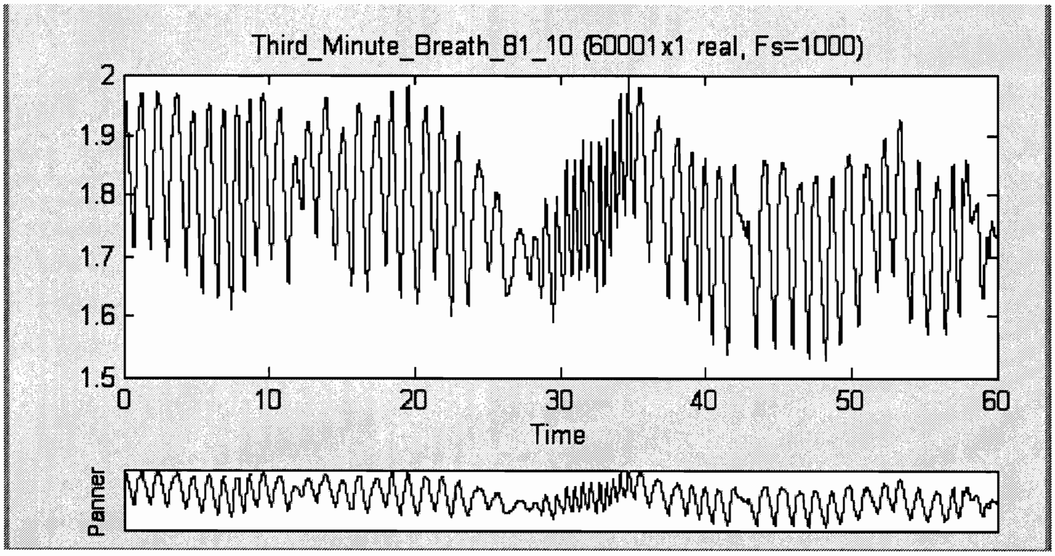

Figure4.91: The third minute of breathing of baby #81, 10th feeding

Table 4.127: The analysis of the third minute of breathing of baby #81,10th feeding

Time Slot	Length	Level of Certainty	Time Slot	Length	Level of Certainty	Time Slot	Length	Level of Certainty
601	1300	0.9413	20221	1140	0.9628	38661	840	0.9683
1901	920	0.9859	21381	1000	0.9704	39521	900	0.9355
2901	1440	0.9783	22441	1220	0.9246	40461	980	0.9509
4341	820	0.9709	23701	1440	0.9799	41621	740	0.8378
5281	1220	0.9302	25141	1020	0.9927	43401	1440	0.9493
6501	680	0.9596	26521	1520	0.9172	44841	960	0.9783
7321	980	0.9080	28601	960	0.8893	45901	1220	0.9602
8301	680	0.9563	30161	660	0.8134	47121	920	0.9675
9041	1120	0.9292	31281	640	0.8418	48161	1140	0.9158
10161	1020	0.9923	31921	440	0.8385	49301	1060	0.9690
11381	900	0.8897	32481	560	0.8451	50441	1420	0.9397
12281	800	0.9443	33041	360	0.8033	51861	880	0.9550
13161	1380	0.9729	33441	500	0.8099	52801	1160	0.9533
14541	960	0.9869	33941	440	0.8283	54021	1200	0.9548
15581	1180	0.9549	34421	680	0.8827	55241	1240	0.9797
16781	1220	0.9859	35101	840	0.9763	56501	920	0.9285
18001	860	0.9535	36041	1400	0.9636	57461	860	0.8615
18941	1260	0.9221	37441	1220	0.9927			

Table 4.128: The evaluation of the third minute of breathing of baby #81, 10th

Agreement(s)	Disagreement(s)
53	0

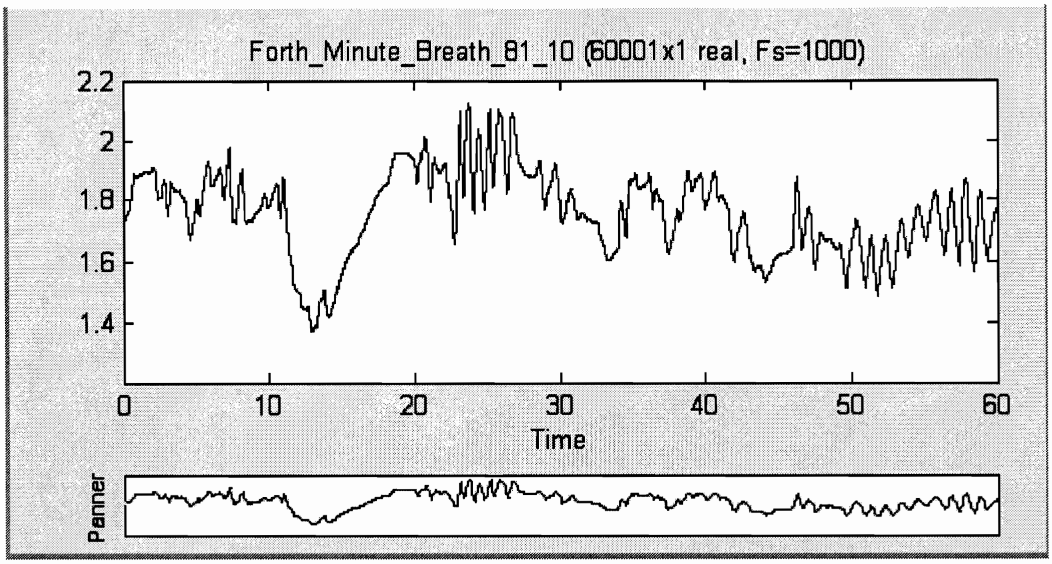

Figure 4.92: The forth minute of breathing of baby #81, 10th feeding

Table 4.129: The analysis of the forth minute of breathing for baby #81,10th feeding

Time Slot	Length	Level of Certainty	Time Slot	Length	Level of Certainty
3001	1520		33941	660	0.8612
5381	860	0.8154	34681	920	0.8321
6881	720	0.8437	38441	740	0.8115
7681	860	0.8856	39181	820	0.8080
10001	860	0.9124	40121	960	0.8936
13201	1020	0.8486	41841	1540	0.9055
18241	1980	0.8981	45841	920	0.8885
20221	940	0.8119	46761	660	0.8878
22861	580	0.9155	49601	1500	0.9531
23441	560	0.8653	51101	560	0.8688
24061	800	0.9490	51781	1120	0.9413
24861	620	0.9500	52961	1020	0.9386
25481	860	0.9204	54041	1120	0.9658
26401	920	0.9844	55161	1120	0.9869
28101	900	0.8976	56341	1080	0.9476
29001	1200	0.8165	57441	840	0.9687
30261	1060	0.9489	58381	1020	0.9124

Table 4.130: The evaluation of the forth minute of breathing of baby #81, 10th

Agreement(s)	Disagreement(s)
33	3

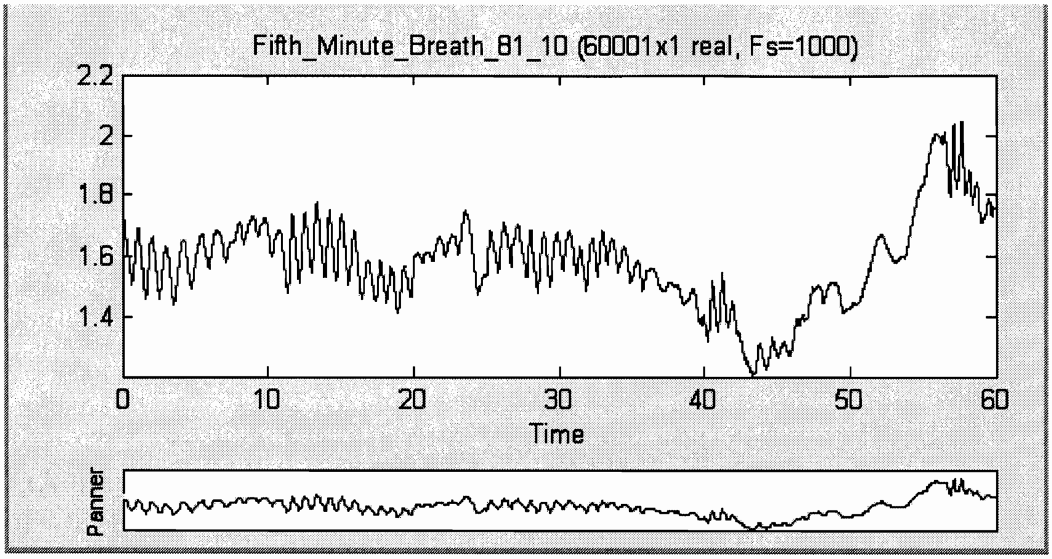

Figure4.93: The fifth minute of breathing of baby #81, 10th feeding

Table 3.131: The analysis of the fifth minute of breathing of baby #81,10th feeding

Time Slot	Length	Level of Certainty	Time Slot	Length	Level of Certainty	Time Slot	Length	Level of Certainty
621	840	0.9236	16861	1000	0.9764	29661	820	0.9329
1461	520	0.8277	17881	940	0.9827	31121	980	0.8942
2021	1040	0.9345	18901	720	0.8648	32661	720	0.8784
3081	980	0.9922	19621	580	0.8703	33381	680	0.8304
4261	960	0.8125	20201	580	0.8983	34281	1980	0.8079
6441	1020	0.8384	20781	540	0.9048	36481	1740	0.8695
8641	1040	0.9275	21341	720	0.9420	46261	900	0.8295
9681	700	0.9342	22061	780	0.9377	47161	940	0.9565
10441	860	0.9529	22841	580	0.8449	48181	1020	0.9105
11981	840	0.8965	23421	720	0.8816	49221	1240	0.9801
12821	680	0.8963	24161	700	0.8396	50581	860	0.8264
13521	840	0.9483	25501	940	0.9061	51481	840	0.9189
14361	720	0.9013	27561	640	0.8092	53761	1160	0.9037
15181	880	0.8793	28621	600	0.8155	57501	1020	0.8673
16061	760	0.9073						

Table 132: The evaluation of the fifth minute of breathing of baby #81, 10th

Agreement(s)	Disagreement(s)
50	2

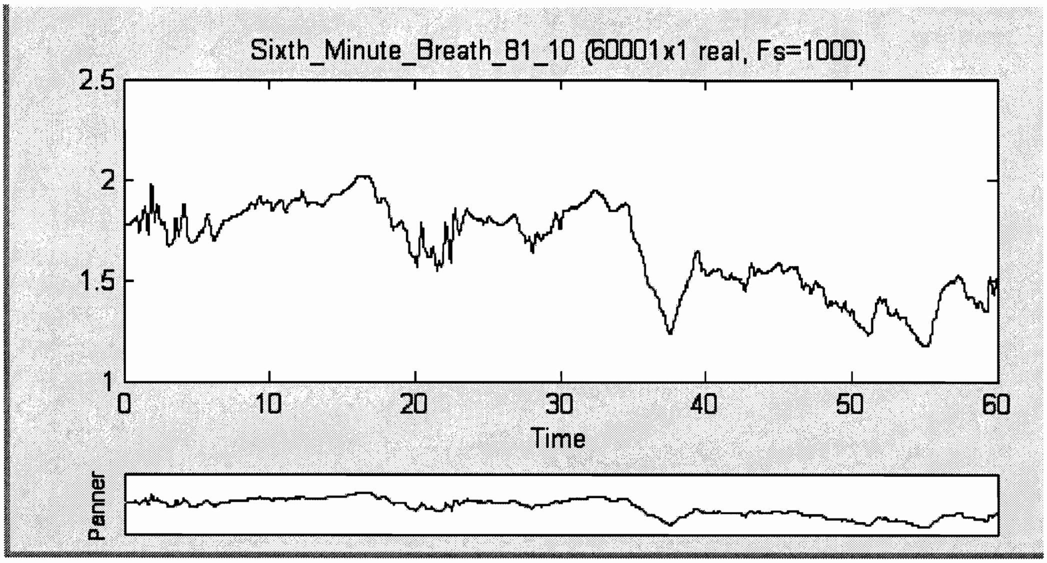

Figure 4.94: The sixth minute of breathing of baby #81, 10th feeding

Table 4.133: The analysis of the sixth minute of breathing of baby #81,10th feeding

Time Slot	Length	Level of Certainty	Time Slot	Length	Level of Certainty
1061	680	0.8830	23161	1040	0.8524
1741	400	0.8341	25881	1680	0.8332
3161	1700	0.8123	31641	1700	0.8749
5001	1340	0.8528	33661	1400	0.8043
10161	1040	0.9624	38701	1540	0.8407
12581	1020	0.8975	40241	980	0.8520
15481	1860	0.8212	44401	1100	0.8879
18461	1040	0.9421	47161	1120	0.8841
20101	840	0.8363	51301	1680	0.8692
21841	680	0.8969	56381	1600	0.8629
22521	560	0.8280			

Table 4.134: The evaluation of the sixth minute of breathing of baby #81, 10th

Agreement(s)	Disagreement(s)
11	10

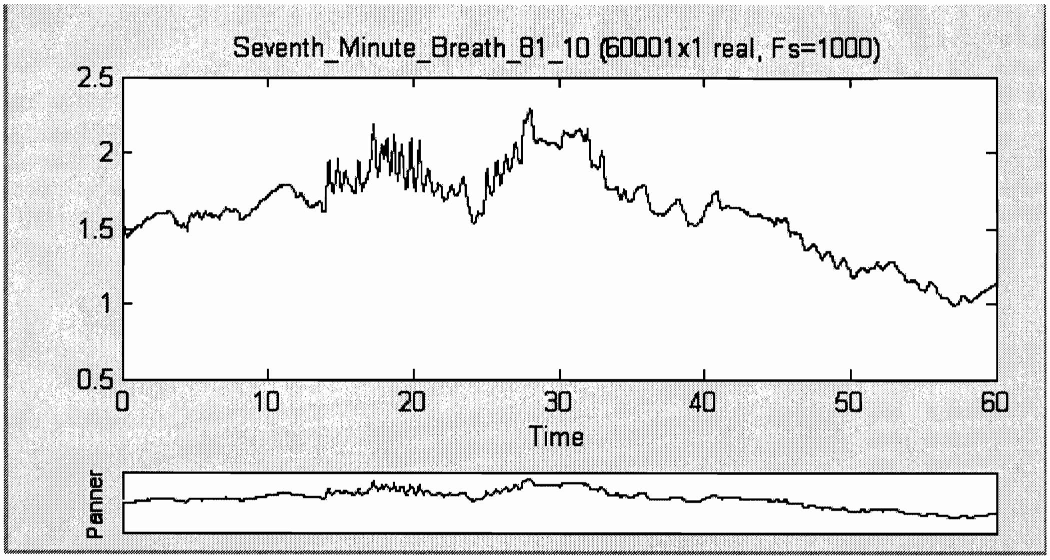

Figure 4.95: The seventh minute of breathing of baby #81, 10th feeding

Table 4.135: The analysis of the seventh minute of breathing of baby #81,10th feeding

Time Slot	Length	Level of Certainty	Time Slot	Length	Level of Certainty	Time Slot	Length	Level of Certainty
1861	1980	0.8150	20181	480	0.8972	34761	1800	0.9283
6541	1760	0.8261	20681	720	0.9052	37261	1640	0.9217
10281	1740	0.8497	21401	700	0.8578	39921	1580	0.8517
12881	1020	0.8089	22201	860	0.8096	46941	1060	0.9155
13901	620	0.8547	23061	700	0.9104	48021	940	0.9608
14521	540	0.8792	24821	580	0.8014	49061	1020	0.9114
15921	620	0.8484	25441	620	0.8887	50361	940	0.8230
16861	780	0.8864	26641	800	0.8610	51301	1020	0.8515
18381	580	0.8779	27441	1020	0.9529	52321	980	0.9716
18961	460	0.8845	30841	1040	0.9091	54941	1280	0.8812
19501	680	0.8889	32601	680	0.8218	57281	1120	0.8447

Table 4.136: The evaluation of the seventh minute of breathing of baby #81, 10th

Agreement(s)	Disagreement(s)
31	4

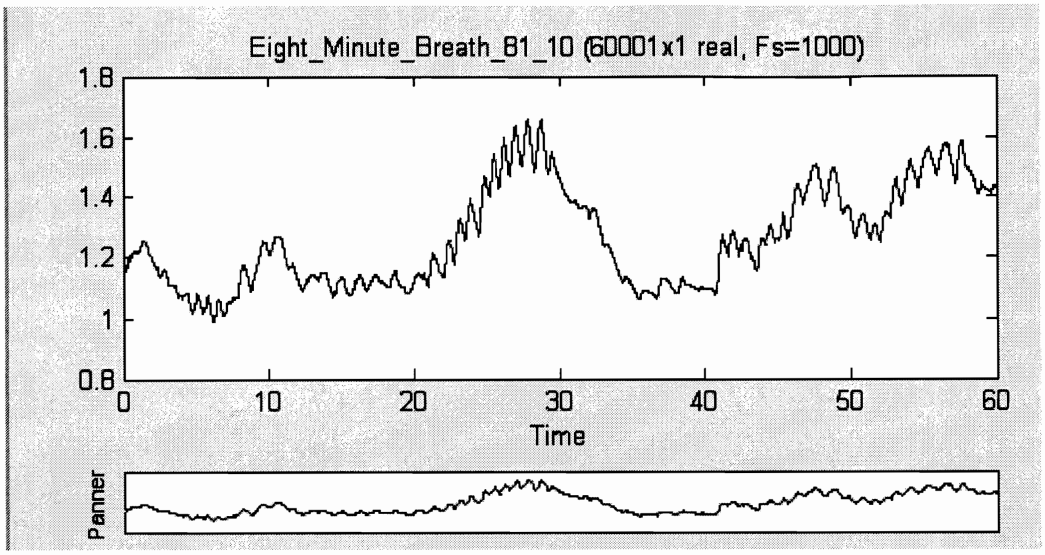

Figure 4.96: The eighth minute of breathing of baby #81, 10th feeding

Table 4.137: The analysis of the eighth minute of breathing of baby #81,10th feeding

Time Slot	Length	Level of Certainty	Time Slot	Length	Level of Certainty	Time Slot	Length	Level of Certainty
341	1820	0.8455	22061	760	0.9239	41641	900	0.9064
4701	880	0.8910	22821	760	0.8927	42321	800	0.8527
6161	840	0.8476	23581	760	0.9027	44101	700	0.8422
7761	1140	0.9199	24581	680	0.8062	45061	860	0.8964
9241	920	0.9111	25261	600	0.8627	45981	1420	0.9849
10161	960	0.9705	25881	740	0.9103	46841	1140	0.9906
12501	960	0.8617	26621	800	0.9417	48281	1140	0.9616
14401	1260	0.9037	27421	860	0.9701	50281	920	0.9057
15701	1080	0.9685	28301	940	0.9694	52701	1040	0.9582
16841	1100	0.8697	35441	1240	0.8463	53641	1220	0.9744
18101	1180	0.8678	36701	1220	0.9114	54741	1160	0.9919
19821	1200	0.9040	40901	740	0.8509	55961	1020	0.8823
21021	800	0.8953	22061	680	0.8361			

Table 4.138: The evaluation of the eighth minute of breathing of baby #81, 10th

Agreement(s)	Disagreement(s)
38	1

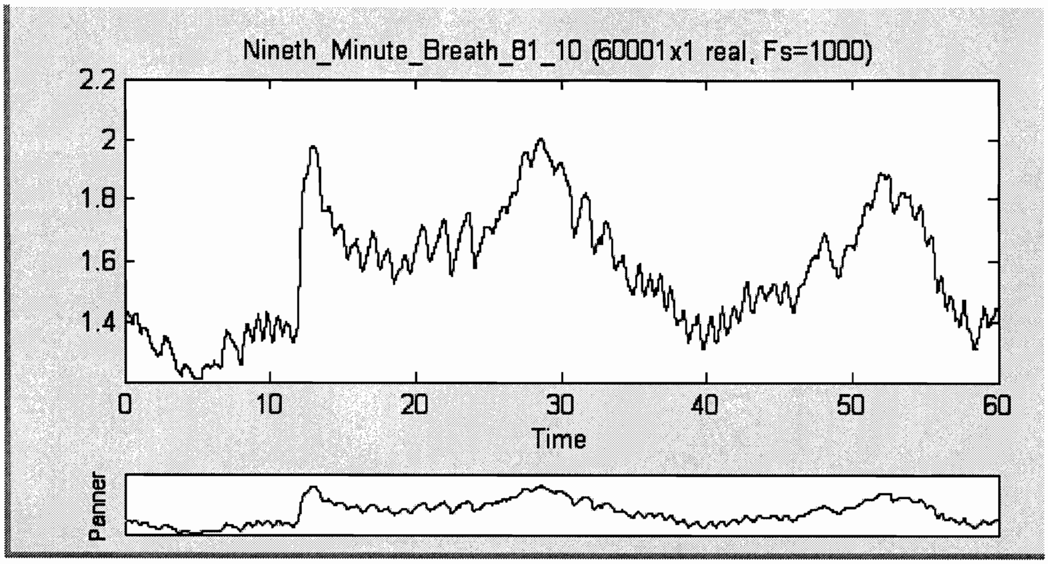

Figure 4.98: The ninth minute of breathing of baby #81, 10th feeding

Table 4.139: The analysis of the ninth minute of breathing of baby #81,10th feeding

Time Slot	Length	Level of Certainty	Time Slot	Length	Level of Certainty	Time Slot	Length	Level of Certainty
2201	1440	0.8645	19821	1280	0.9684	38801	980	0.9634
3701	1020	0.9055	21101	1420	0.9401	39841	900	0.9363
6441	1600	0.9074	22621	1620	0.9370	40741	700	0.8844
8041	820	0.8598	27121	920	0.8785	41481	840	0.8611
8861	640	0.8250	28081	1060	0.9782	42321	880	0.9512
9501	660	0.8735	29481	940	0.8874	43261	900	0.8760
10161	720	0.8744	30881	1560	0.9408	44161	900	0.8767
12081	1720	0.9620	32441	1280	0.9028	45061	840	0.9260
14381	860	0.8054	33721	900	0.8746	47381	1480	0.9029
15281	1040	0.9451	34901	960	0.9016	51281	1680	0.9468
16401	1240	0.9563	36401	860	0.8846	52961	1280	0.9193
17641	840	0.8863	37261	600	0.8227	57321	720	0.8535
18721	1020	0.8740	37901	880	0.8031	58621	840	0.8491

Table 4.140: The evaluation of the ninth minute of breathing of baby #81, 10th

Agreement(s)	Disagreement(s)
38	2

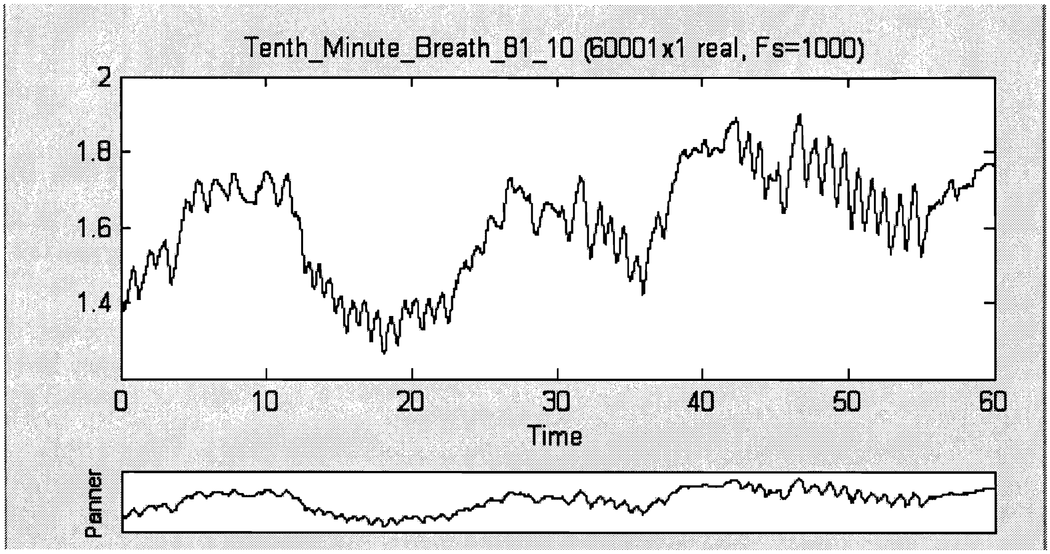

Figure 4.99: The 10th minute of breathing of baby #81, 10th feeding

Table 4.141: The analysis of the 10th minute of breathing of baby #81,10th feeding

Time Slot	Length	Level of Certainty	Time Slot	Length	Level of Certainty	Time Slot	Length	Level of Certainty
361	41241	0.9083	18121	960	0.9560	41241	1660	0.8962
1621	43501	0.8561	19141	840	0.8058	43501	860	0.8953
2501	45761	0.9185	20721	960	0.9111	45761	1580	0.9201
4781	47341	0.9338	21681	820	0.8787	47341	760	0.8042
6081	48161	0.8339	25061	1060	0.8497	48161	1100	0.9744
7281	49261	0.8996	26361	900	0.8105	49261	900	0.9742
9161	50201	0.9201	28801	1360	0.8291	50201	980	0.9587
10901	51181	0.9779	30741	1720	0.9396	51181	860	0.9579
13201	52041	0.8794	32461	940	0.9375	52041	840	0.9418
14701	52961	0.8385	34061	1000	0.9187	52961	1120	0.9337
15501	54081	0.9404	35061	840	0.9077	54081	880	0.9749
16401	56461	0.8663	36441	980	0.8818	56461	1080	0.9257
17161	41241	0.9572						

Table 4.142: The evaluation of the 10th minute of breathing of baby #81, 10th

Agreement(s)	Disagreement(s)
36	2

Tables (4.143) and (4.144) show the result of evaluation for baby # 87 and baby # 81 respectively.

Table 4.143: The evaluation of all three signals for baby # 87, seventh feeding

Baby # 87	Agreement(s)	Disagreement(s)
Suck	427	52
Swallow	41	22
Breath	277	13

Table 4.144: The evaluation of all three signals for baby # 81, 10th feeding

Baby # 81	Agreement(s)	Disagreement(s)
Suck	77	21
Swallow	18	17
Breath	418	29

4.6.2. Result of Analysis the Relationships between the Signals

In this section, the results of analysis the relationship between the signals are presented. The following plots demonstrate the relationship between suck, swallow and breath for each 10 seconds of a specific minute. Therefore, the time slot is 500 ms (0.5 s). As was mentioned before the third, forth , fifth , sixth , seventh, 13th and 14th minutes for baby #87 are analyzed. For baby #81 the second, third, eighth and ninth minutes are selected for analysis.

The Analysis of the Third Minute of Baby #87 Feeding

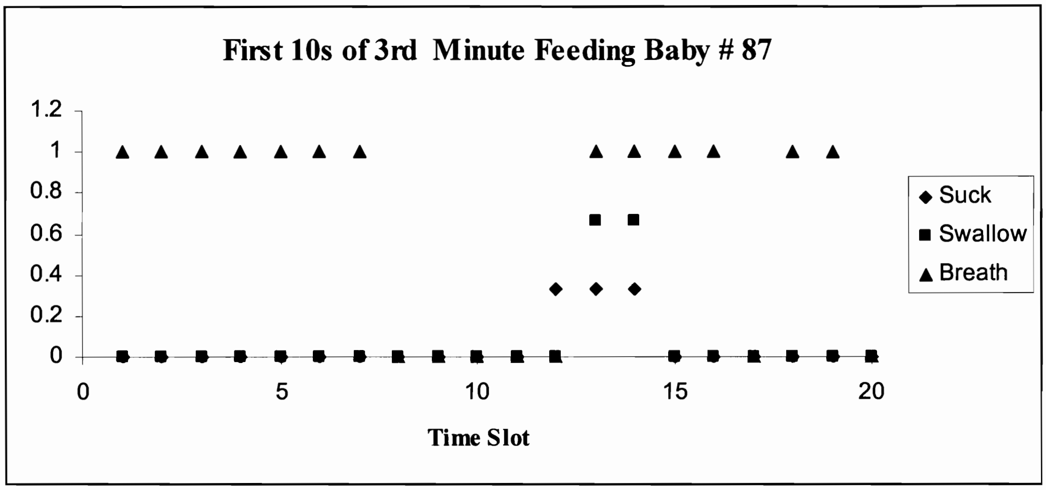

Figure 4.100: The third minute of baby #87's feeding (t =1 to 10 s)

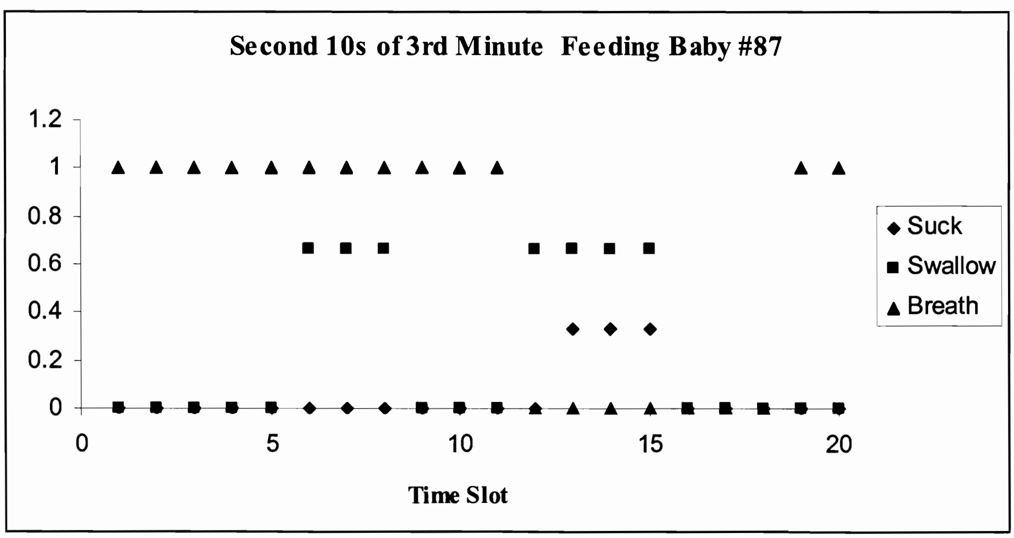

Figure 4.101: The third minute of baby #87's feeding (t=11 to 20 s)

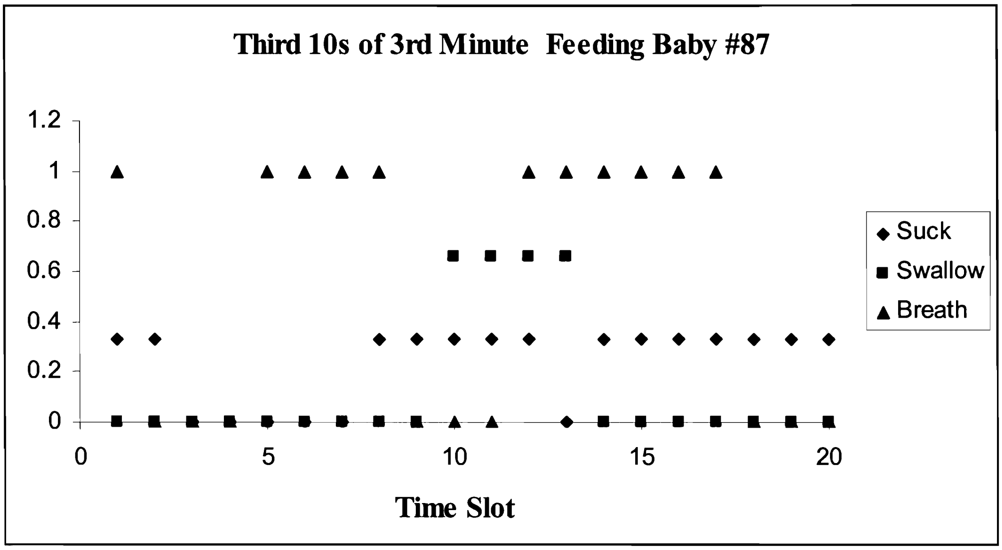

Figure 4.102: The third minute of baby #87's feeding (t= 21 to 30s)

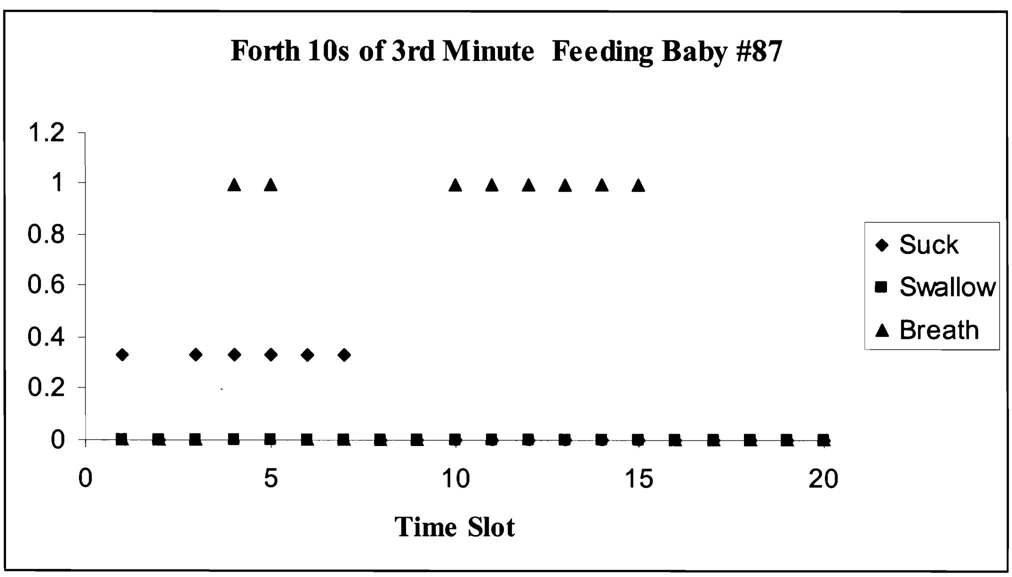

Figure 4.103: The third minute baby #87's feeding (t=31 to 40s)

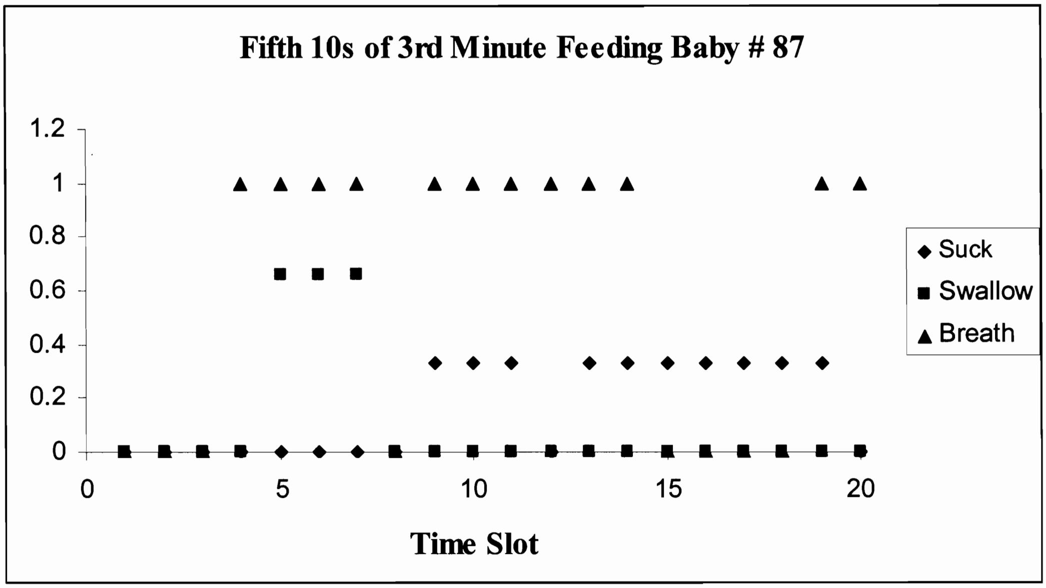

Figure 4.104: The third minute of baby #87's feeding (t= 41 to50)

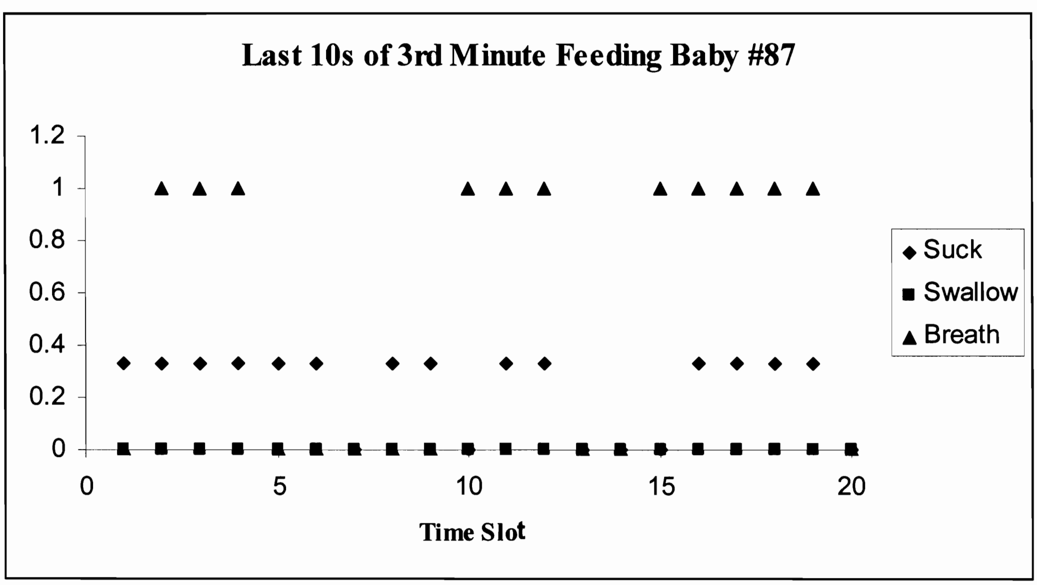

Figure 4.105: The third minute baby #87's feeding (t=51 to 60)

<u>The Analysis of the Forth Minute of Baby # 87's Feeding</u>

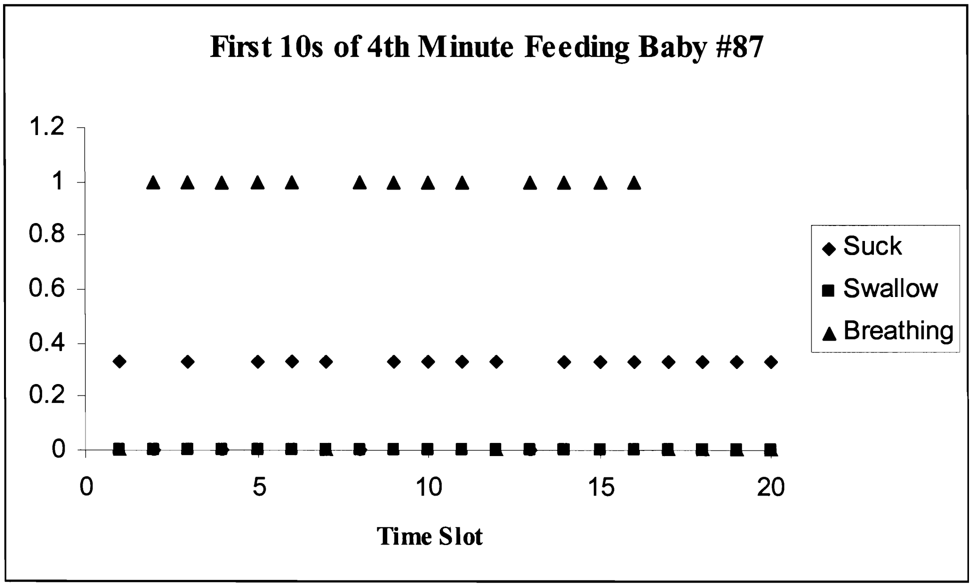

Figure 4.106: The forth minute of baby #87's feeding (t=1 to 10)

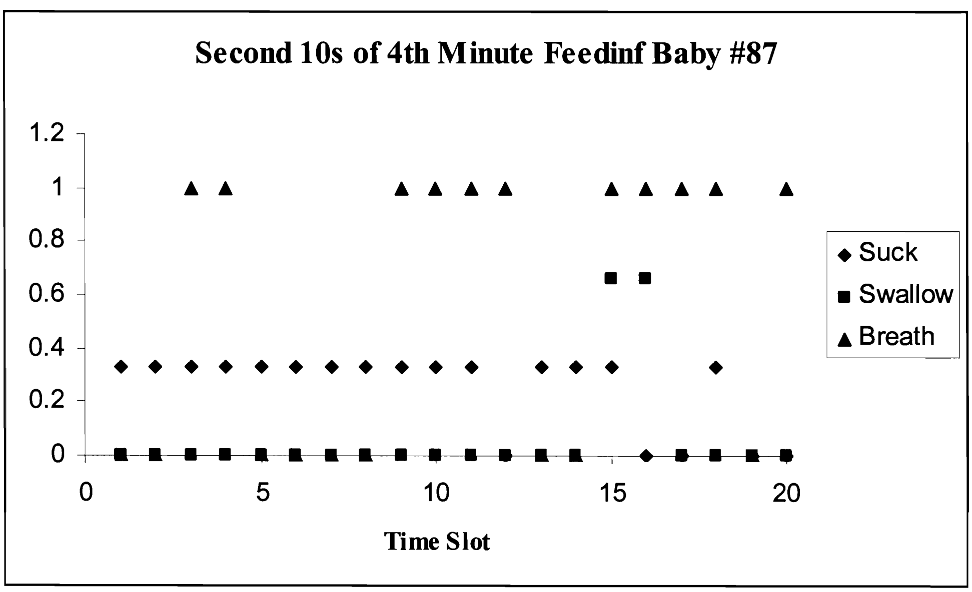

Figure4.107: The forth minute of baby #87's feeding (t=11 to 20)

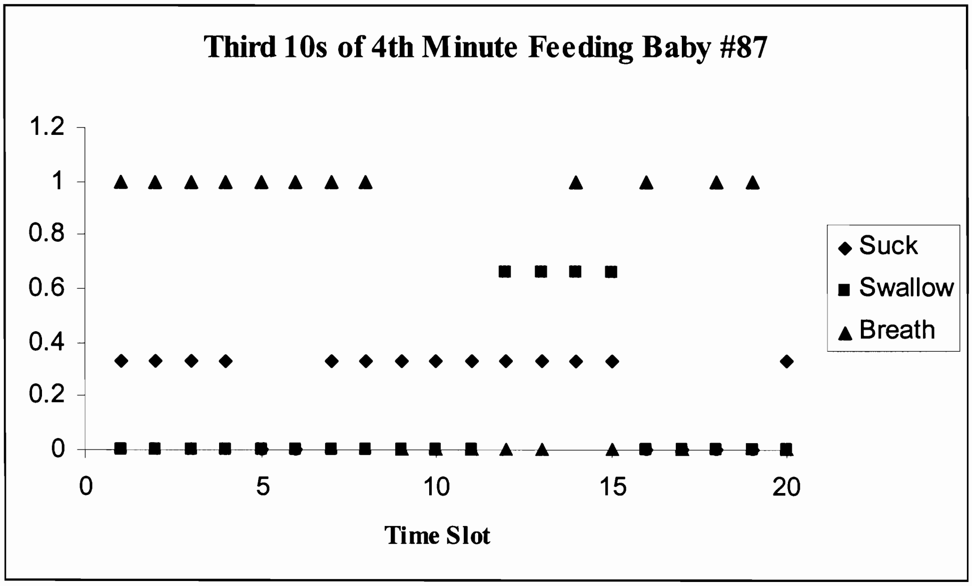

Figure 4.108: The forth minute of baby #87's feeding (t=21 to 30)

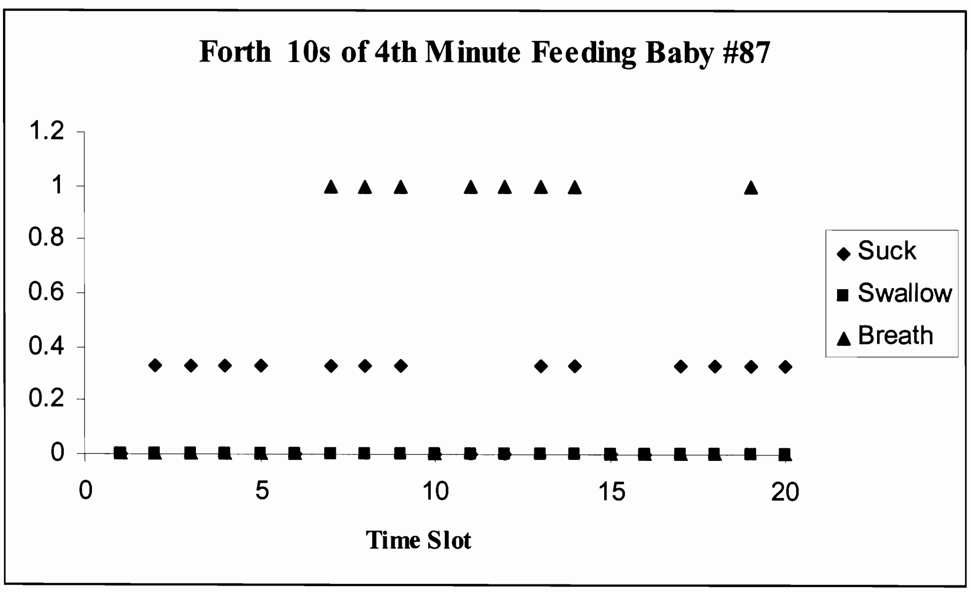

Figure 4.109: The forth minute of baby #87's feeding (t=31 to 40)

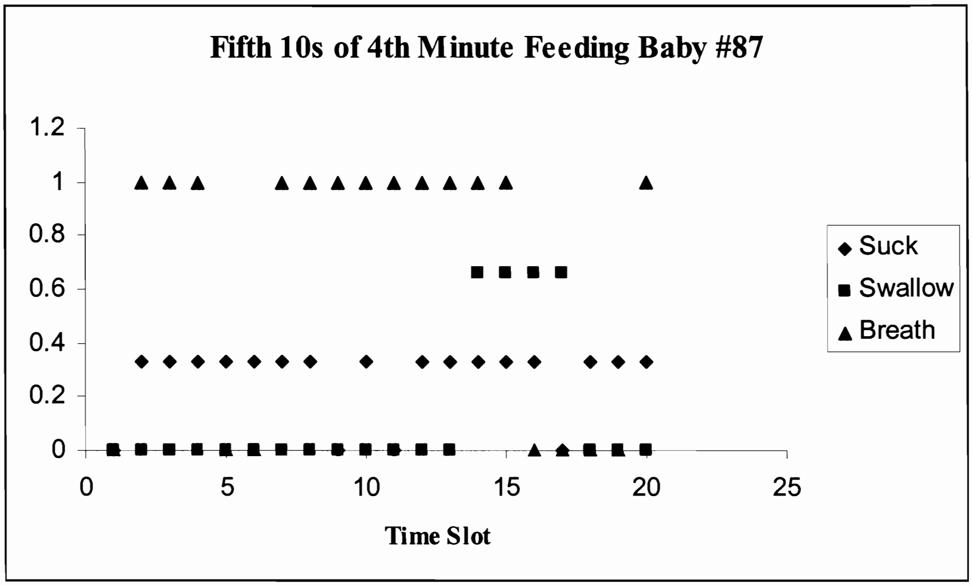

Figure 4.110: The forth minute of baby #87's feeding (t=41 to 50)

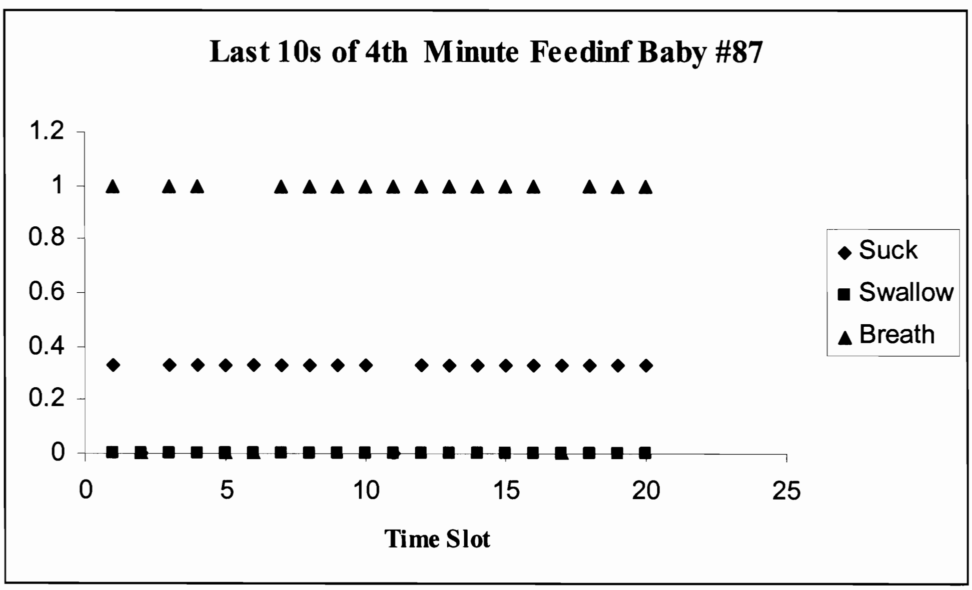

Figure 4.111: The forth minute of baby #87's feeding (t=51 to 60)

<u>The Analysis of the Fifth Minute of Baby # 87's Feeding</u>

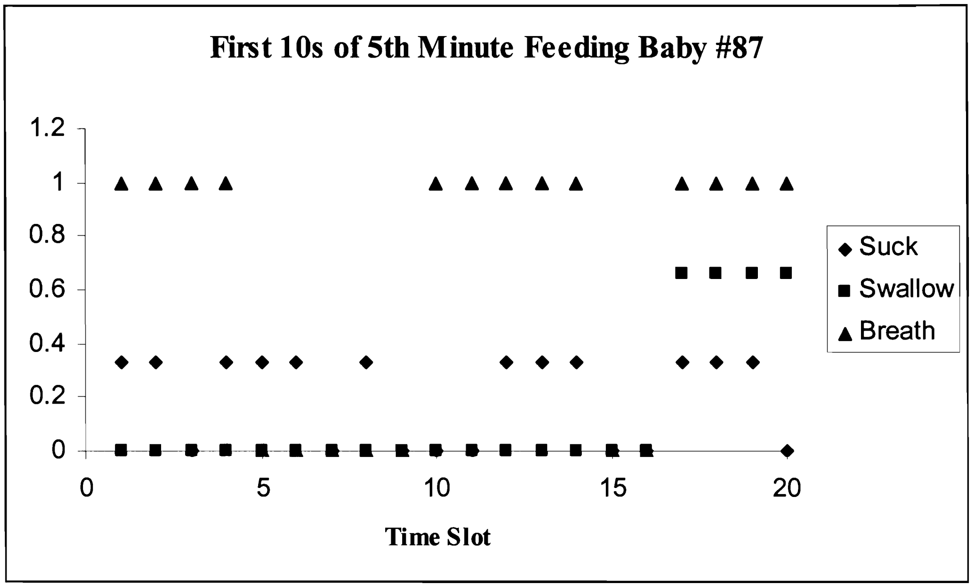

Figure 4.112: The fifth minute of baby #87's feeding (t=1 to 10)

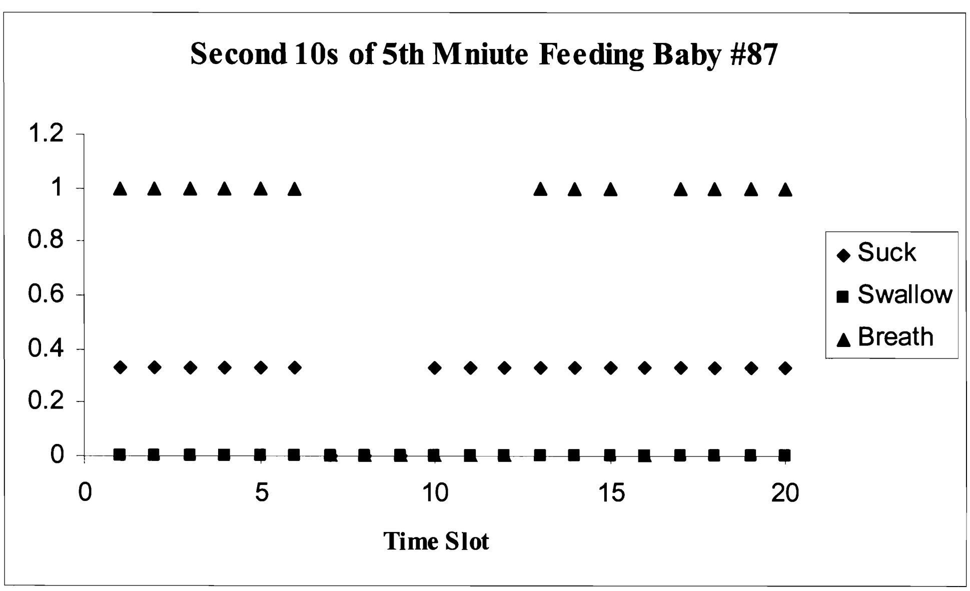

Figure 4.113: The fifth minute of baby #87's feeding (t=11 to 20)

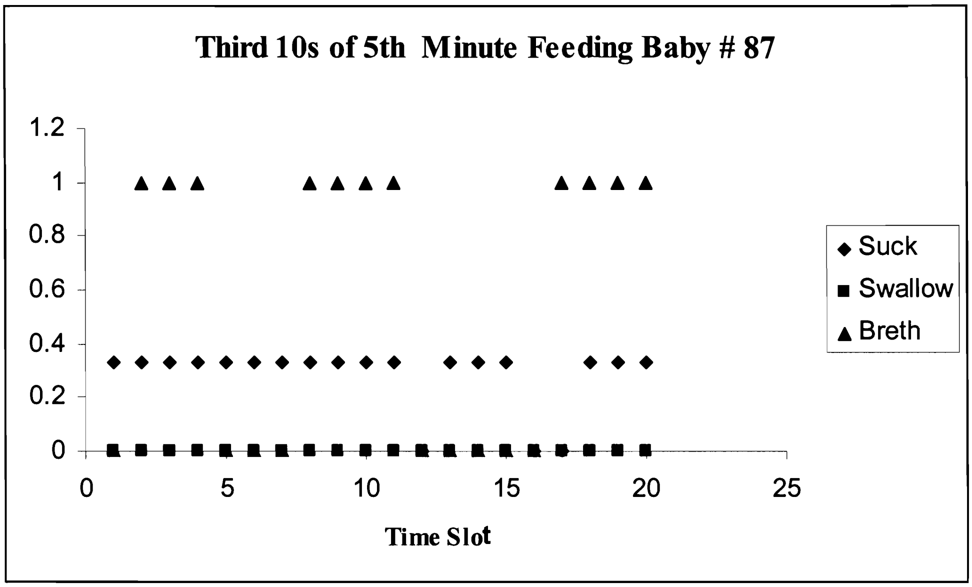

Figure 4.114: The fifth minute of baby #87's feeding (t=21 to 30)

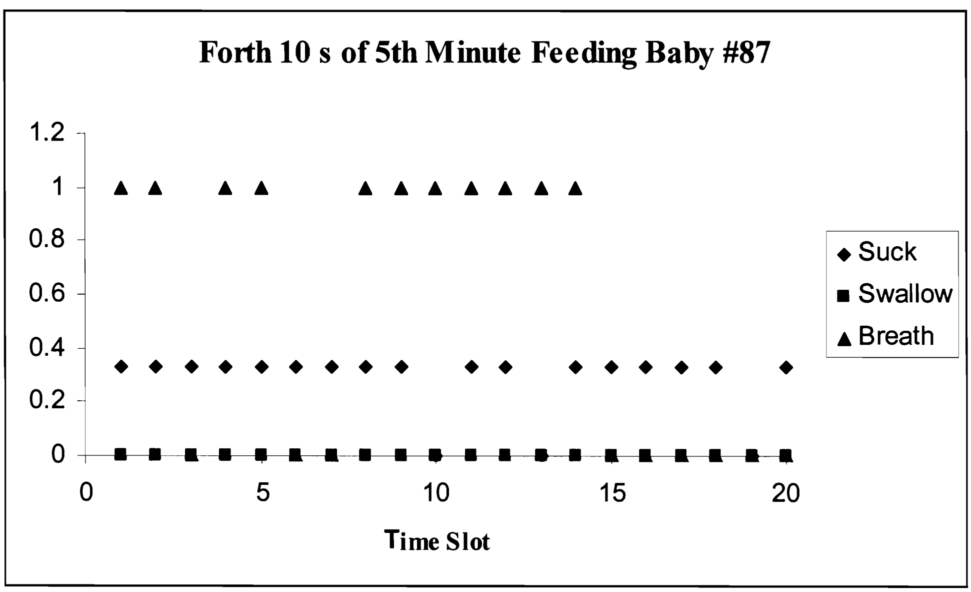

Figure 4.115: The fifth minute of baby #87's feeding (t=31 to 40)

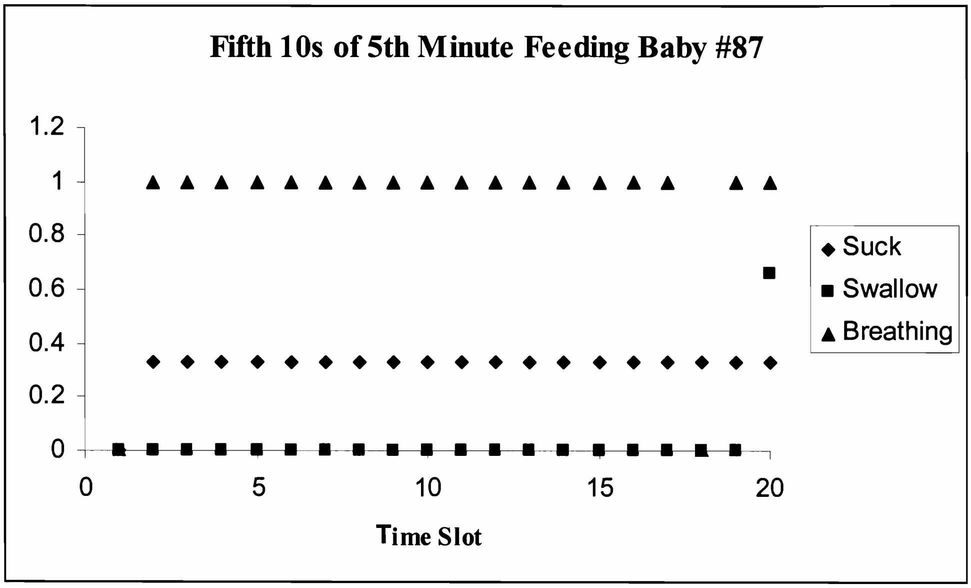

Figure4.116: The fifth minute of baby #87's feeding (t=41 to 50)

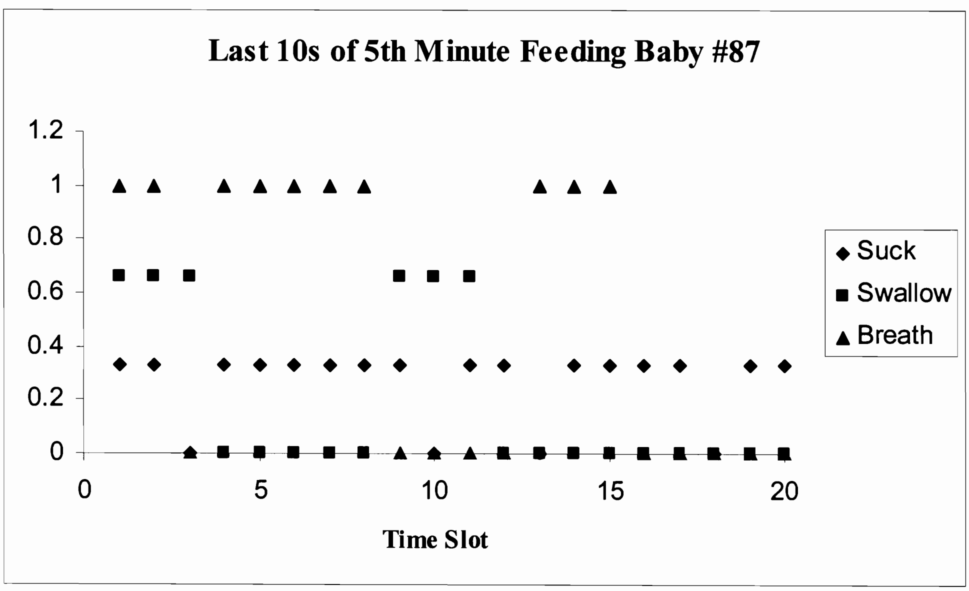

Figure 4.117: The fifth minute of baby #87's feeding (t=51 to 60)

The Analysis of the Sixth Minute of Baby # 87's Feeding

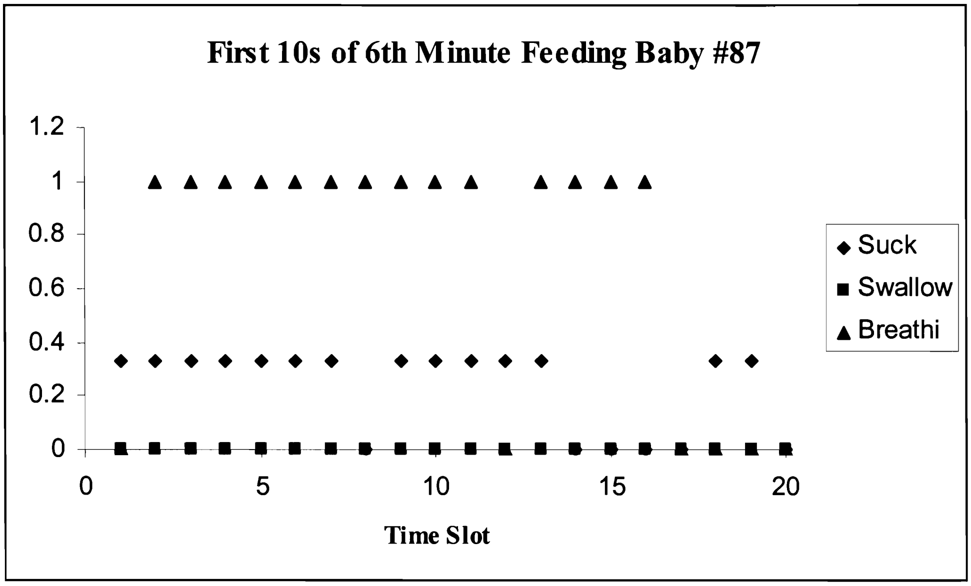

Figure 4.118: The sixth minute of baby #87's feeding (t=1 to 10s)

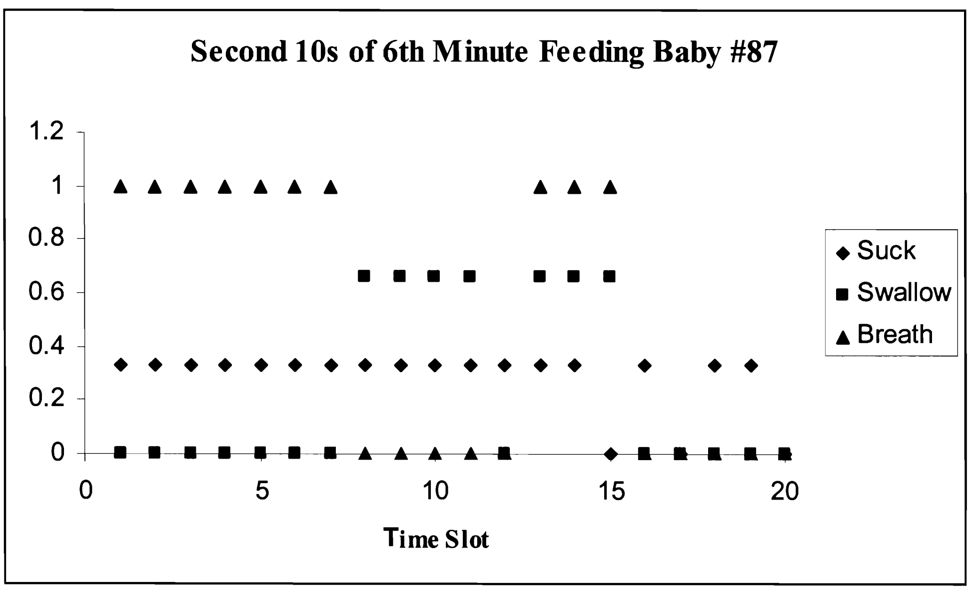

Figure 4.119: The sixth minute of baby #87's feeding (t=11 to 20s)

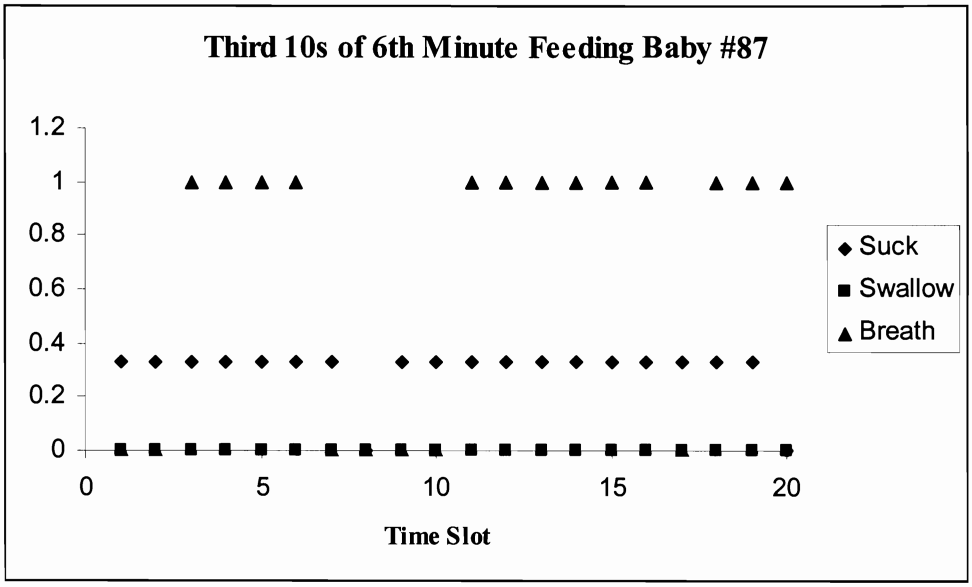

Figure 4.120: The sixth minute of baby #87's feeding (t=21 to 30s)

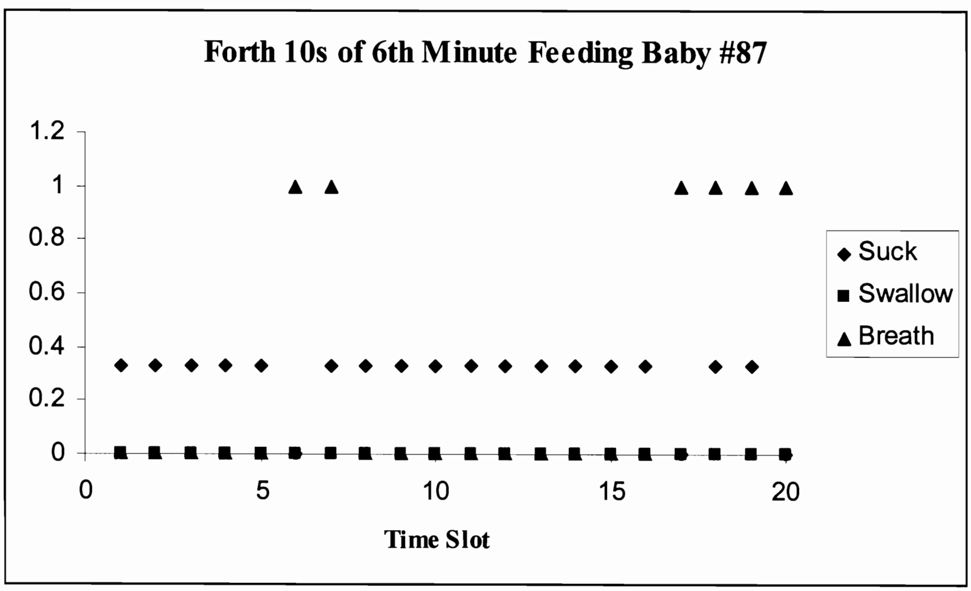

Figure 4.121: The sixth minute of baby #87's feeding (t=31 to 40s)

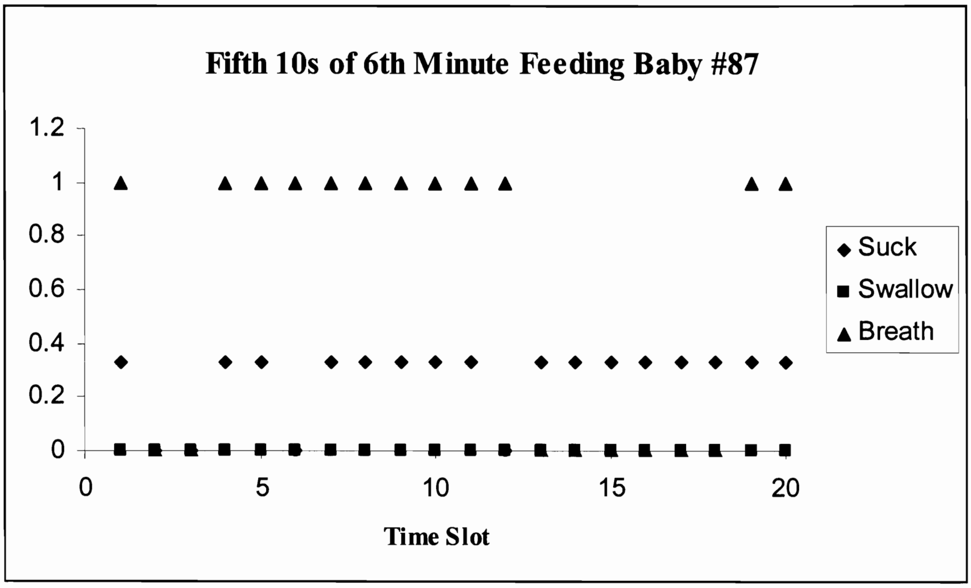

Figure 4.122: The sixth minute of baby #87's feeding (t=41 to 50s)

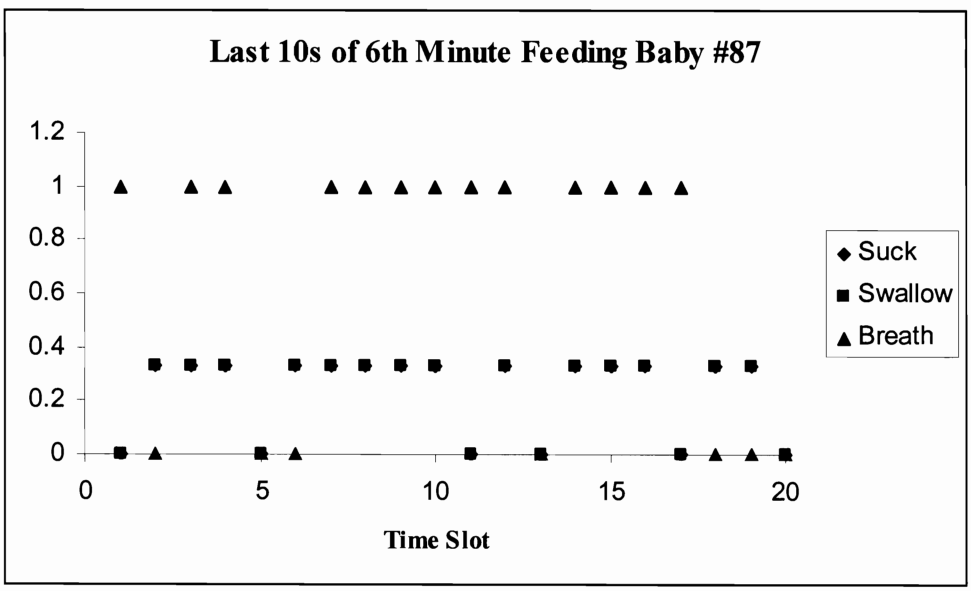

Figure 4.123: The sixth minute of baby #87's feeding (t=51 to 60s)

The Analysis of the Seventh Minute of Baby #87's Feeding

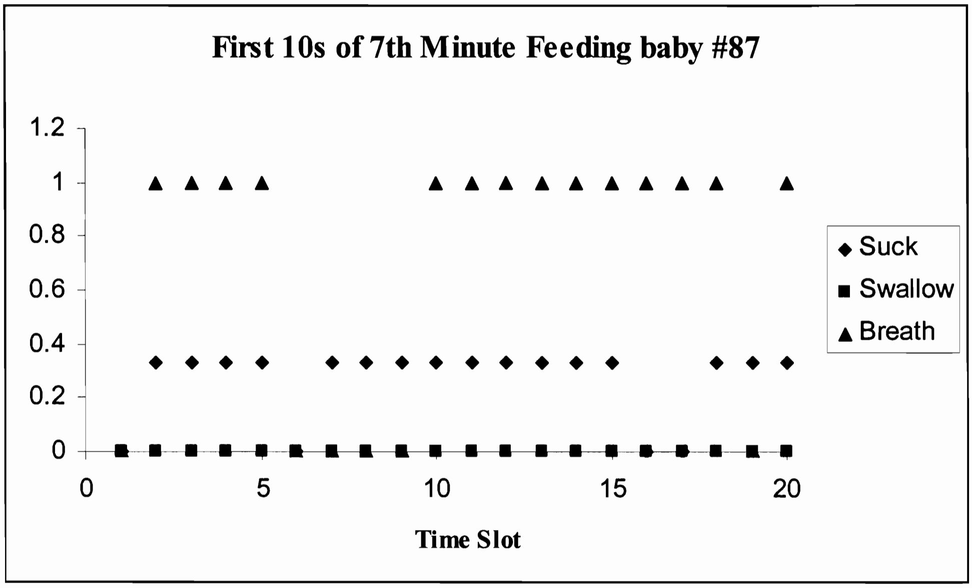

Figure4.124: The seventh minute of baby #87's feeding (t=1 to 10s)

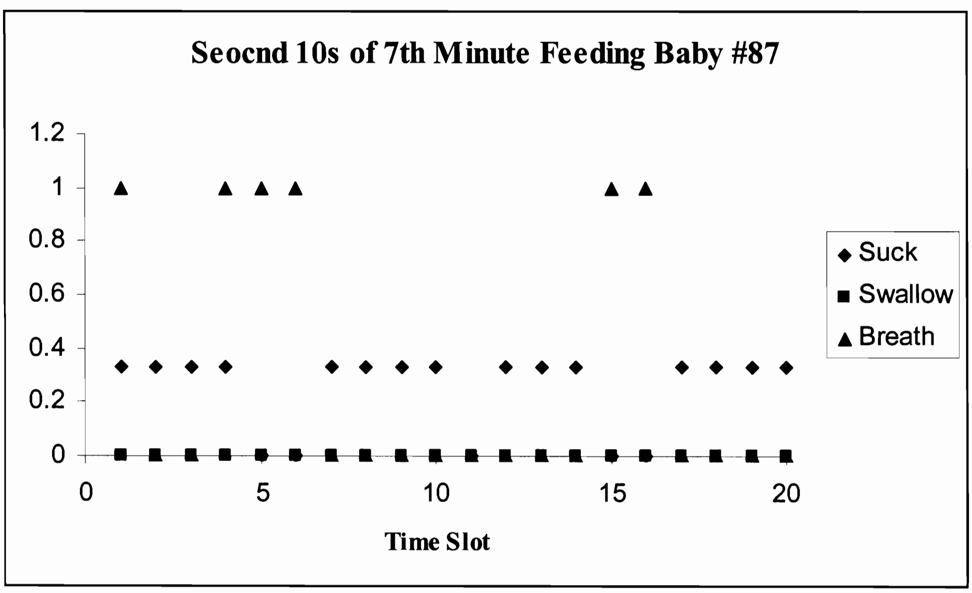

Figure4.125: The seventh minute of baby #87's feeding (t=11 to 20s)

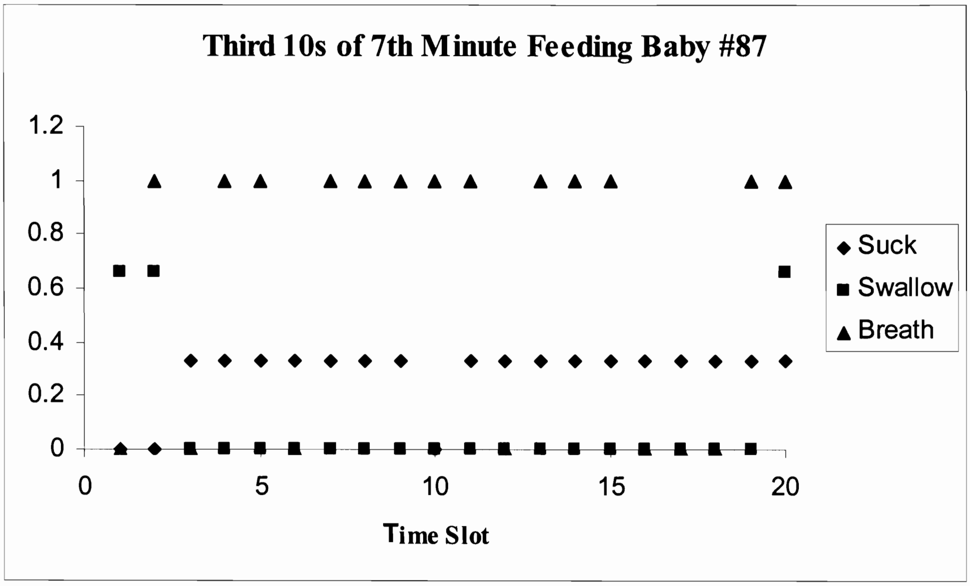

Figure 4.126: The seventh minute of baby #87's feeding (t=21 to 30s)

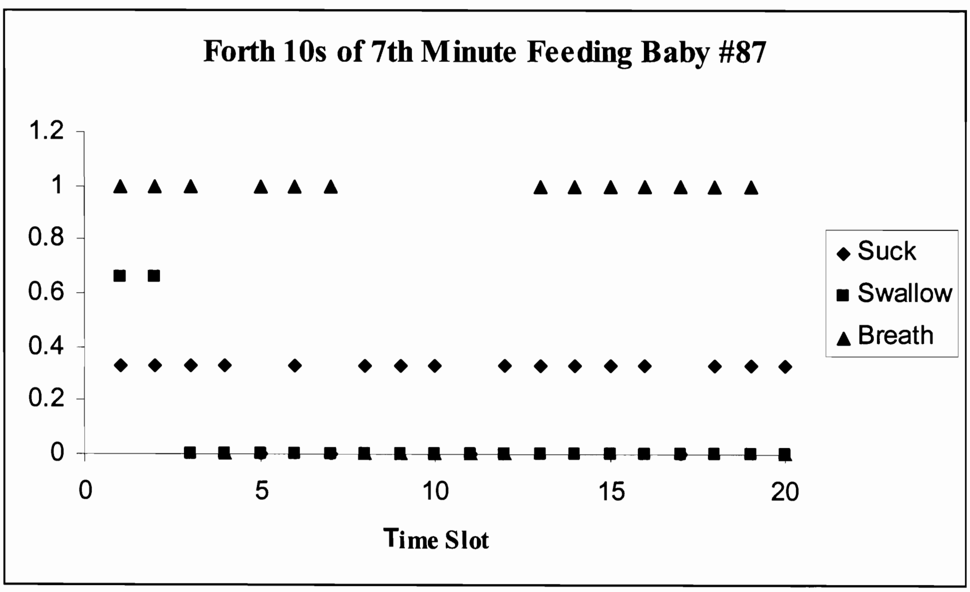

Figure 4.127: The seventh minute of baby #87's feeding (t=31 to 40s)

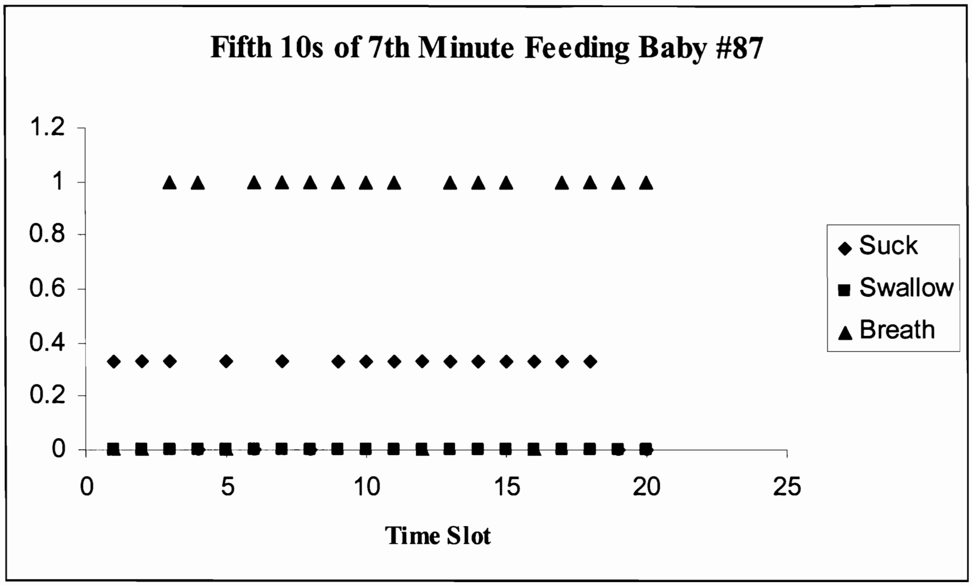

Figure 4.128: The seventh minute of baby #87's feeding (t=41 to 50s)

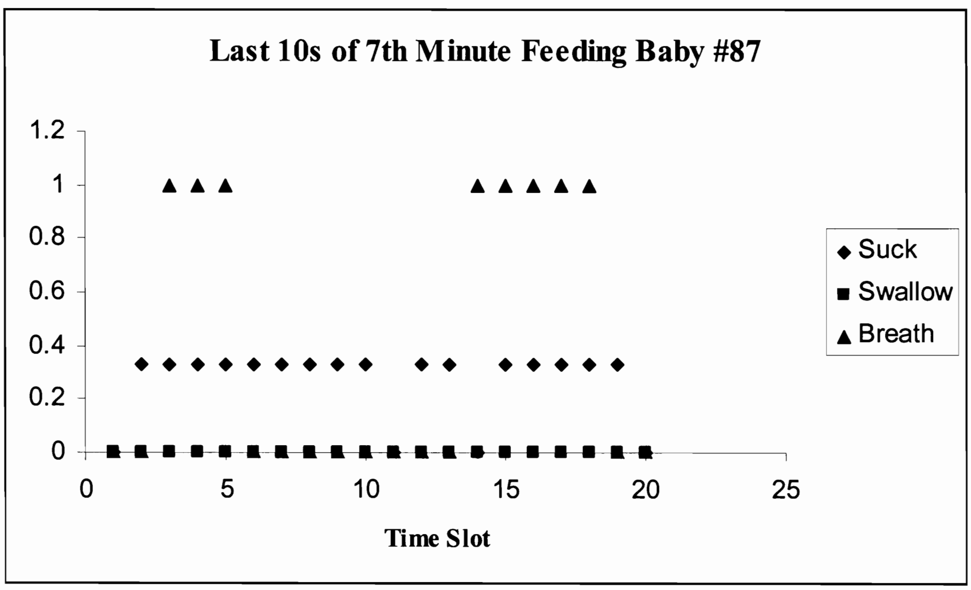

Figure 4.129: The seventh minute of baby #87's feeding (t=51 to 60s)

The Analysis of the 13th Minute of Baby #87's Feeding

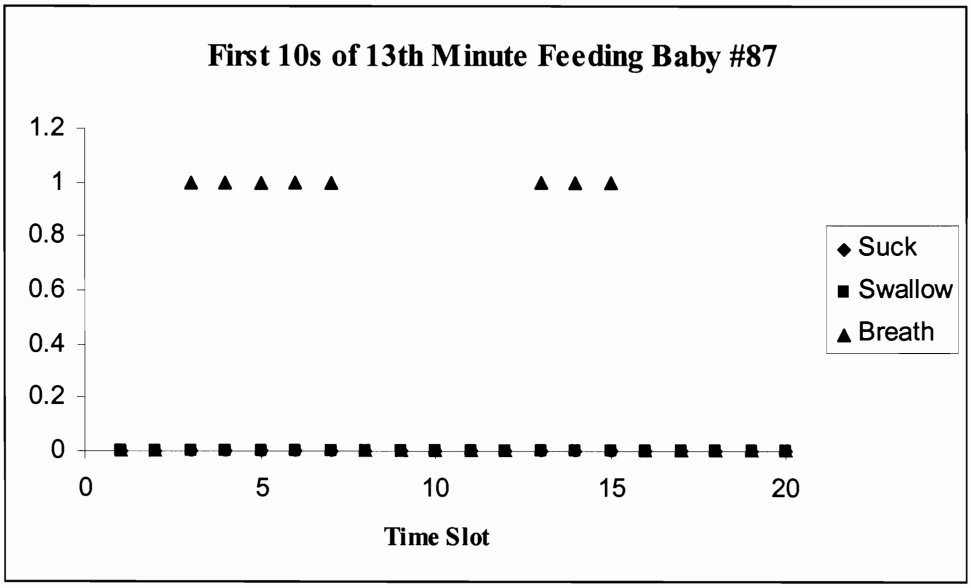

Figure 4.130: The 13th minute of baby #87's feeding (t=1 to 10s)

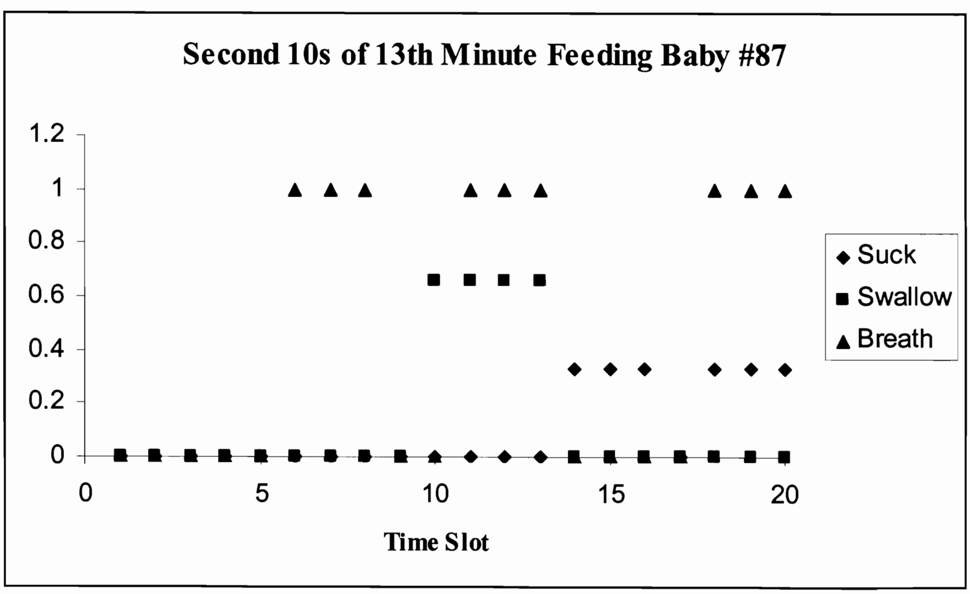

Figure 4.131: The 13th minute of baby #87's feeding (t=11 to 20s)

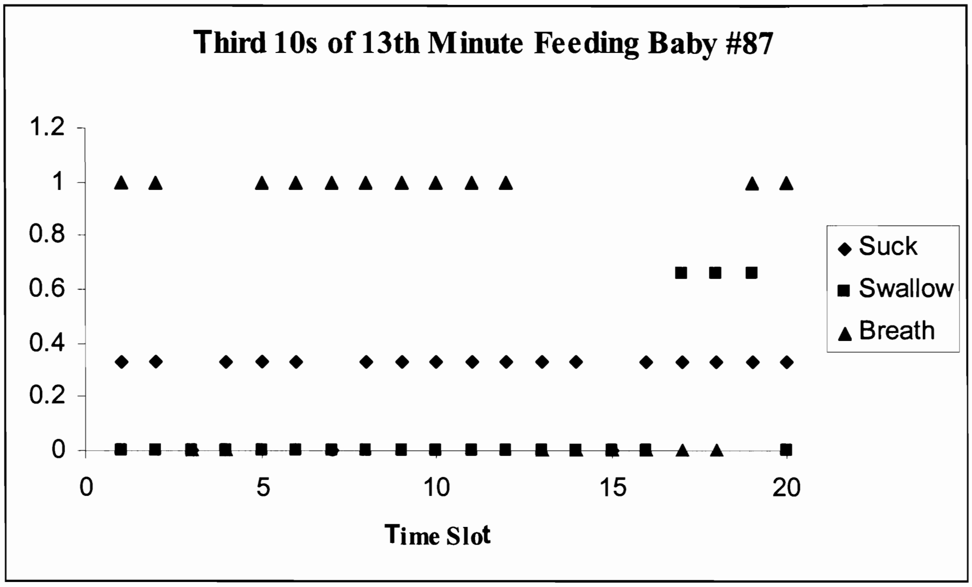

Figure 4.132: The 13th minute of baby #87's feeding (t=21 to 30s)

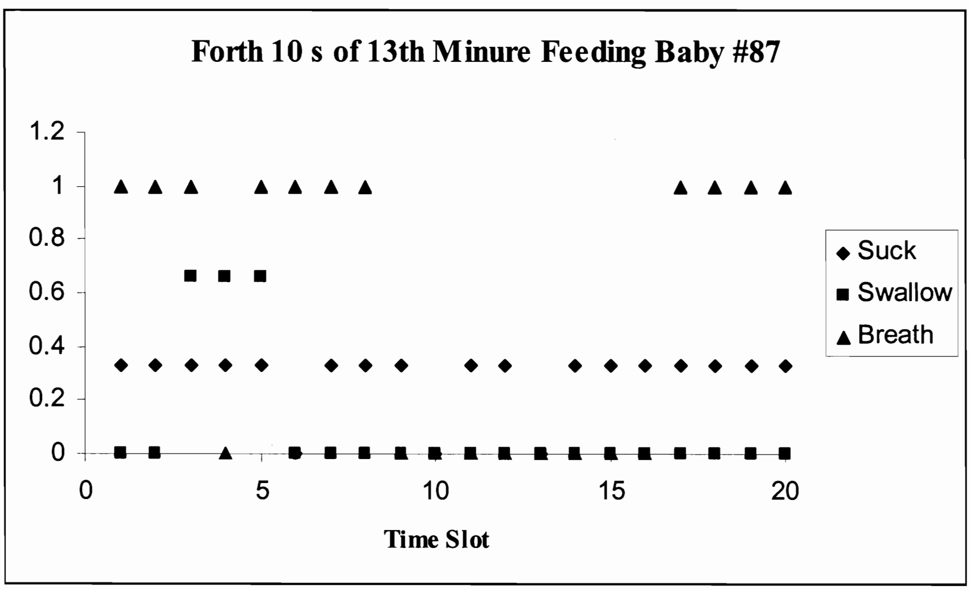

Figure 4.133: The 13th minute of baby #87's feeding (t=31 to 40s)

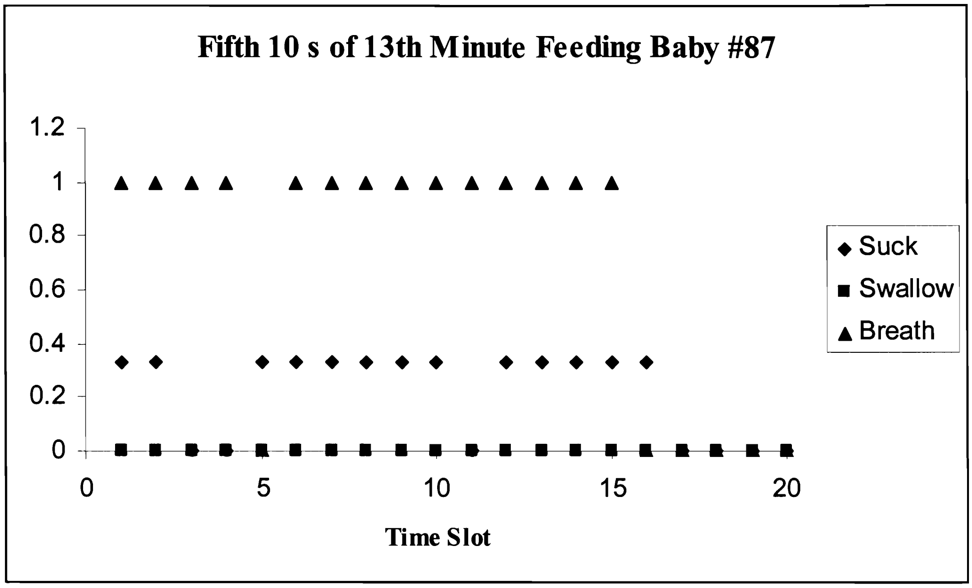

Figure 4.134: The 13th minute of baby #87's feeding (t=41 to 50s)

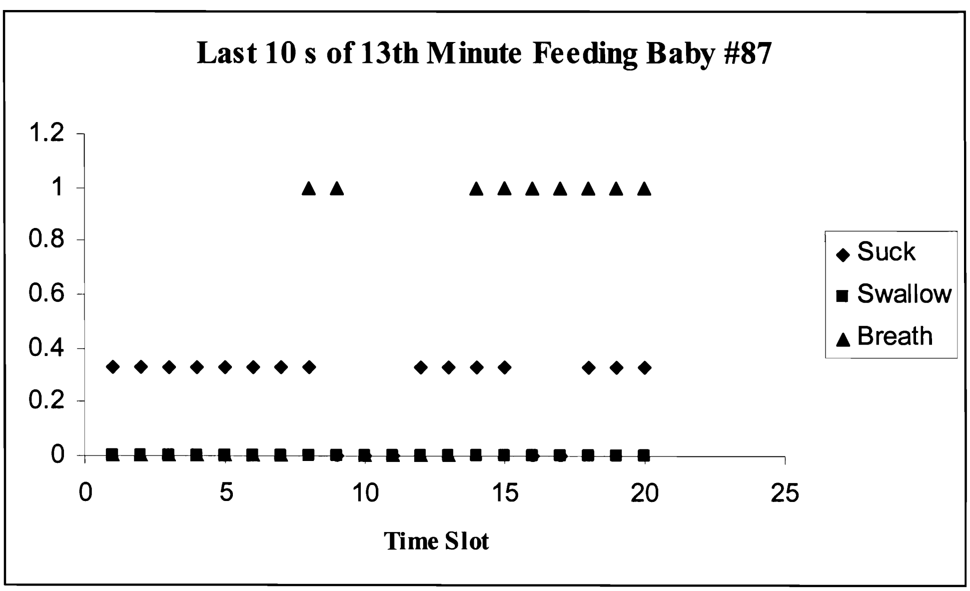

Figure 4.135: The 13th minute of baby #87's feeding (t=51 to 60s)

The Analysis of the 14th Minute of Baby #87's Feeding

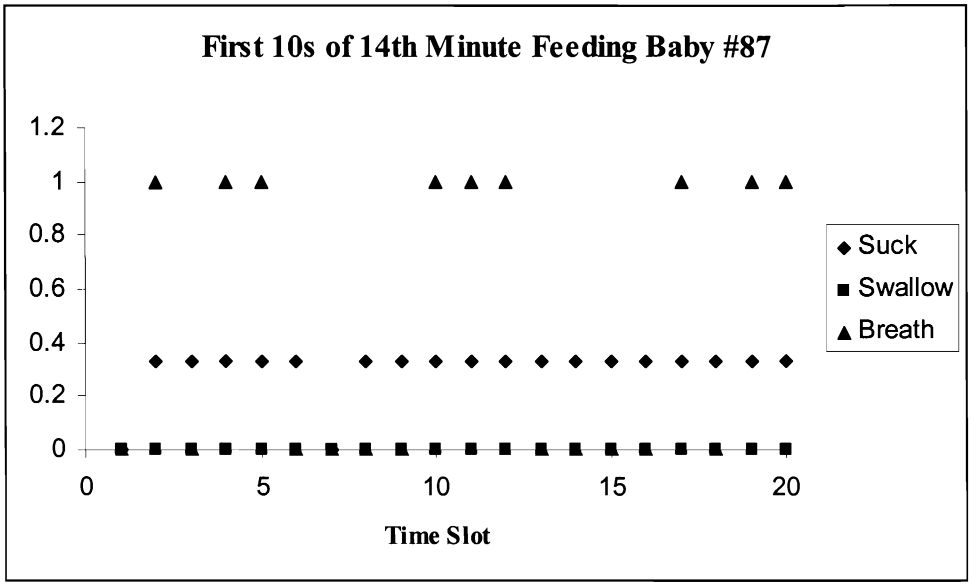

Figure 4.136: The 14th minute of baby #87's feeding (t=1 to 10s)

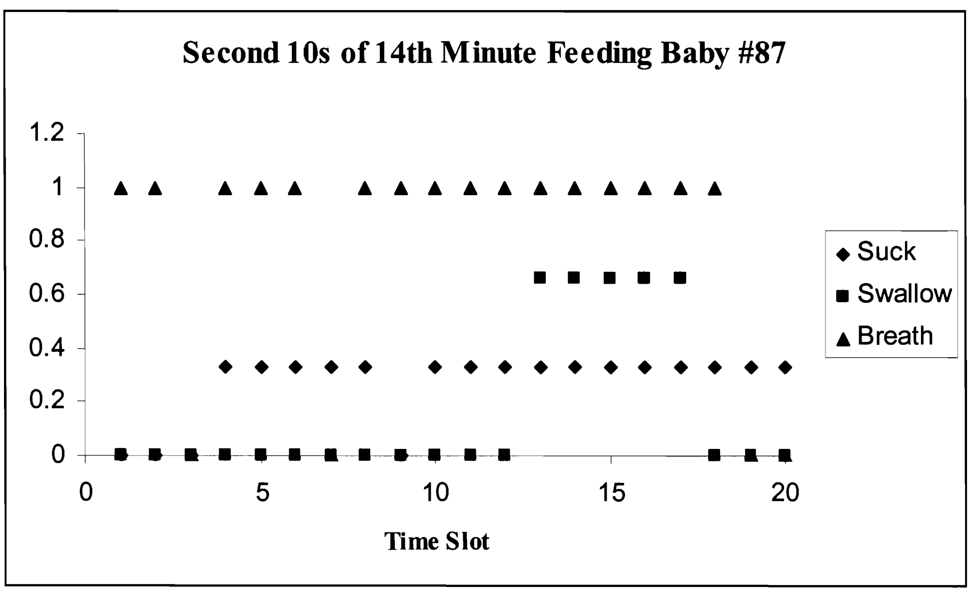

Figure 4.137: The 14th minute of baby #87's feeding (t=11 to 20s)

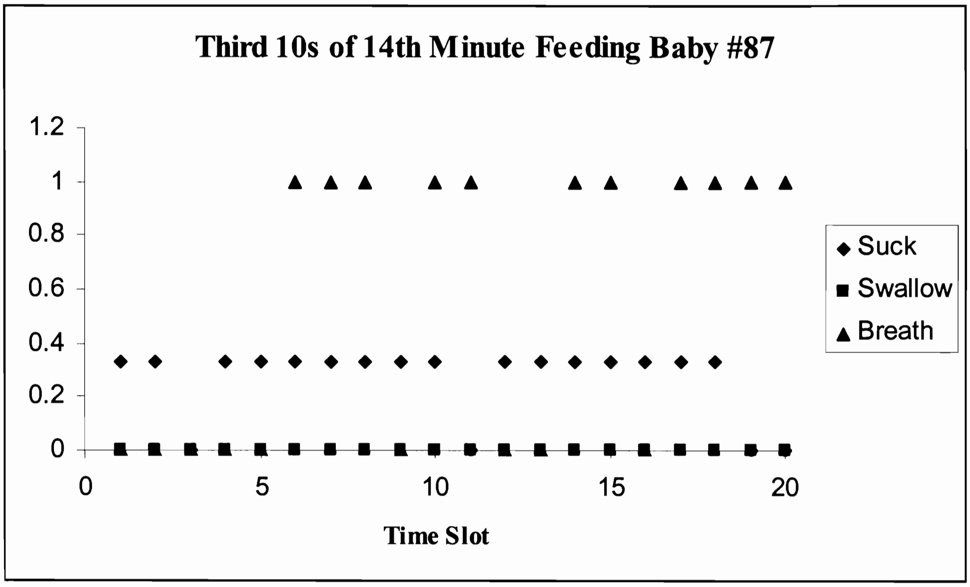

Figure 4.138: The 14th minute of baby #87's feeding (t=21 to 30s)

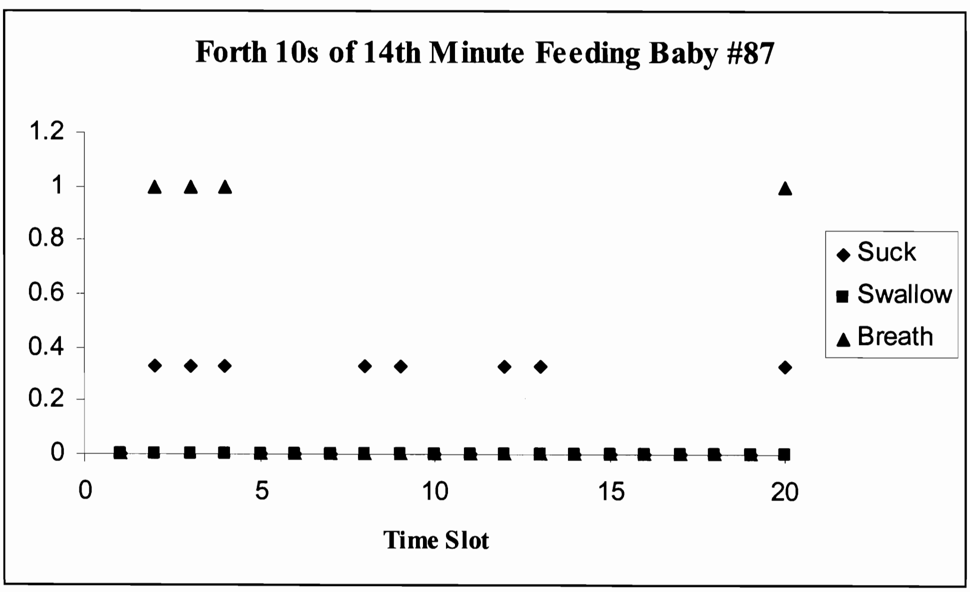

Figure 4.139: The 14th minute of baby #87's feeding (t=31 to 40s)

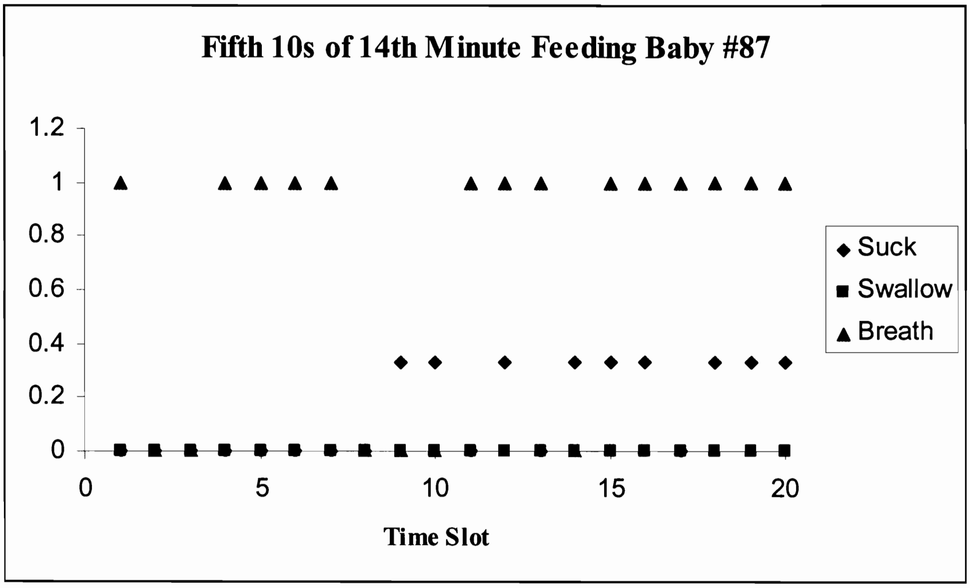

Figure 4.140: The 14th minute of baby #87's feeding (t=41 to 50s)

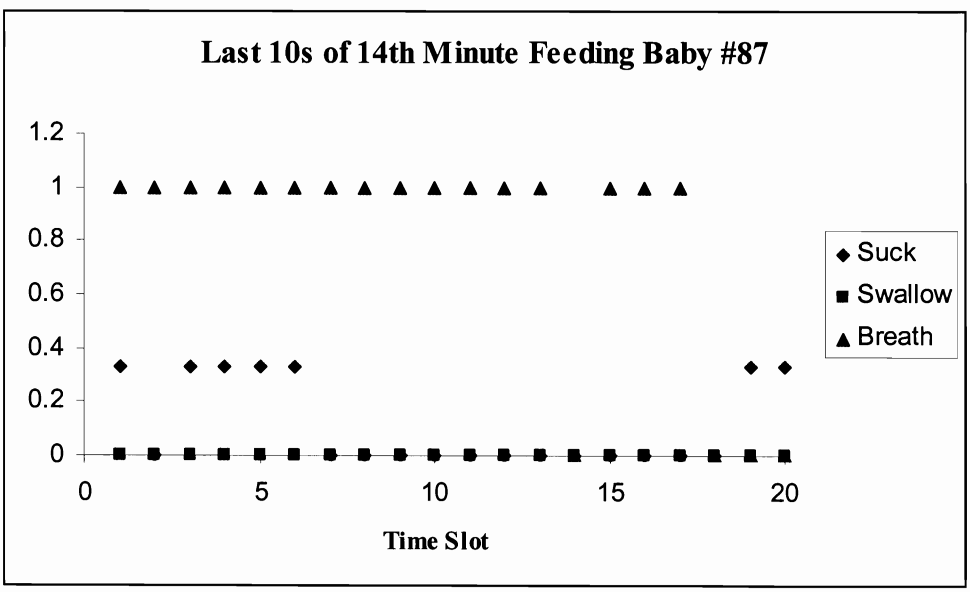

Figure 4.141: The 14th minute of baby #87's feeding (t=51 to 60s)

The Analysis of the Second Minute of Baby #81's

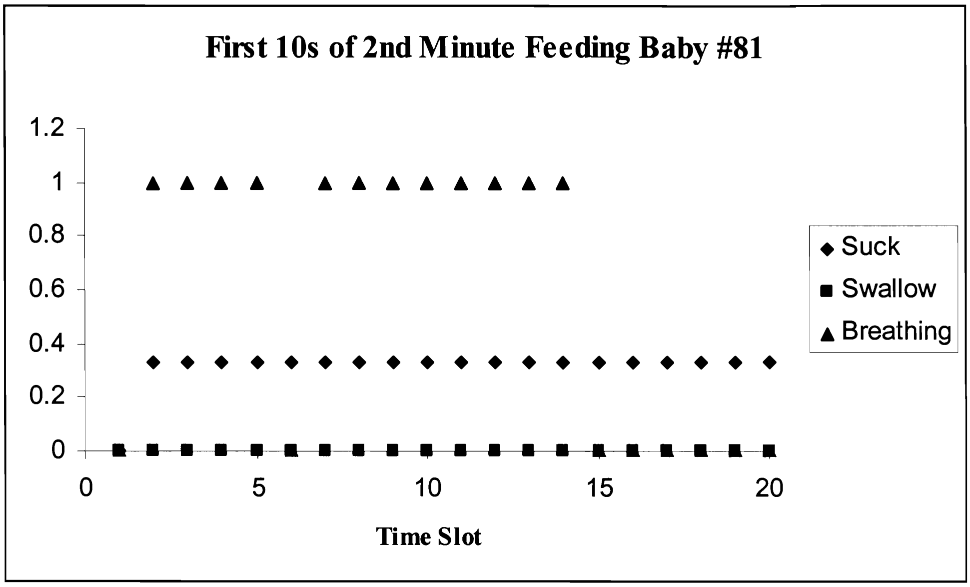

Figure 4.142: The second minute of baby #81's feeding (t=1 to 10s)

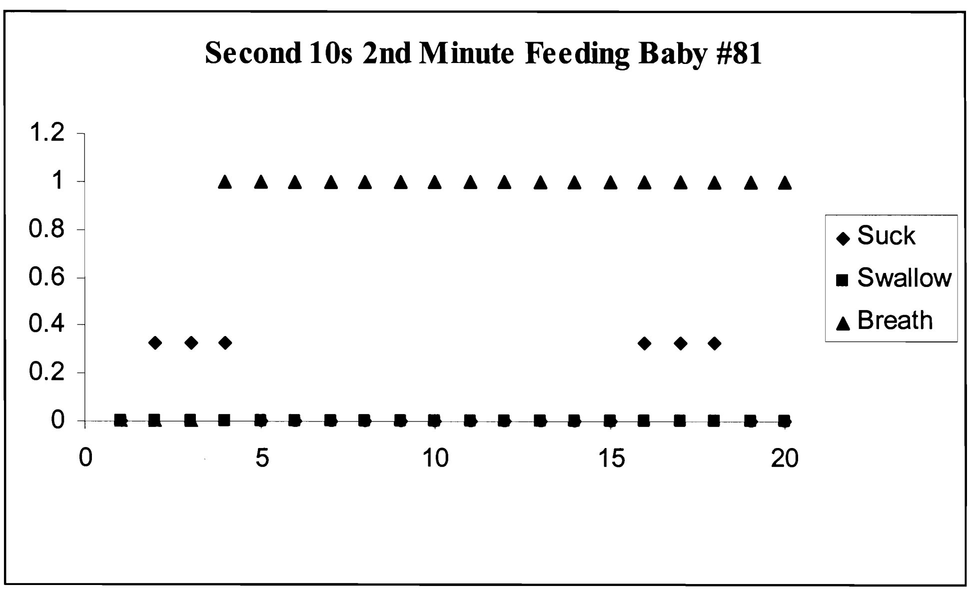

Figure 4.143: The second minute of baby #81's feeding (t=21 to 30s)

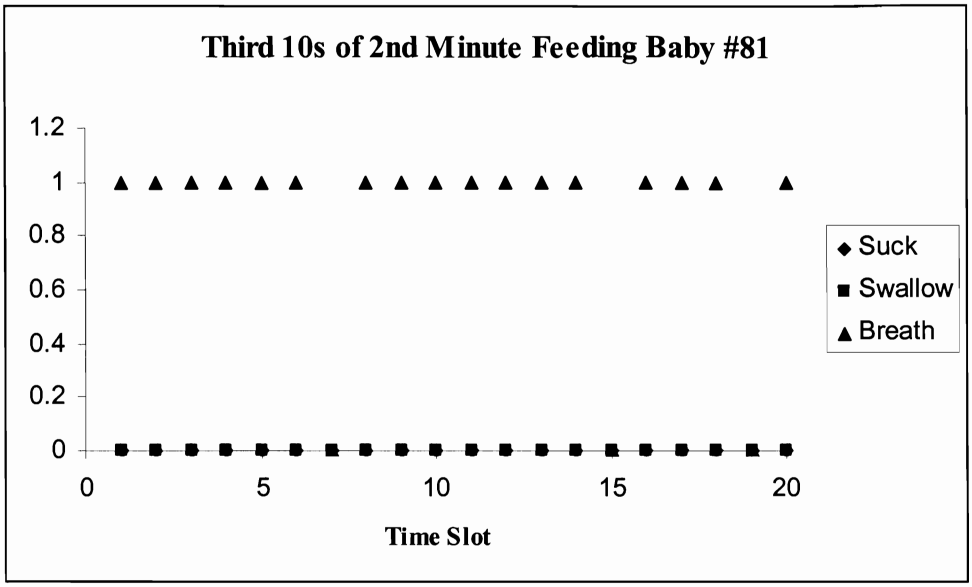

Figure 4.144: The second minute of baby #81's feeding (t=21 to 30s)

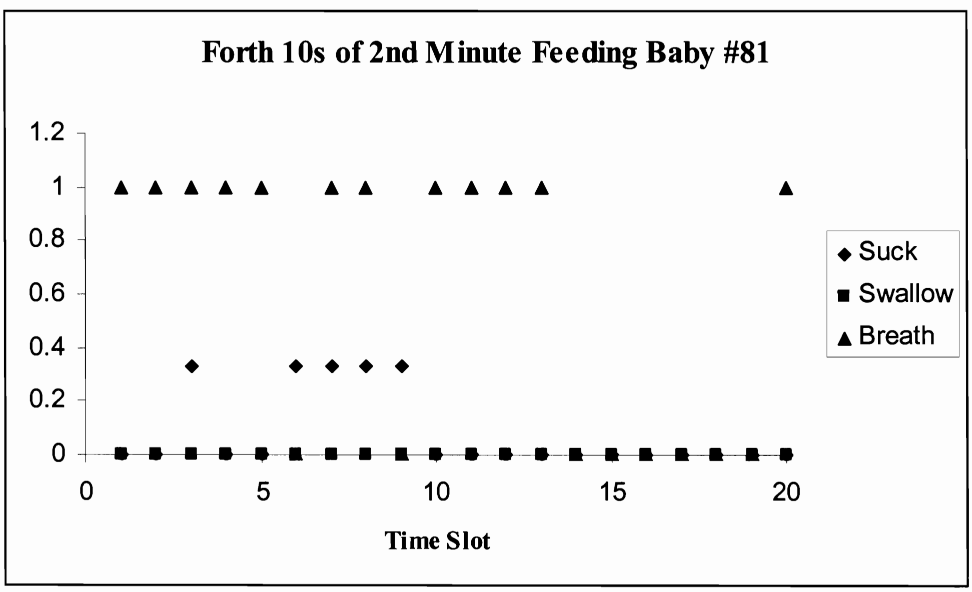

Figure 4.145: The second minute of baby #81's feeding (t=31 to 40s)

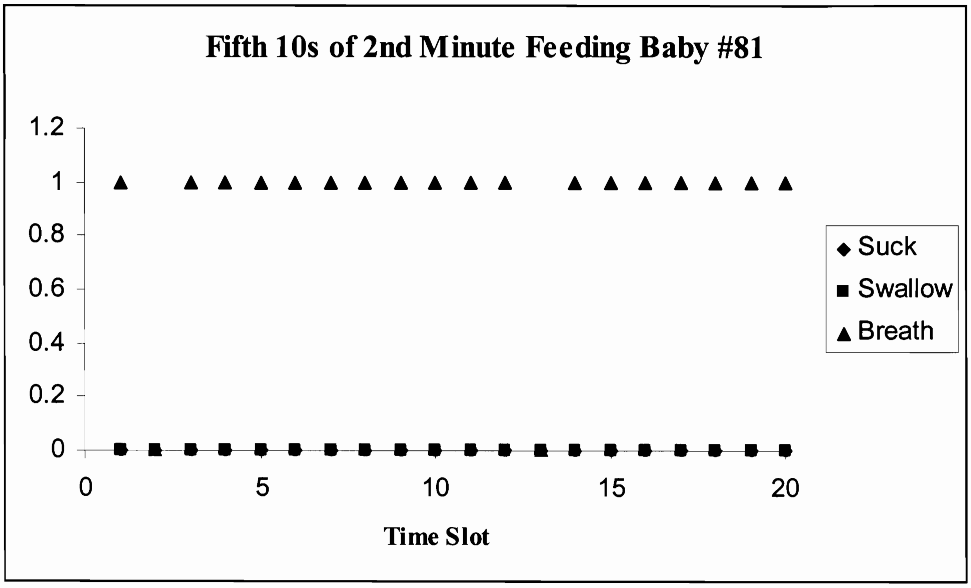

Figure 4.146: The second minute of baby #81's feeding (t=41 to 50s)

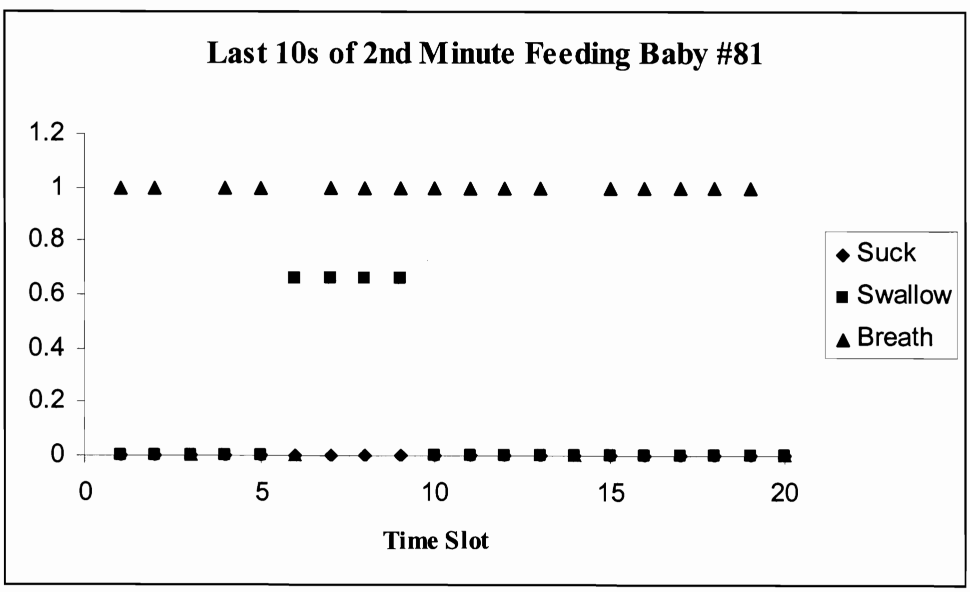

Figure 4.147: The second minute of baby #81's feeding (t=51 to 60s)

The Analysis of the Third Minute of Baby #81's Feeding

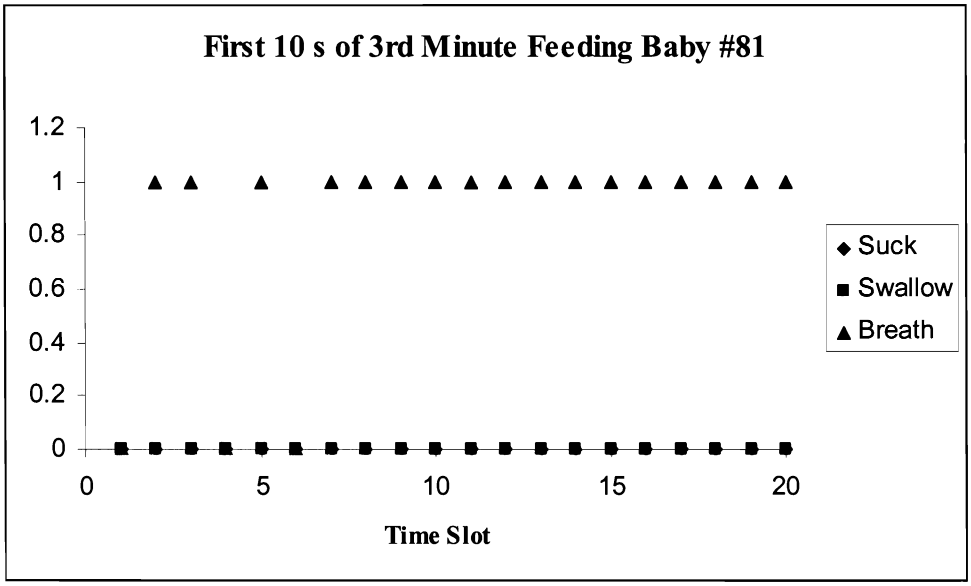

Figure4.148: The third minute of baby #81's feeding (t=1 to 10s)

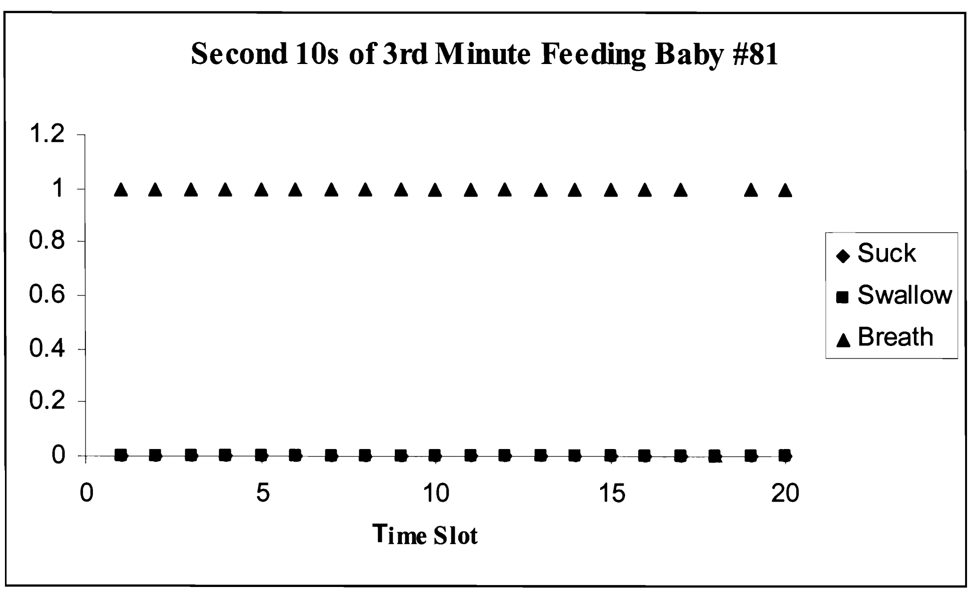

Figure 4.149: The third minute of baby #81's feeding (t=11 to 20s)

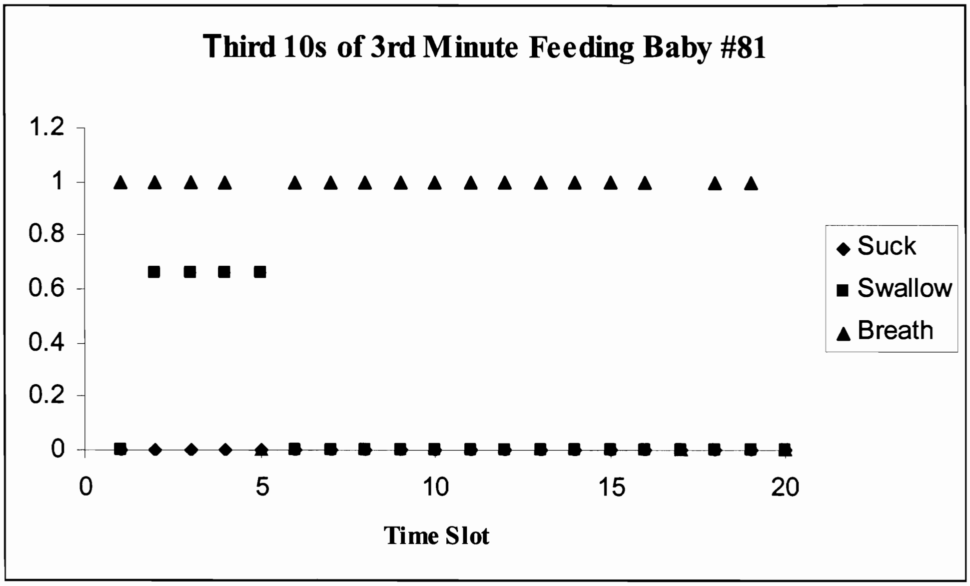

Figure 4.150: The third minute of baby #81's feeding (t=21 to 30s)

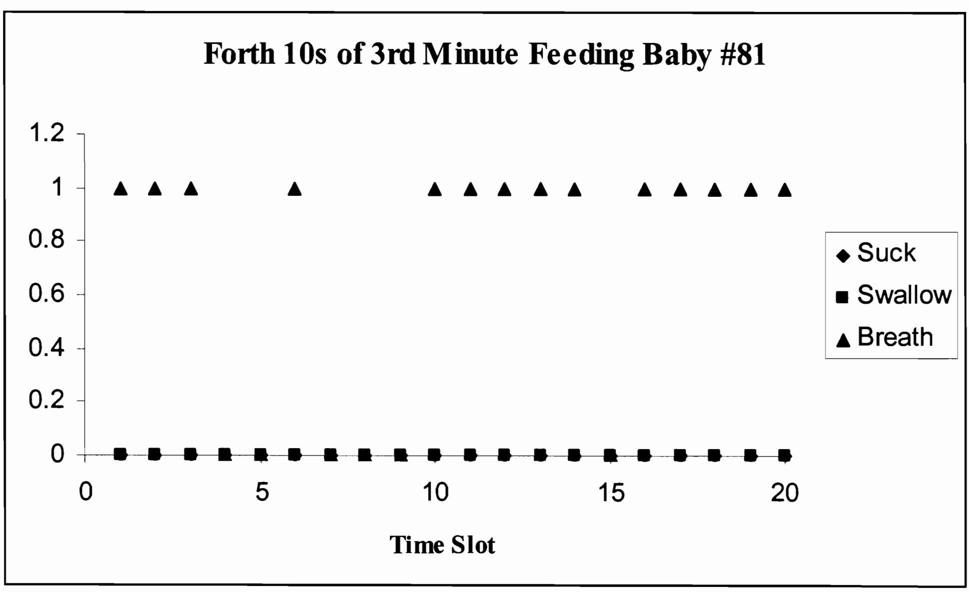

Figure 4.151: The third minute of baby #81's feeding (t=31 to 40s)

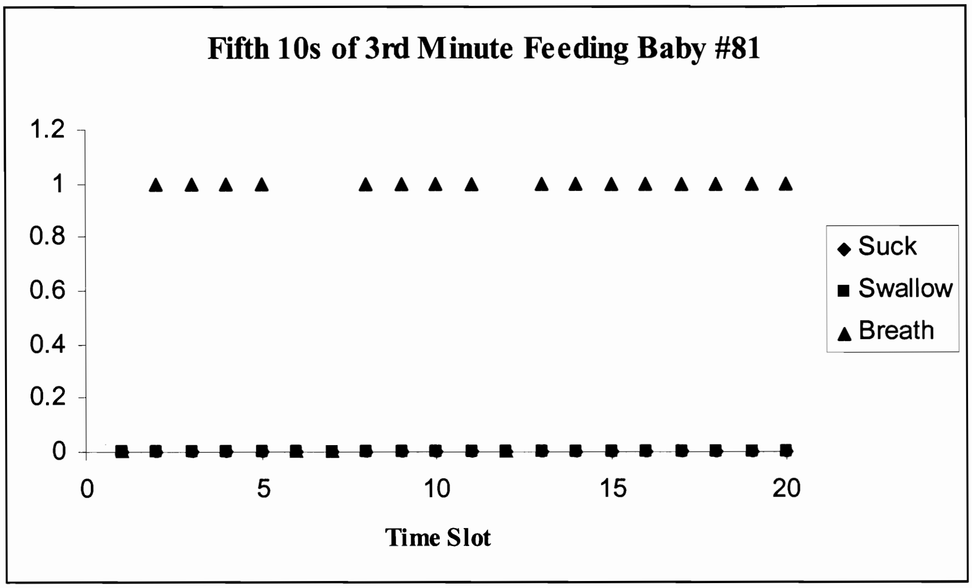

Figure 4.152: The third minute of baby #81's feeding (t=41 to 50s)

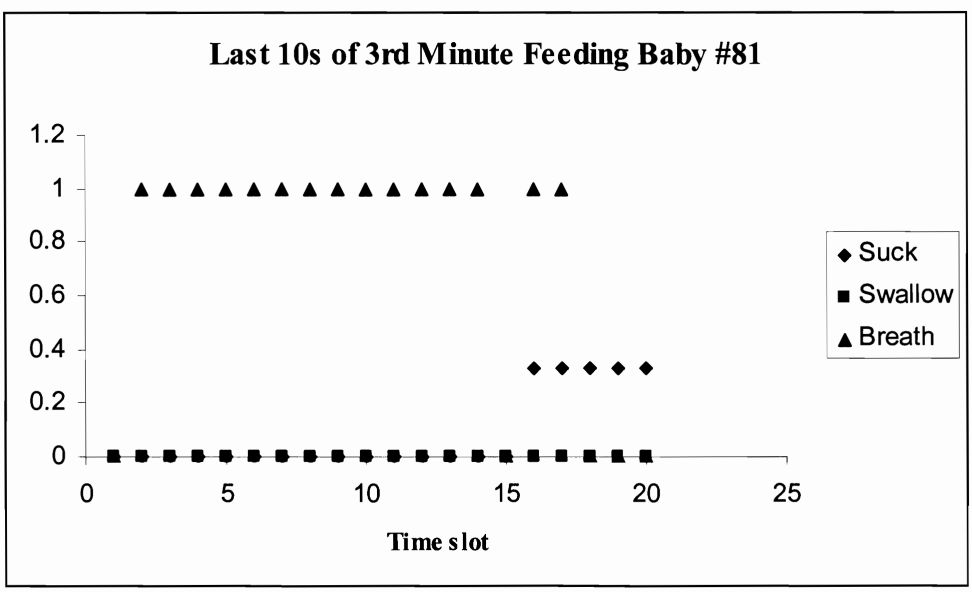

Figure 4.153: The third minute of baby #81's feeding (t=51 to 60s)

The Analysis of the Eighth Minute of Baby #81's Feeding

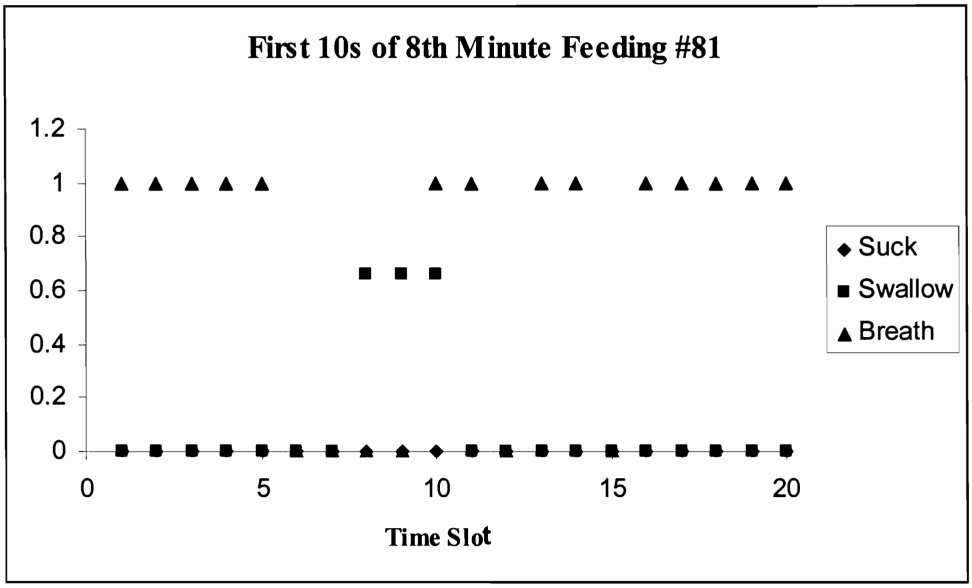

Figure 4.154: The eighth minute of baby #81's feeding (t=1 to 10s)

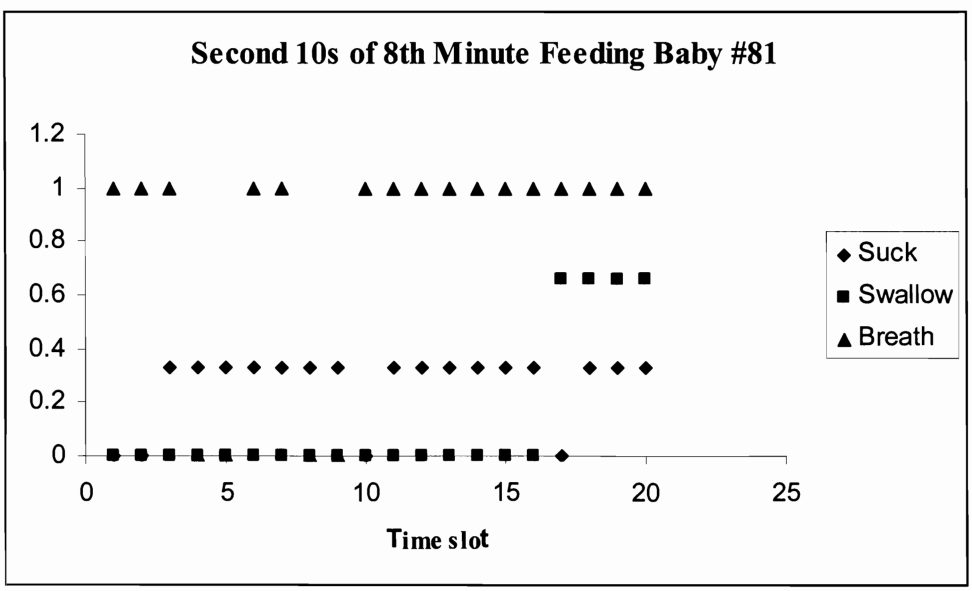

Figure 4.155: The eighth minute of baby #81's feeding (t=11 to 20s)

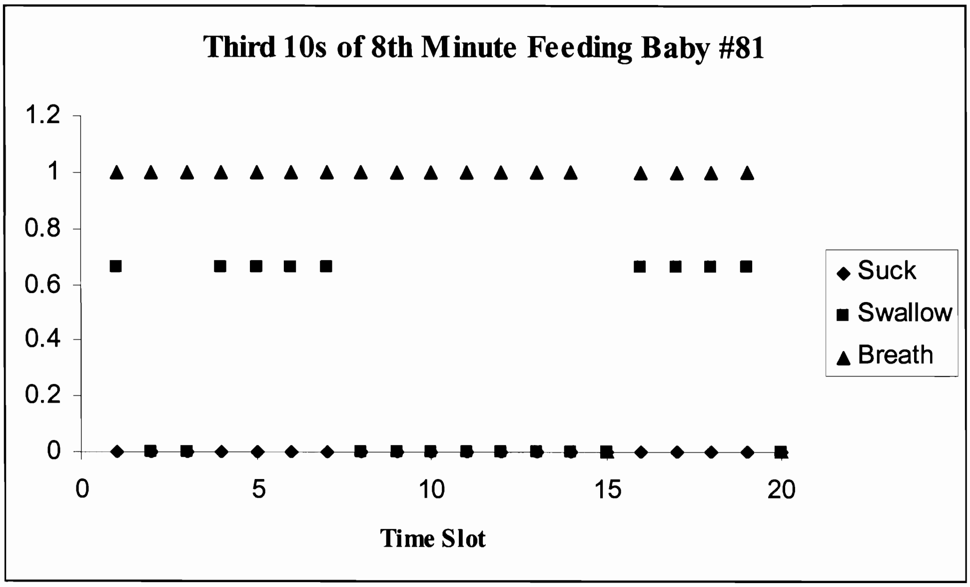

Figure 4.156: The eighth minute of baby #81's feeding (t=21 to 30s)

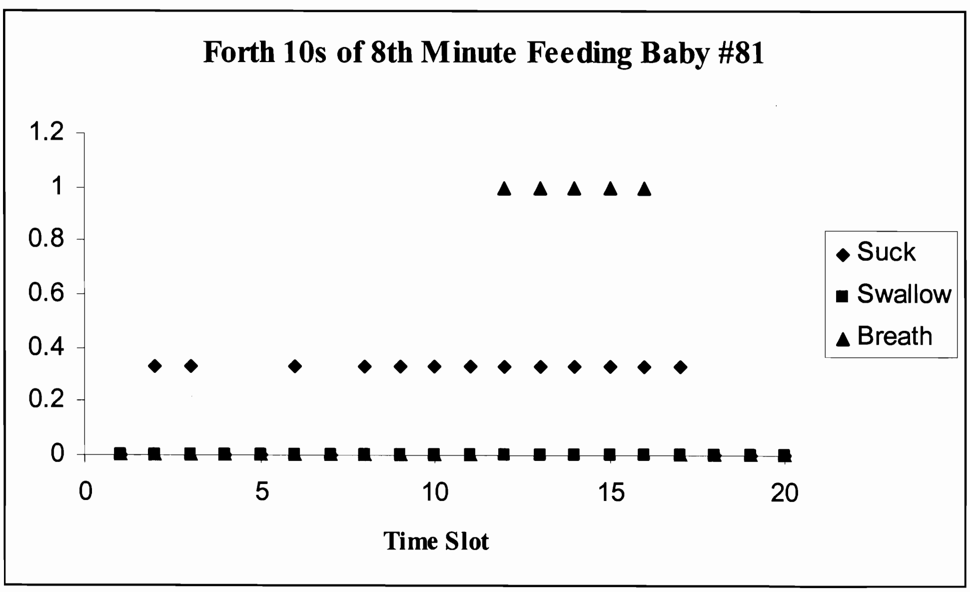

Figure 4.157: The eighth minute of baby #81's feeding (t=31 to 40s)

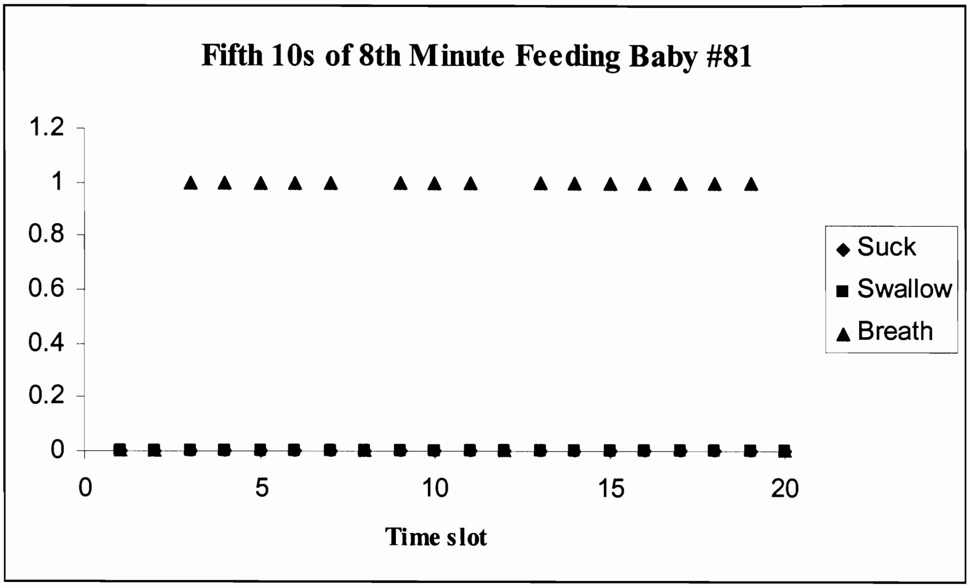

Figure 4.158: The eighth minute of baby #81's feeding (t=41 to 50s)

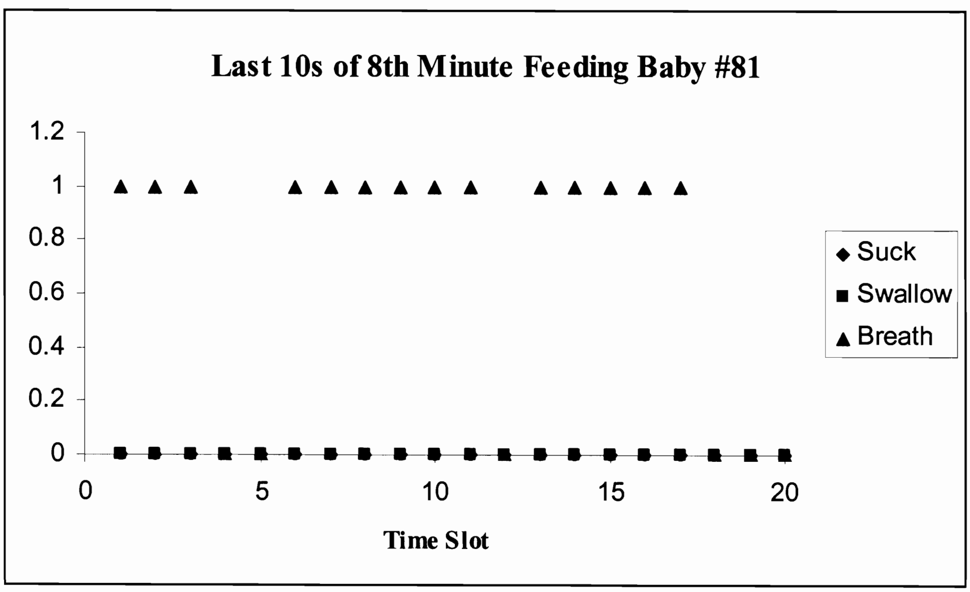

Figure 4.159: The eighth minute of baby #81's feeding (t=51 to 60s)

The Analysis of the Ninth Minute of Baby #81's Feeding

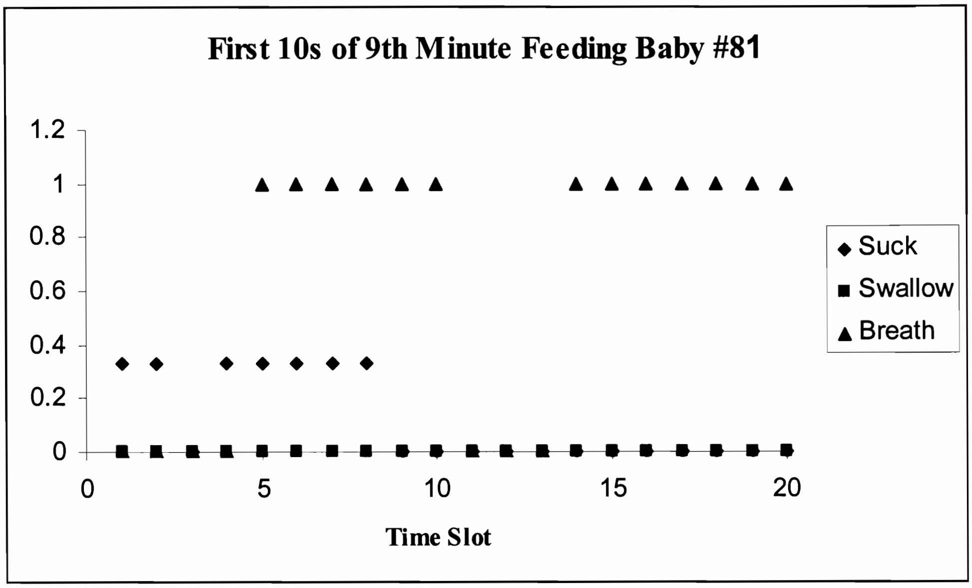

Figure 4.160: The ninth minute of baby #81's feeding (t=1 to 10s)

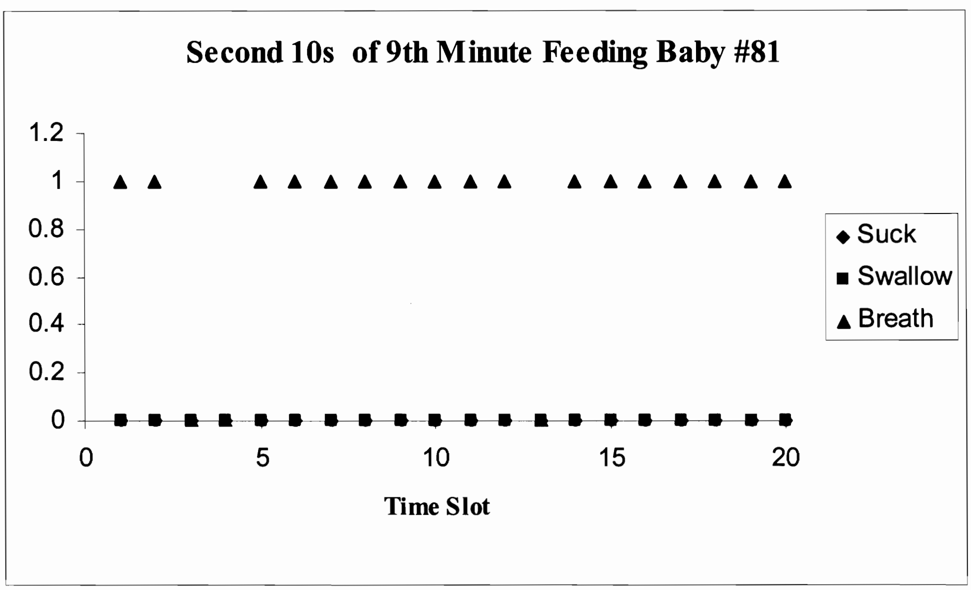

Figure 4.161: The ninth minute of baby #81's feeding (t=11 to 20s)

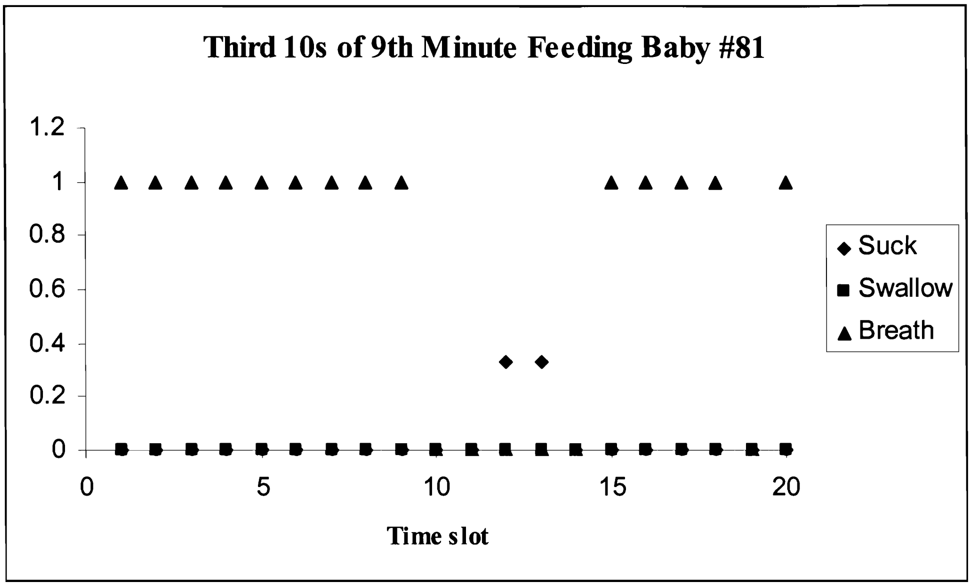

Figure 4.162: The ninth minute of baby #81's feeding (t=21 to 30s)

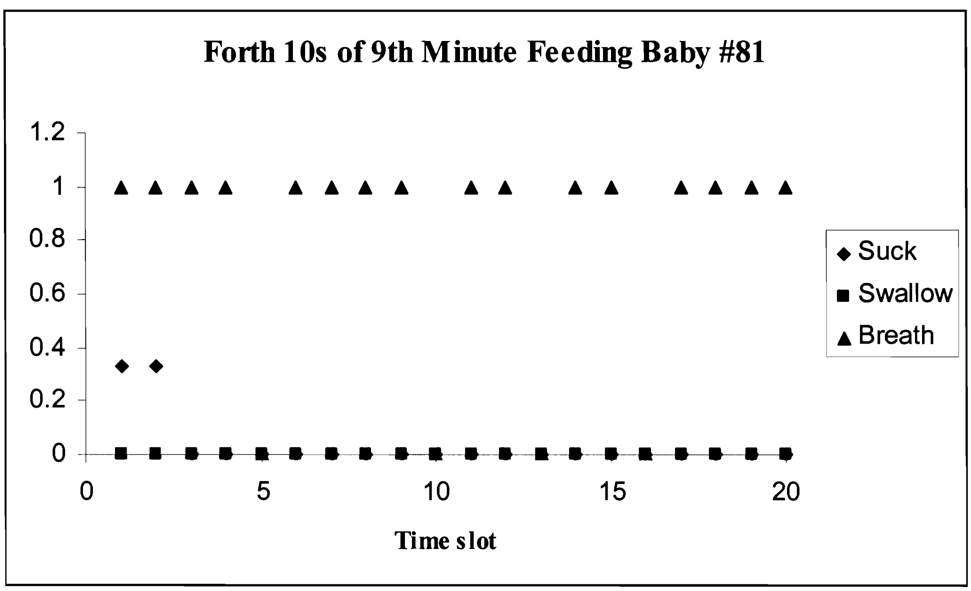

Figure 4.163: The ninth minute of baby #81's feeding (t=31 to 40s)

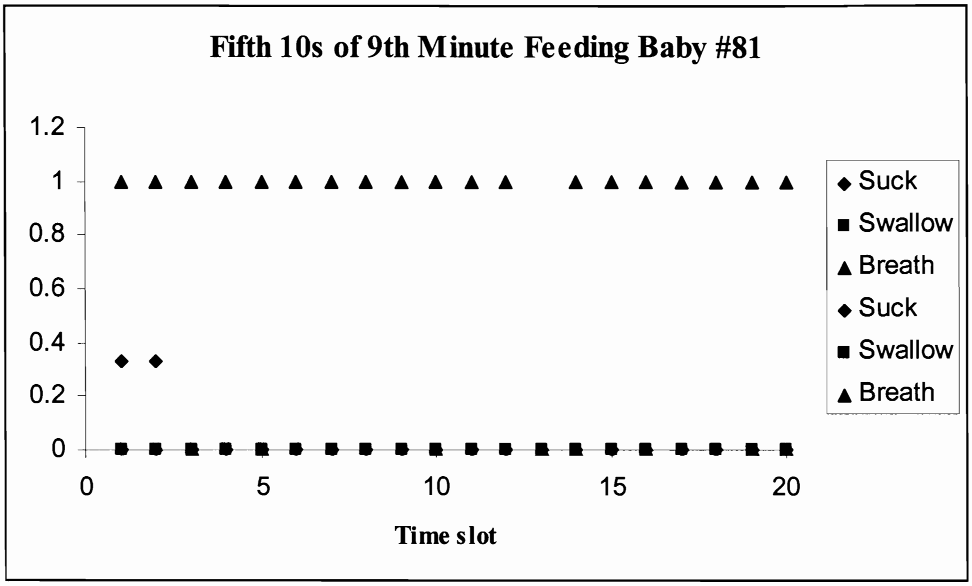

Figure 4.164: The ninth minute of baby #81's feeding (t=41 to 50s)

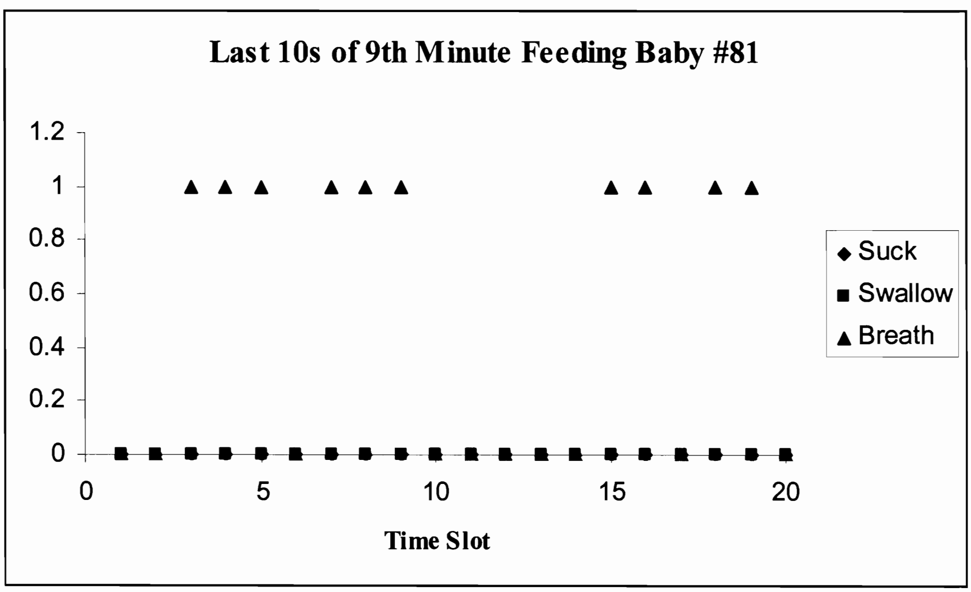

Figure 4.165: The ninth minute of baby #81's feeding (t=51 to 60s)

4.7. Discussion

According to Tables (4.143) and (4.144) (evaluation of signals), this method has satisfactory results for the detection of the breathing signal for both babies (277 agreements vs. 13 disagreements in baby #87 and 418 agreement vs. 29 disagreements in baby #87). This is mainly because the correlation between breathing and non-breathing patterns is very low in breathing waveform. In other words, breathing and non-breathing are dissimilar.

As Tables (4.143) and (4.144) show, for sucking signals, there are 427 agreements vs. 52 disagreements for baby #87 and 77 agreements vs. 21 disagreements for baby #81. The results of the detection of sucking is also reliable but at a lesser degree in comparison with the breathing signal. This is the result of a higher correlation between suck and non-suck signals. Also, there were some cases where non-suck patterns were very similar to the prototype.

According to Tables (4.143) and (4.144) the results for swallowing are not satisfactory (41 agreements vs. 22 disagreements in baby #87 and 18 agreements vs. 17 disagreements for baby #81). This is because in many cases non-swallow patterns are highly correlated with the prototype. As was mentioned earlier, the quality of the swallowing signal was not satisfactory in this study; therefore, there were insufficient number of patterns to develop the prototype for swallowing. Also, in many cases non-swallow patterns were highly correlated with the prototype leading to high error in detection of the swallowing signal. By improving the signal measurement there can be

more candidate patterns available to develop the swallowing prototype and less correlation between non-swallow and prototype.

During segmentation and matched filtering, frames were overlapped with 20 samples. By decreasing the size of overlap, accuracy of the system will improve.
The speed of the system in detection is fairly slow. This is because of the Matlab's slow performance. Although Matlab provides many features for signal processing and designs, its performance is rather slow in some applications. This is mainly because Matlab is interpretative software. By transferring the program from the Matlab environment to other high level languages like C++, the speed of the system can be improved. In addition, the size of overlap between frames can be minimized leading to a more accurate result.

In the current system, there are several cases during matched filtering where the suck, swallow or breath pattern in the current frame was not correlated with the prototype. This may be the result of inaccurate development of the prototype. As was mentioned previously, 55 patterns (for baby #87) and 23 patterns (for baby #81) were used to develop the prototype for the breathing and sucking signals. However, the performance of the system could be improved by defining a class of prototypes instead of just one prototype providing the opportunity to compare the current frame with several templates. As such, during matched filtering, the correlation of the current frame would be assessed with a class of prototypes instead of one prototype.

In the current system, it was necessary to define a prototype for each baby independently. This is mainly because the form of sucking, swallowing and breathing

patterns of one baby differs from another. Also, the shape of sucking, swallowing and breathing of a baby changes over time and feeding as the baby grows. As a result, it is necessary to develop a whole new prototype for that baby. Therefore, by developing a class of prototypes and updating this set as the baby grows can solve this problem.

According to the results of the analysis of the relationships between suck, swallow and breathing signals of baby #81 and baby #87 (Figures (4.100) to (4.165)), there were several incidents when these babies attempted to swallow and breath at the same time. These incidents are summarized in Tables (4.145) and (4.146).

Table4.145: Simultaneous swallow and breath in Baby #81

Minute #	Second (s)	Incident	Duration(ms)
2nd	53	Simultaneous swallow and breath	1500
3rd	20.5	Simultaneous swallow and breath	1500
8th	0.5	Simultaneous swallow and breath	500
8th	18.5	Simultaneous swallow and breath	500
8th	19	Simultaneous suck, swallow and breath	1500
8th	20.5	Simultaneous swallow and breath	500
8th	28	Simultaneous swallow and breath	2000

According to Table (4.145) and Table (4.146), baby # 81 had seven incidents of simultaneous swallow and breath over two minutes of feeding while baby # 87 has 19 incidents of simultaneous swallow and breath over seven minutes feeding.

Table (4.146): Simultaneous swallow and breath in Baby #87

Minute #	Second (s)	Incident	Duration(ms)
3rd	6.5	Simultaneous suck, swallow and breath	1000
3rd	13	Simultaneous swallow and breath	1500
3rd	26	Simultaneous suck, swallow and breath	500
3rd	26.5	Simultaneous swallow and breath	500
3rd	42.5	Simultaneous swallow and breath	1500
4th	17.5	Simultaneous suck, swallow and breath	500
4th	18	Simultaneous swallow and breath	500
4th	27	Simultaneous suck, swallow and breath	500
4th	47	Simultaneous suck, swallow and breath	1000
5th	8.5	Simultaneous suck, swallow and breath	1500
5th	10	Simultaneous swallow and breath	500
5th	50.5	Simultaneous suck, swallow and breath	1000
6th	16.5	Simultaneous suck, swallow and breath	1000
6th	17	Simultaneous swallow and breath	500
7th	21	Simultaneous swallow and breath	500
7th	30	Simultaneous suck, swallow and breath	1500
13th	15.5	Simultaneous swallow and breath	1500
13th	32.5	Simultaneous suck, swallow and breath	500
14th	16.5	Simultaneous suck, swallow and breath	2500

As it is clear, more that one feeding for a baby must be investigated to decide whether the baby has reached to the point to coordinate the suck, swallow and breathing processes.

4.8. Conclusion

In this approach, the integration of correlation and matched filtering in time domain was investigated. As the result shows, this method had promise result for the detection of suck and breathing signal but not for the swallowing waveform. From a theoretic point of view, this method must also have acceptable results for the swallowing signal but due to the poor quality of the measurement of the swallowing signal, the error level is high.

For analysis the relationship between the signals, transforming the occurrence matrix of each signal to a binary stream and investigating the relationships of signals using corresponding decision tables seems satisfactory to see whether or not the baby is able to coordinate suck, swallow and breathing.

Overall Conclusions

5.1. Overall Conclusions

In this study, three different methods of signal analysis were investigated to detect, identify and classify three physiological measurements including suck, swallow and breathing activity in premature infants during bottle-feeding.

In the first approach, the integration of wavelet packet transform with neural network was examined. In this method, wavelet packet energy nodes were introduced as a set of parameters to characterize each frame of a specific signal. These parameters were then fed to the neural network in order to classify the frame being processed. As a feature extraction method, wavelet packet energy nodes do not emphasize the duration of the signal being processed. Therefore, two similar signals with different durations cannot be distinguished by this method. In addition, loss of localized time property of the signal is unavoidable. Since the energy differences are not sufficient to distinguish shape differences of the waveforms, applying a feature extraction method that takes into account the duration and shape of a signal is necessary.

Wavelet packet energy nodes are formed based on the existing wavelet packet decomposition coefficients. Although this method is compact and avoids the use of a large number of coefficients, it fails to emphasize the localized time property. In order to reveal the localized time property and shape differences of the waveforms, another category of feature extraction method that directly uses the decomposition coefficients may be investigated.

In the second approach, an arbitrary window size of one minute was used to investigate the frequency content of each specific signal. The results showed that

differences in waveform shape could not be adequately distinguished by examination of the frequency content. Because the Welch method involves with averaging over frequency for the different segments, it is likely that the spectral content associated with the event of interest is hidden somewhere. In order to reveal the difference of frequency content, the size of the window needs to be reduced close to the actual duration of an event. Matching the window size to the actual duration of an event may reveal greater relationships between the shape of the signal and its frequency content.

In the third approach, a method including correlation and matched filtering was studied. In order to perform matched filtering to detect an activity in a specific waveform, a prototype (template) for each waveform was developed based on an average of several candidate patterns. Candidates were selected based on the opinion of a subject expert. The match filtering process incrementally slides the prototype over the unknown signal and computes the correlation between them within the time interval. To perform the correlation signals are resampling to have the same size. Signals that are not correlated to the prototype will have in a correlation coefficient close to zero. If a matching frame is detected the correlation coefficient becomes closer one with a maximum value of one for a perfect match. In this case, the start time, the length of the current frame and the correlation coefficient were recorded in a matrix called the occurrence matrix.

In order to analyze the relationship between the three signals (suck, swallow and breathing), the corresponding occurrence matrices were transformed into a binary stream. To perform this, each minute of a specific signal was divided into consequent time slots and using the corresponding matrix, the occurrence of that specific activity in different

time slots was examined. If the activity has occurred in the time slot the value would be one otherwise it would be zero. At the end of the detection procedure for all three signals for a specific baby, the binary streams for all three signals were combined in a table called decision table. The decision table can be used to determine whether suck, swallow and breathing have occurred in a coordinated fashion or not. As the results showed the third approach is reliable for detection of suck and breathing signals but due to the poor quality of measurements of swallowing signal in this study, the error in detection of swallowing signal is rather high.

List of References

References

"Life Science Suite: PONEMAH Physiology Platform", Gould Instrument System Inc., 2001.

"Matlab User's Guide", The Mathworks Inc., 2000.

"Neural Network Toolbox User's Guide", The Mathworks Inc., 2000.

"Signal Processing Toolbox User's Guide", The Mathworks Inc., 2000.

Akay M., "Nonlinear Biomedical Signal Processing: Volume I", IEEE Press, New York, 2000.

Baher H., "Analog & Digital Signal Processing", John Wiley & Sons Ltd., 20001.

Bamford O., Taciak V., Gewolb I. H., "The Relationship between Rhythmic Swallowing and Breathing during Suckle Feeding in Term Neonates", Pediatr Res, 31(6):619-624, 1992.

Bendat J. S., Piersol A. G.," Engineering Applications of Correlation and Spectral Analysis", John Wiley & Sons, 1993.

Berne R. M., Levy M. N., Bruce M. K., Bruce A. S., "Physiology", Mosby-Year Book, 2004.

Bose N. K., Rao C. R., "Signal Processing and its Applications", Elsvier Science Publishers B.V., 1993.

Bu'Lock F., Woolridge M. W., Baum J. D., "Infants' Coordination of Sucking Swallowing and Breathing", Developmental Medicine and Child Neurology, 32: 669-678, 1990.

Castanie F., "Spectral Analysis: Parametric and Non-parametric Digital Methods", ISTE Ltd., 2006.

Convey A., "Instruments in Neonatal Research: Measuring Preterm Infant Feeding Ability, Part I: Bottle-Feeding", Neonatal Network, 13(4): 71-73, June 1994.

Deckardt R., Steward D. J., "Noninvasive Arterial Hemoglobin Oxygen Saturation versus Transcutaneous Oxygen Tension Monitoring in the Preterm Infants", Crit Care Med., 12:935-939, 1984.

Eberhart R. C., Dobbins R.W., “Early Neural Network Development History: The Age of Camelot”, IEEE Engineering in Medicine and Biology, 9:15-18. 1990.

Enderle J., Blanchard S., Bronino J., “Introduction to Biomedical Engineering”, Academic Press, 2000.

Eugene N. B., “Biomedical Signal Processing and Signal Modeling”, John Wiley & Sons Inc., 2001.

Firebaugh M. W., “Artificial Intelligence: A Knowledge-based Approach”, Boyd and Fraser, Boston, MA, 1988.

Gallant S. I., “Neural Network Learning and Expert Systems”, The MIT Press, 1993.

Guez A., Protopopesu V., Barhen J., “On the Stability, Storage Capacity, and Design of Nonlinear Continuous Neural Networks”, IEEE Trans. on System Man and Cybernetics 18(1):80-87,1988.

Haykin S., “Neural Networks: A Comprehensive Foundation” Prentice Hall, 1999.

Hippenstiel R. D.,” Detection Theory”, CRC Press, 2002.

Hiss S. G., Treole K., Stuart A., “Effects of Age, Gender, Bolus Volume, and Trial on Swallowing Apnea Duration and Swallow/Respiratory Phase Relationships of Normal Adults”, Dysphagia, 16(2): 128-135, 2001.

Hornik K., Stinchcombe M., White H., “Universal Approximation of an Unknown Mapping and its Derivatives Using Multilayer Feed-Forward Networks”, Neural Networks, 3(5):551-560, 1990.

Jain L. C., Martin N. M., “Fusion of Neural Network, Fuzzy Sets, and Genetic Algorithms: Industrial Application”, CRC Press, 1999.

Kaiser G.,”A Friendly Guide to Wavelets”, Birkhauser, 1994.

Klein M. R., Methlie L. B., “Knowledge-Based Decision Support System: with Application in Business”, Wiley, 1995.

Koos B. J., Maeda T., Jan C.,” Adenosine A_1 and A_{2A} Receptors Modulate Sleep State and Breathing in Fetal Sheep”, Appl Physiol, 91: 343-350, 2001

Kramer S. S.,” Special Swallowing Problems in Children”, Gastrointest Radiol, 10:259–265, 1985.

Lau C., Alagugurusamy R., Schanler R. J., Smith E. O., Shulman R. J., "Characterization of the Developmental Stages of Sucking in Preterm Infants during Bottle-Feeding" Acta Paediatr, 89: 846-52, 2000.

Lau C., Schanler R. J.," Oral Motor Function in the Neonate", Clinics in Perinatology, 23(2):161-178, June 1996.

Lau C., Sheena H. R., Shulman R. J., Schanler R. J., " Oral Feeding in Low Birth Weight Infants", The Journal of Pediatrics, 130: 561-9, 1997.

Lau C., Smith E. O., Schanler R. J." Coordination of Suck-Swallow and Swallow-Respiration in Preterm Infants", Acta Paediatr, 92(6):721-7, June 2003.

Linden D. W., Paroli E. T., Doron M. W., "Preemies: the Essential Guide for Parents of Premature Babies", New York : Pocket Books, 2000.

Looney C. G.," Pattern Recognition Using Neural Networks", Oxford University Press, 1997.

Lutovac M. D., Tosic D. V., Evans B. L., "Filter Design for Signal Processing using Matlab and Mathematica", Prentice Hall, 2001.

Mallat S., "A Wavelet Tour of Signal Processing", Academic Press, 1998.

Manolakis D. G., Ingle V. K., Kogon S. M., "Statistical and Adaptive Signal Processing", McGraw-Hill Higher Education, 2000.

Mathew O. P., "Respiratory Control during Nipple Feeding in Infants" Pediatr Pulmonol. 5:220-224, 1988.

Medsker L. R., "Hybrid Neural Network and Expert System", Kluwer Academic Publishers, 1994.

Medoff-Cooper B., Wendy R.," Neonatal Sucking Behaviors", Journal of Nursing Scholarship, 27(3): 195-200, 1995.

Medoff-Cooper B., Bilker W. B., Kaplan J. M., "Suckling Behavior as a Function of Gestational Age: a Cross-Sectional Study", Infant Behavior & Development 24: 83-94, 2001.

Mitra P., Pesaran B., "Analysis of Dynamic Brain Imaging Data", Biophysical Journal 76(2):691–708, 1999.

Mizuno K., Ueda A., "The Maturation and Coordination of Sucking, Swallowing, and Respiration in Preterm Infants", Journal of Pediatrics, 142(3):233-4, March 2003.

Newman L. A., "Infant Swallowing and Dysphagia", Head Neck Surg., 4:182–186, 1996.

Newman L. A., Keckley C., Petersen M. C., Hamner A., "Swallowing Function and Medical Diagnoses in Infants Suspected of Dysphagia", Pediatrics, Vol. 108 No. 6, pp. 106, December 2001.

Nyqvist K. H., Sjoden P., Ewald U., "The Development of Preterm Infants' Breastfeeding Behavior", Early Human Development, 55:247-264, 1999.

Nguyen H. T., Walker E. A., "A First Course in Fuzzy Logic", CRC Press, 1997.

Ott R. L., Longnecker M., "An Introduction to Statistical Methods and Data Analysis", Wadsworth Group, 2001.

Pal S. K., Wang P. P., "Genetic Algorithms for Pattern Recognition", CRC Pres, 1996.

Pickler R. H., "Bottle-Feeding Readiness in Preterm infants", NINR/NIH 1 R01 NR005182-01, 1999.

Priestley M. B.," Spectral Analysis and Time Series", Volume 1, Academic Press, 1981.

Proakis J. G., Manolakis D. G., "Digital Signal Processing: Principles, Algorithms, and Applications" Prentice Hall, 1996.

Qian S., "Introduction to Time-Frequency and Wavelet Transform", Prentice Hall, 2002.

Reddy S., Ryan M. W. "Dysphagia", Grand Rounds Presentation, UTMB, Dept. of Otolaryngology, November 21, 2001.

Redshaw M. E., Rivers R. A., Rosenblatt D. B., "Born Too Early", Oxford University Press, 1985.

Rumelhart D.E. , McClelland J.L.," Parallel Distributed Processing: Explorations in the Microstructure of Cognition", MIT Press, 1986 .

Sarkar t. K., Salazar-Palma M., Wicks M. C., "Wavelet Application in Engineering Electromagnetics", Artech House Inc., 2002.

Selley W. G., Ellis R. E., Flack F. C., Brooks W. A., "Coordination of Sucking, Swallowing and Breathing in the Newborn: its Relationship to Infant Feeding and Normal Development", Br J Disord Commun, 25(3): 311-327, 1990.

Selley W. G., Ellis R. E., Flack F. C., Curtis H., Callon M., "Ultrasonographic Study of Sucking and Swallowing by Newborn Infants", Dev Med Child Neurol, 28(6): 821-823, 1986.

Smith J. O., "Mathematics of the Discrete Fourier Transform", W3K Publishing,, 2003.

Stocia P., Moses R. L., "Introduction to Spectral Analysis", Prentice Hall, 1997.

Walnut D. F., "An Introduction to Wavelet Analysis", Birkauser Boston, 2002.

Webster J. G., "Medical Instrumentation", John Wiley &Sons Inc., 1998.

Weismiller D. G., "Preterm Labor", American Family Physician, Feb 1, 1999.

Winter G., Perinaux J., Galan M., Cuesta P., "Genetic Algorithms in Engineering and Computer Science", John Wiley & Sons Inc., 1995.

Wu T., Carl W. A., "Pulmonary Physiology of Neonatal Resuscitation", Neoreviews, 2: 45-50, 2001.

Yager R. R., Filev D. P., " Essential of Fuzzy Modeling", John Wiley & Sons Inc., 1994.

Yen G.G., Lin K.C., "Wavelet Packet Feature Extraction for Vibration Monitoring", IEEE Trans Industrial Electronics, 47(3):650-667, 2000.

Appendix 1

Appendix 1

The List of the Functions and Data Structure Used in WPT and NN

```
%%%%%%%%%%%%%%%%%%%%%%%%%%%%%%%%%%%%%%%%%%%%
%%%%%                 SCAN                 %%%%%
%%%%%%%%%%%%%%%%%%%%%%%%%%%%%%%%%%%%%%%%%%%%

% This function scan the signal to detect whether an activity has occurred or not

 function occurance=scan(signal,net,meane,stde,meant,stdt)

smallest_breath=500;
j=1;
counter=1; % begining the signal
while (counter+smallest_breath)<=5000          % not end of signal
   catch_a_breath=0;          % There is no breath pattern
   window_size=smallest_breath;           % smallest breath pattern 500
   while ~catch_a_breath && window_size<=2000
      data=signal(counter:counter+window_size); % read a window
     % extract features and normalize them
      E=parameters(data);
      En=trastd(E,meane,stde);
      y=poststd(sim(net,En),meant,stdt);
      if y>=0.80
         is_breath=1;
      else
         is_breath=0;
      end
      if is_breath  % if there is breath in this window
         catch_a_breath=1;
         occurance(1,j)=counter;  %time  time of breath
         occurance(2,j)=window_size;   %length of breath
          j=j+1;
         counter=counter+window_size;  % go to the end of the breath

      else
         window_size=window_size+5;   %strech the window
      end
   end

      if ~catch_a_breath
         counter=counter+5;  %if you didn't find any breath  then move the window
```

```
    end

end

%%%%%%%%%%%%%%%%%%%%%%%%%%%%%%%%%%%%%%%%%%%%%%
%%%%%                    PARAMETERS                    %%%%%
%%%%%%%%%%%%%%%%%%%%%%%%%%%%%%%%%%%%%%%%%%%%%%

%This function characterizes a signal using wavelet packet transform
%It decomposes the signal to level 3 and caculates the enegry of teminal
%nodes (7,8,9,10,11,12,13,14) in a vector named E.
%E=(E1,E2,...,E8) is the parameter that characterizes the signal

function EN=parameters(signal)
if nargin>1
   error('Too many input argument');
end
EN=[];
wpThree=wpdec(signal,3,'db2');
for i=7:14
   coefs=wpcoef(wpThree,i);
   EN(i-6)=energy(coefs);
end
EN=EN';


%%%%%%%%%%%%%%%%%%%%%%%%%%%%%%%%%%%%%%%%%%%%%%
%%%%%                    NET_8_1                    %%%%%
%%%%%%%%%%%%%%%%%%%%%%%%%%%%%%%%%%%%%%%%%%%%%%

net_8_1 =

   Neural Network object:

   architecture:

        numInputs: 1
        numLayers: 3
      biasConnect: [1; 1; 1]
     inputConnect: [1; 0; 0]
     layerConnect: [0 0 0; 1 0 0; 0 1 0]
    outputConnect: [0 0 1]
    targetConnect: [0 0 1]
```

```
   numOutputs: 1  (read-only)
   numTargets: 1  (read-only)
numInputDelays: 0  (read-only)
numLayerDelays: 0  (read-only)

subobject structures:

       inputs: {1x1 cell} of inputs
       layers: {3x1 cell} of layers
      outputs: {1x3 cell} containing 1 output
      targets: {1x3 cell} containing 1 target
       biases: {3x1 cell} containing 3 biases
 inputWeights: {3x1 cell} containing 1 input weight
 layerWeights: {3x3 cell} containing 2 layer weights

functions:

     adaptFcn: 'trains'
      initFcn: 'initlay'
   performFcn: 'sse'
     trainFcn: 'trainrp'

parameters:

   adaptParam: .passes
    initParam: (none)
 performParam: (none)
   trainParam: .epochs, .show, .goal, .time,
               .min_grad, .max_fail, .delt_inc, .delt_dec,
               .delta0, .deltamax

weight and bias values:

           IW: {3x1 cell} containing 1 input weight matrix
           LW: {3x3 cell} containing 2 layer weight matrices
            b: {3x1 cell} containing 3 bias vectors

other:
     userdata: (user stuff)
```

The Shape of the Patterns Used to Train the Neural Network

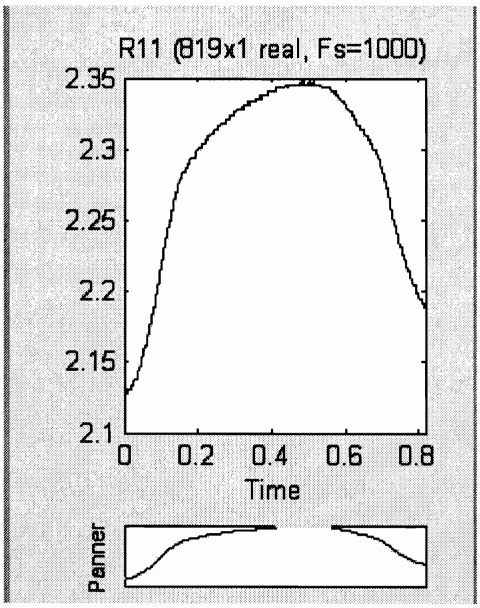

Figure 7.1: R11 used to train the NN

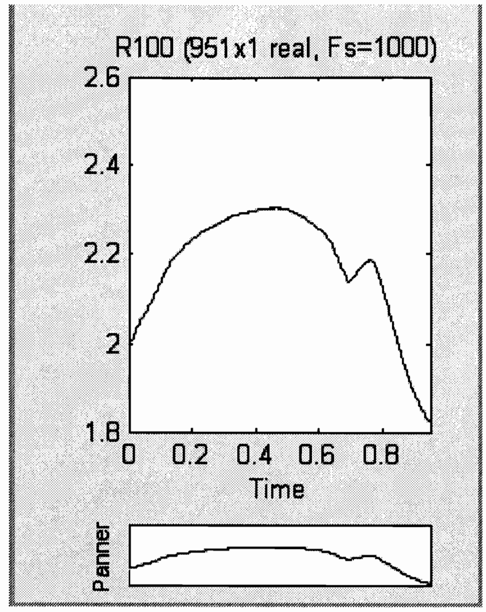

Figure 7.2: R100 used to train the NN

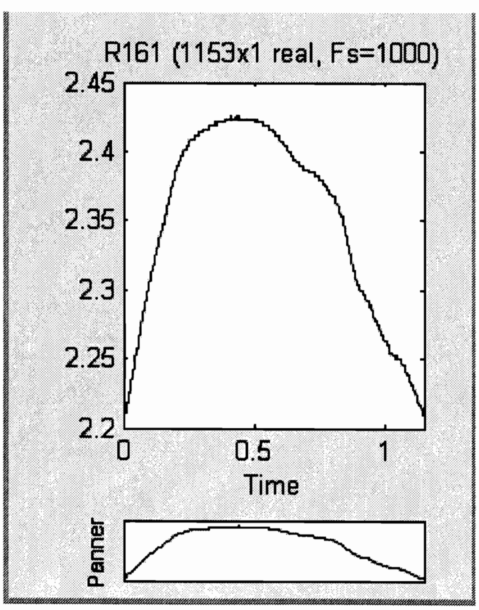

Figure 7.3: R161 used to train the NN

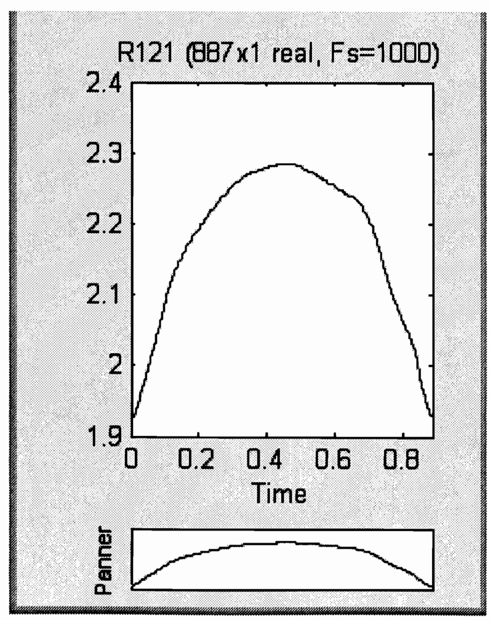

Figure 7.4: R121 used to train the NN

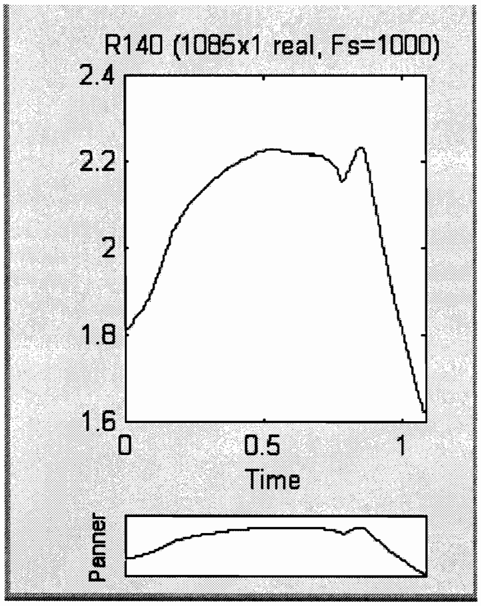

Figure 7.5: R140 used to train the NN

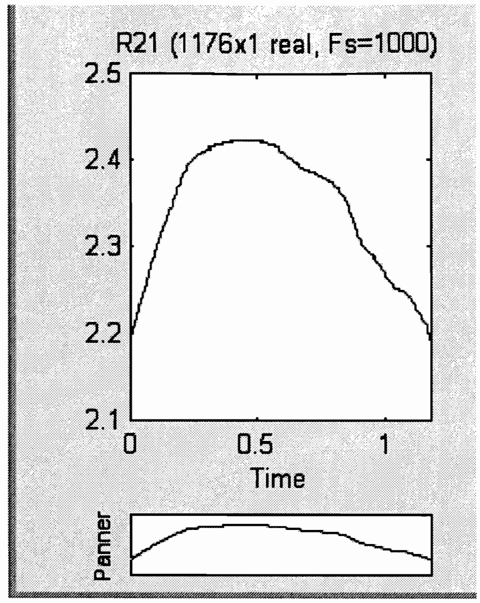

Figure 7.6: R21 used to train the NN

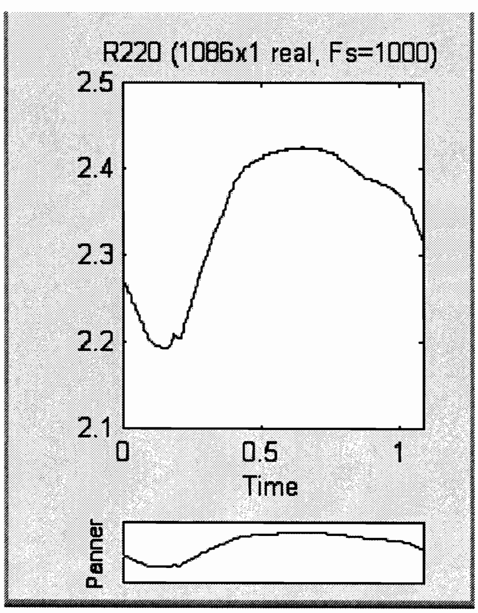

Figure 7.7: R220 used to train the NN

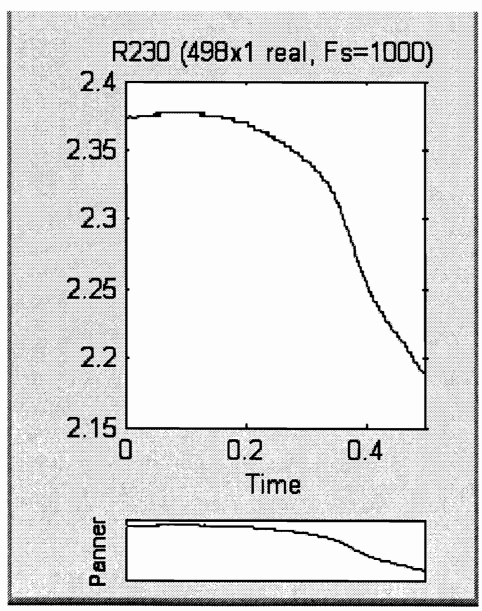

Figure 7.8: R230 used to train the NN

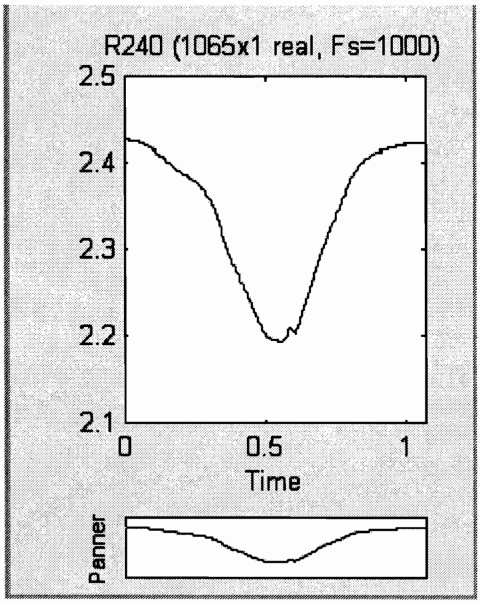

Figure 7.9: R240 used to train the NN

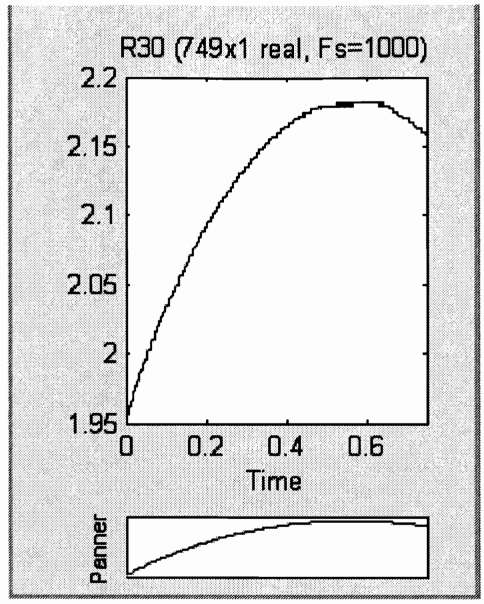

Figure 7.10: R30 used to train the NN

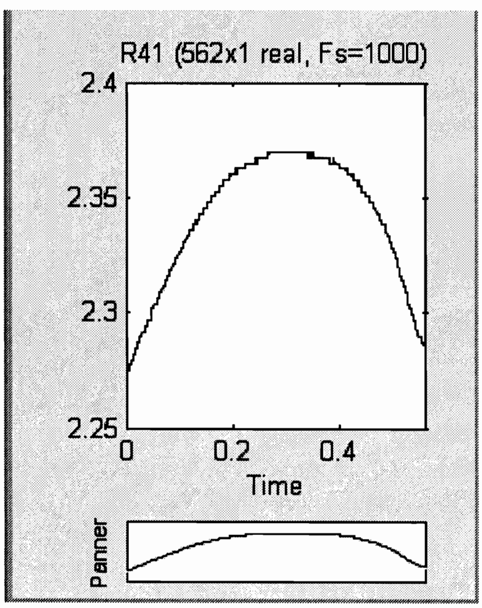

Figure 7.11: R41 used to train the NN

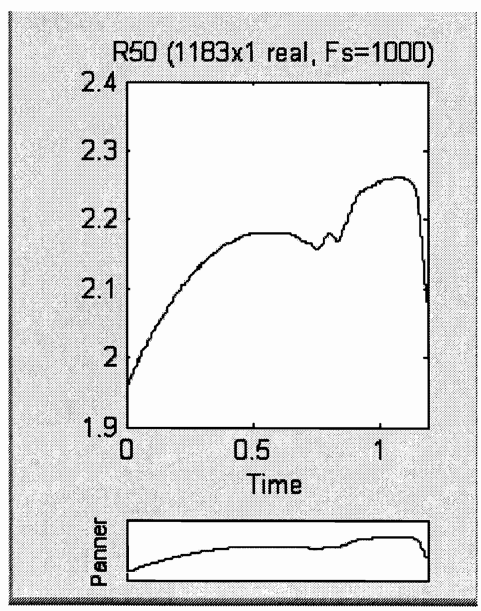

Figure 7.12: R50 used to train the NN

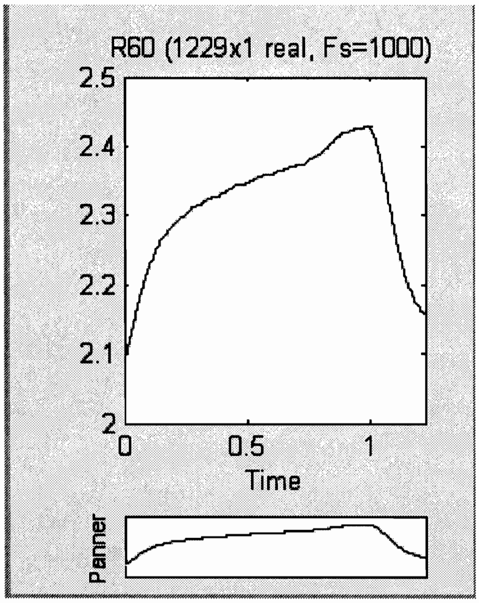

Figure 7.13: R60 used to train the NN

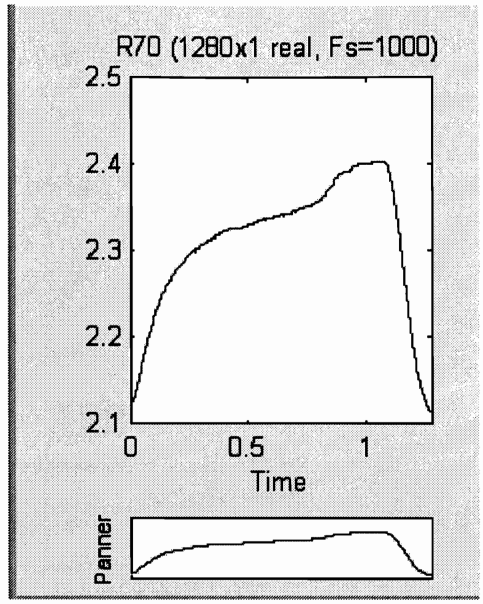

Figure 7.14: R70 used to train the NN

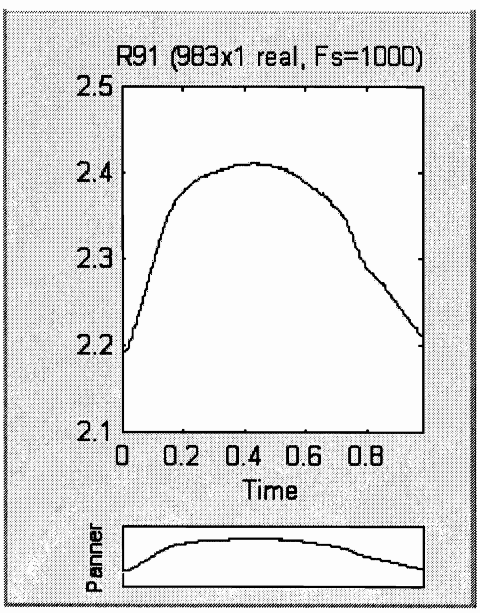

Figure 7.15: R91 used to train the NN

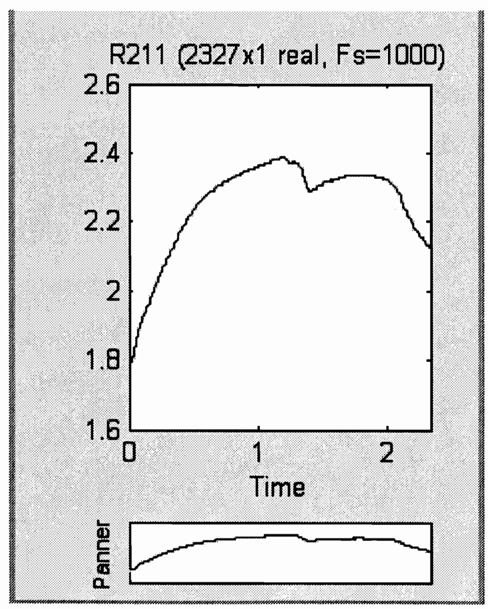

Figure 7.16: R211 used to train the NN

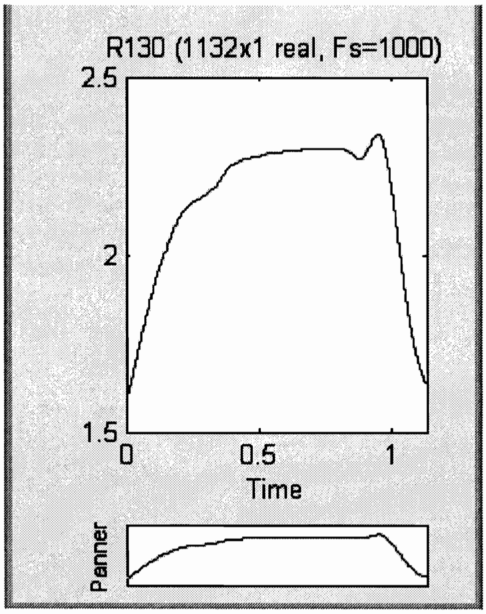

Figure 7.17: R130 used to train the NN

The Shape of the Signals Used to Test the Neural Network

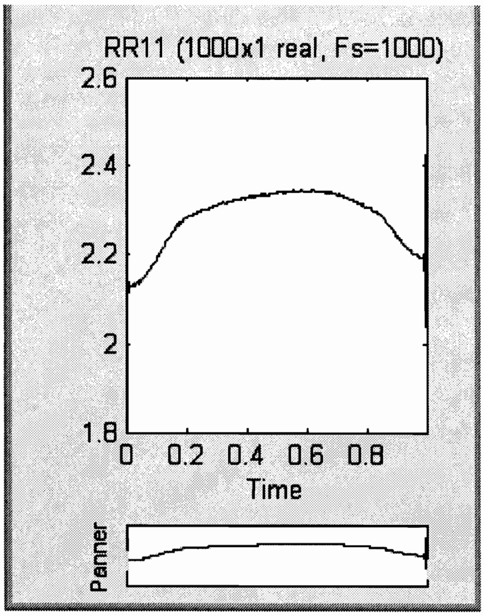

Figure 7.18: RR11 used to test the NN

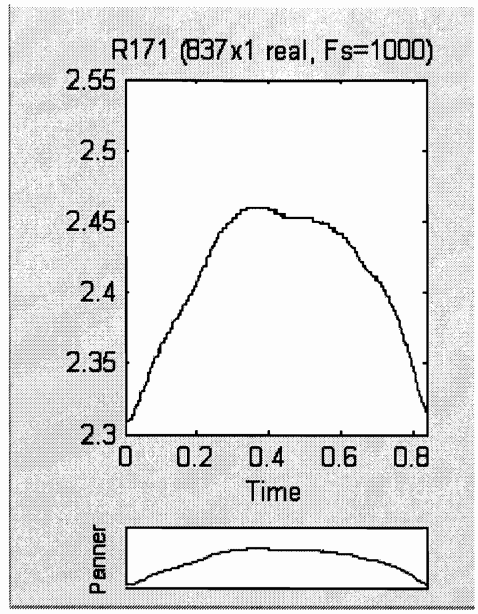

Figure 7.19: R171 used to test the NN

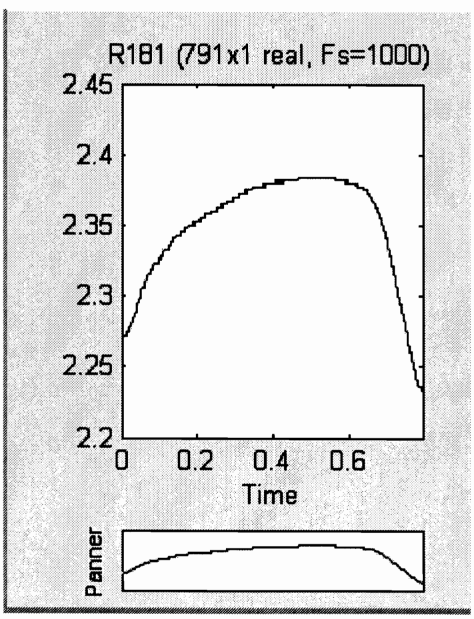

Figure 7.20: R181 used to test the NN

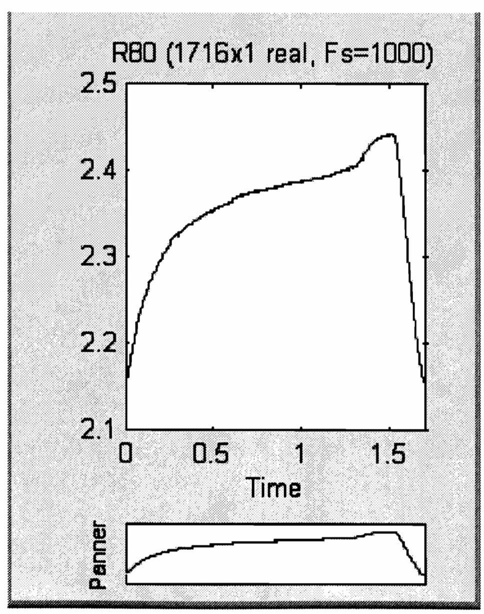

Figure 7.21: R80 used to test the NN

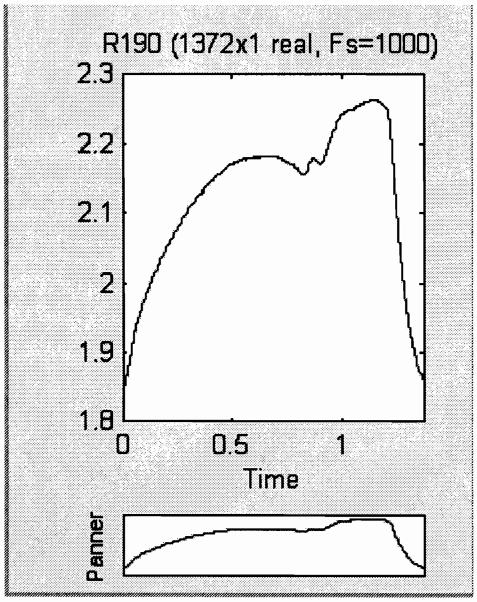

Figure 7.22: R190 used to test the NN

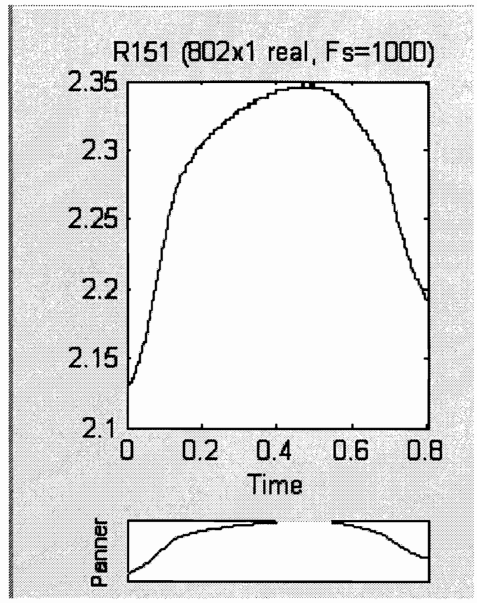

Figure 7.23: R151 used to test the NN

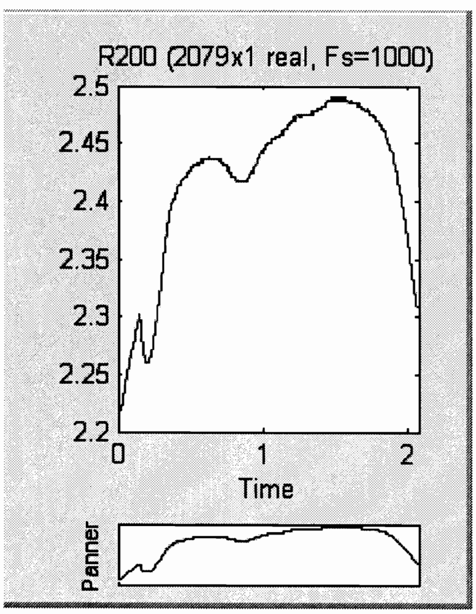

Figure 7.24: R200 used to test the NN

Appendix 2

Appendix 2

The List of the Functions Used in Correlation and Matched Filtering

```
%%%%%%%%%%%%%%%%%%%%%%%%%%%%%%%%%%%%%%%%%%%%%%%%%
%%%%%%%%%          CREAT_PROTOTYPE_81_10      %%%%%%%%%%%%
%%%%%%%%%%%%%%%%%%%%%%%%%%%%%%%%%%%%%%%%%%%%%%%%%


function
prototype=creat_prototype_81_10(X1,X2,X3,X4,X5,X6,X7,X8,X9,X10,X11,X12,X13,X
14,X15,X16,X17,X18,X19,X20,X21,X22,X23)
for i=1:1000

prototype(i)=(X1(i)+X2(i)+X3(i)+X4(i)+X5(i)+X6(i)+X7(i)+X8(i)+X9(i)+X10(i)+X11(i
)+X12(i)+X13(i)+X14(i)+X15(i)+X16(i)+X17(i)+X18(i)+X19(i)+X20(i)+X21(i)+X22(i)
+X23(i))/23;
end



%%%%%%%%%%%%%%%%%%%%%%%%%%%%%%%%%%%%%%%%%%%%%%%%%
%%%%%%%%%          CREAT_PROTOTYPE_87_7       %%%%%%%%%%%%
%%%%%%%%%%%%%%%%%%%%%%%%%%%%%%%%%%%%%%%%%%%%%%%%%
function
prototype=creat_prototype_87_7(X1,X2,X3,X4,X5,X6,X7,X8,X9,X10,X11,X12,X13,X1
4,X15,X16,X17,X18,X19,X20,X21,X22,X23,X24,X25,X26,X27,X28,X29,X30,X31,X32
,X33,X34,X35,X36,X37,X38,X39,X40,X41,X42,X43,X44,X45,X46,X47,X48,X49,X50,
X51,X52,X53,X54,X55)
for i=1:1000

prototype(i)=(X1(i)+X2(i)+X3(i)+X4(i)+X5(i)+X6(i)+X7(i)+X8(i)+X9(i)+X10(i)+X11(i
)+X12(i)+X13(i)+X14(i)+X15(i)+X16(i)+X17(i)+X18(i)+X19(i)+X20(i)+X21(i)+X22(i)
+X23(i)+X24(i)+X25(i)+X26(i)+X27(i)+X28(i)+X29(i)+X30(i)+X31(i)+X32(i)+X33(i)
+X34(i)+X35(i)+X36(i)+X37(i)+X38(i)+X39(i)+X40(i)+X41(i)+X42(i)+X43(i)+X44(i)
+X45(i)+X46(i)+X47(i)+X48(i)+X49(i)+X50(i)+X51(i)+X52(i)+X53(i)+X54(i)+X55(i))
/55;
end
```

```
%%%%%%%%%%%%%%%%%%%%%%%%%%%%%%%%%%%%%%%%%%%%
%%%%%%%%%                SWALLOW_SCAN          %%%%%%%%%%%%
%%%%%%%%%%%%%%%%%%%%%%%%%%%%%%%%%%%%%%%%%%%%


function occurance=swallow_scan(signal,prototype)

smallest_swallow=1000;
widest_swallow=2000;
step1=20;
step2=20;
j=1;
correlation_coeff=0.85;
counter=1; % begining the signal
size_of_signal=size(signal);
occurance=[];
while (counter+smallest_swallow)<=size_of_signal(1,1)          % not end of signal
   catch_a_swallow=0;           % There is no swallow pattern
   window_size=smallest_swallow;            % smallest swallow pattern
   while ~catch_a_swallow && window_size<=widest_swallow &&
(counter+window_size)<=size_of_signal(1,1)
      data=signal(counter:counter+window_size); % read a window
      % scale data and do the correlation
      data=resample_1000(data);
      coeff=corrcoef(data,prototype);
      y=coeff(1,2);
      if y>=correlation_coeff
         is_swallow=1;
         go_ahead=1;
         while go_ahead && (counter+window_size+step2)<= size_of_signal(1,1)&&
window_size+step2<=widest_swallow  %as far as you see a better signal move the end
of the window (beginning is fixed)
            window_size=window_size+step2;
            data=signal(counter:counter+window_size);
            data=resample_1000(data);
            coeff=corrcoef(data,prototype);
            x=coeff(1,2);
            if x>=y
               y=x;
            else
              go_ahead=0;
              window_size=window_size-step2;
            end
         end
```

```
        go_ahead=1;
        while go_ahead  && counter+window_size+step2<= size_of_signal(1,1)&&
window_size-step2>=smallest_swallow%as far as you see a better signal move the
begining of the window (end is fixed)
            counter=counter+step2;
            window_size=window_size-step2;
            data=signal(counter:counter+window_size);
            data=resample_1000(data);
            coeff=corrcoef(data,prototype);
            x=coeff(1,2);
            if x>=y
                y=x;
            else
               go_ahead=0;
               counter=counter-step2;
               window_size=window_size+step2;
            end
         end

      else
         is_swallow=0;
      end

      if is_swallow && window_size>=smallest_swallow && (max(data)-
min(data))>=0.75 % if there is swallow in this window and window is big enough and the
shape is deep enough
         catch_a_swallow=1;
         occurance(1,j)=counter;  % time of swallow
         occurance(2,j)=window_size;   %length of swallow
         occurance(3,j)=y;
         j=j+1;
         counter=counter+window_size;  % go to the end of the swallow

      else
         window_size=window_size+step1;   %strech the window
      end
   end

      if ~catch_a_swallow
         counter=counter+step1;  %if you didn't find any swallow  then move the window
      end
end
%%%%%%%%%%%%%%%%%%%%%%%%%%%%%%%%%%%%%%%%
%%%%%%%%                 SUCK_SCAN          %%%%%%%%%%%
```

```
%%%%%%%%%%%%%%%%%%%%%%%%%%%%%%%%%%%%%%%%%%%

function occurance=suck_scan(signal,prototype)

smallest_suck=500;
widest_suck=2000;
step1=20;
step2=20;
j=1;
correlation_coeff=0.85;
counter=1; % begining the signal
size_of_signal=size(signal);
occurance=[];
while (counter+smallest_suck)<=size_of_signal(1,1)          % not end of signal
   catch_a_suck=0;           % There is no suck pattern
   window_size=smallest_suck;           % smallest suck pattern
   while ~catch_a_suck && window_size<=widest_suck &&
(counter+window_size)<=size_of_signal(1,1)
      data=signal(counter:counter+window_size); % read a window
      % scale data and do the correlation
      data=resample_1000(data);
      coeff=corrcoef(data,prototype);
      y=coeff(1,2);
      if y>=correlation_coeff
         is_suck=1;
         go_ahead=1;
         while go_ahead && (counter+window_size+step2)<= size_of_signal(1,1)&&
window_size+step2<=widest_suck  %as far as you see a better signal move the end of
the window (beginning is fixed)
            window_size=window_size+step2;
            data=signal(counter:counter+window_size);
            data=resample_1000(data);
            coeff=corrcoef(data,prototype);
            x=coeff(1,2);
            if x>=y
               y=x;
            else
              go_ahead=0;
              window_size=window_size-step2;
            end

         end
         go_ahead=1;
```

```
        while go_ahead  && counter+window_size+step2<= size_of_signal(1,1)&&
window_size-step2>=smallest_suck%as far as you see a better signal move the begining
of the window (end is fixed)
            counter=counter+step2;
            window_size=window_size-step2;
            data=signal(counter:counter+window_size);
            data=resample_1000(data);
            coeff=corrcoef(data,prototype);
            x=coeff(1,2);
            if x>=y
                y=x;
            else
               go_ahead=0;
               counter=counter-step2;
               window_size=window_size+step2;
            end
          end



      else
         is_suck=0;
      end

      if is_suck && window_size>=smallest_suck  % if there is suck in this window and
window is big enough
         catch_a_suck=1;
         occurance(1,j)=counter;  % time of suck
         occurance(2,j)=window_size;   %length of suck
         occurance(3,j)=y;
         j=j+1;
         counter=counter+window_size;  % go to the end of the suck

      else
         window_size=window_size+step1;   %strech the window
      end
   end

      if ~catch_a_suck
         counter=counter+step1;  %if you didn't find any suck  then move the window
      end

end
```

```
%%%%%%%%%%%%%%%%%%%%%%%%%%%%%%%%%%%%%%%%%%%%%%%%%%%
%%%%%%%%%                BREATH_SCAN          %%%%%%%%%%%
%%%%%%%%%%%%%%%%%%%%%%%%%%%%%%%%%%%%%%%%%%%%%%%%%%%

function occurance= breath_scan(signal,prototype)

smallest_breath=300;
widest_breath=2000;
step1=20;
step2=20;
j=1;
correlation_coeff=0.8;
counter=1; % begining the signal
size_of_signal=size(signal);
occurance=[];
while (counter+smallest_breath)<=size_of_signal(1,1)          % not end of signal
   catch_a_breath=0;           % There is no breath pattern
   window_size=smallest_breath;           % smallest breath pattern
   while ~catch_a_breath && window_size<=widest_breath &&
(counter+window_size)<=size_of_signal(1,1)
      data=signal(counter:counter+window_size); % read a window
      % scale data and do the correlation
      data=resample_1000(data);
      coeff=corrcoef(data,prototype);
      y=coeff(1,2);
      if y>=correlation_coeff
         is_breath=1;
         go_ahead=1;
         while go_ahead && (counter+window_size+step2)<= size_of_signal(1,1)&&
window_size+step2<=widest_breath   %as far as you see a better signal move the end of
the window (beginning is fixed)
            window_size=window_size+step2;
            data=signal(counter:counter+window_size);
            data=resample_1000(data);
            coeff=corrcoef(data,prototype);
            x=coeff(1,2);
            if x>=y
               y=x;
            else
              go_ahead=0;
              window_size=window_size-step2;
            end
```

```
        end
        go_ahead=1;
        while go_ahead  && counter+window_size+step2<= size_of_signal(1,1)&&
window_size-step2>=smallest_breath%as far as you see a better signal move the
begining of the window (end is fixed)
            counter=counter+step2;
            window_size=window_size-step2;
            data=signal(counter:counter+window_size);
            data=resample_1000(data);
            coeff=corrcoef(data,prototype);
            x=coeff(1,2);
            if x>=y
                y=x;
            else
              go_ahead=0;
              counter=counter-step2;
              window_size=window_size+step2;
            end
         end



      else
        is_breath=0;
      end

      if is_breath && window_size>=smallest_breath % if there is breath in this window
and window is big enough
        catch_a_breath=1;
        occurance(1,j)=counter;  % time of breath
        occurance(2,j)=window_size;   %length of breath
        occurance(3,j)=y;
        j=j+1;
        counter=counter+window_size;  % go to the end of the breath

      else
        window_size=window_size+step1;   %strech the window
      end
    end

      if ~catch_a_breath
        counter=counter+step1;  %if you didn't find any breath  then move the window
      end
```

```
end


%%%%%%%%%%%%%%%%%%%%%%%%%%%%%%%%%%%%%%%%%%%%%%%%%%%%
%%%%%%%%%           TRANSFER_TO_ONE_ZERO        %%%%%%%%%%%%
%%%%%%%%%%%%%%%%%%%%%%%%%%%%%%%%%%%%%%%%%%%%%%%%%%%%

% This function creat the binary stream corresponding to the occurrence matrix

function output=transfer_to_one_zero(matrix,length)

time_slot=500;
size_of_output=round(length/time_slot);
output(1:size_of_output)=0;  % lenght is the size of a signal that we are analyzing for
now its 60000
index=1;
[x y]=size(matrix);
for index=1:y
   beginning=matrix(1,index);
   ending=matrix(2,index)+matrix(1,index);
   a=fix(beginning/time_slot);
   b=fix(ending/time_slot);
   r1=beginning-a*time_slot;
   r2=ending-b*time_slot;   % residue
   a=a+1;
   b=b+1;
   output(a:b)=1;
   if (time_slot-r1)<=(time_slot/5)          % if the activity has started in the very end of
this section, ignore it (zero it)
      output(a)=0;
   end
   if (time_slot-r2)>=4*(time_slot)/5
      output(b)=0;   % if the activity has ended in the very beginning of this section,
ignore it (zero it)
   end
end
```